



<https://theses.gla.ac.uk/>

Theses Digitisation:

<https://www.gla.ac.uk/myglasgow/research/enlighten/theses/digitisation/>

This is a digitised version of the original print thesis.

Copyright and moral rights for this work are retained by the author

A copy can be downloaded for personal non-commercial research or study, without prior permission or charge

This work cannot be reproduced or quoted extensively from without first obtaining permission in writing from the author

The content must not be changed in any way or sold commercially in any format or medium without the formal permission of the author

When referring to this work, full bibliographic details including the author, title, awarding institution and date of the thesis must be given

Enlighten: Theses

<https://theses.gla.ac.uk/>
research-enlighten@glasgow.ac.uk

A THESIS FOR THE DEGREE OF DOCTOR OF PHILOSOPHY

THE THERMAL DEGRADATION OF
POLY(-D)- β -HYDROXYBUTYRIC ACID)

BY
ERIC JAMES MURRAY

SUPERVISORS: PROFESSOR N. GRASSIE
DR. P. A. HOLMES

CHEMISTRY DEPARTMENT
UNIVERSITY OF GLASGOW
OCTOBER, 1980

ProQuest Number: 10984236

All rights reserved

INFORMATION TO ALL USERS

The quality of this reproduction is dependent upon the quality of the copy submitted.

In the unlikely event that the author did not send a complete manuscript and there are missing pages, these will be noted. Also, if material had to be removed, a note will indicate the deletion.



ProQuest 10984236

Published by ProQuest LLC (2018). Copyright of the Dissertation is held by the Author.

All rights reserved.

This work is protected against unauthorized copying under Title 17, United States Code
Microform Edition © ProQuest LLC.

ProQuest LLC.
789 East Eisenhower Parkway
P.O. Box 1346
Ann Arbor, MI 48106 – 1346

C O N T E N T S

	Page
CONTENTS	(i)
PREFACE	(vii)
SUMMARY	(viii)
ABBREVIATIONS	(x)

CHAPTER 1 INTRODUCTION

1.1 Biopolymers	1
1.2 History of Poly(-(D)- β -Hydroxybutyric Acid)	2
1.3 General Considerations on Biopolymers	5
1.4 Degradation of Polymers	7
1.5 Classification of Degradation Reactions	7
(1) Main Chain Scission	8
(2) Side Chain or Substituent Reactions	12
1.6 General Consideration of Polymer Degradation	14
1.7 Aim of this Work	15

CHAPTER 2 EXPERIMENTAL TECHNIQUES

2.1 Sources of Reagents	17
2.2 Isolation of PHB from Cell Cultures and its Purification	17
2.3 Fractionation of PHB	18
2.4 Thermal Methods of Analysis	20
(i) Thermal Gravimetric Analysis (TG)	20
(ii) Differential Thermal Analysis (DTA)	21
(iii) Differential Scanning Calorimetry (DSC)	21
(iv) Thermal Volatilisation Analysis (TVA)	22
(v) Subambient Thermal Volatilisation Analysis (SATVA)	27
(vi) Melt Flow Index (MFI)	29

<u>CHAPTER 2</u>	Page
2.5 Analytical Techniques	31
(i) Infra-Red Spectroscopy (IR)	31
(ii) Quantitative Estimation of Volatile Products by IR Spectroscopy	32
(iii) Ultra-Violet Spectroscopy (UV)	35
(iv) Nuclear Magnetic Resonance Spectroscopy (NMR)	35
(v) Mass Spectrometry (MS)	35
(vi) Thin Layer Chromatography (TLC)	35
(vii) Gas Liquid Chromatography (GLC)	35
(viii) Trace Impurity Analysis	39
2.6 Molecular Weight Determination	39
(i) Gel Permeation Chromatography (GPC)	39
(ii) Viscometry The Mark Houwink-Sakurada Equation	47
2.7 X-Ray Crystallography	54
2.8 Treatment of Errors	54
2.9 Degradation Techniques Under Glass	55
(i) Vacuum	55
(ii) Under an Atmosphere of Nitrogen	57
(iii) Under an Atmosphere of Static Air	59
(iv) Closed system	59
2.10 Preparation of a Single Crystal Mat	59
2.11 Classification of PHB Samples Studied in This Work	60

	Page
<u>CHAPTER 3</u> <u>THE PRODUCTS OF THERMAL DEGRADATION OF PHB</u> <u>UNDER VACUUM</u>	
3.1 Introduction	62
3.2 Thermogravimetric Analysis	62
3.3 Differential Thermal Analysis	65
3.4 Differential Scanning Calorimetry	65
3.5 Thermal Volatilisation Analysis	65
3.6 Thermal Volatilisation Analysis with Differential Condensation of Products	68
3.7 Subambient TVA of the Volatile Degradation Products (ambient to 500°C)	71
3.8 The Cold Ring Fraction (ambient to 500°C)	89
3.9 Residue (ambient to 500°C)	103
3.10 An Investigation of the Products Formed upon a Programmed Degradation of PHB Under Vacuum from:-	103
(i) Ambient to 338°C	103
(ii) The resultant Residue of (i) from ambient to 500°C	105
(iii) Ambient to 500°C in a Horizontal Degradation Tube	108
3.11 Closed System Degradation of Crotonic Acid	109
3.12 Closed System Degradation of PHB	109
3.13 Products Formed on Heating PHB at 200°C for Six Hours	109
3.14 Conclusions	112

<u>CHAPTER 4</u>	<u>THE PRODUCTS OF THE THERMAL DEGRADATION OF PHB UNDER A NITROGEN ATMOSPHERE</u>	Page
4.1	Introduction	121
4.2	Differential Thermal Analysis and Differential Scanning Calorimetry Under Nitrogen	121
4.3	The Thermal Degradation of PHB Under a Nitrogen Atmosphere	121
4.4	Subambient TVA of the Products Isolated in the Cold Trap	122
4.5	The Cold Ring Fraction Obtained by Degrading PHB Under a Nitrogen Atmosphere	122
4.6	The Residue Formed upon Heating PHB to 500°C under Nitrogen	123
4.7	Conclusions	133
<u>CHAPTER 5</u>	<u>QUANTITATIVE ANALYSIS OF THE PRODUCTS OF THERMAL DEGRADATION OF PHB UNDER VACUUM AND NITROGEN</u>	
5.1	Introduction	135
5.2	Conditions of Measurement and Calibration Curves for Degradation Products	135
5.3	Quantitative Analysis of the Products formed in the Thermal Degradation of PHB under Vacuum	140
5.4	Quantitative Analysis of the Products formed from the Thermal Degradation of PHB under Nitrogen	148
5.5	General Conclusions	153

<u>CHAPTER 6</u>	<u>MOLECULAR WEIGHT IN PHB ON ISOTHERMAL HEATING</u>	Page
6.1	Introduction	156
6.2	Weight Loss on Isothermal Heating of PHB	156
6.3	Molecular Weight Changes under Vacuum	156
6.4	Molecular Weight Changes under Nitrogen	178
6.5	Molecular Weight Changes under Static Air	189
6.6	Effect of a Cyclic Heating Programme on Molecular Weight	203
6.7	Correlation between Melt Flow Index and Molecular Weight	209
6.8	General Conclusions	211
<u>CHAPTER 7</u>	<u>CRYSTALLINITY IN PHB AND ITS EFFECT ON THERMAL DEGRADATION</u>	
7.1	Introduction	220
7.2	Preparation of Polymer Samples	221
7.3	Measurement of Crystallinity	221
7.4	X-Ray Powder Photograph of PHB, Sample SX	224
7.5	Differential Scanning Calorimetry	224
7.6	Thermogravimetric Analysis	231
7.7	TVA with Differential Condensation of Products	233
7.8	Effect of Crystallinity on the Rate of Chain Scission	233
7.9	Discussion and Conclusions	242

<u>CHAPTER 8</u>	<u>EFFECT OF INITIAL MOLECULAR WEIGHT ON STABILITY</u>	Page
8.1	Introduction	247
8.2	DSC	247
8.3	TG Analysis	249
8.4	TVA	254
8.5	Quantitative Analysis of Products	254
8.6	Rate of Depolymerisation	259
8.7	Conclusions	267
<u>CHAPTER 9</u>	<u>GENERAL CONCLUSIONS AND DISCUSSION</u>	
9.1	General Conclusions	269
9.2	General Discussion	271
9.3	Suggestions for Future Work	273
REFERENCES		275

P R E F A C E

The work described in this thesis was carried out by the author between October, 1977 and September, 1980 at the University of Glasgow, in the Physical Chemistry Department which is under the general supervision of Professor G. A. Sim, and at the Research Laboratories of Imperial Chemical Industries Limited situated at Runcorn and Billingham.

I am indebted to the Science Research Council and Imperial Chemical Industries Limited for the award of a grant during the tenure of which this work was carried out.

I should like to thank my supervisors, Professor N. Grassie, University of Glasgow, and Dr. P. A. Holmes, I.C.I. Ltd., for their interest, advice and continual encouragement throughout the course of this work.

My thanks are also due to my colleagues in the Macromolecular Chemistry Group for invaluable assistance and helpful discussions, and to various members of the Departmental Technical Staff, in particular Mr. G. McCulloch and Mr. J. Gorman.

Finally, I thank my wife, Janice, for her patience, understanding and support during the period of this work, and my mother for the typing of this thesis.

Eric S. Murray

Eric James Murray

SUMMARY

The exponential increase in the price of crude oil combined with the recent upsurge of public concern over pollution and ecology has led to an increasing commercial interest in polymers that are either dependant on a non-oil based feedstock or are biodegradable. Poly(-(D)- β hydroxybutyric acid) (PHB) is such a polymer, which combines both these properties.

Among biopolymers, PHB is exceptional in possibly being suitable for commercial exploitation as a processable thermoplastic polymer. This field, to date, has been dominated almost exclusively by synthetic polymers. The work described in this thesis was undertaken to increase our understanding of the products, kinetics and mechanisms involved in the thermal degradation of PHB, isolated from a culture of the bacterium *Azotobacter beijerinckii*, with a view to providing information relevant to the assessment of PHB as a viable commercial polymer.

Reviews of PHB and the most probable reactions involved in the thermal degradation of polymers are presented in Chapter 1.

A list of the chemicals used in this study are given in Chapter 2, along with the isolation, purification and fractionation conditions employed for PHB. Details of the experimental techniques and apparatus used for degrading the polymer, and of the analytical techniques employed in this investigation are also included in this Chapter. Values for the constants in the Mark Houwink-Sakurada Equation for PHB in CHCl_3 at 30°C are reported.

The results from the various methods of thermal analysis when applied to PHB are recorded in Chapter 3 and the products of thermal degradation under vacuum are identified and possible

mechanisms for their formation proposed and discussed. A similar study of PHB under an atmosphere of dynamic nitrogen is described in Chapter 4.

Chapter 5 presents a quantitative study of the various degradation fractions obtained from PHB under vacuum and under a nitrogen atmosphere. Oligomers of PHB are shown to account for greater than 90% of the weight of the initial polymer under both conditions, and the changes in product composition as the temperature rises is investigated.

Evidence for a random chain scission reaction with short zip length occurring in the temperature range $170^{\circ}\text{C} - 200^{\circ}\text{C}$ is presented in Chapter 6. An ester-pyrolysis mechanism has been proposed for this reaction and its rate calculated at various temperatures ($170^{\circ}\text{C}-200^{\circ}\text{C}$) under vacuum, nitrogen and air from which a value of energy of activation has been calculated. The presence of a competing esterification reaction, of limited duration, associated with the condensation of hydroxyl and carboxyl end groups on PHB was also observed in this temperature region. A relationship between MFI and \bar{M}_w was shown to exist at 190°C .

The effect of crystallinity on stability is reported in Chapter 7 and in Chapter 8 the effect of initial degree of polymerisation is investigated.

The main results from Chapter 3 to 8 are summarised in Chapter 9 which also includes suggestions for future work.

ABBREVIATIONS

- β BL - β -butyrolactone
- 4 Methyl-2-oxetanone
- Cis crotonic acid - cis but-2-enoic acid
- Crotonic acid - trans but-2-enoic acid
- PHB - Poly(-(D)- β -hydroxybutyric acid)
- Poly(oxo-(1-methyl-3-oxo)trimethylene)

CHAPTER 1

INTRODUCTION

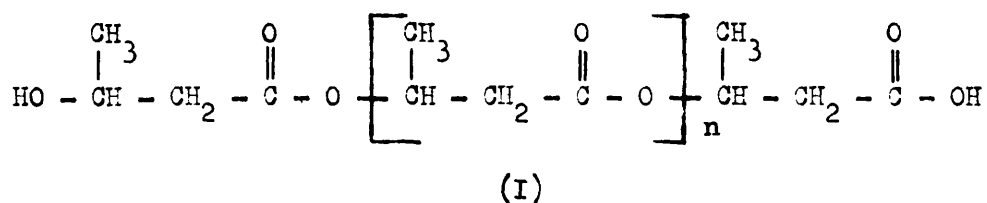
1.1 BIOPOLYMERS

High polymers are abundant in living cells, the main classes being polypeptides, proteins, nucleic acids and polysaccharides. Non food applications for a large variety of these polymers are evident in everyday life, for example as textile fibres (wool), and construction materials (wood, paper). Synthetic polymers, however, have enjoyed a virtual monopoly in application as far as thermoplastic technology is concerned. This is due principally to the fact that the biological polymers are unsuitable for processing. A possible exception to this is Poly(-(D)- β -hydroxybutyric acid), a highly crystalline polyester.

As the price of crude oil, the basis of the synthetic polymer industry, continues to rise steadily, and with the possibility of oil shortages in the next century, the search for new sources of chemical feedstocks and new polymers dependant on non oil-based sources has increased in recent years. Of note, in this field, is the renewed interest in the manufacture of chemicals from coal (Ref. 1). Increasing public concern about pollution and the treatment of waste materials has stimulated the study of the biodegradation of synthetic polymers. As a group, aliphatic polyesters are known to be generally susceptible to biological attack (Ref. 2-4). Thus any new commercially viable polymer should ideally be non dependant on oil related chemicals as a feedstock and biodegradable. Such a polymer is poly(-(D)- β -hydroxybutyric acid) a naturally occurring biodegradable polyester. (Ref. 5)

1.2 HISTORY OF POLY(-(D)- β -HYDROXYBUTYRIC ACID)

Poly(-(D)- β -hydroxybutyric acid)*, (I), hereafter referred to as PHB, is a naturally occurring polyester, synthesised by various types of bacteria by the condensation of D-(-)- β -hydroxybutyryl coenzyme A. It was first cited in the literature in 1927, by the French scientist M. Lemoigne (Ref.5).



It is hardly surprising that the bulk of investigations into the properties of PHB have been of a biological nature. The function, formation and bacterial synthesis of PHB has been extensively studied, mainly by Doudoroff and Stanier (Ref.7) Gibbons (Ref. 8), Schlegel (Ref. 9), Wilkinson (Ref.10), and their collaborators. PHB is found in the intracellular granules of bacterium, which were demonstrated to consist of 90% PHB and 10% lipid in *Bacillus cereus* and *B. megaterium* (Ref.10). The polyester has been reported to constitute as much as 80% of the dry weight of bacterium (Ref.11), and functions as a food reserve and carbon source for the bacterium, being accumulated when food is abundant and cell division prevented, and consumed when a food supply is absent (Ref. 12). A further study of PHB biosynthesis, metabolism and regulation has been undertaken in recent years by

* Systematic name, according to IUPAC Information Bulletin No.29 November 1972: poly[oxy-(1-methyl-3-oxo) trimethylene].

Senior and Dawes and their co-workers (Ref. 13-17). This work showed that only oxygen limitation of bacterial growth initiated accumulation of PHB and culminated in the proposal of a biochemical pathway for the regulation of PHB metabolism (Figure 1.1).

Surprisingly little has been published on the chemical and physical properties of PHB. Only the crystallographic and morphological properties have been studied in any depth (Ref.18-21). The crystal structure of PHB involves a left handed (2/1) helix consisting of an orthorombic unit cell with dimensions $a = 5.76 \text{ \AA}$, $b = 13.20 \text{ \AA}$ and c (the fibre period) = 5.96 \AA . Recently, the molecular weight distribution of native D-PHB has been studied (Ref. 22). Only the following observations, on the thermal degradation of PHB, have been reported. (Ref. 23, 24)

- (a) The polyester degrades relatively rapidly at temperatures a few degrees above the melting point.
- (b) A rapid drop in the intrinsic viscosity is observed in the polymer at these temperatures.
- (c) The reaction can be followed by the increase in the presence of crotonate ester in the degrading polymer.
- (d) The final product of complete degradation is crotonic acid.

Poly(-(D)- β -hydroxybutyric acid) is one of the few biopolymers which can be synthesised also in vitro. The first reports of the synthesis of DL-PHB from DL- β -butyrolactone using organometallic catalysts showed that polymers are produced with properties much different from those of bacterial PHB (Ref. 25, 26). Great improvements in this process were achieved by D. E. Agostini et al (Ref. 27, 28) who used a

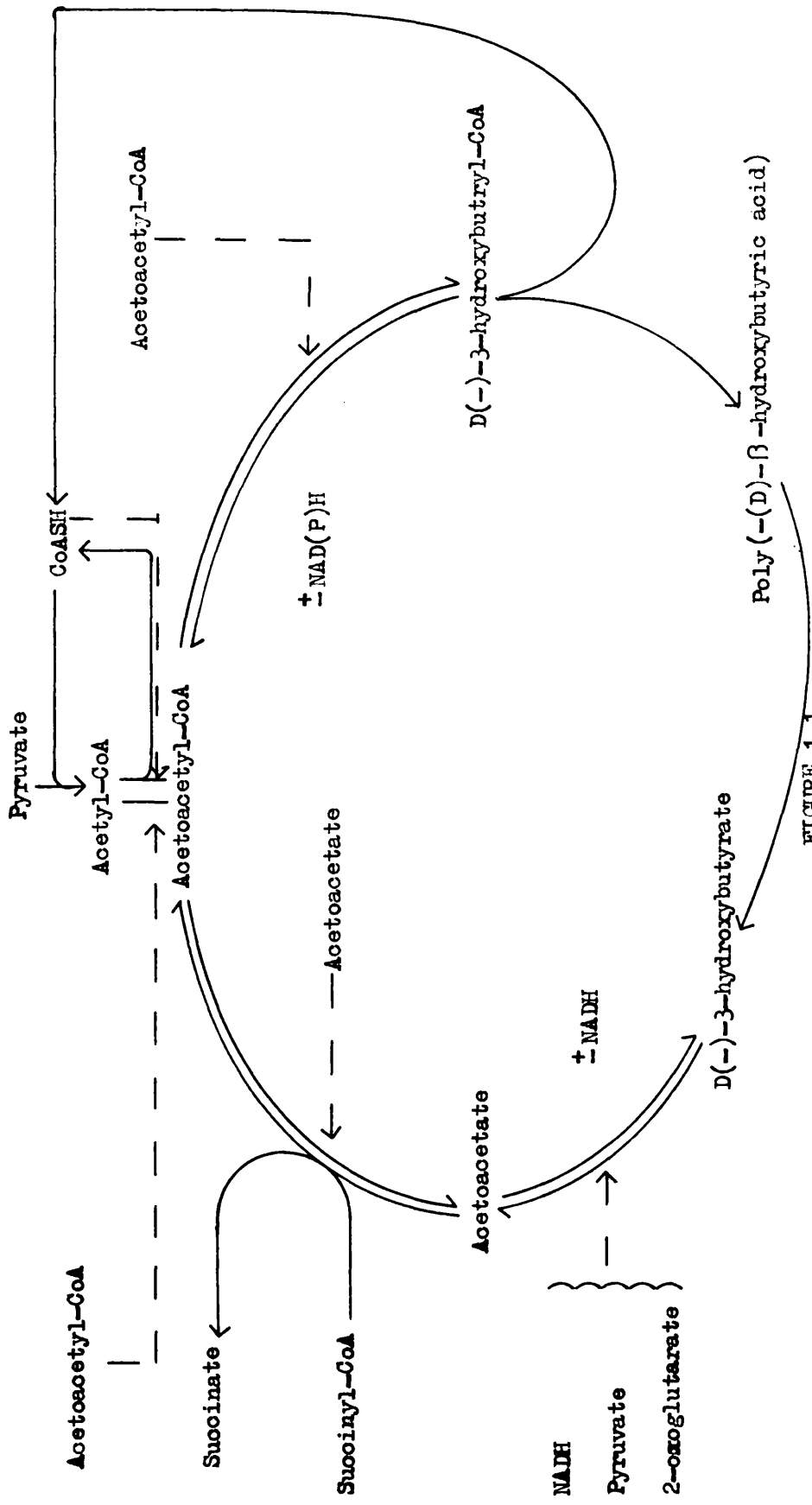


FIGURE 1.1

REGULATION OF PHB METABOLISM IN A. BEIJERINCHII

(Inhibition is indicated by broken lines) [Senior and Dawes Ref.17]

triethylaluminium catalyst with water as co-catalyst. They eventually synthesised D-PHB from D(+)- β -butyrolactone. The chemical and physical properties of the synthetic polymer were found to be essentially the same as those of the bacterial produced polymer, except that the molecular weight of the synthetic polymer was much lower than that of its biological equivalent. Vergara and Figini (Ref. 29), have recently achieved a notable increase in the molecular weight of the polymer by undertaking the procedures of preparation and purification of initiator, purification of the monomer and the polymerisation under conditions of extreme exclusion of moisture and oxygen in a jointless all glass apparatus. This process, however, could still only produce a polymer with weight average molecular weight 1/6th that of the biologically produced polymer studied during the course of this work. In the same year a comprehensive study of the effect of substituents on the stereospecific polymerisation of β -Alkyl- β -propiolactones (Ref. 30) led to the development of a polymeric catalyst capable of producing PHB with $\bar{M}_v = 400,000$, still only 1/3rd that of the PHB used in this present study.

1.3 GENERAL CONSIDERATIONS ON BIOPOLYMERS

When dealing with a "biologically" produced polymer from a living source the limitation of contaminants to which the polymer is exposed during formation cannot be as easily controlled as in a laboratory prepared synthetic polymer. PHB prepared by bacteria must, of necessity, be exposed to many biological substances such as enzymes, coenzymes, polylipids and inorganic material in the nutrient medium which sustains the bacterium. The separation of these substances from the final polymer is often a difficult and

expensive process. The purification of PHB is further complicated by its extraordinary chelating properties. "Biological" PHB has been shown to contain many inorganic contaminants (greater than 26 (Ref. 31)) derived from the added nutrient and concentrated from the aqueous media. In fact PHB has been shown to enrich, from the nutrient medium and Thames water supply in which the bacterium are suspended, Zn, Cd, Hg by a factor of >1800, Cu by 80 and Mn by >25 (Ref. 31). Thus it is a formidable task to prepare samples of PHB of high purity. An extensive study has been carried out (Ref. 32) to attempt to relate melt stability to impurity concentration within the polymer. However, due to the vast number of variables, this has proved a fruitless task. PHB will also differ from "synthetic" PHB in that, despite the theoretical biochemical pathway leading only to ester linkages, other groups such as -CHO, -SH, -CH=N-, -NH₂ could also be present (Ref. 31). The difficulty of identifying and measuring the concentration of a few such groups in a polymer of molecular weight $\sim 5 \times 10^5$ is formidable.

Measurements of a few of these contaminants have been recorded (Chapter 2.11) for every polymer used in the course of this study. The majority of the work described in this thesis was performed on a single sample of PHB, thus enabling comparison between experimental results without detailed consideration of impurity effects. Only in work, where this was impossible, such as a comparison of the effect of initial degree of polymerisation on stability (Chapter 8), have the results from more than one polymer sample been compared.

Therefore, throughout this work it should be noted that it is a polymer sample from a living source that is being investigated

and not a "sterile" synthetic polymer.

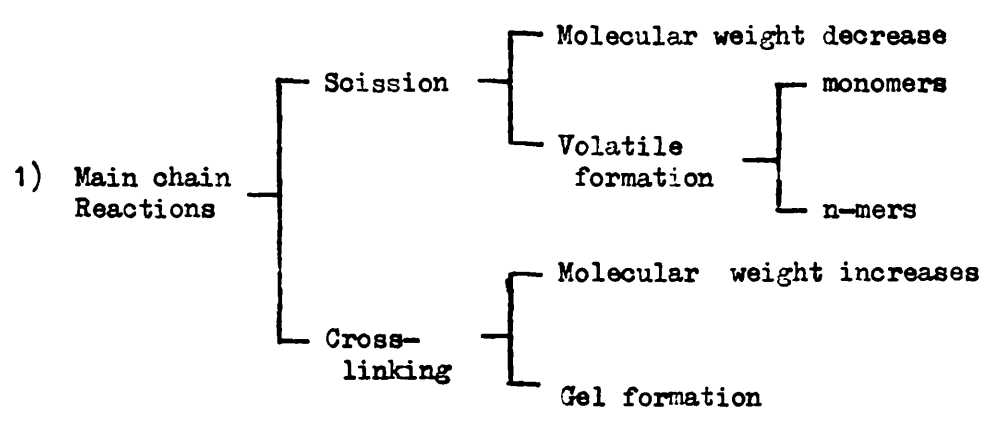
1.4 DEGRADATION OF POLYMERS

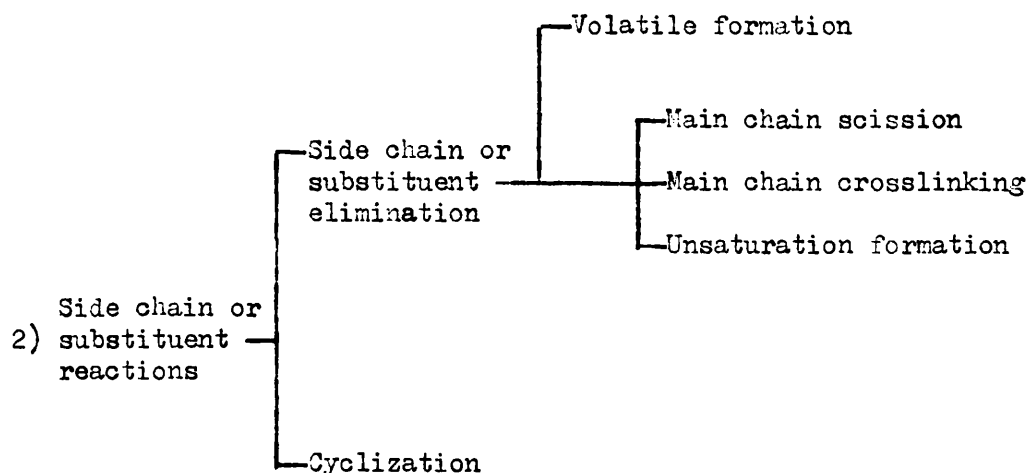
A polymer may "degrade" when exposed to external agencies which include the physical action of heat, light and mechanical stress or chemical influences such as oxidation and hydrolysis. Polymers are normally subjected to degradative agencies, which may act separately or together depending on the environment surrounding the polymer, during fabrication and the subsequent useful life of the fabricated article. Most research however has involved the study of one of these variables under closely controlled conditions.

Studies on the thermal degradation of polymers are of extreme importance from a practical point of view. They cannot only explain the behaviour of polymers at elevated temperatures, but possibly more important may help in selecting the correct polymer for a particular application or suggest the design and synthesis of new materials to meet new or existing requirements.

1.5 CLASSIFICATION OF DEGRADATION REACTIONS

The commonest types of thermal degradation reactions may be summarised as follows:-





Thus the reactions involved in polymer degradation can be split into two main categories:

- (1) Main chain reactions, and,
- (2) Side chain or substituent reactions.

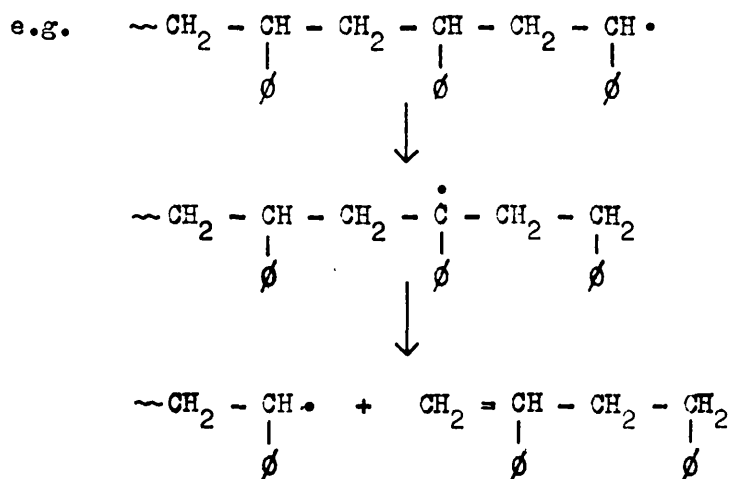
(1) Main Chain Reactions

Main Chain Scission leads to depolymerisation such that monomer units are always distinguishable in the products. Such reactions are characterised by a decrease in molecular weight and/or the formation of volatile products, the relationship between the two giving an insight into the site of chain scission, whether at random along the chain or at labile chain ends.

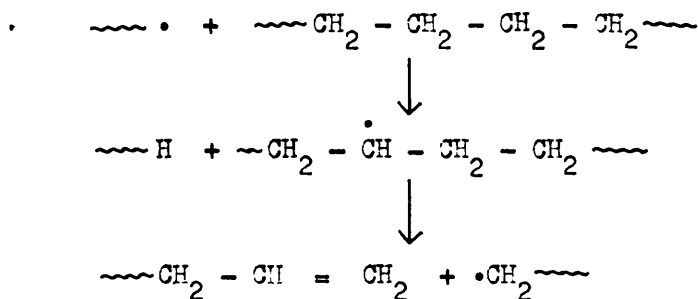
The classic example of a polymer which undergoes a chain scission reaction is poly(methylmethacrylate) PMMA. Monomer is the exclusive product of degradation in the 150°C to 500°C temperature range and at temperatures below 270°C, the reaction is initiated at the double bonds situated at chain ends and formed by radical disproportionation during polymerisation. Above 270°C end initiation and random initiation occur simultaneously. The initiation process in

this reaction involves scission of the molecule to produce radicals which then depropagate or unzip to produce monomer (Ref. 33-35).

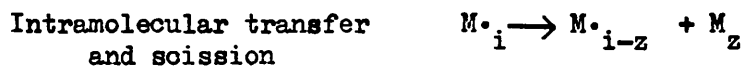
This example of main chain scission is unique in its simplicity. Polystyrene, for example, yields 42% monomer, at 300°C the remainder being dimer, trimer, tetramer and pentamer (Ref. 36) while polyethylene yields an apparently continuous spectrum of hydrocarbon from 1 to 70 carbon atoms (Ref. 37, 38). The former has been explained by intramolecular transfer reactions which are in direct competition with the monomer producing depropagation process, (Ref. 39)



The continuous spectrum of hydrocarbons formed from polyethylene is accompanied by a rapid decrease in molecular weight. Little monomer is formed however, thus depropagation cannot be significant. It has been demonstrated that the large proportion of mono-olefins are formed by an intramolecular transfer process of the type illustrated above for polystyrene while the larger fragments are formed in intermolecular transfer reactions as follows: (Ref. 40)



The following general reaction scheme, proposed by Simha, Wall and Blatz (Ref. 41-43) includes all these kinds of free radical depolymerisation processes, the ratio of monomer to larger chain fragments being governed by the relative rates of depropagation and transfer, with intramolecular transfer being regarded as a special case of depropagation in which a stable volatile fragment larger than monomer is produced.



n is the chain length of the starting material and M_i , M_j , etc., and $M\cdot_i$ and $M\cdot_j$ etc. represent respectively 'dead' polymer molecules and long chain radicals, i , j , etc. monomer units in length.

All depolymerisation reactions, however, do not involve free radical mechanisms, especially if the polymer backbone contains heteroatoms such as oxygen and nitrogen. In this case reactions cannot be unified by a single reaction scheme since they depend entirely on the chemical nature of the functional groups. For example, the decomposition of poly(oxyethylene) was shown to take place exclusively from hydroxyl chain ends since it is inhibited by acetylation. (Ref. 44). Molecular, free radical and ionic mechanisms were considered for this process by Grassie and Roche (Ref. 44). The absence of any secondary volatile products, which would result from an end initiated radical reaction, are strong arguments against a free radical mechanism. Nylon 6,6 and nylon 6,10 also degrade by a non-free radical mechanism, via a complex mechanism which has recently been re-examined by Wiloth (Ref. 45). Similarly, the initial scission process in the degradation of poly(ethylene terephthalate), which occurs at random, involves ester decomposition. This and subsequent reactions have been elucidated in great detail through studies of model compounds. (Ref. 46, 47)

Main Chain Crosslinking leads to an increase in molecular weight and in extreme cases to gel formation. Poly(methylacrylate) forms gels in some cases (Ref. 48,50) which can be explained by a free radical mechanism (Ref. 51) in which recombination of two radicals of the type, $\sim\dot{C} - CH_2$ occurs.

$$\begin{array}{c} \cdot \\ | \\ \sim C - CH_2 \\ | \\ COOCH_3 \end{array}$$

On the other hand, investigations of the thermal degradation of polysiloxanes with terminal hydroxyl groups (Ref. 52) indicate that, at low conversion to volatile products, increase in the molecular weight of the polymer occurs in the range 170°C to 300°C. This was assigned to a polycondensation involving the terminal hydroxyl groups. Subsequent increase in temperature decomposes the polymer and decreases its molecular weight.

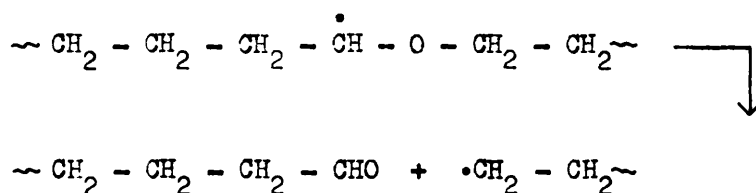
(2) Side Chain or Substituent Reactions

Side Chain or Substituent Elimination leads to the formation of volatile products accompanied by main chain scission, crosslinking or unsaturation. A common reaction of this kind is that of substituent elimination accompanied by unsaturation, the classic example of which is the thermal decomposition of poly(vinylchloride) PVC. A form of unzipping of HCl molecules is thought to occur with the unsaturation resulting from decomposition of one vinylchloride unit activating the decomposition of an adjacent unit since colour develops very early in the decomposition. (Ref. 53)

The reaction is also thought to be initiated at labile structural abnormalities formed during polymerisation or fabrication. (Ref. 54) Although some controversy still exists as to the nature of the mechanism, it would appear that the bulk of the evidence now points towards a radical mechanism first proposed by Stromberg et al in 1959 (Ref. 55).

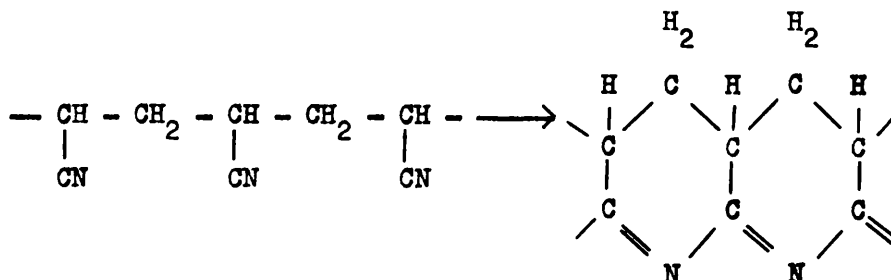
Other reactions of this type are elimination of acetic acid from poly(vinylacetate) which is thought to proceed via a non-radical chain mechanism (Ref. 56, 57) and elimination of H₂O from poly(vinylalcohol). (Ref.58).

Examples of substituent elimination leading to the formation of volatile products and main chain scission can be found in the thermal degradation of certain polyethers such as poly(tetramethyleneoxide) (Ref. 59). Initiation was shown to occur at the carbon in the α position to the oxygen atom. Rupture of the C-H bond is followed by breaking of the main chain according to



The terminal macroradical thus formed initiates the decomposition kinetic chain, which is the main source of the volatile products of degradation.

Side Chain Reactions Leading to Cyclisation are frequently observed in polymer degradation, a typical example of which is the heat-resistant cyclized structure formed in heated poly(acrylonitrile), PAN,



which has been extensively studied (Ref. 60-62).

Several other examples of this type of reaction are to be found in the literature, two of which are, the formation of cyclic anhydrides from poly(methacrylic acid), (Ref. 63)

and cyclic α - β unsaturated ketones from poly(methylvinylketone). (Ref.64).

1.6 GENERAL CONSIDERATION OF POLYMER DEGRADATION

In order to have a full understanding of the mechanism of the thermal degradation of organic polymers, it is necessary to have information about three things in particular:

- (a) The change in molecular weight of the polymer as a function of temperature and extent of degradation.
- (b) The qualitative and quantitative composition of the volatile and non-volatile products of degradation.
- (c) The rates and activation energies of the degradation processes.

Each of these can be ascertained by thermal analysis and analytical chemical methods and a detailed reaction mechanism formulated.

There are numerous reviews of this field to be found in the literature. (Ref. 65-67).

The use of model compounds to predict the mechanism and kinetics of polymeric materials must only be undertaken with due caution. While it is true that many polymeric esters predominantly decompose to form acid and olefin, e.g. polyacrylates and poly(vinylacetate), in a similar manner to simple esters like ethyl acetate, poly(ethylmethacrylate) gives high yields of monomer at 250°C, while model primary ethyl esters decompose to ethylene and the corresponding acid at about 450°C. Similarly PVC thermally decomposes to form products similar to those obtained from simple chloroparaffins but at a temperature some 200°C lower than the corresponding model. Behaviour of this type is quite common in

polymers and mechanistic studies have shown two principle reasons for its occurrence. Firstly, polymer chains, although normally represented by linear sequences of monomer units, contain abnormalities such as branches and unsaturation. This, along with the chain ends, may constitute weak points in the polymer molecules at which degradation may be initiated. Secondly, many reactions encountered in polymer degradation have been shown to consist of chain processes running along the polymer backbone which have no analogues in simple model compounds.

The thermal stability and degradation mechanisms of co-polymers and polymer blends has been extensively studied in these laboratories, and these topics have been the subject of two recent reviews (Ref. 68, 70). The presence of a comonomer can deeply affect the thermal behaviour of polymers. A comonomer can in some cases confer stability but in others may render a homopolymer unstable. An example of the former is the co-polymer of methylmethacrylate and acrylonitrile. This stabilisation was first reported by Grassie and Melville (Ref. 33) and later re-examined by Grassie and Farish (Ref. 69). At 220°C the degradation is initiated at unsaturated chain ends but radical depolymerisation cannot pass through acrylonitrile units. Degradation is thus stopped at the first acrylonitrile unit. Random chain scission occurs at a slow rate at 220°C producing unsaturated chain ends, which increase in concentration and since they are unstable at 220°C the rate of volatilisation increases. The stabilisation effect is lost at 280°C because acrylonitrile units are liberated in the depropagation process at this temperature.

Poly(acrylonitrile) is destabilised if methylvinylketone units are incorporated into the molecules. The accelerating effect of

methylvinylketone units on the rate of thermal colouration of the polymer has been ascribed to their behaviour as initiators (Ref.64). Similar stabilising and destabilising effects have been reported for polymer blends. (Ref. 70).

1.7 AIM OF THIS WORK

The work described in this thesis will be concerned with the thermal degradation properties of biologically produced PHB. A study of the rates and activation energy of the depolymerisation reaction occurring in PHB under various atmospheres at temperatures in the region suitable for processing will be described. This shall be combined with a qualitative and quantitative study of the products of degradation in order to gain not only an understanding of the mechanism of degradation of PHB but also information relevant to the possible commercial exploitation of PHB as a thermoplastic. This work forms an integral part of an examination, by a multi-disciplined team of scientists into the problems associated with the production, processability and future commercial uses of bacterially produced PHB as a thermoplastic polymer which is not dependant on oil related feedstocks and has a biodegradable character.

Samples of PHB were obtained from a culture of the bacterium *Azotobacter beijerinckii* and were supplied by Imperial Chemical Industries Ltd., Corporate Division, Runcorn, in the form of either dead bacterium or partially purified polymer.

CHAPTER 2

EXPERIMENTAL TECHNIQUES

2.1 SOURCES OF REAGENTS

Propan-1-2-diol, crotonic acid and ethyl crotonate were obtained from B.D.H. Chemicals Ltd. All other reagents and solvents used in this study were of Analar grade.

2.2 ISOLATION OF PHB FROM CELL CULTURES AND ITS PURIFICATION

Once fully cultured the bacterium was killed by addition of mercuric chloride. The dead bacterial cells were then dyemilled to commence the procedure of rupturing the cell walls before being spray dried. Dyemilling consists of passing the cells through a column, under pressure, which contains many rotating discs each with only a small slit. The slits are not lined up so that the cells are pounded against the walls of the column and the discs. PHB as supplied by I.C.I. Corporate Division was in the form of spray dried cells, light brown in colour.

A 1% w/v solution of these spray dried cells in chloroform was refluxed for $1\frac{1}{2}$ hours to extract the polyester. The resultant solution was filtered through a filter cloth and then Whatman's glass-fibre GF/A filter paper to remove the cell debris prior to precipitation in petroleum-ether. The polymer was isolated by filtration and washed with diethyl-ether prior to drying under vacuum at room temperature. The polyester was repeatedly dissolved in chloroform, precipitated into petroleum-ether, filtered and washed with diethyl-ether until snow-white in appearance. By this method a fibrous form of PHB was obtained.

A powder sample of PHB was obtained by slow addition of a 1% w/v solution to five volumes of methanol with vigorous stirring. The PHB was separated by filtration and vacuum dried at room temperature for 24 hours. The resultant polymer cake was ground in a mortar and pestle at liquid nitrogen temperatures to give a fine powder. This powder was vacuum dried at room temperature for 48 hours and stored for use.

NOTE: The precipitation of PHB from solution in chloroform of higher concentration than 1% w/v by methanol resulted in the formation of a fibrous form of PHB.

2.3 FRACTIONATION OF PHB

Polymer fractionation was carried out on the basis of the decreasing solubility of a polydisperse sample with increasing molecular weight. For general theory on this method see Ref. 71.

The experimental set up was as shown in Figure 2.1.

A 6g sample of PHB, S1 (see Chapter 2.11) was dissolved in 800 cm³ of chloroform and poured into the central cylinder of the fractionating column. This was left overnight, the water jacket being maintained at 303K.

The following morning 440 cm³ of propan-1-2-diol, the precipitating agent, was added dropwise via the dropping funnel with continuous stirring. A cloudy precipitate formed which disappeared on raising the temperature of the water jacket to 308K. While continuing the stirring the temperature of the water jacket and polymer solution was allowed to cool to 303K whereupon stirring was stopped and the temperature held at 303K overnight. On the following morning the solution consisted of two phases - (a) a lower gel phase and (b) a clear solution. The gel was removed via the

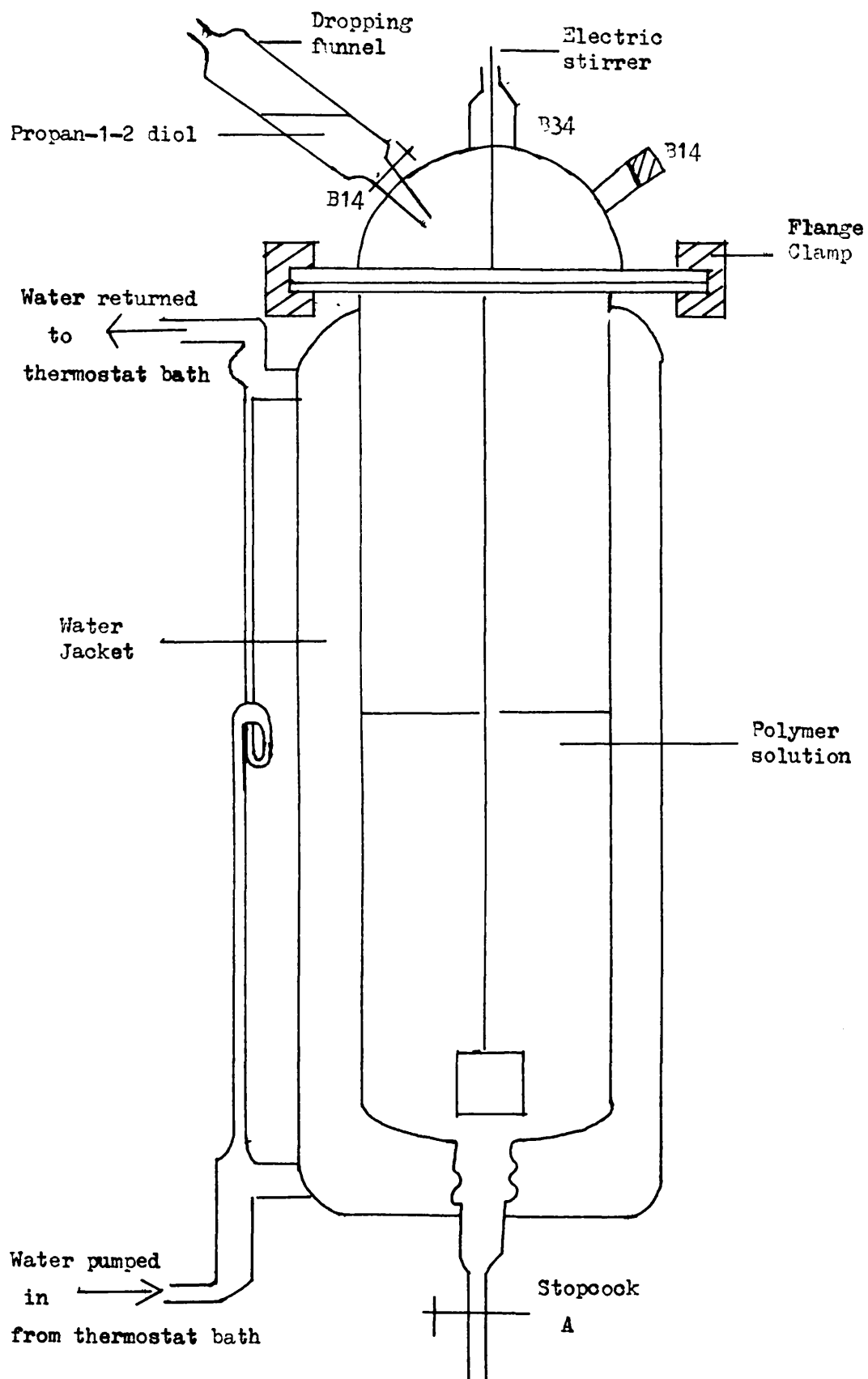


FIGURE 2.1

FRACTIONATION APPARATUS

stopcock A, dissolved in approximately 200 cm³ of chloroform by refluxing for $\frac{1}{2}$ an hour, and precipitated into an excess of methanol. The PHB precipitate was recovered by filtration, vacuum dried at room temperature and labelled Fraction 1 (F1) - High Molecular Weight Fraction. ($\sim 1.4g$).

A further 10 cm³ of propan-1-2-diol was added and the above procedure followed to obtain Fraction 2 (F2) - Medium High Molecular Weight. ($\sim 1.7g$)

Fraction 3 (F3) - Medium Low Molecular Weight was obtained by the above procedure on addition of a further 20 cm³ of propan-1-2-diol. ($\sim 1.4g$).

The remaining solution in the fractionating column was added to excess (5,000 cm³) methanol. The precipitate formed was recovered by filtration and vacuum dried at room temperature. This was labelled Fraction 4 (F4) - Low Molecular Weight Fraction. ($\sim 1.5g$).

The whole procedure was repeated eight times. The eight Fraction 1 samples were dissolved together in chloroform and precipitated in methanol, filtered and vacuum dried. Fractions F2, F3 and F4 were treated similarly giving over 10g of each fraction.

The molecular weight distribution of the PHB fractions were determined by gel permeation chromatography (See Chapter 2.6(i)).

2.4 THERMAL METHODS OF ANALYSIS

(i) Thermal Gravimetric Analysis TG

Thermal gravimetric analyses were carried out on two instruments, (a) a Du Pont 950 thermobalance and (b) a Du Pont 951 thermobalance.

The polymer samples (5-10mg) were placed on a boat-shaped platinum holder and the temperature measuring thermocouple placed 0.1 cm from the powdered sample.

In a programmed heating run a flow of nitrogen gas (a) 80 cm³/min., (b) 40 cm³/min. was maintained throughout the degradation. The samples were heated from ambient to 500°C at a rate of 10°C/min.

For experiments in air the procedure was identical, except that the samples were maintained in an atmosphere of static air.

In an isothermal experiment the sample was heated rapidly to 200°C, the recording pan set to 100% and after 5 minutes the pan was lowered and the temperature held at 200°C for 3 hours. All isothermal TG's were run on instrument (b) at a temperature of 200°C under an atmosphere of nitrogen with a flow rate of 50 cm³/min.

(ii) Differential Thermal Analysis DTA

A Du Pont 900 Thermoanalyser instrument was used to obtain DTA curves. Two identical tubes, 25mm long by 4mm diameter, were placed in a heating block. The reference tube was packed with small glass beads and the sample tube with approximately 10mg of powdered polymer, each tube also contained a thermocouple. The tubes were heated from ambient to 500°C at a rate of 10°C/min. under an atmosphere of nitrogen with a flow rate of 80 cm³/min.

(iii) Differential Scanning Calorimetry DSC

DSC was carried out on a Du Pont 910 Thermoanalyser. Powdered samples (3mg to 5mg) were placed in aluminium pans and an aluminium pan lid crimped on top. The sample pan and an empty reference pan were placed on the heating block.

An inert atmosphere was maintained by passing nitrogen gas over the sample at a rate of $50 \text{ cm}^3/\text{min}$. while heating the sample block from ambient to 500°C , at a rate of $10^\circ\text{C}/\text{min}$.

(iv) Thermal Volatilisation Analysis TVA

TVA has been used to study the degradation properties of many polymers and is now a well-established thermal analysis technique, being well documented by a series of publications by McNeill (Ref. 72, 73). It may be informative however to discuss briefly some general aspects and practical details involved in this work.

The basic TVA method involves heating a polymer sample at a linear rate of temperature increase, usually $10^\circ\text{C}/\text{min}$, in a flat-bottomed tube under vacuum with continuous pumping, the degradation products being collected in a liquid nitrogen trap some distance from the sample. The pressure of volatiles is continuously measured somewhere between sample and cold trap and plotted as a function of temperature or time as the sample is heated. A typical oven set up for TVA is depicted in Figure 2.2.

TVA with Differential Condensation of Products
(Ref. 74, 75) involves four cold traps at different temperatures arranged in parallel with geometrically equivalent routes from the sample to a liquid nitrogen trap as depicted in Figure 2.3.

Pirani gauges A, B, C and D are placed after each cold trap to give a measure of the pressure of volatiles, which pass through the respective cold traps. Pirani E, after the liquid nitrogen trap, gives a measure of non-condensable gases passing through the system. The oven temperature together with the output from each pirani head is displayed on a 12

A = Degradation Tube

B = Thermocouple

C = Cooling Jacket

D = Removable flange
head

E = F11 Oven

F = Temperature
Programmer

G = Fan

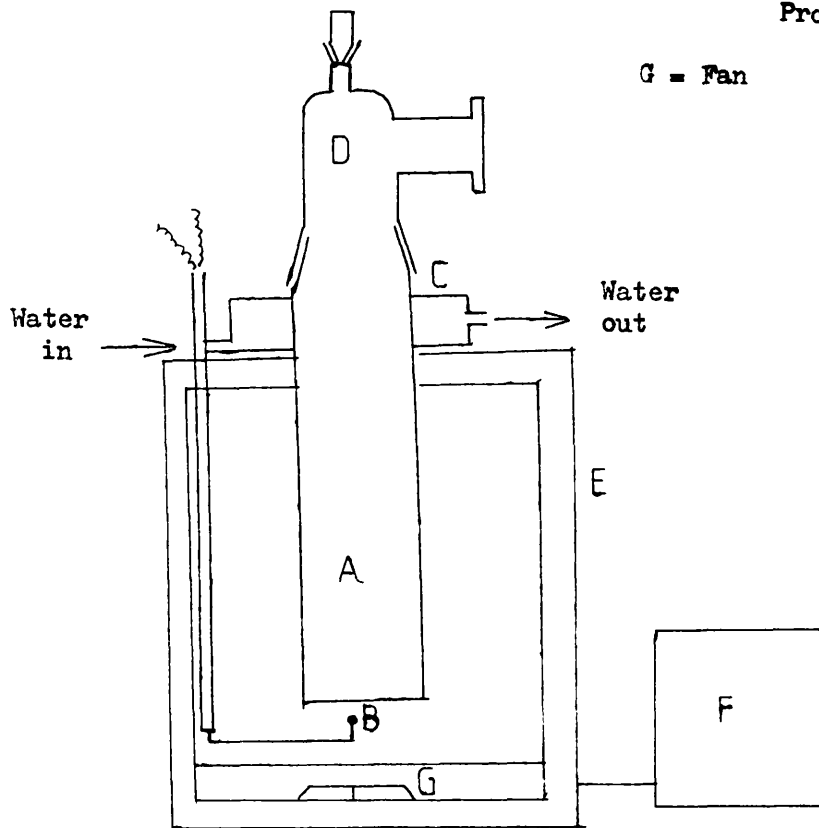


FIGURE 2.2

TYPICAL OVEN ARRANGEMENT FOR TVA

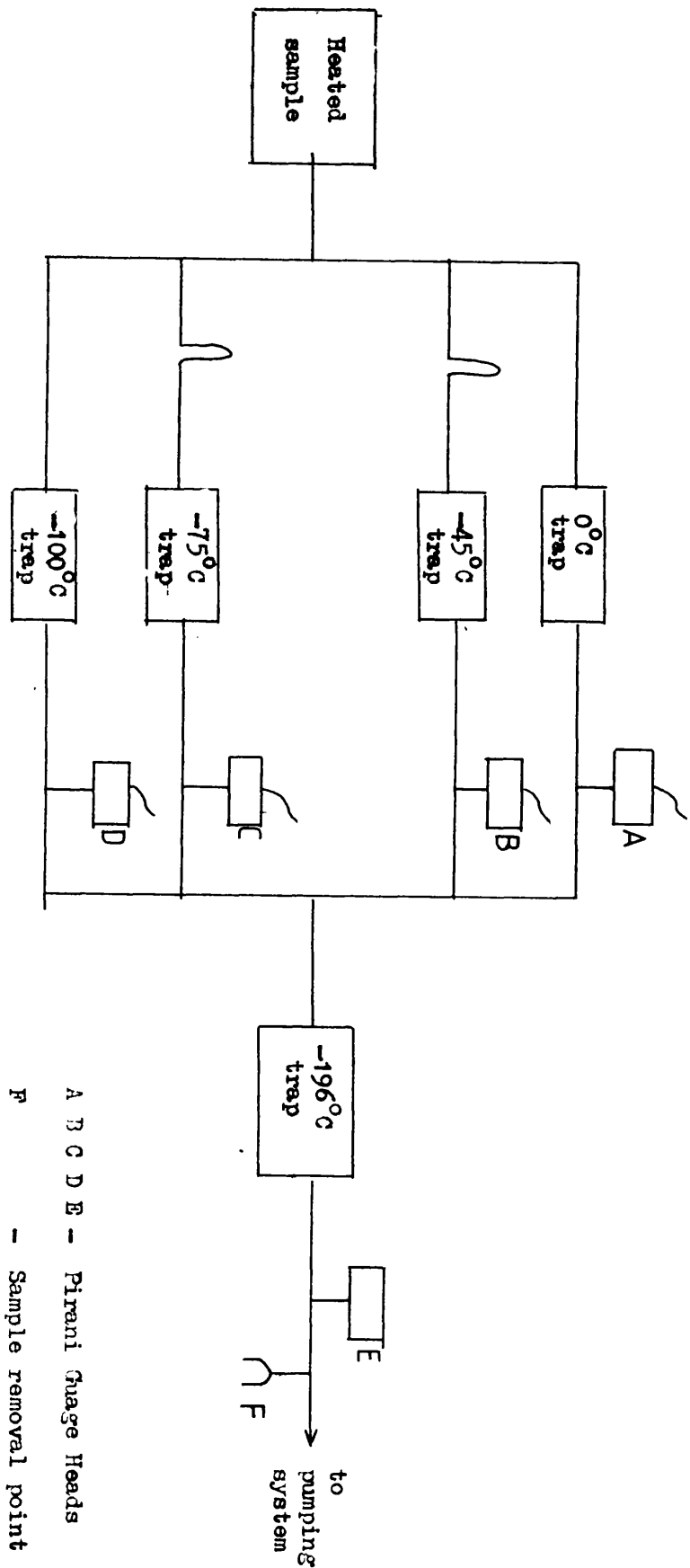


FIGURE 2.3

VACUUM SYSTEM FOR TVA WITH DIFFERENTIAL CONDENSATION OF PRODUCTS

A B C D E - Pirani Gauge Heads
 F - Sample removal point

channel recorder unit via a multihead switch unit.

Thus a preliminary impression of the distribution of condensable products from thermal degradation on the basis of their condensabilities is obtained. A typical trace of this type is shown in Figure 2.4.

The products of degradation can be divided into two main categories:-

1. The involatile residue.
2. The volatile products which can further be sub-divided into three categories.
 - (a) Those products which are volatile at oven temperature but non-volatile at room temperature. (cold ring fraction).
 - (b) Those products which are volatile at degradation temperatures but condense in one of the five cold traps (0, -45, -75, -100 and -196°C) (the condensables).
 - (c) Products volatile even at liquid nitrogen temperatures (non-condensables).

The involatile residue, left at the base of the degradation tube, can be removed for analysis by dissolving in a suitable solvent or by being scraped out of the degradation tube.

The cold ring fraction which collects at the top of the degradation tube can be removed for analysis by methods similar to that employed for the involatile residue.

The volatile products can be removed at (F) in Figure 2.3 by condensation into a gas cell or cold finger for subsequent analysis.

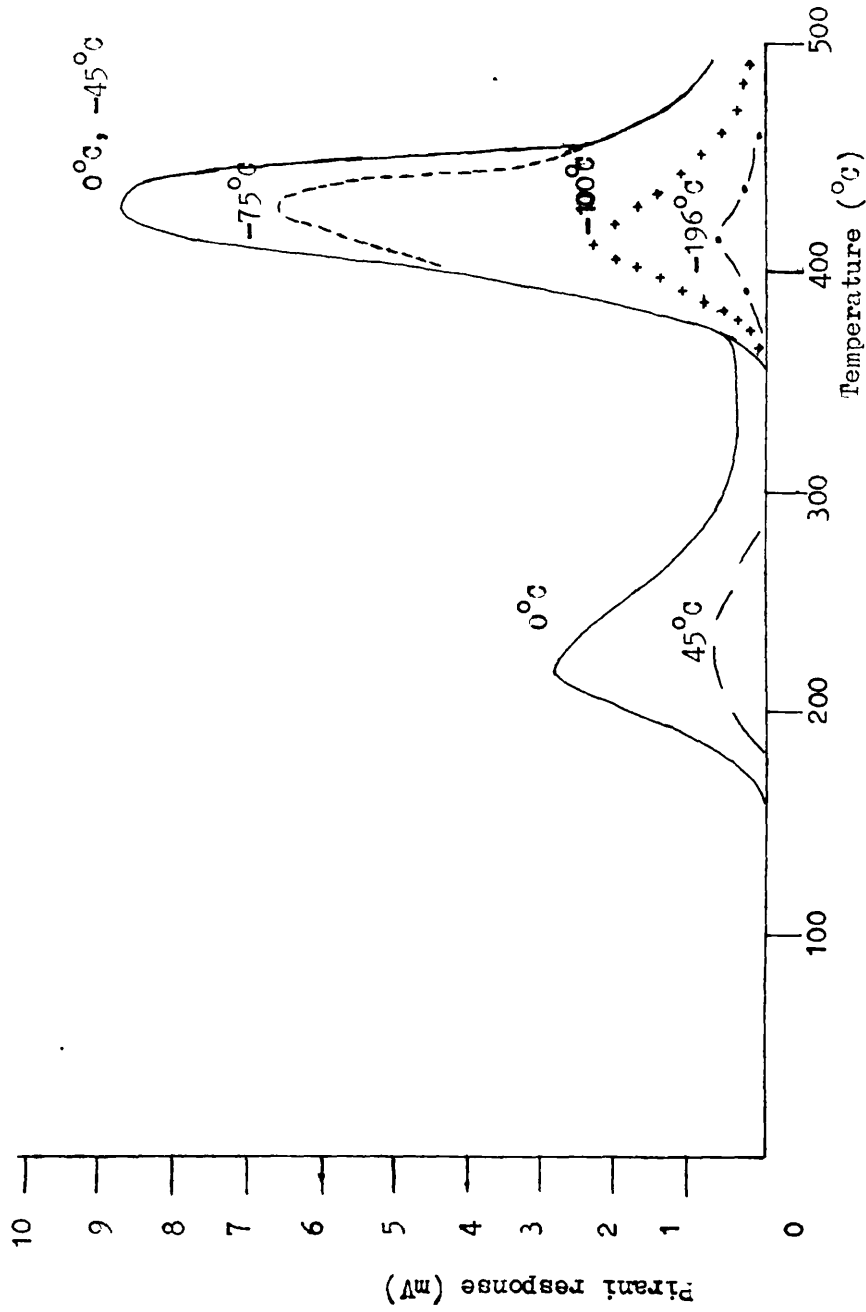


FIGURE 2.4
A TYPICAL TVA TRACE WITH DIFFERENTIAL CONDENSATION OF PRODUCTS

Non-condensables are best investigated by means of a closed system technique described by McNeill. (Ref. 76).

(v) Subambient Thermal Volatilisation Analysis SATVA

At the end of a TVA experiment the various products of degradation of the polymer sample, except gases not condensable at -196°C , are condensed in cold traps in the vacuum system, from which they are then removed for analysis. SATVA is a process developed in this laboratory by McNeill (Ref.77) from an approach by Ackerman (Ref. 78) in which these products can be separated according to their volatility.

The process operates on the principle that when a frozen mixture of products is slowly heated under high vacuum with continuous pumping, a separation occurs which depends upon the volatilities of the various products.

The apparatus used for SATVA is illustrated in Figure 2.5. At the end of the TVA experiment all the condensable products can be collected in a cold trap at -196°C (B). If the liquid nitrogen level round the para-xylene jacket (F) is raised to the level of the bottom of the U-tube (E) as shown, then once equilibrium has been reached there will be a temperature gradient between the base $[-196^{\circ}\text{C}]$ and the top $[\sim \text{ambient}]$. Once the bottom of (E) has reached -196°C as measured by thermocouple (G), stopcocks (A) and (H) are closed and the cold trap round (B) removed. The products then distil over onto the walls of (E) where they will be partially separated due to the temperature gradient. This is monitored by means of pirani head (C) and once all the products have condensed in (E) the liquid nitrogen level round

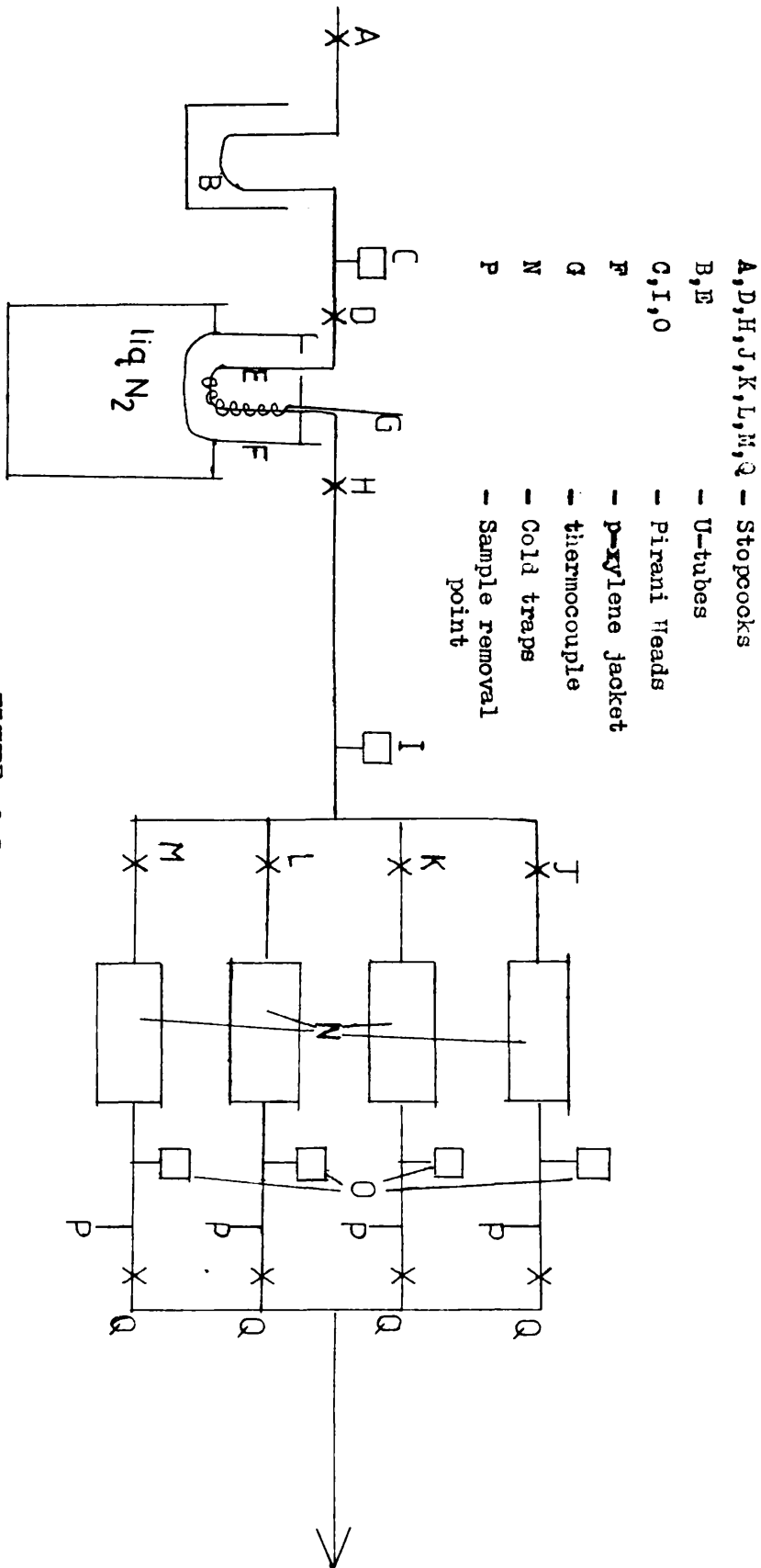


FIGURE 2.5

VACUUM SYSTEM FOR SAWA

(F) is raised to the level of the para-xylene so that the entire p-xylene jacket is lowered to a temperature of -196°C . When this has been achieved stopcock (D) is closed and (H) opened. Cold traps (N) for the collection of products are prepared at -196°C and all but one of stopcocks (J), (K), (L), and (M) closed. If the cold trap round (F) is removed then the temperature of the para-xylene and U-tube (E) will slowly rise. As each product distills pirani head (I) will measure a change in pressure.

The thermocouple reading along with that of pirani head (I) are continuously recorded on a multi-channel recorder. A typical trace is shown in Figure 2.6. The products responsible for each peak can be collected separately in cold traps (N) by manipulation of stopcocks (J) to (M). The products can be removed from the system by distillation into a gas cell or cold finger at (P), this process being monitored by pirani heads (O).

Depending upon the products involved, separation is not always complete but this technique makes identification, especially of minor products, which are often masked by major products, much simpler. The results of these procedures are reproducible.

The advantage of this process is its ability to separate volatile products both for qualitative and quantitative analysis.

(vi) Melt Flow Index MFI

A Davenport Melt Indexer instrument, whose design is exactly specified by ASTM Designation D1238, was used for obtaining melt flow index data. The instrument is

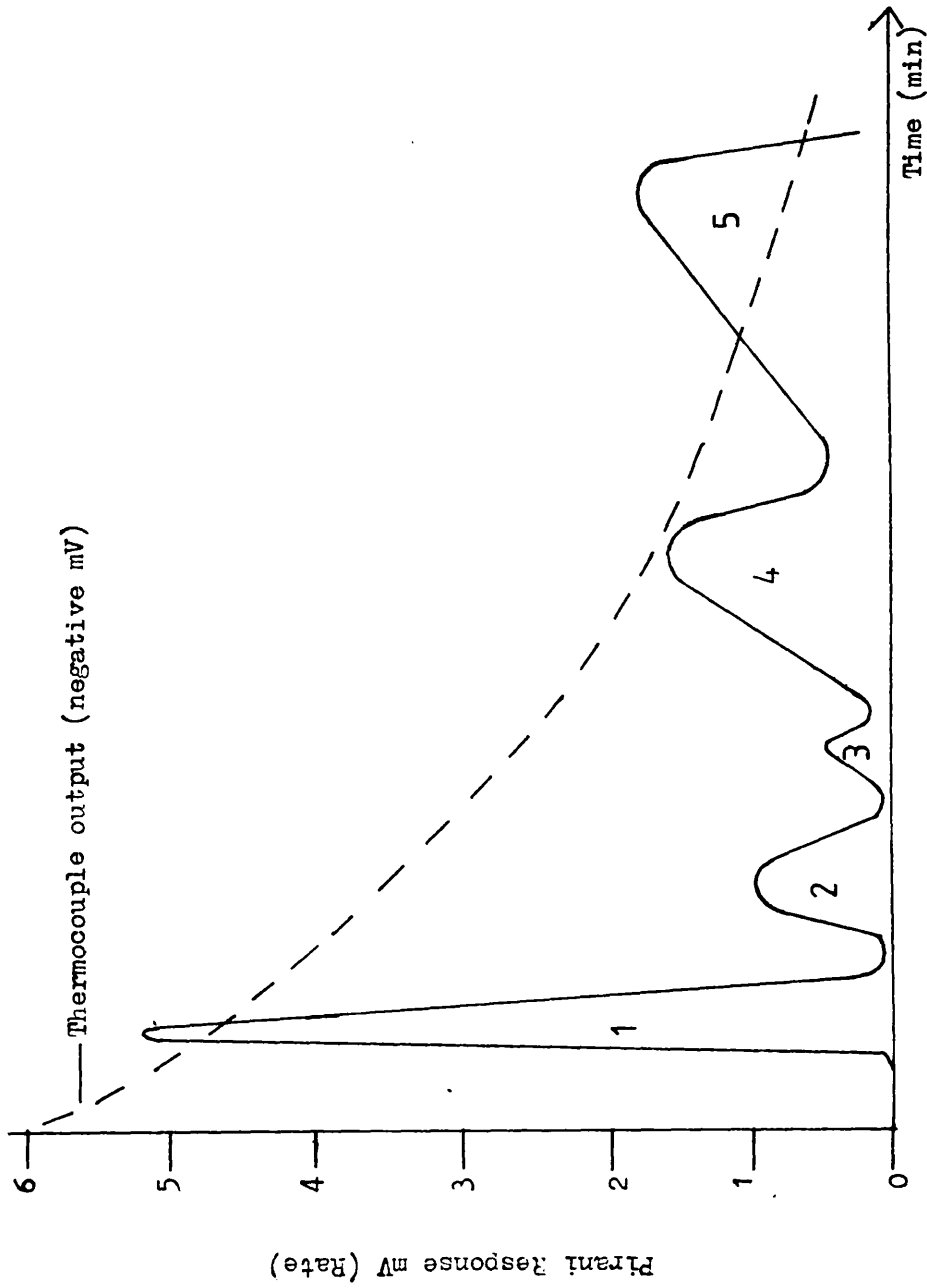


FIGURE 2.6
A TYPICAL SATVA TRACE SHOWING THE SEPARATION OF VOLATILE
PRODUCTS INTO 5 SEPARATE PEAKS

essentially a dead weight piston driven capillary extrusion viscometer having a thermostated barrel reservoir with a removable capillary orifice at the bottom. The polymer in the reservoir is driven through the orifice by a constant load applied to the plunger in the form of an added weight and the melt index is obtained from the resulting flow rate in the units grams of polymer per 10 minutes.

Procedure

The barrel, at a temperature of 190°C , was charged up over a 2 minute period and left to equilibrate for 5 minutes. Thirty seconds prior to the expiry time of the 5 minute equilibration time a load of 2.16kg was placed on the piston. After the 5 minute equilibration time the polymer was extruded through a hole, $9.5504 \pm 0.0076\text{mm}$ in diameter.

Sixty second cuts of the polymer strands produced were taken at various times throughout a 6 minute period and converted to a value of melt index in grams of polymer/10 minutes. This was assumed to be the average MFI over the 60 second time period of the cut or the MFI at the mid-point of the time interval.

2.5. ANALYTICAL TECHNIQUES

(i) Infra-Red Spectroscopy

Spectra were recorded on a Perkin Elmer 257 grating spectrometer. All PHB samples, cold ring fractions, and volatile products distilling over under high vacuum with continuous pumping at temperatures above -90°C were run in solution, all other volatile products being examined in the

gaseous phase.

(ii) Quantitative Estimation of Volatile Products by Infra-Red Spectroscopy

(a) Gaseous Products

A gas cell of known volume was calibrated for quantitative analysis of some gaseous degradation products using the apparatus described in Figure 2.7. The method involves obtaining a plot of optical density, for a particular absorption peak, against the pressure of the reference gas in torr. The gaseous degradation product can be isolated in the gas cell by means of subambient TVA, the optical density measured and related to pressure, by means of the ideal gas equation $PV = nRT$, which holds for low pressures and temperatures well above the boiling points of the gases. The pressure of gas can then be related to the number of moles present.

The volume of the gas cell was found by repeated filling of the gas cell with a suitable liquid from a burette: the temperature was taken as 293K.

The system was evacuated with all taps open, with a cylinder of reference gas attached at (F). Taps (A) and (G) were closed and the reference gas from the cylinder introduced into the line to a pressure of approximately 500mm of Hg (torr) as measured by manometer (I). Tap (E) was closed and the reference gas condensed into reservoir (C) by means of a liquid N_2 trap.

The cylinder was then replaced by the gas cell (J),

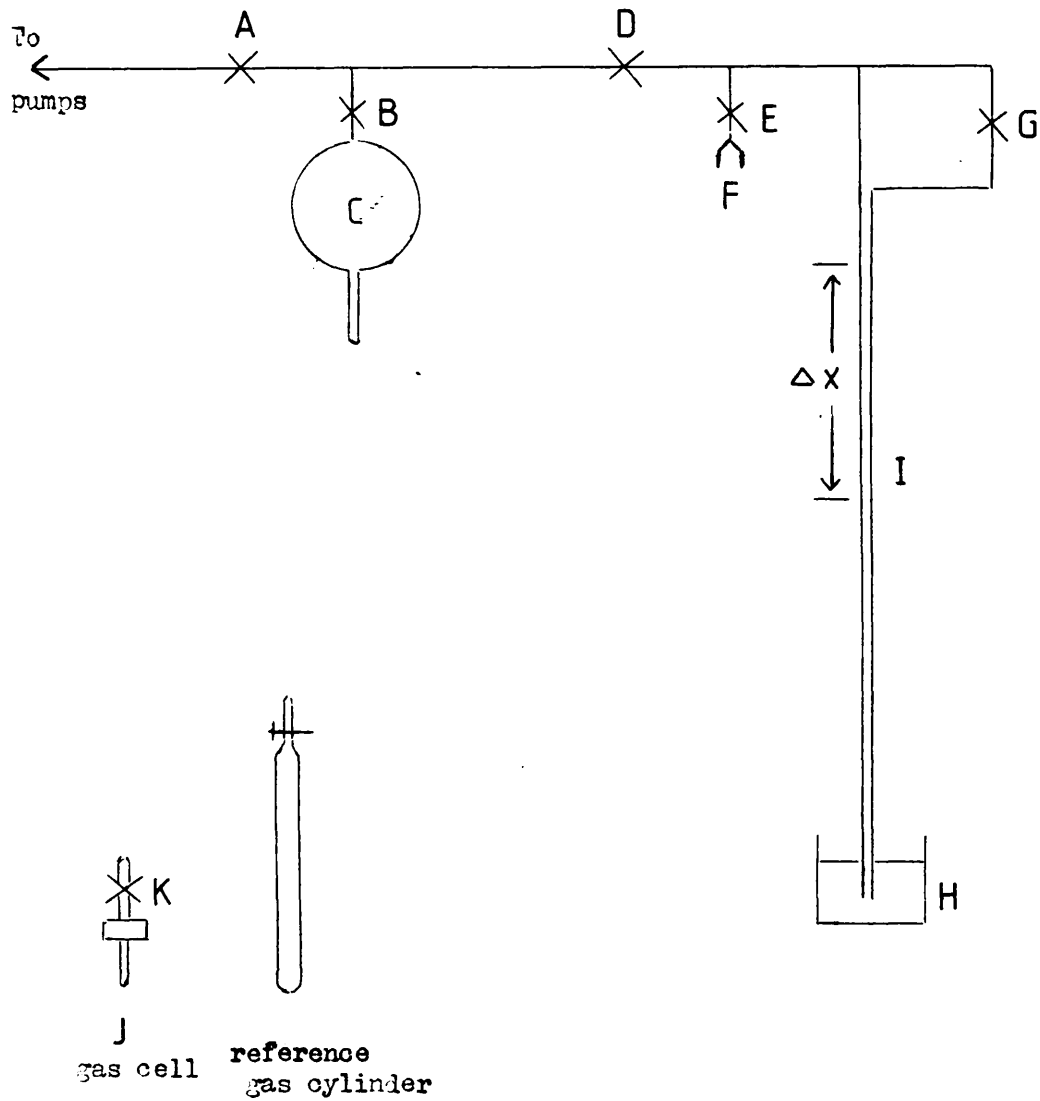


FIGURE 2.7

VACUUM SYSTEM FOR THE CALIBRATION OF A GAS CELL

- A, B, D, E, G and K - Stopcocks
- C - Reservoir
- F - B14 inlet
- H - Mercury reservoir
- I - Manometer
- J - Gas cell

and evacuated with all taps except (B) open. Taps (A) and (G) were closed and by manipulation of Tap (B) gas was introduced into cell (J). The pressure of gas present in (J) was measured by the fall in mercury level Δx . Taps (J) and (K) were closed and the IR Spectrum obtained. The gas cell (J) was then replaced on the line and the above procedure repeated with a different pressure of reference gas in the gas cell.

In this way a calibration graph of optical density, measured as absorbance difference between the filled and empty gas cell, versus pressure was constructed for each gas.

When pure reference gas was not available the following procedure was followed.

The gas cell, containing the gaseous degradation product in question was attached at (F) (Figure 2.7) and all but the gas cell evacuated. Taps (D) and (G) were closed and the gas in the cell allowed to expand into the system. The pressure of gas in the system was measured by the manometer and knowing the volumes of the system and gas cell the original pressure of gas within the closed gas cell can be evaluated. For this purpose a vacuum system of the design illustrated in Figure 2.7, but with the smallest feasible dimensions was used.

(b) Solution

Solutions of pure reference samples of degradation products which were non-gaseous at atmospheric pressure, were prepared in different concentrations in carbon

tetrachloride. The IR spectra of these solutions were run and the optical density measured for a particular absorption peak. These optical densities were plotted against the concentration of the solution.

Non-gaseous (at 1atm pressure) degradation products isolated by SATVA were dissolved in a known volume of CCl_4 , the optical density measured and related to concentration and hence number of moles.

If more than one suitable wavelength was available for quantitative analysis of any product then an average result obtained by using these different wavelengths was calculated.

(iii) Ultra-Violet Spectroscopy UV

Spectra were recorded on a Unicam SP800 Spectrometer, all samples being run in solution.

(iv) Nuclear Magnetic Resonance Spectroscopy NMR

Spectra were recorded on a Varion T60 60 MHz and a Varion HA100 100 MHz spectrometer. All samples were run as solutions in CDCl_3 .

(v) Mass Spectrometry MS

This was carried out on a 90° sector AE1 MS12 mass spectrometer. (Ref. 79).

(vi) Thin Layer Chromatography TLC

Two-dimensional TLC was carried out using two chromatographic tanks -

Tank (a) contained propan-1-ol : methyl ethyl ketone : ammonia in the ratio of 5:5:3 by volume.

Tank (b) contained propan-1-ol : methyl ethyl ketone 1:1 by volume.

Both tanks were freshly prepared and left to equilibrate overnight prior to each run.

Standard 20cm x 20cm Merck silica gel 60 plates with a layer thickness of 0.25mm were used. These plates were activated before spotting by heating to 120°C for 30 minutes in an oven.

The following procedure was followed for each run. A plate was lightly spotted in the bottom left hand corner 2cm from each edge and placed in tank (a). When the solvent front had travelled its course the plate was removed, dried in a stream of air and the change in position of the spot observed under a UV lamp. The plate was then placed in tank (b) and the spots run in the other direction before being dried and observed under a UV lamp.

The ammonia present in the eluent of tank (a) converted any acids present to ammonium salts in which form they were then separated. (Ref. 80).

(vii) Gas Liquid Chromatography GLC (Ref.81)

Analyses were carried out using a Perkin-Elmer F11 gas chromatograph with flame ionisation detector connected to a linear temperature programmer. The column used was a 10' 1% OV1 of $\frac{1}{8}$ inch diameter. The sample, dissolved in chloroform, was injected by syringe through the self sealing rubber septum and the oven programmed to heat from 50°C to 260°C at a heating rate of 5°C/min. The temperature was held at 260°C for 10 minutes after the heating programme had terminated.

Use of Carbon Number

It has been shown that for a homologous series each

increment decreases the vapour pressure of the component by a constant amount. Therefore under isothermal conditions there is a linear relationship between $\log V_g$ (V_g = retention volume) and number of carbon atoms or increment units.

In the case of a linear programmed heating rate a near linear relationship between V_g and number of increment units is expected.

In order to verify the relationship between V_g and increment units of a homologous series under a linear temperature programme, a solution was prepared containing members of the series of linear hydrocarbons. This was run on the column as above and from the GLC trace a plot of relative retention (r) versus carbon number was found to be nearly linear. Figure 2.8.

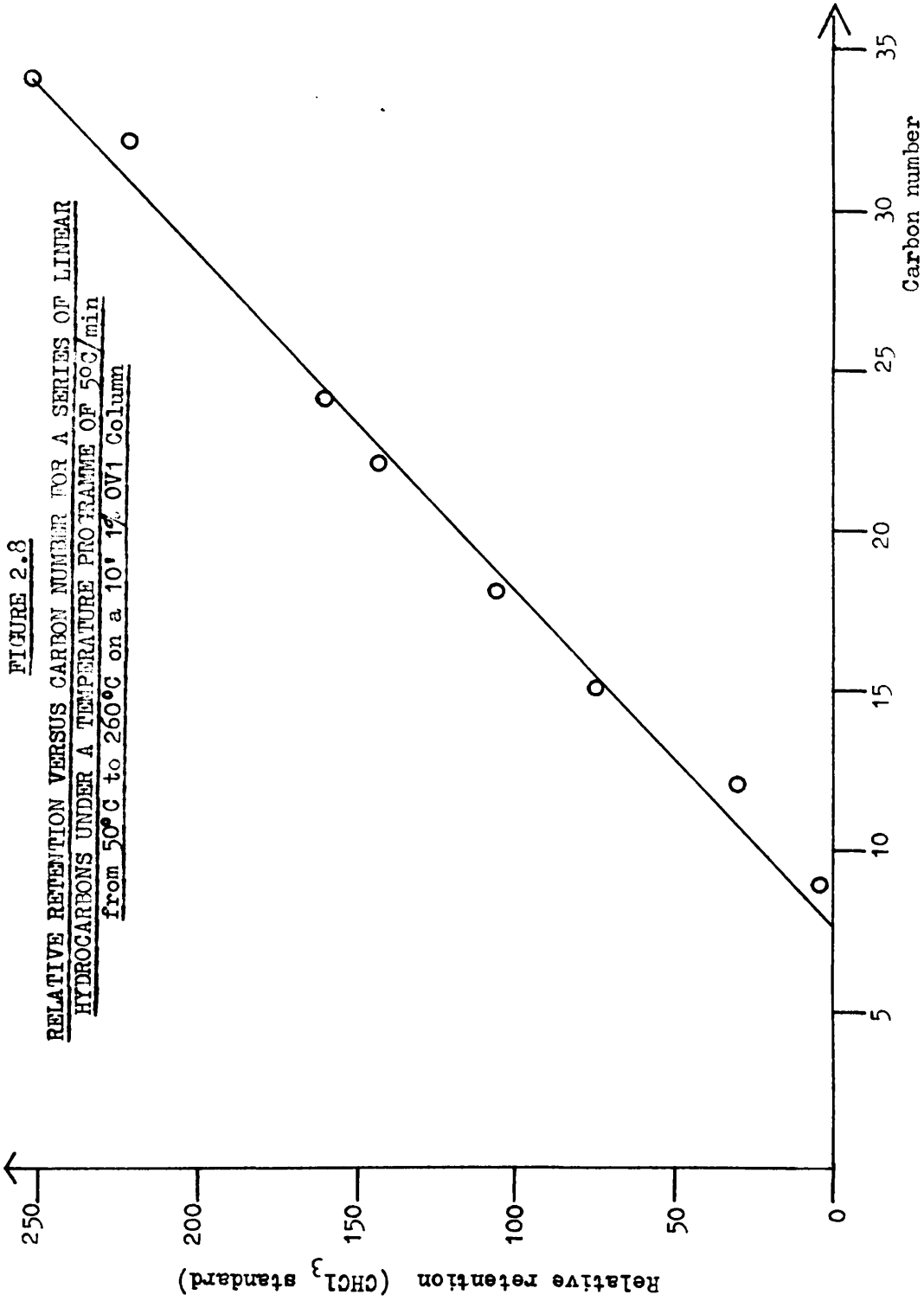
NOTE: Relative retention = $\frac{\text{retention distance for component}}{\text{retention distance for standard compound}}$

Thus relative retention varies directly with the number of increment units in a homologous series under a linear temperature programme.

Normalisation Method for Quantitative Analysis

This method depends on making the assumption that the chromatogram represents a known proportion of the sample. Then, by use of pure components the column is calibrated by obtaining a relative response factor R_f which is defined as the ratio of the detector response factor for a component and that for a selected standard component. This is done for each component by measuring the peak areas from chromatograms obtained from samples of known concentration.

For a flame ionisation detector the response increases



with percentage carbon in the molecule. Thus for a homologous series, e.g. monomer, dimer, trimer the relative response factors (taking the monomer as standard) will be 1 : 2 : 3 respectively. In this case relative response characteristics can be defined without recourse to pure samples of each component in the mixture.

(viii) Trace Impurity Analysis

The presence of impurities in the polymer samples was determined by standard trace analysis techniques for the elements thought to be relevant.

This work was carried out on samples supplied by the author to I.C.I. Agricultural Division Laboratories, Billingham, Cleveland.

2.6 MOLECULAR WEIGHT DETERMINATION

(i) Gel Permeation Chromatography GPC (Ref. 82)

This technique was used to determine the molecular weight distribution MWD of different polymer samples of PHB giving a measure of the number average molecular weight \bar{M}_n , the weight average molecular weight \bar{M}_w , the viscosity average molecular weight \bar{M}_v and the polydispersity $D = \bar{M}_w / \bar{M}_n$.

Two instruments were used during the course of this work. The first, Instrument A, was an Applied Research Laboratories Instrument containing prepacked columns filled with a cross-linked polystyrene divinyl benzene gel as supplied by Polymer Laboratories Ltd. There were five columns contained within the instrument each of 60cms length with pore size of 10^7 \AA , 10^6 \AA , 10^5 \AA , 10^4 \AA and 10^3 \AA with a macrogel diameter size of $20 \mu\text{m}$. The GPC was run at a temperature of 30°C using

chloroform as a solvent with a flow rate of $0.75\text{cm}^3/\text{min}$.

The detector system was an infra-red spectrometer set at a constant wavelength of $5.75\mu\text{m}$ with a flow through cell in the IR beam.

The second, Instrument B, was a Du Pont Chromatographic Pump and column chamber within which were 4 prepacked columns filled with a cross-linked polystyrene divinyl benzene gel, as supplied by Polymer Laboratories Ltd. The 4 columns were each of length 30cm with pore sizes of 10^6 \AA , 10^5 \AA , 10^4 \AA , and 10^3 \AA , respectively and a microgel diameter of $10\mu\text{m}$. The internal diameter of the columns was 7.7mm. The GPC was run at 35°C with a flow rate of $1\text{cm}^3/\text{min}$. and a pressure drop of 50 torr. A Du Pont IR analyser set at a wavelength of $5.85\mu\text{m}$ with a flow through cell was used as a detector system.

Interpretation of a GPC Chromatogram

A diagrammatical summary of the steps in the conversion of a GPC chromatogram to a MWD curve are given in Figure 2.9.

The raw GPC chromatogram (i) is first normalised to give unit area under the curve. Heights h_i are measured at various intervals along the retention volume (V_r) axis and each value divided by $\sum h_i$. The normalised ordinate values h^1 may then be plotted against V_r (ii) to give the normalised elution curve. From this curve and the calibration curve (iii) a set of pairs of values for dw/dV_r and V_r , and $d(\log M)/dV_r$ for the same V_r values and a corresponding range of values for M can be generated (iv). Suitable manipulation of these terms enables dw/dM to be calculated and the normalised weight differential molecular weight distribution curve to be constructed (v). This procedure is best carried out by

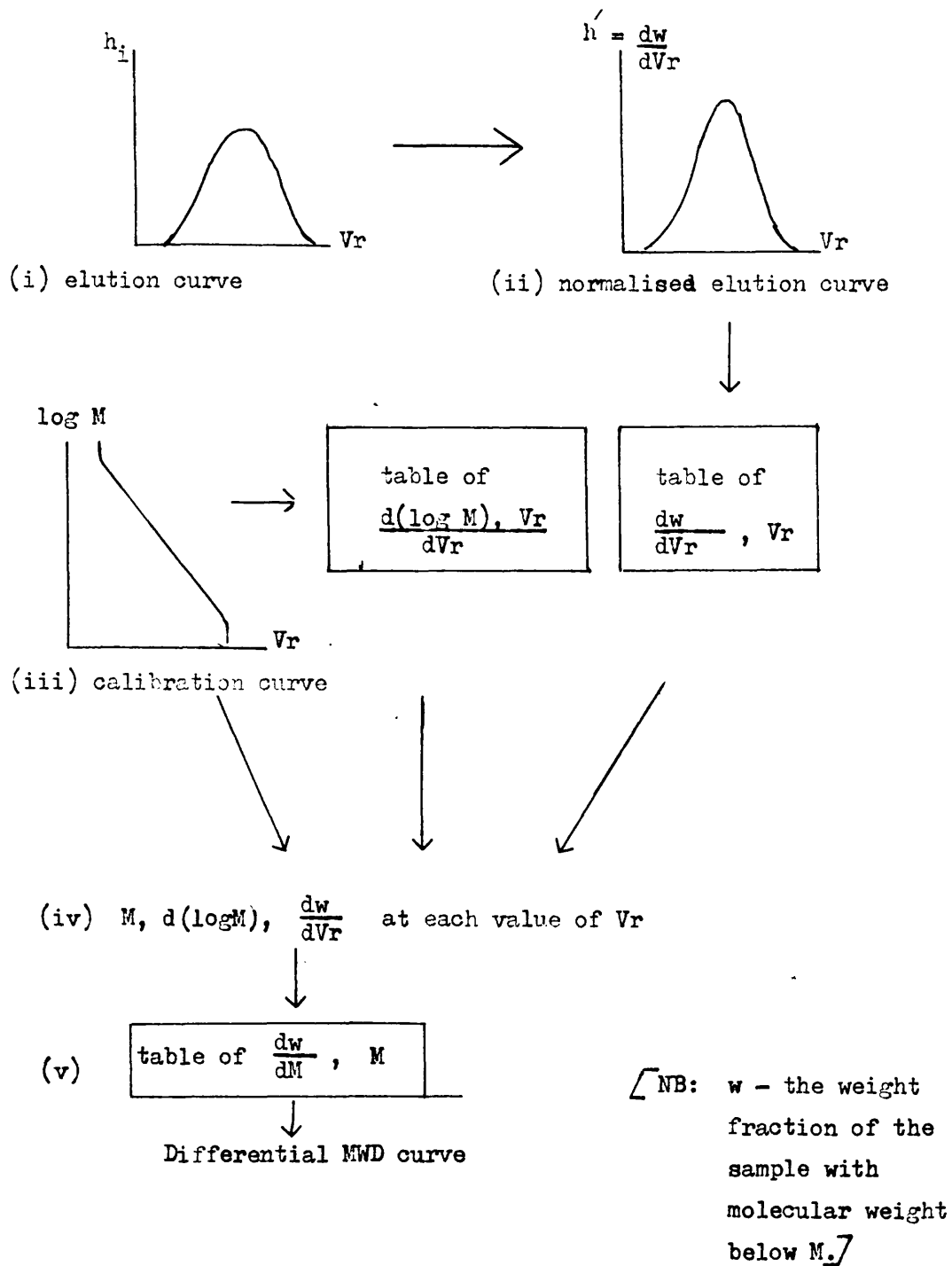


FIGURE 2.9

SUMMARY OF THE STEPS IN THE CONVERSION OF A
GPC CHROMATOGRAM TO A GPC MOLECULAR WEIGHT DISTRIBUTION CURVE

computer and typical programme by Picket et al (Ref.83)

produces \bar{M}_n , \bar{M}_w , \bar{M}_v as well as the MWD curve.

Method

The solutions were injected via an injection coil and were of approximate concentration $\frac{1}{2}$ % w/v.

Instrument A - The elution curve was measured automatically at regular intervals and the results stored on magnetic tape. The results were then fed into a Commodore PET computer using a programme modified by Burgess (Ref. 84) to produce a differential MWD curve. A typical example of a differential MWD curve is illustrated in Figure 2.10.

Instrument B - The elution curve was measured manually at regular intervals (1cm) giving approximately 20 values. These values were fed into a PET computer and a MWD curve obtained. A typical elution curve obtained on Instrument B is depicted in Figure 2.11.

Calibration of Columns for PHB

Since standards of PHB were not readily available the columns were calibrated using commercially available polystyrene samples. For this purpose chromatograms were obtained of different mixtures of polystyrene standards dissolved in chloroform. A typical chromatogram is depicted in Figure 2.12. The IR detector was set at a wavelength of $3.43\mu\text{m}$ while running polystyrene samples. Thus it was possible to relate the retention volume V_R to polystyrene equivalent molecular weight. The calibration curve of $\log M$ versus V_R for polystyrene samples run on Instrument B is depicted in Figure 2.13.

Since GPC separates on a molecular size basis rather than

FIGURE 2.10

A DIFFERENTIAL MOLECULAR WEIGHT DISTRIBUTION

CURVE FOR A SAMPLE OF PHB

NUMBER AVERAGE 683600

WEIGHT AVERAGE 1621000

D = MW/MN 2.37

VISCOSITY AVERAGE 1472600

ALPHA 0.70

ELUTION TRACE, COUNT 89 TO 150

CALIBRATION ... ARL-PL 8 31-10-79

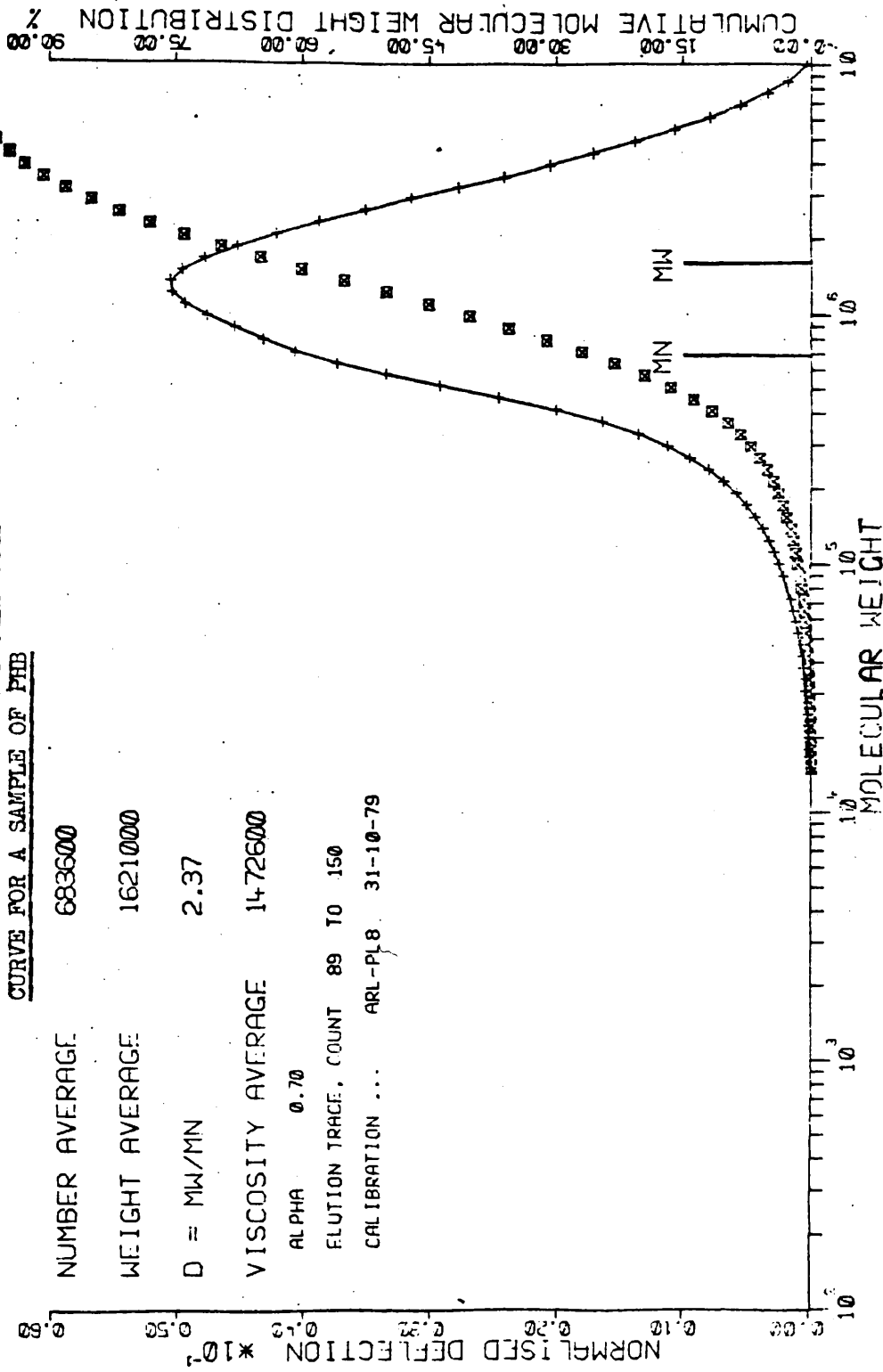


FIGURE 2.11

AN ELUTION CURVE FOR A SAMPLE OF PHB OBTAINED FROM INSURMENT B

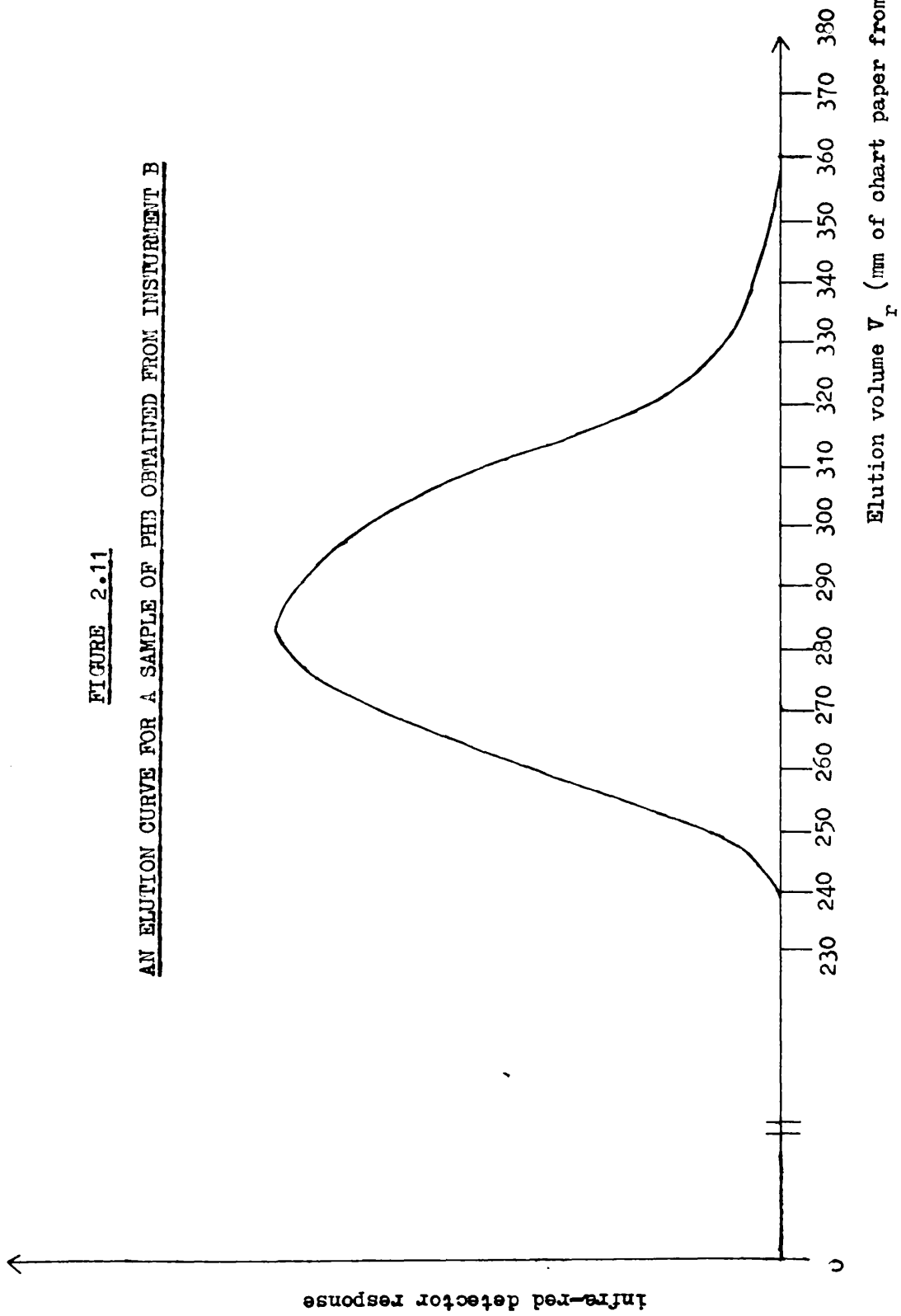


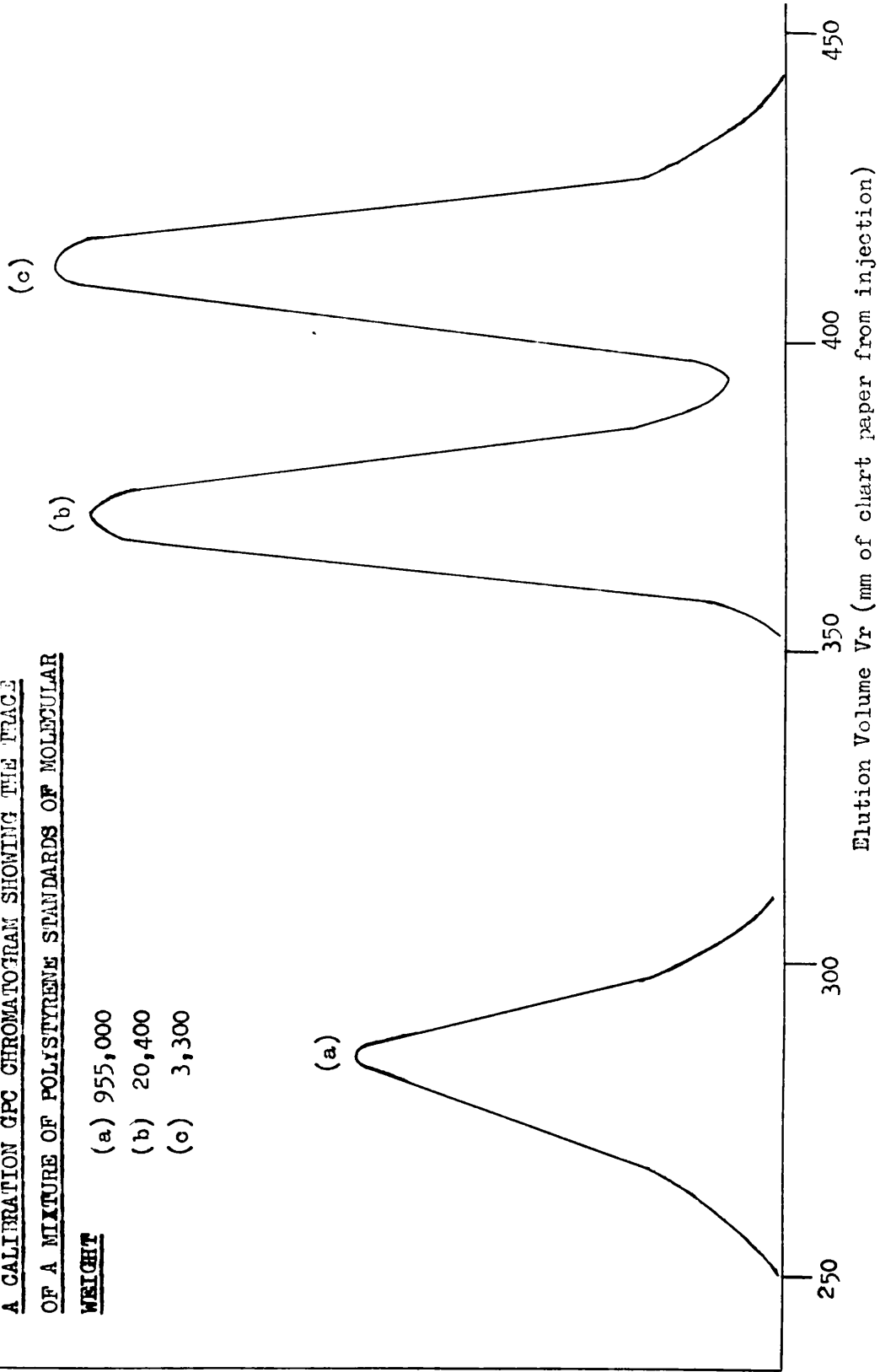
FIGURE 2.12

A CALIBRATION GPC CHROMATOGRAM SHOWING THE TRACE
OF A MIXTURE OF POLYSTYRENE STANDARDS OF MOLECULAR

WEIGHT

- (a) 955,000
- (b) 20,400
- (c) 3,300

infra-red detector response



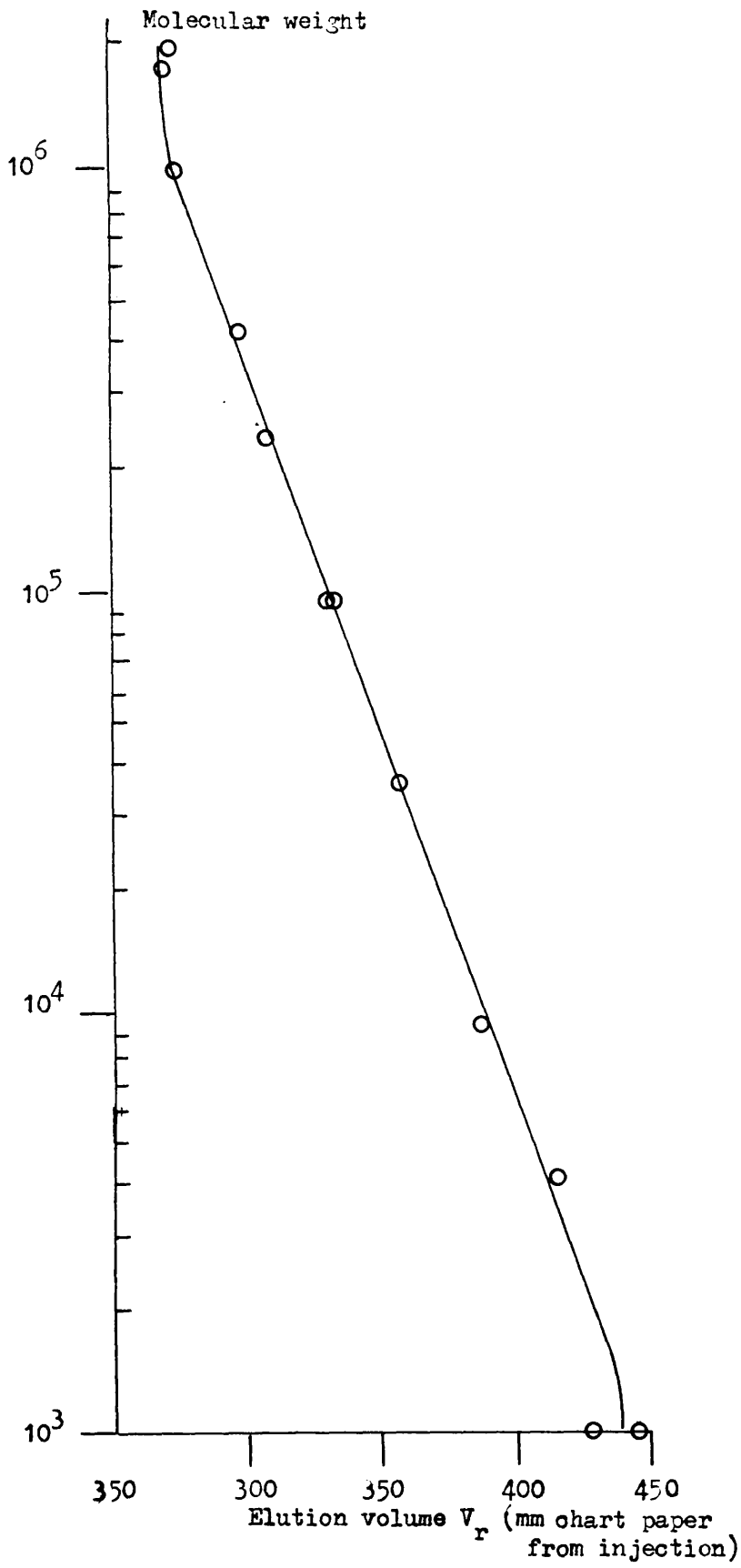


FIGURE 2.13

CALIBRATION CURVE FOR GPC OF LOG (MOLECULAR WEIGHT) OF POLYSTYRENE SAMPLE VERSUS ELUTION VOLUME ON INSTRUMENT B

on molecular weight, the values obtained from this calibration are polystyrene equivalent molecular weights rather than true PHB molecular weights. Thus a correction has to be applied to obtain true PHB molecular weights.

By comparing a measurement of the molecular weight of a sample of PHB measured as above and independantly by osmometry, viscometry or light scattering then a relationship of the following form is obtained. (Ref. 85).

$$\log_{10} \left[\frac{\text{true molecular weight of PHB}}{\text{polystyrene equivalent molecular weight}} \right] = -0.21 \dots\dots\dots \text{Eq 2.1}$$

All values of molecular weights measured by GPC reported in this work have been corrected using the above expression.

(ii) Viscometry

Viscometry was employed as a means of rapid determination of molecular weight which could be carried out at Glasgow. This technique was also investigated as a means of molecular weight determination in an industrial production setting.

Method

An Ubbelohde suspended level dilution viscometer immersed in a thermostated water bath set at 25°C was used throughout. The flow time of each sample solution on reaching thermal equilibrium was measured using a stop-watch graduated in 0.2 second intervals. The reduced specific viscosity

$$\frac{1}{c} \frac{\eta - \eta_0}{\eta_0} \quad \text{where}$$

c = concentration (g/dl)
 η = flow time of sample solution
 η_0 = flow time of pure solvent Eq 2.2

was measured over an average of 5 flow times.

The intrinsic viscosity $[\eta]$ was determined by extrapolating a plot of reduced specific viscosity versus concentration to zero concentration (a minimum of 5 values of reduced specific viscosity were obtained from each PHB sample).

The temperature of 25°C was chosen as being the lowest suitable temperature for taking measurements in an industrial production setting where ease of operation has to be coupled with safety in controlling chloroform vapour.

The Relationship between Molecular Weight and $[\eta]$ -
The Mark-Houwink-Sakurada Equation

For a given polymer-solvent system at a specified temperature, $[\eta]$ can be related to molecular weight through the Mark-Houwink-Sakurada Equation.

$$[\eta] = KM^a \quad \text{where } [\eta] = \text{intrinsic viscosity}$$

$$a, K = \text{constants}$$

$$M = \text{molecular weight} \dots\dots\dots \text{Eq 2.3}$$

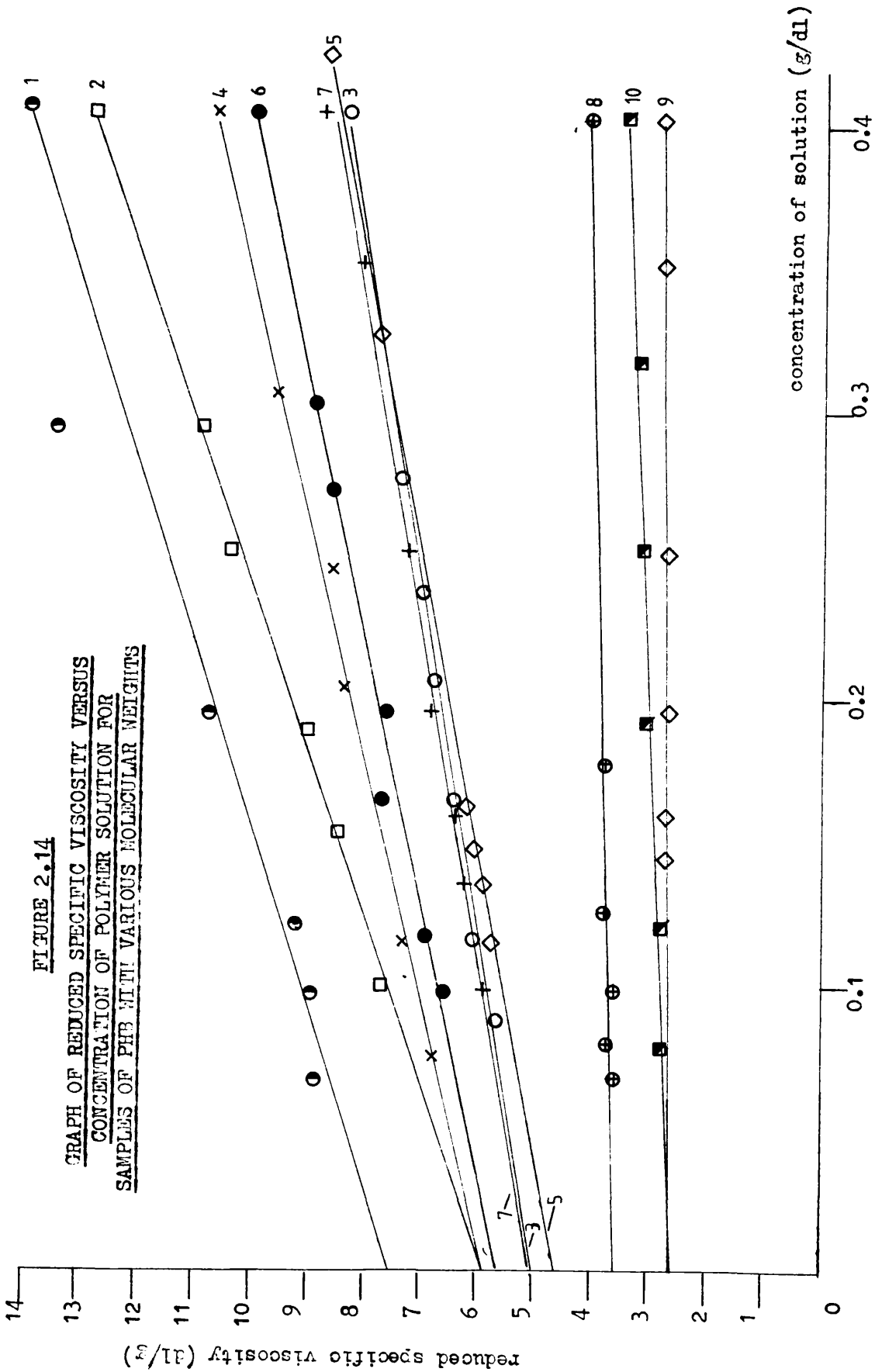
This is an empirical equation in which K and a are constants which depend upon the solvent, the polymer and the temperature. The exponent "a" should be ≈ 1.8 for a "rigid rod" solvent and $0.5 < a \leq 0.8$ for a "random coil" solvent.

\bar{M}_n versus $[\eta]$ i.e. $[\eta] = K_n \bar{M}_n^a$

The value for K_n is particularly sensitive to MWD and for this reason the relationship was examined only for samples of narrow distribution, e.g. polydispersity D in the range 1.56 to 1.76.

The intrinsic viscosities of fractions F1 to F3 mentioned in Chapter 2.3 were measured as in Figure 2.14. A graph of

The molecular weight distributions of the polymer samples giving rise to the curves designated 1-10 below are listed in Table 2.A (page 53).



$[\eta]$ versus $\log \bar{M}_n$ was plotted as in Figure 2.15, a least squares fit giving the following relationship.

$$[\eta]_{\text{CHCl}_3}^{298} = 3.92 \times 10^{-6} \bar{M}_n^{1.07 \pm 0.7} \quad [[\eta] \text{ in dl/g}]$$

..... Eq 2.4

The high error in "a" is due to the small number of samples (3) used in its determination. This equation is only of limited industrial value as it applies only to polymer samples with $1.50 < D < 1.80$.

$$\bar{M}_w \text{ versus } [\eta] \text{ i.e. } [\eta] = K_w \bar{M}_w^{a_w}$$

A far more useful expression can be obtained for the relationship between $[\eta]$ and \bar{M}_w since K_w is far less sensitive to MWD than K_n .

The intrinsic viscosities of polymer samples (10 in number) in the range $448,999 < \bar{M}_w < 1,030,000$ with polydispersity $1.56 < D < 8.14^*$ were measured as in Figure 2.14. A graph of $[\eta]$ versus $\log \bar{M}_w$ was plotted Figure 2.16, a least squares fit giving the following relationship.

$$[\eta]_{\text{CHCl}_3}^{298} = 5.72 \times 10^{-7} \bar{M}_w^{1.17 \pm 0.1} \quad [[\eta] \text{ in dl/g}]$$

..... Eq 2.5

***NOTE:** 8 of the samples had polydispersity in the range $1.56 < D < 2.68$.

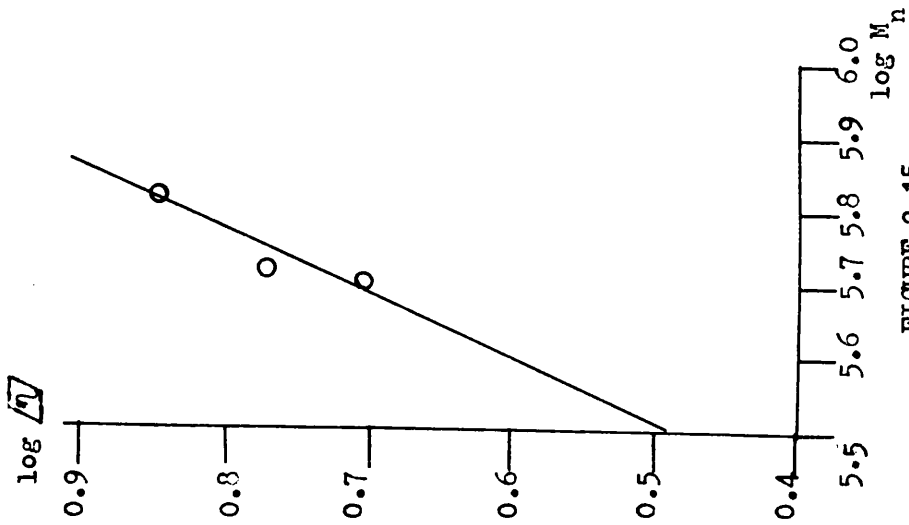


FIGURE 2.15

RELATIONSHIPS BETWEEN $\log \sqrt{[\eta]}$ AND
 $\log (M_n)$ FOR PHB SAMPLES WITH
 POLYDISPERSITY IN THE RANGE
1.56 to 1.76

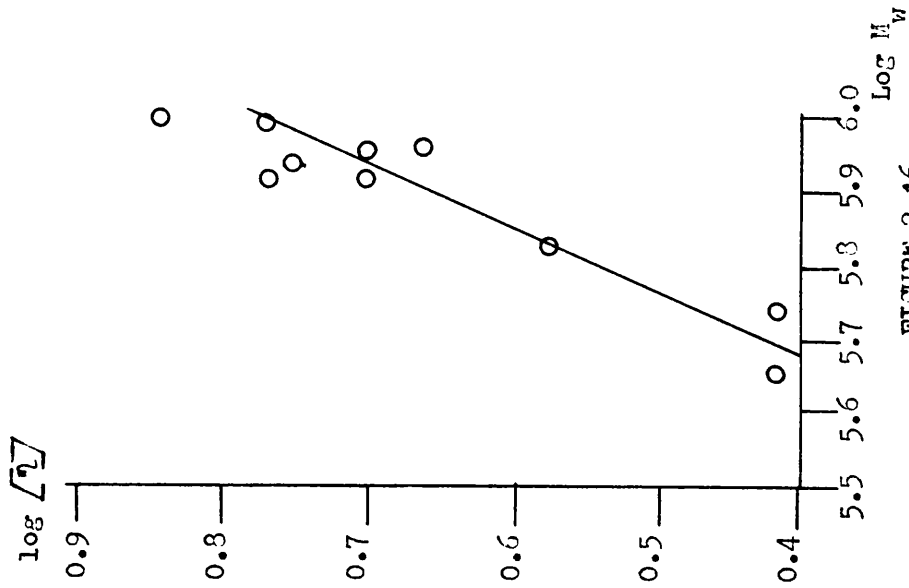


FIGURE 2.16

RELATIONSHIP BETWEEN $\log \sqrt{[\eta]}$ AND
 $\log (M_w)$ FOR PHB SAMPLES WITH
 POLYDISPERSITY IN THE RANGE
1.56 to 3.14

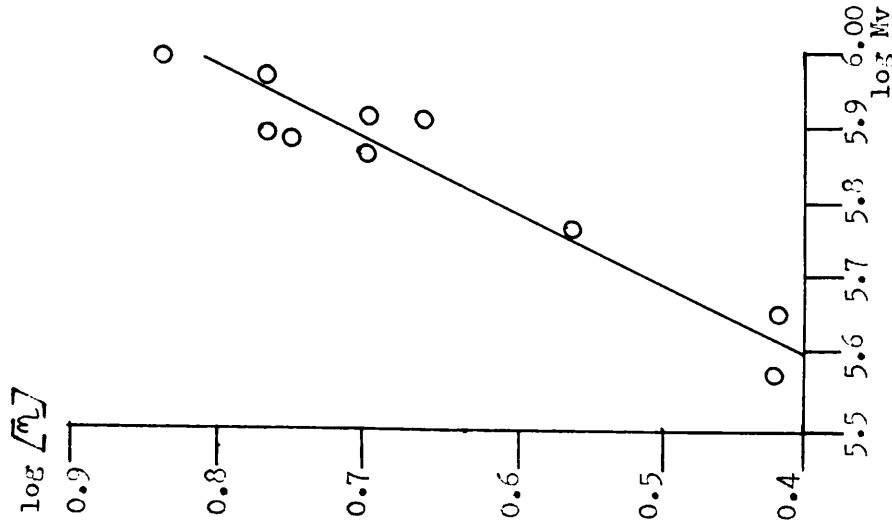


FIGURE 2.17

RELATIONSHIP BETWEEN $\log \sqrt{[\eta]}$
 AND $\log (M_w)$ FOR PHB SAMPLES
 WITH POLYDISPERSITY IN THE
 RANGE 1.56 to 3.14

$$\underline{\bar{M}_v \text{ versus } [\eta]} \quad \text{i.e. } [\eta] = K_v \bar{M}_v^{a_v}$$

The intrinsic viscosities of the 10 samples noted above were plotted against $\log \bar{M}_v$ Figure 2.17, a least squares fit giving the following relationship.

$$[\eta]_{\text{CHCl}_3}^{298} = 2.62 \times 10^{-6} \bar{M}_v^{1.07 \pm 0.1} \quad [[\eta] \text{ in dl/g}] \quad \dots\dots\dots \text{Eq 2.6}$$

Summary

The MWD of the polymer samples used in the above calibrations were obtained by means of GPC, see Chapter 2.6(i), using instrument A. This data plus the values for intrinsic viscosity are tabulated in Table 2.A.

Since the standard deviation of "a" calculated from the least squares fit amounts to 0.1 for a_w and a_r it seems therefore more correct to apply the following equations, 2.7, 2.8 and 2.9, rather than 2.1, 2.2 and 2.3.

$$\left. \begin{aligned} [\eta]_{\text{CHCl}_3}^{298} &= 3.9 \times 10^{-6} \bar{M}_n^{1.1} && \dots\dots\dots \text{Eq 2.7} \\ [\eta]_{\text{CHCl}_3}^{298} &= 5.7 \times 10^{-7} \bar{M}_w^{1.1} && \dots\dots\dots \text{Eq 2.8} \\ [\eta]_{\text{CHCl}_3}^{298} &= 2.6 \times 10^{-6} \bar{M}_v^{1.1} && \dots\dots\dots \text{Eq 2.9} \end{aligned} \right\} \begin{array}{l} [[\eta] \text{ in dl/g}] \\ \text{in all cases} \end{array}$$

Equation 2.8 would appear to be at variance with a similar equation derived by Marchessault (Ref. 86) and Herrera de Mola (Ref. 22) for PHB in chloroform at 30°C.

$$[\eta]_{\text{CHCl}_3}^{303} = 7.7 \times 10^{-5} \bar{M}_w^{0.82} \quad \text{and} \quad \dots\dots\dots \text{Eq 2.10}$$

$$[\eta]_{\text{CHCl}_3}^{303} = 1.90 \times 10^{-4} \bar{M}_v^{0.74} \quad \text{respectively} \quad \dots\dots\dots \text{Eq 2.11}$$

TABLE 2.A
MOLECULAR WEIGHT AND VISCOSITY RESULTS
FOR THE SAMPLES USED IN EVALUATING THE RELEVANT
MARK-HOUWINK-SAKURADA EQUATION

	\bar{M}_n	\bar{M}_w	\bar{M}_v	D	$\frac{[\eta]}{dl/g}$	
1	658,000	1,029,000	975,000	1.56	6.96	(a)(b) F1
2	525,000	838,000	790,000	1.60	5.86	(a)(b) F2
3	506,000	890,000	834,000	1.76	5.01	(a)(b) F3
4	486,000	1,002,000	934,000	2.14	5.89	(b)
5	381,000	922,000	828,000	2.42	4.61	(b)
6	329,500	863,000	772,000	2.62	5.59	(b)
7	315,000	829,000	741,000	2.63	5.01	(b)
8	243,000	652,000	586,000	2.68	3.60	(b)
9	85,000	449,000	389,000	5.29	2.62	(b)
10	63,000	546,000	465,000	8.71	2.62	(b)

NOTE: (a) - samples used in evaluating Eq. 2.4

(b) - samples used in evaluating Eqs. 2.5, 2.6

All molecular weights were obtained via GPC -
 see Chapter 2.6 (i) on Instrument A.

1-10 refer to the curves of Figure 2.14

This is especially true since K and a become mostly insensitive to temperature when a exceeds 0.7, being approximately constant 10°C either side of the quoted temperature. (Ref.87) However the increase in a from 0.8 at 30°C to 1.1 at 25°C can be explained by light scattering experiments performed by Cornibert (Ref. 88) which indicated that as the temperature is decreased the particle length in solution increases. This is thought to be due to chain-folding in solution forming a more rigid rod-like particle.

Equations 2.8 and 2.9 were used to relate molecular weight measurements carried out by GPC and viscometry. In the following text this has been done only where indicated.

The use of these relationships in a production setting might be severely limited by the temperature dependence of the relevant Mark-Houwink-Sakurada Equation.

2.7 X-RAY CRYSTALLOGRAPHY

Powdered X-ray photographs of various polymer samples were obtained on a powder camera of 65mm radius.

The conditions of the film exposure were as follows:

M.A. = 10
K.V. = 35
Exposure Time = 7 hours
Tube = Co with an Fe filter.

The intensities of the resultant rings on the x-ray film were measured using a densitometer.

2.8 TREATMENT OF ERRORS

The gradients and intercepts of all linear graphs were obtained

using a least squares fit on the points.

An estimate of the standard deviation of scatter around the least squares fit was obtained for equations of the form $y = mx + c$ using the following equations.

$$S_{xy} = \sqrt{\frac{\sum (y_i - Y_i)^2}{n-2}} \quad \text{where } y_i = \text{experimental value of } y \text{ at } x_i \dots\dots\dots \text{Eq 2.12}$$

Y_i = least squares fit value of y at x_i

n = number of values for x at which values for y were obtained experimentally.

$$S_m = \frac{S_{xy}}{\sqrt{\sum x^2 - \bar{x} \sum x}} \quad \text{where } S_m = \text{standard deviation of } m \dots\dots\dots \text{Eq.2.13}$$

$$S_o = \sqrt{\frac{\sum x^2}{n \sum x^2 - (\sum x)^2}} \dots\dots\dots \text{Eq 2.14}$$

For further details on error calculations see reference 89.

2.9 DEGRADATION TECHNIQUES UNDER GLASS

(i) Vacuum

The oven and vacuum line system were as described previously in Chapter 2.4, Figures 2.2. and 2.5.

The pumping system consisted of an Edwards Vapour Pump Model E10 and an Edwards Oil Rotary Pump, Spedivac Single Stage Model 1S50.

A weighed polymer sample was placed at the base of the degradation tube (see Figure 2.18) connected to the vacuum system and evacuated to a pressure of 10^{-5} torr before

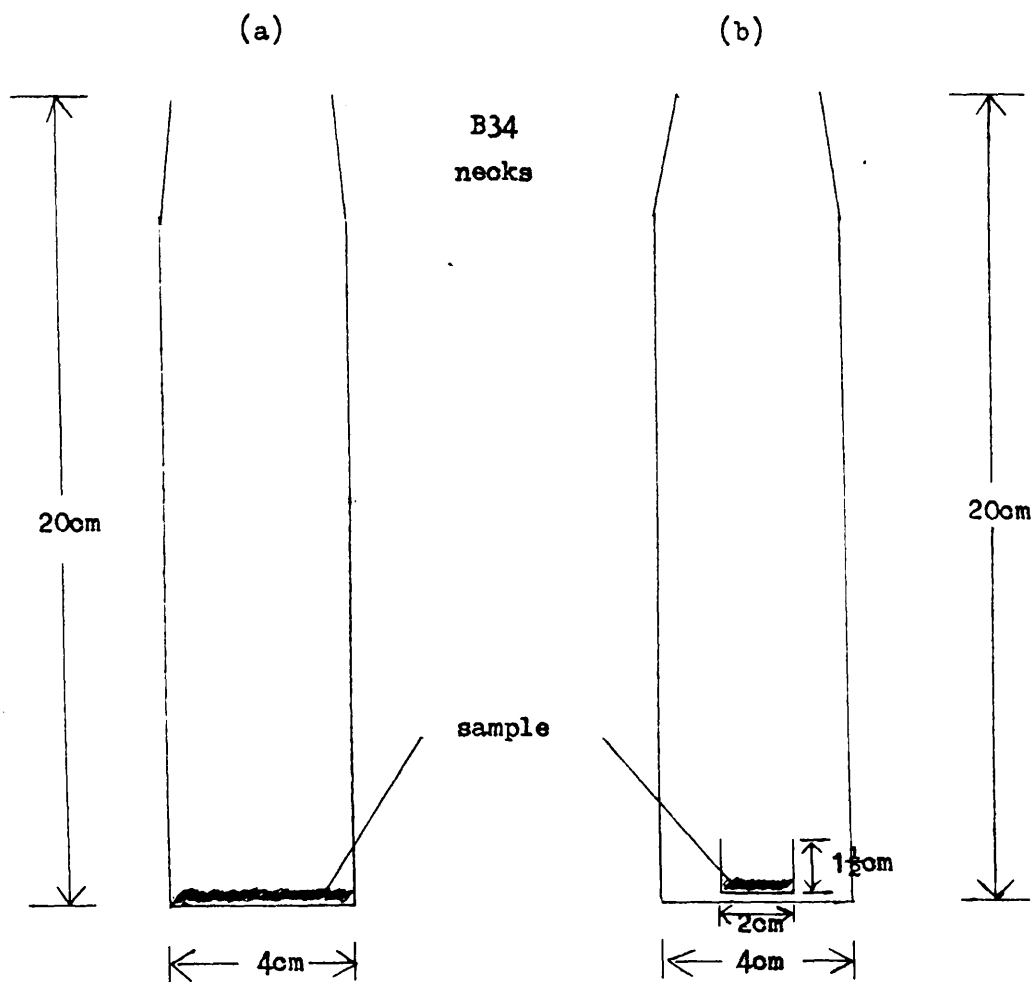


FIGURE 2.18

DEGRADATION TUBES

- (a) Polymer sample placed on base of tube for TVA and SATVA.
- (b) Polymer sample placed in sample bottle at base of degradation tube for ease of removal for molecular weight studies.

commencing the heating programme for thermal analysis (see Chapter 2.4).

Isothermal experiments, used to measure molecular weight changes on heating, the polymer sample was placed in a small sample tube inside the degradation tube (Figure 2.18) and connected to the vacuum system (Figures 2.2 and 2.5) and evacuated. A cold trap, -196°C , was placed at (B) (Figure 2.5) and the oven temperature set for the desired temperature (T). The temperature rise of the sample was followed by means of thermocouple (B) (Figure 2.2) whose reading was printed out on a multihead recorder unit. Zero time was taken when thermocouple (B) gave a reading corresponding to (T). The temperature was held at (T) for a specific time whereupon the oven was set to cool. Once the degradation tube had cooled the polymer sample was removed, re-weighed and the molecular weight measured by one of the methods described in Chapter 2.6.

(ii) Under an atmosphere of Nitrogen

The experimental set up is described in Figure 2.19. Tap (C) and (K) were closed and the nitrogen permitted to flush the system for 15 minutes at a rate of $100\text{ cm}^3/\text{min}$. While keeping the nitrogen flow at this level cold traps (-196°C) were then raised at (B) and (G). The nitrogen flow was set at $80\text{ cm}^3/\text{min}$ and either an isothermal programme as above or a linear temperature programme (from ambient to 500°C at a linear rate of temperature increase of $10^{\circ}\text{C}/\text{min}$) carried out. Tap (C) was opened and Tap (E) and (J) closed once the degradation tube had cooled. The system could now be opened to vacuum by opening Tap (K) and a subambient

- A, C, E, and K, L, M - Stopcocks
- B, G - spiral cold traps
- D, I - Drechsel Bottle
- F. - Oven as in Figure 2.2
- H - GEC Elliot 1100 Rotameter - flow meter.
- J - Water jacket

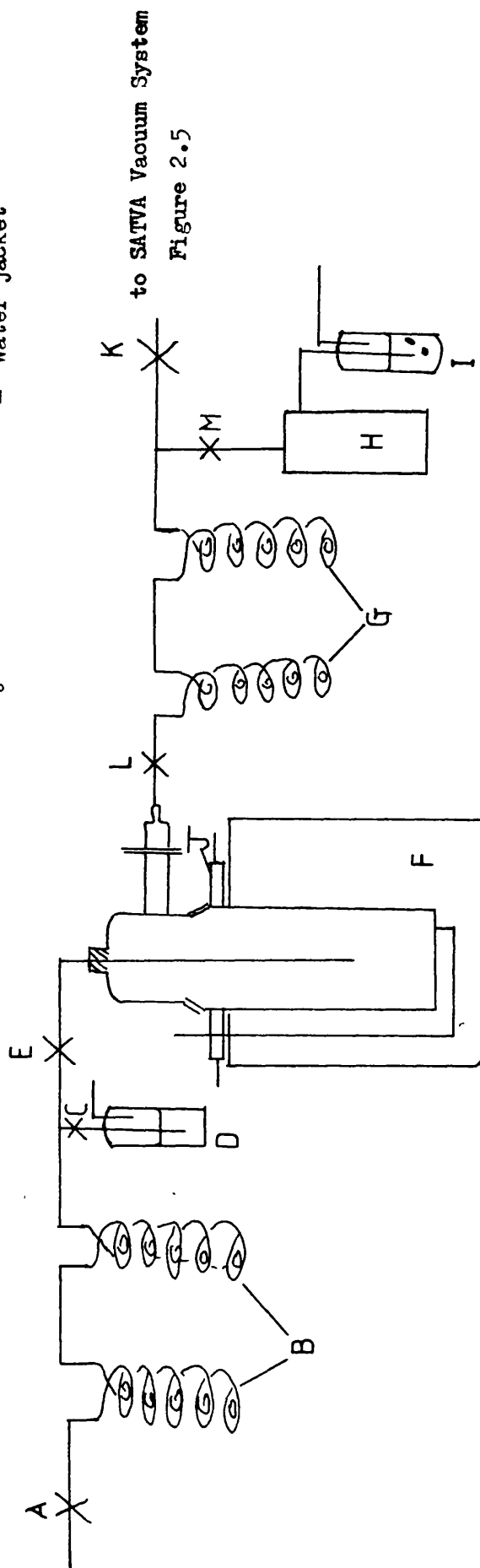


FIGURE 2.19

EXPERIMENTAL ARRANGEMENT FOR DEGRADATION CARRIED OUT UNDER NITROGEN

TVA carried out on the degradation products condensed in (G) or the polymer sample removed for measurement of molecular weight as described in Chapter 2.6.

(iii) Under an Atmosphere of Static Air

The experimental set up was as described in Figure 2.2 the sample being exposed to static air by leaving the B14 outlet open. The method and treatment of polymer samples was as described in 2.9 (i) above, except that the sample was under an atmosphere of static air rather than vacuum.

(iv) Closed System

This was used mainly to investigate the non-condensable products of thermal degradation. The method employed was essentially that described by McNeill. (Ref.76)

2.10 PREPARATION OF A SINGLE CRYSTAL MAT

The method used to prepare a single crystal mat of PHB was similar to that described by Alper et al (Ref.20).

To a 0.1% solution of PHB in CHCl_3 an equal volume of ethanol was added, the resultant solution being refluxed for 1 hour at 50°C . On cooling the flask containing the solution was stoppered and placed in a freezer at -20°C for 24 hours by which time a fluffy white precipitate had formed. This was compacted into a smaller volume by centrifugation at a temperature of -20°C prior to filtration using Whatman's No.42 Ashless filter paper.

The resultant highly crystalline sample (labelled SX) (see x-ray data page 22) was ground to a powder at liquid nitrogen temperatures and vacuum dried.

2.11 CLASSIFICATION OF PHB SAMPLES STUDIED IN THIS WORK

Table 2.B lists all the polymer samples studied during the course of this work. The molecular weight distribution data was measured by GPC (Chapter 2.6 (i)) and the impurities as detailed in Chapter 2.5 (viii).

The designations, e.g. S1 in the first column of Table 2.B shall be used throughout this work.

TABLE 2.B

CHARACTERISATION OF PHB SAMPLES USED IN THIS STUDY

PHB Polymer	MOLECULAR WEIGHT DISTRIBUTION					TRACE IMPURITIES						
	Number Average Molecular Weight \bar{M}_n	Viscosity Average Molecular Weight \bar{M}_v	Weight Average Molecular Weight \bar{M}_w	Poly-dispersity D	Ca ppm	Mg ppm	Zn ppm	Fe ppm	Al ppm	P ppm	S ppm	
S1	468,000	934,000	1,002,000	2.14	<20	6.9	-	46	-	-	-	
S2	126,000	192,000	201,000	1.59	-	-	-	-	-	-	-	
BLDX01	329,500	772,000	863,000	2.62	205	9.9	9.7	81	-	-	-	
SX	329,500	772,000	863,000	2.62	210	27.0	42.0	135	-	-	-	
F1	658,000	975,100	1,029,000	1.56	48	8.1	5.5	55	<20	20	195	
F2	525,000	790,000	838,000	1.60	77	5.2	<4	58	<20	15	95	
F3	506,000	834,000	890,000	1.76	110	11.0	9.5	66	<20	15	265	
F4	63,000	465,000	546,000	8.71	<20	<4	<4	57	<20	5	290	

NOTE: (a) Molecular weight distribution was obtained by GPC using Instrument A. (Chapter 2.6(i)).

(b) Values of trace impurities were obtained as detailed in Chapter 2.5 (viii)

CHAPTER 3

THE PRODUCTS OF THERMAL DEGRADATION OF PHB UNDER VACUUM

3.1 INTRODUCTION

The aim of the work described in this chapter was to investigate fully, using the various methods of thermal analysis, the products formed on heating PHB under vacuum, and, having accomplished this, to propose possible mechanisms for their formation. The effect of these products on the processing of PHB will also be discussed.

Unless otherwise stated the work described in this chapter was carried out on sample S1 of PHB (see Chapter 2.11).

3.2 THERMOGRAVIMETRIC ANALYSIS

TG was performed on approximately 5mg samples of PHB under, (a) a dynamic nitrogen flow, (b) vacuum, and (c) static air, with a heating programme of $10^{\circ}\text{C}/\text{min}$ from ambient to 500°C (see Chapter 2.4 (i)). The traces are illustrated in Figure 3.1 and the results summarised in Table 3.A.

In each case a one step weight loss was observed, between approximately 250°C and 300°C , leaving a residue of 0-2.5%.

As expected the earliest signs of weight loss were recorded under vacuum where volatile material can diffuse most readily from the degrading polymer. The first sign of weight loss under static air (230°C) occurred 10°C lower than under flowing nitrogen perhaps indicating a slightly increased reactivity of PHB in air. The lower rate of weight loss in air was expected, due to the static atmosphere.

KEY: (a) N₂ flow of 80cm³/min.
(b) static air
(c) N₂ flow of 40cm³/min.
(d) Vacuum
Heating rate 10°C/min

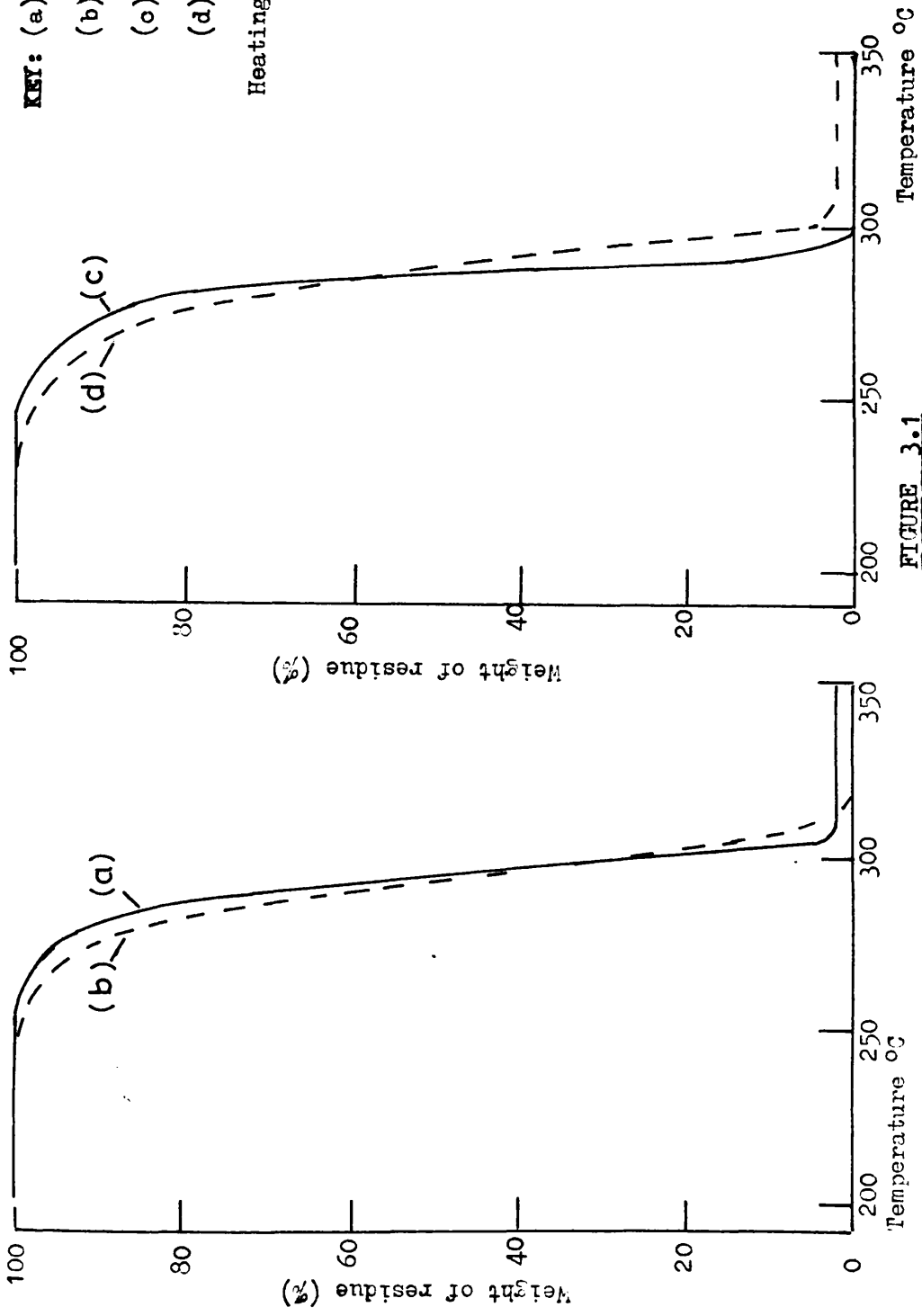


FIGURE 3.1
TG TRACES OF PHB UNDER VARIOUS ATMOSPHERES

TABLE 3.A

A SUMMARY OF THE TG TRACES ILLUSTRATED IN FIGURE 3.1

Instrument	Atmosphere	Temperature of onset of weight loss °C	Extrapolated temperature of onset of weight loss °C	Temperature at which 50% weight loss is recorded °C	Temperature at which weight loss terminated °C	Weight of residue (% of original)
950	N ₂ flow of 3 80cm ³ /min	240	281	292	307	2
950	Static Air	230	276	292	320	0
951	N ₂ flow of 3 40cm ³ /min	242	273	285	300	0
951	Vacuum	225	275	289	303	2.5

3.3 DIFFERENTIAL THERMAL ANALYSIS

Figure 3.2 illustrates a DTA trace obtained as described in Chapter 2.4 (ii). The trace shows two peaks,

- (a) a melting endotherm from 135°C to 185°C peaking at 176°C and,
- (b) An endotherm due to degradation from 235°C to 310°C .

The shape of this endotherm is typical of rapid evolution of volatiles from a viscous liquid.

Thus DTA shows that this sample of PHB melts in the range 135°C to 185°C and degrades with rapid evolution of volatiles between 235°C and 310°C with no further reaction above 310°C .

3.4 DIFFERENTIAL SCANNING CALORIMETRY

DSC was carried out on a 5mg sample of PHB as outlined in Chapter 2.4 (iii). The resultant trace, illustrated in Figure 3.3, shows two endotherms,

- (a) occurring in the temperature range 143°C to 190°C with a peak maximum at 180°C due to melting and,
- (b) occurring in the temperature range 250°C to 308°C with a peak maximum at 295°C due to degradation.

The sharp peak at 280°C in this sample was reproducible and an explanation for this is given in Chapter 6.8 p 216

No endotherms or exotherms were observed above 310°C .

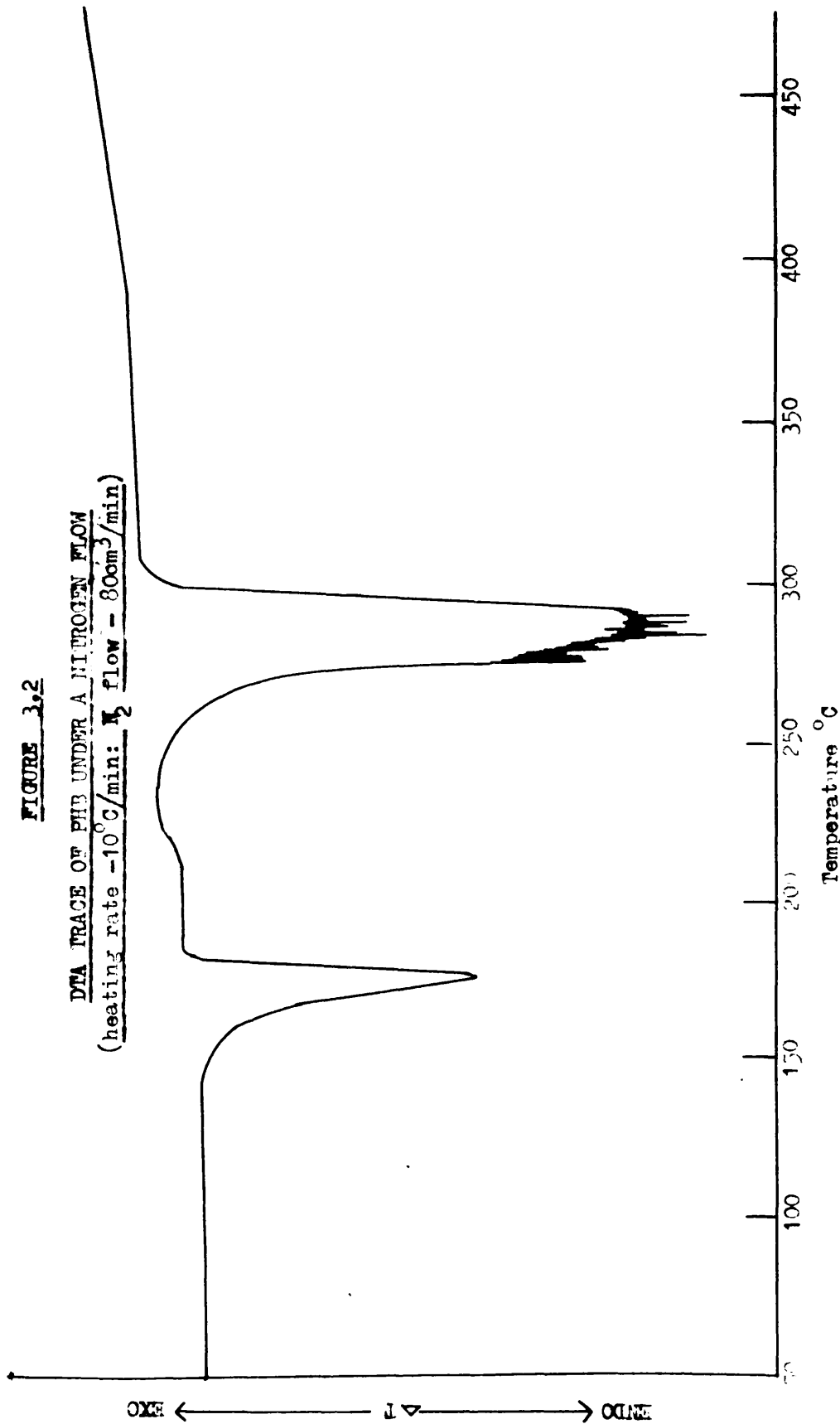
Thus all degradation seems to occur between 250°C and 310°C .

3.5 THERMAL VOLATILISATION ANALYSIS

A 60mg sample of PHB was heated at a programmed rate of $10^{\circ}\text{C}/\text{min}$ from ambient to 500°C . The evolution of volatiles was measured

FIGURE 3,2

DTA TRACE OF PHB UNDER A NITROGEN FLOW
(heating rate $-10^{\circ}\text{C}/\text{min}$; N_2 flow $- 80\text{cm}^3/\text{min}$)



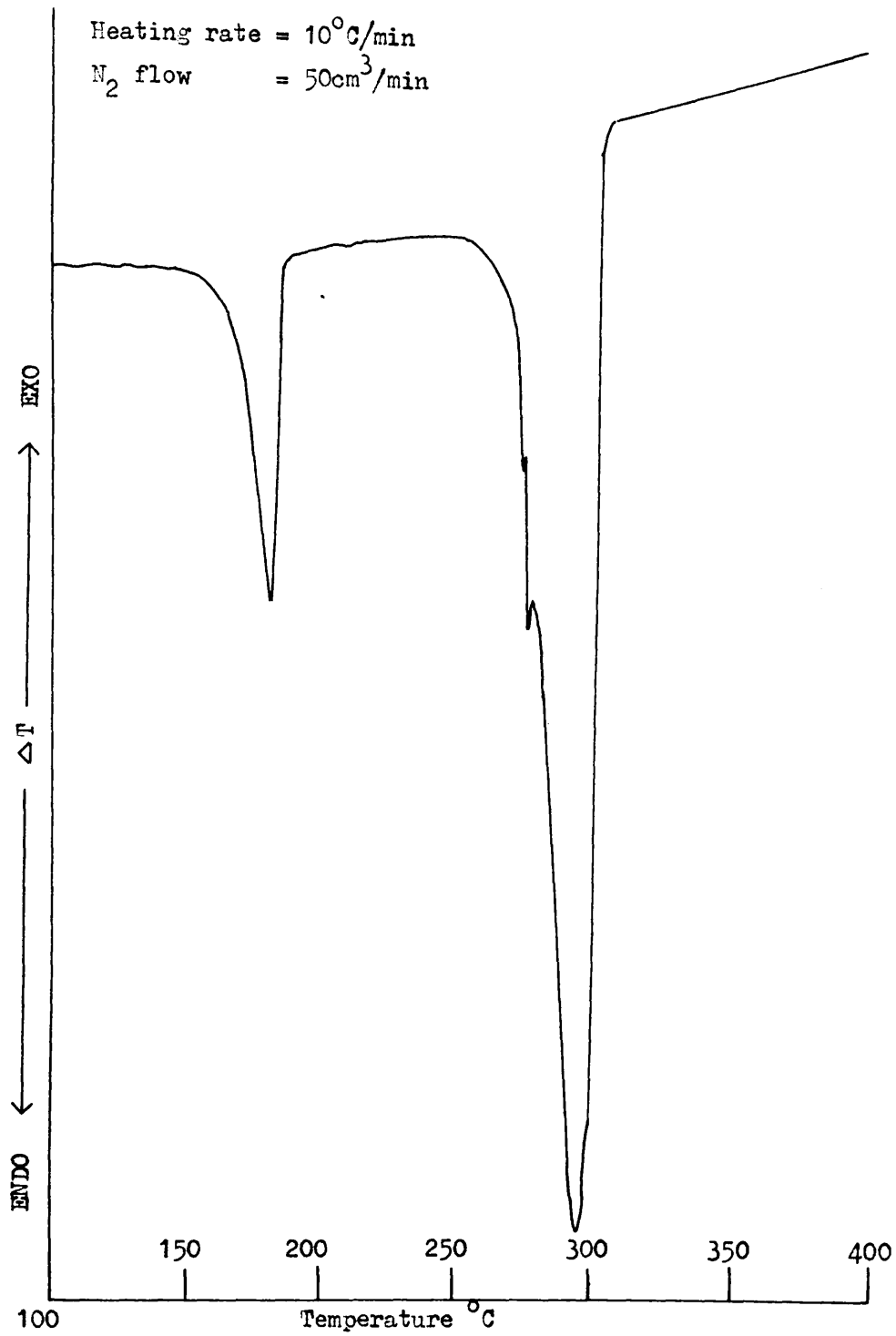


FIGURE 3.3
DSC TRACE OF PNB

as a function of oven temperature as described in Chapter 2.4 (iv).

From the trace, illustrated in Figure 3.4, it can be seen that the evolution of volatiles occurs in two distinct stages. In the first, volatile products were first detected around 240°C reaching a maximum at 310°C before falling to a minimum at 338°C . The second stage evolution of volatiles occurs at temperatures above 340°C resulting in a broader peak with a maximum in the region of 441°C .

This two stage evolution of volatiles appears to contradict the TG, DTA and DSC results in which no reaction was observed above 310°C . This was therefore further investigated.

3.6 THERMAL VOLATILISATION ANALYSIS WITH DIFFERENTIAL CONDENSATION OF PRODUCTS

Figure 3.5 illustrates the trace obtained from TVA with differential condensation of products.

The volatile products evolved between 240°C and 338°C (Stage 1) consist mainly, wholly below 285°C , of products which condense in all but the 0°C trap. Above 285°C volatiles which pass through the 0°C and the -45°C trap are observed. The -45°C trace goes through a minimum at 338°C . Volatiles which condense only in the -196°C trap were observed between 309°C and 323°C and then again at temperatures above 351°C . The small response in the -196°C trace above 429°C demonstrates the formation of a small proportion of products volatile at -196°C (non-condensables).

The relative difference in response from each Pirani head at a given time gives a rough guide to the relative proportions of products of various volatilities, since each Pirani is matched to give the same response to a given pressure. Thus the major

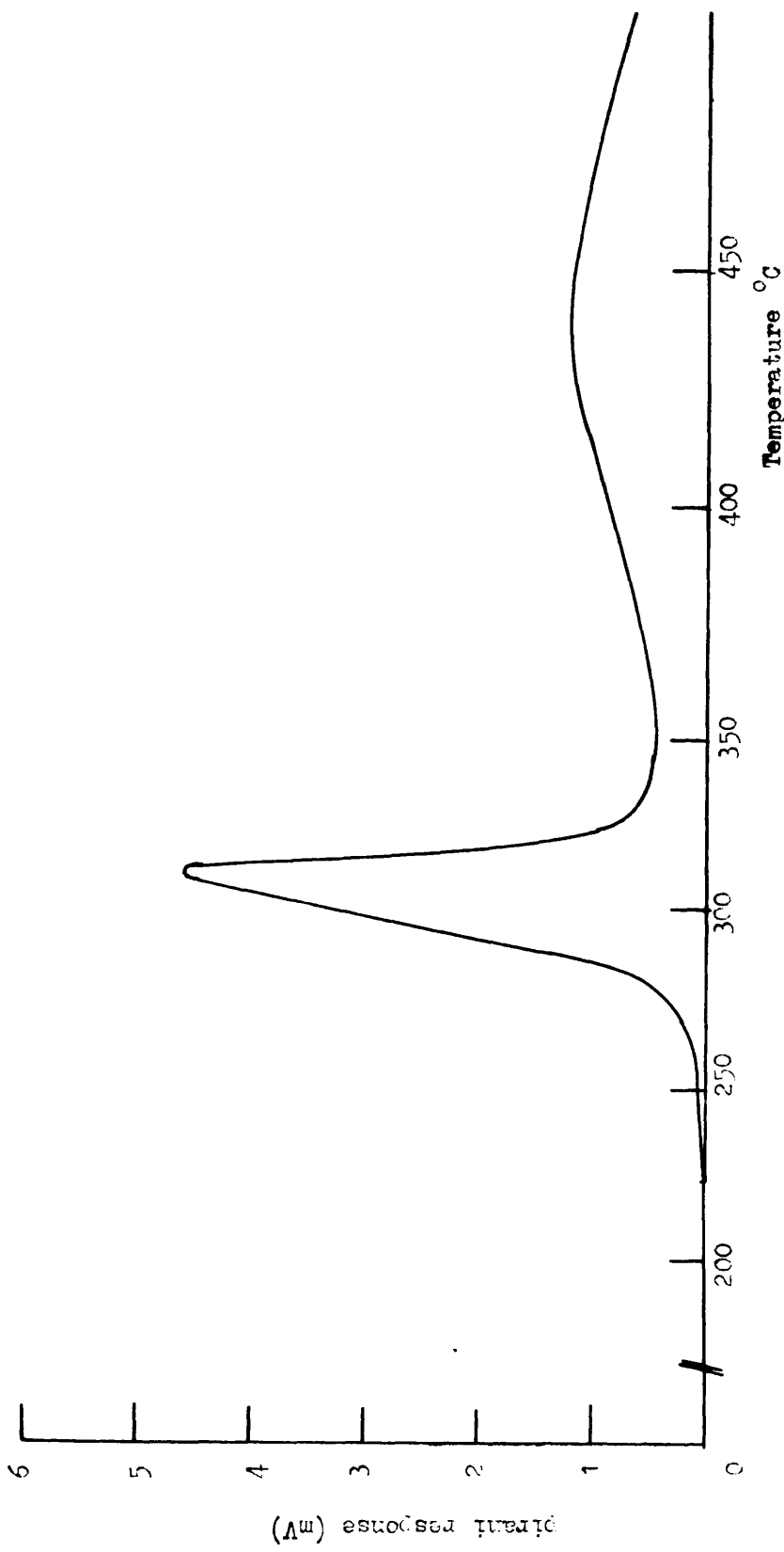


FIGURE 3.4

TVA TRACE OF PHB

(50ml sample, heating rate 10°C/min from ambient to 500°C)

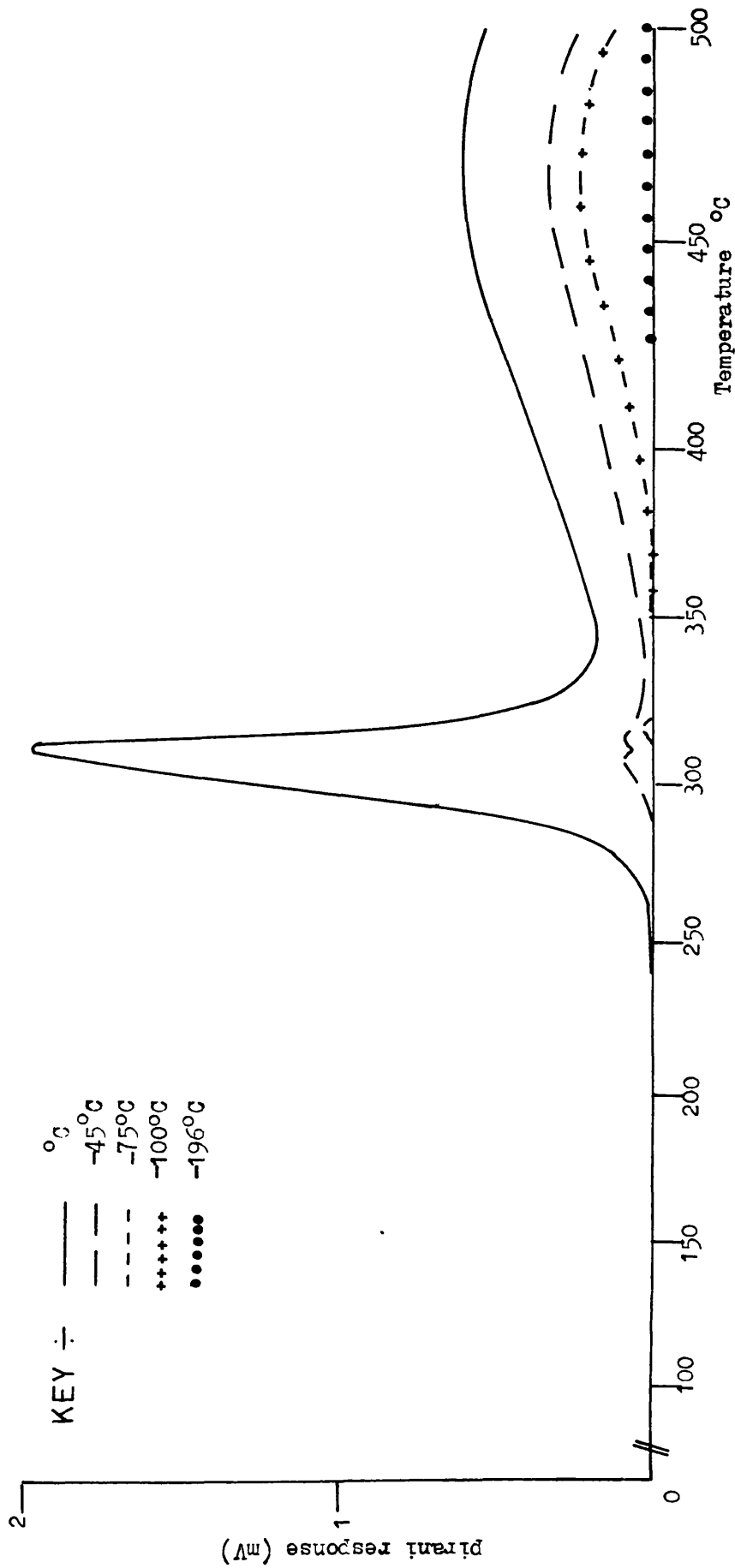


FIGURE 3.5
PVA WITH DIFFERENTIAL CONDENSATION OF PRODUCTS OF PFB TRACE
 (60mg sample, heating rate 10°C/min from ambient to 500°C)

product(s) from the thermal degradation of PHB under the above conditions condenses at -45°C under vacuum and it is only at temperatures above 340°C that products of higher volatility are produced in any quantity.

The products responsible for the TVA trace were identified by SATVA.

3.7 SUBAMBIENT TVA OF THE VOLATILE DEGRADATION PRODUCTS (ambient to 500°C)

The volatile products in cold trap B of Figure 2.5 were isolated and analysed by means of SATVA as outlined in Chapter 2.4 (v).

The SATVA trace, illustrated in Figure 3.6, shows 6 peaks at temperatures ranging from -150°C to ambient. The product(s) responsible for each peak were removed from the vacuum system as described in Chapter 2.4 (v) and identified by the various analytical techniques outlined in Chapter 2.5.

The products from peak A were isolated and identified from their IR spectra, in the gaseous state, Figure 3.7, as carbon dioxide (CO_2), ketene (CH_2CO) and propene (CH_2CHCH_3) by comparison with standard gas IR spectra. (Ref. 90-92)

The material responsible for peak B was identified from its gas phase IR spectrum, Figure 3.8, as acetaldehyde (CH_3CHO) by comparison with standard spectra (Ref. 93). and from its MS, molecular ion $m/e = 44$.

The product responsible for peak C was identified from its MS, molecular ion $m/e = 18$, as water (H_2O).

The IR spectrum of the product of peak D, its NMR spectrum and mass spectrum are illustrated in Figures 3.9(a), 3.10(a)

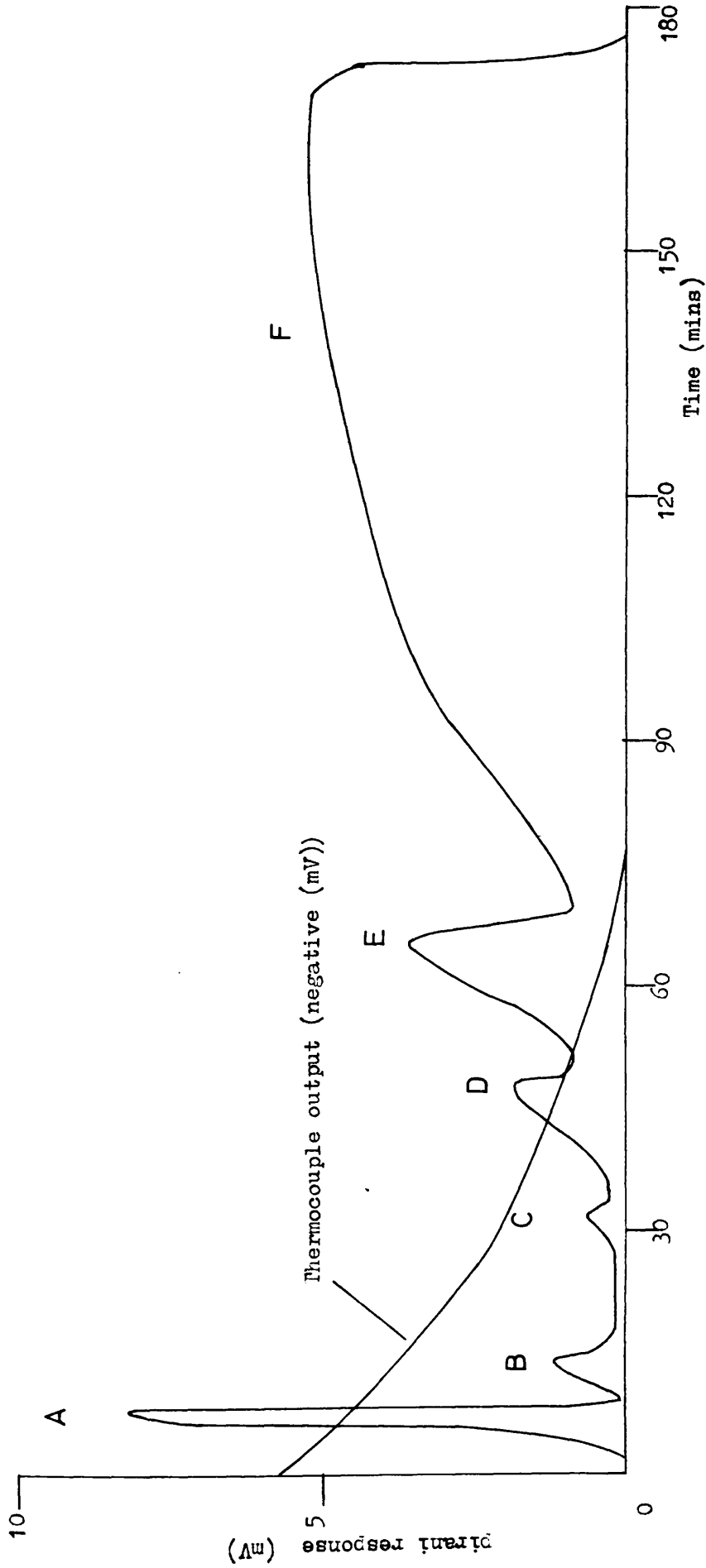


FIGURE 3.6

SATVA TRACE OF THE PRODUCTS OF THERMAL DEGRADATION OF PHB
 (60mg sample, heating rate 10°C/min from ambient to 500°C)

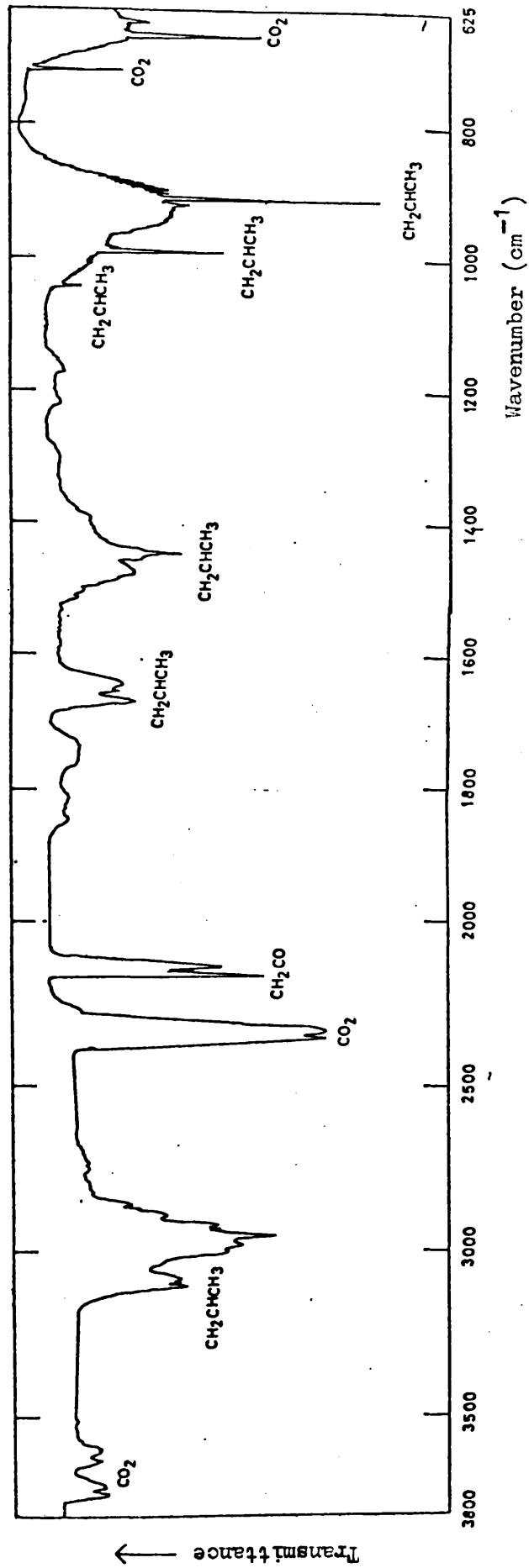


FIGURE 3.7

IR SPECTRUM OF THE PRODUCTS OF PEAK A

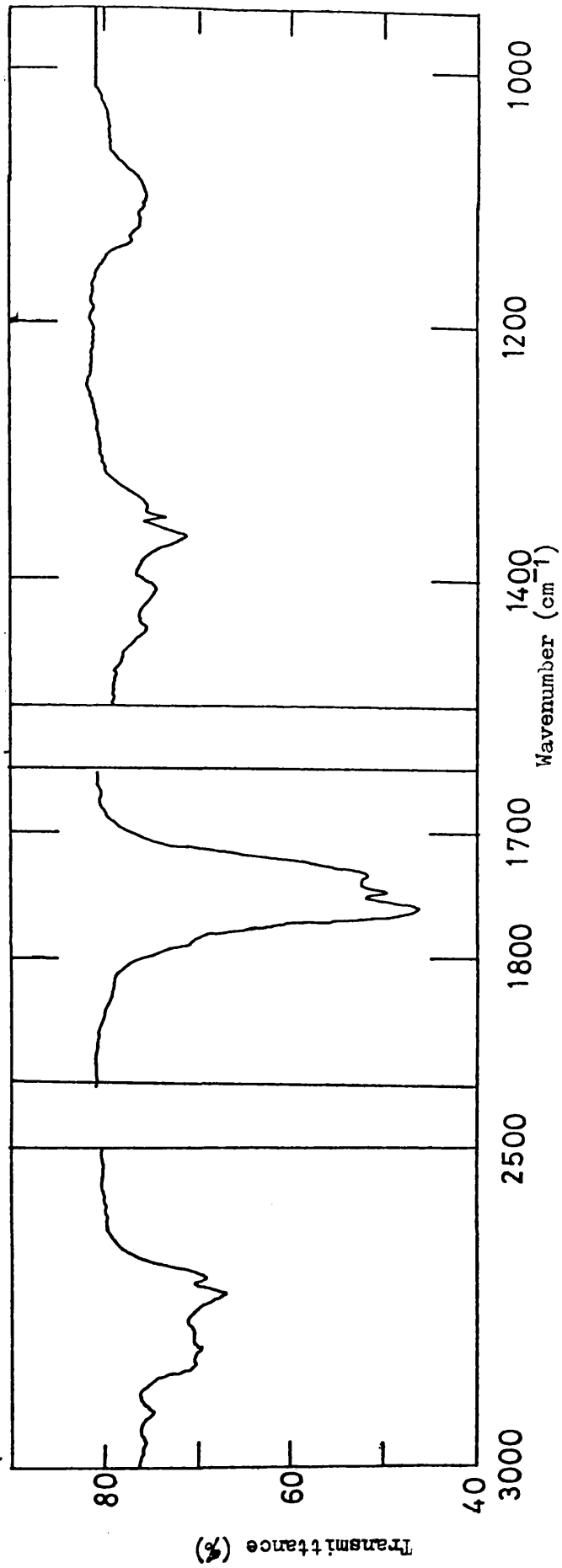


FIGURE 3.8

IR SPECTRUM OF THE PRODUCT OF PEAK B

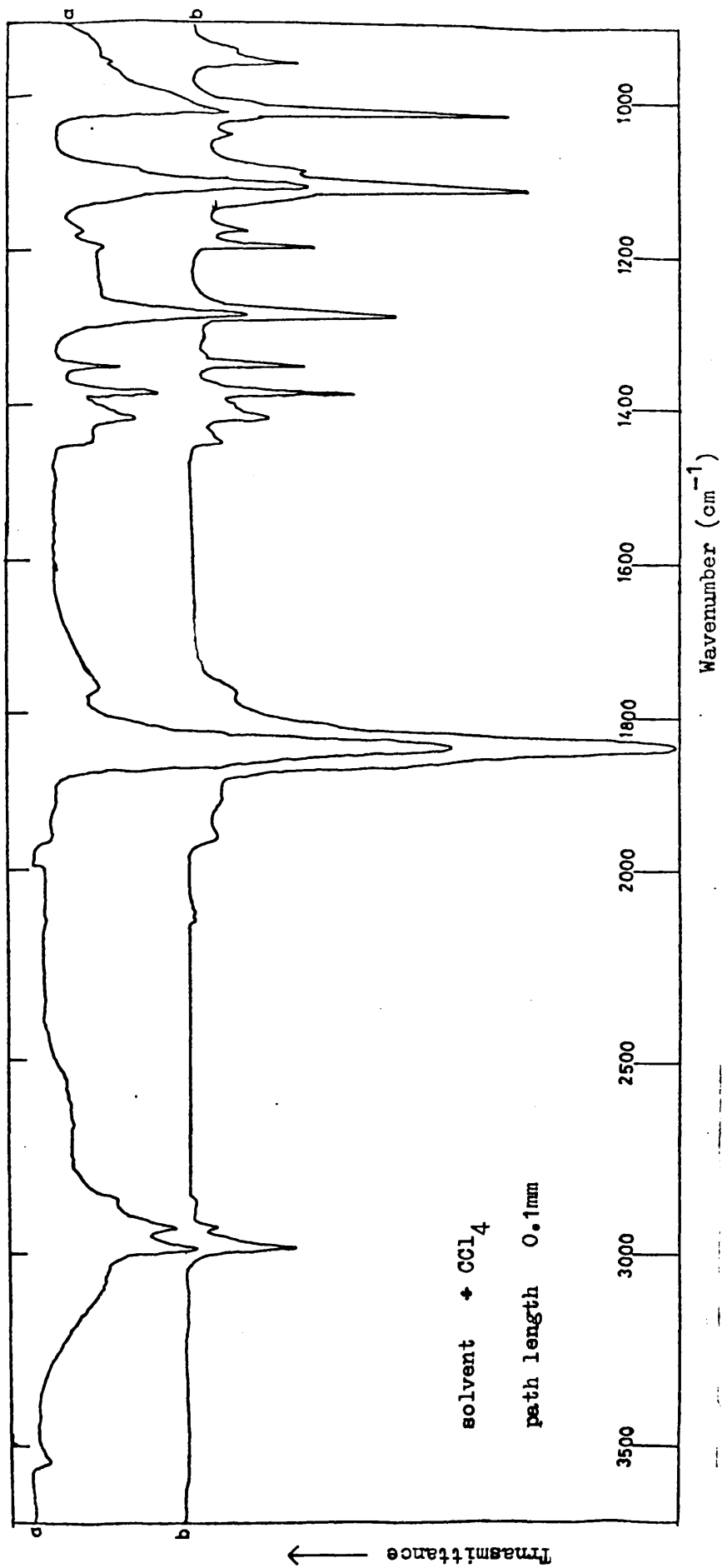
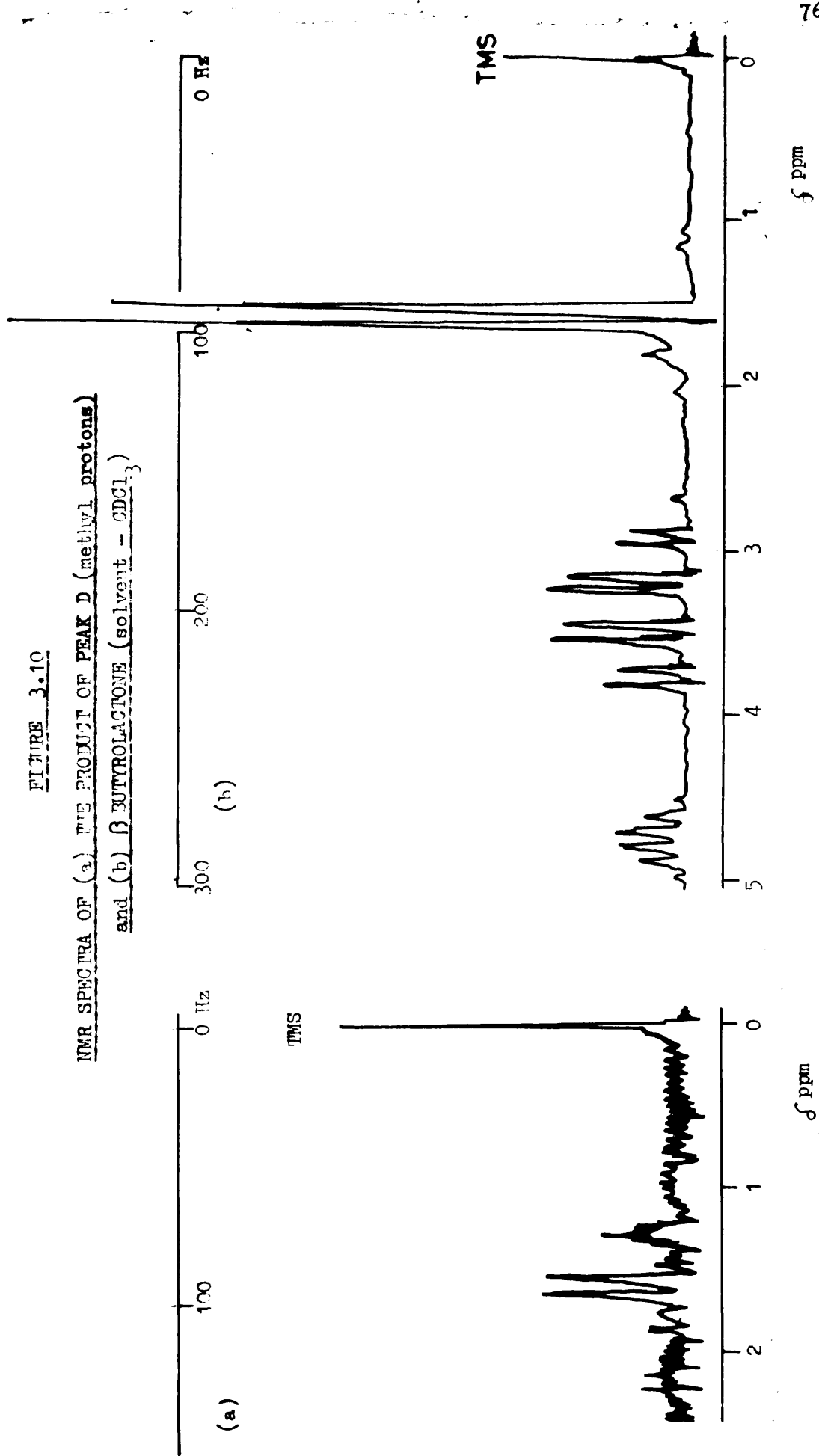


FIGURE 3.9
IR SPECTRA OF (a) THE PRODUCT OF PEAK D
AND (b) β -BUTYROLACTONE

FIGURE 3.10

NMR SPECTRA OF (a) THE PRODUCT OF PEAK D (methyl protons)
and (b) β BUTYROLACTONE (solvent - $CDCl_3$)



and 3.11 respectively. The stretching frequency of the C=O bond at 1840cm^{-1} in the IR was in the region characteristic of a 4 membered ring lactone, which, along with the molecular ion peak in the MS of $m/e = 86$ suggests that peak D is due to β -butyrolactone (4-methyl-2-oxetanone or β BL). The IR compared favourably with standard literature reference spectra of β BL (Ref. 94, 95). A pure sample of β BL was prepared from β -bromobutyric acid by the method outlined by Agostini et al (Ref. 27) and was purified by vacuum distillation. The IR and NMR spectra of this material are shown in Figures 3.9(b) and 3.10(b) respectively. A comparison of the NMR spectra is made in Table 3.B. From this information it is clear that, Peak D, is indeed due to β -butyrolactone.

Peak F will be discussed before Peak E since knowledge of the nature of peak F is relevant to the discussion of Peak E.

Figure 3.6 demonstrates that the material of peak F is the major condensable degradation product. Mass spectra, IR and NMR spectra of peak F were compared with equivalent spectra of crotonic acid, Figures 3.12, 3.13, 3.14 and Table 3.C and were shown to be identical. Therefore crotonic acid (trans but-2-enoic acid) is responsible for peak F.

The product responsible for peak E was removed from the vacuum system and MS, IR and NMR spectra obtained as in Figures 3.15, 3.16 and 3.17 respectively. Comparison with the respective spectra for crotonic acid, Figures 3.12(b), 3.13(b), 3.14(b), demonstrates the following.

- (a) The MS of peak E is essentially identical to that of crotonic acid.

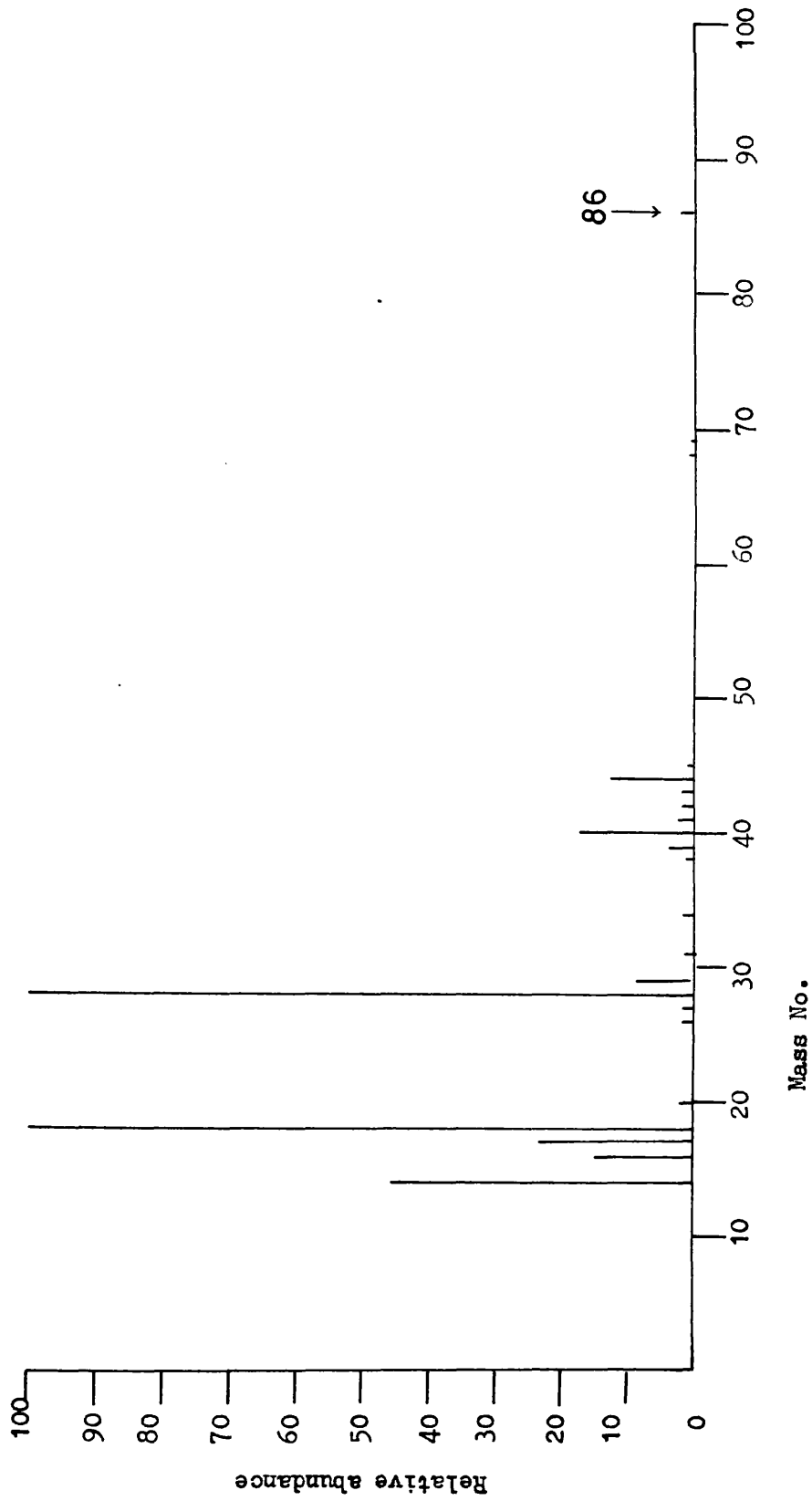


FIGURE 3.11

MASS SPECTRUM OF THE PRODUCT OF PEAK D

TABLE 3.B

COMPARISON OF THE NMR OF PEAK D WITH THAT OF PURE β BL

PEAK D			β BL			
δ ppm	J Hz	Int	δ ppm	J Hz	Int	
1.52	6.6	1	1.53	6	1)	
1.63		1	1.63		1)	3
Too weak to be observed			2.88		1	
			2.95		1)	
			3.18		4)	
			3.23		4)	
			3.47		4)	2
			3.54		4)	
			3.71		1)	
		3.81		1)		
Too weak to be observed			4.50		1)	
			4.60		4)	
			4.70		8)	1
			4.78		8)	
			4.88		4)	
			4.96		1)	

Key: δ = chemical shift ppm.

J = coupling constant Hz

Int = integral of peak area.

Errors: Estimated absolute errors in δ and J due to measurements from spectra alone are -

$$\delta = \pm 0.02 \text{ ppm}$$

$$J = \pm 1 \text{ Hz}$$

Instrument: spectra were run on a 60 MHz machine in CDCl_3 .

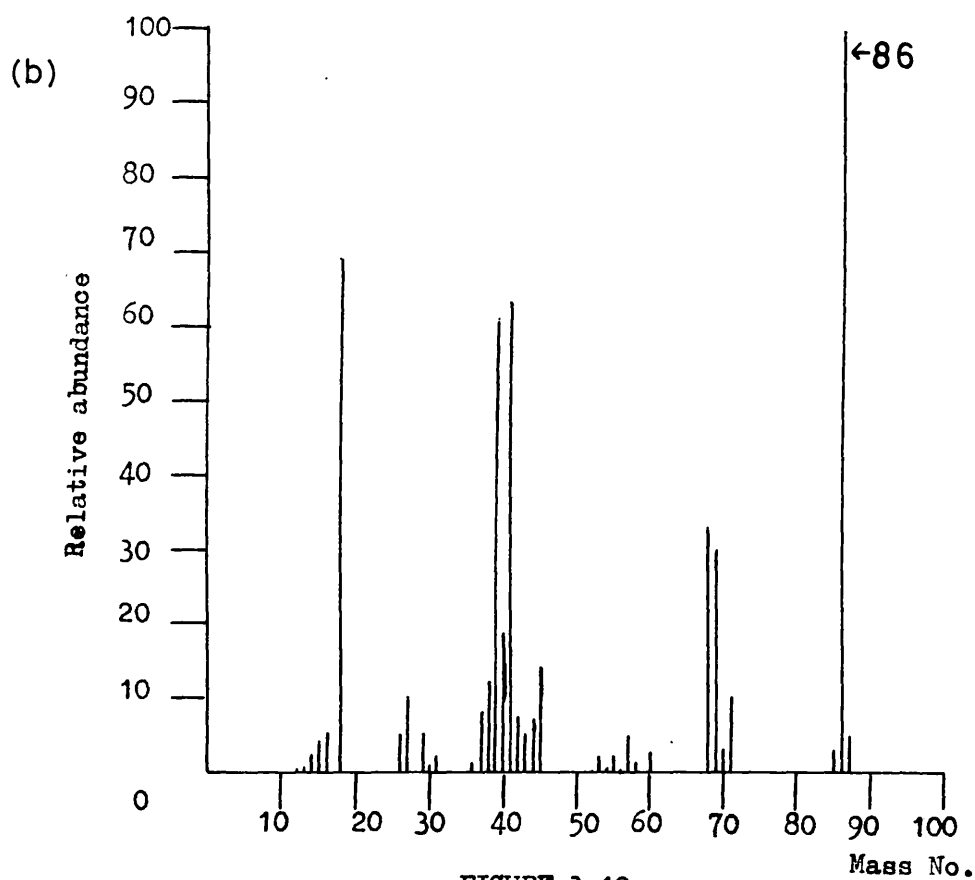
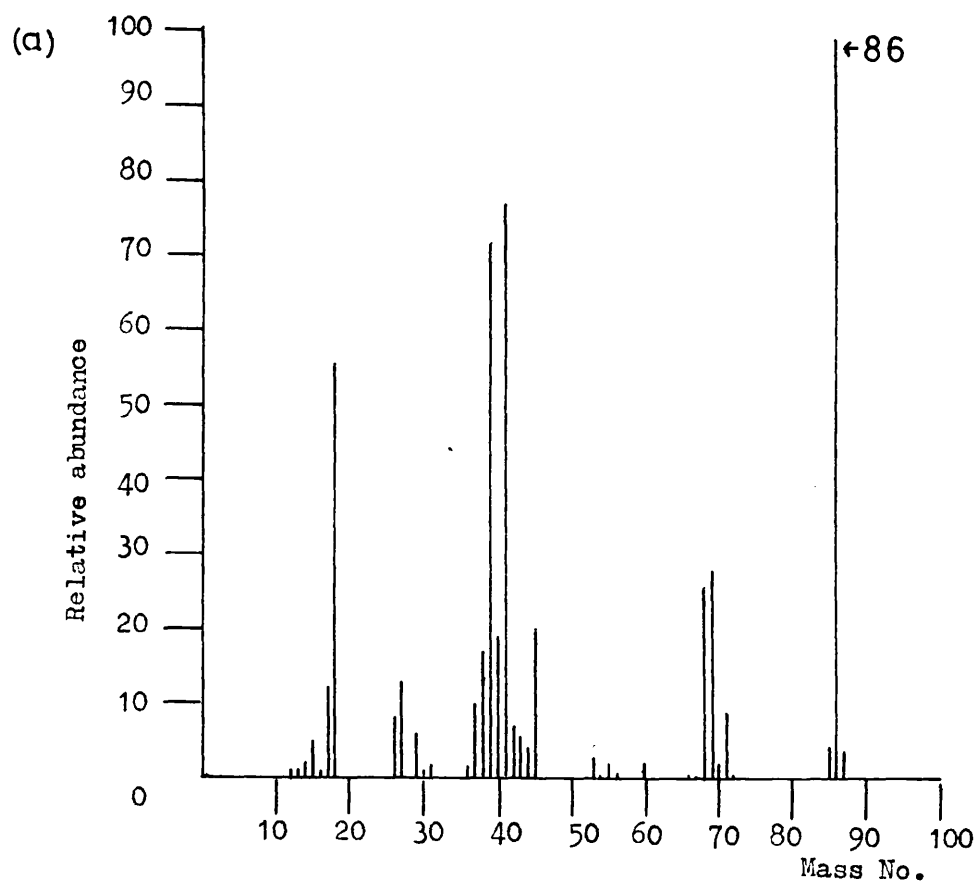


FIGURE 3.12

**MASS SPECTRUM OF (a) THE PRODUCT OF PEAK F AND
(b) CROTONIC ACID**

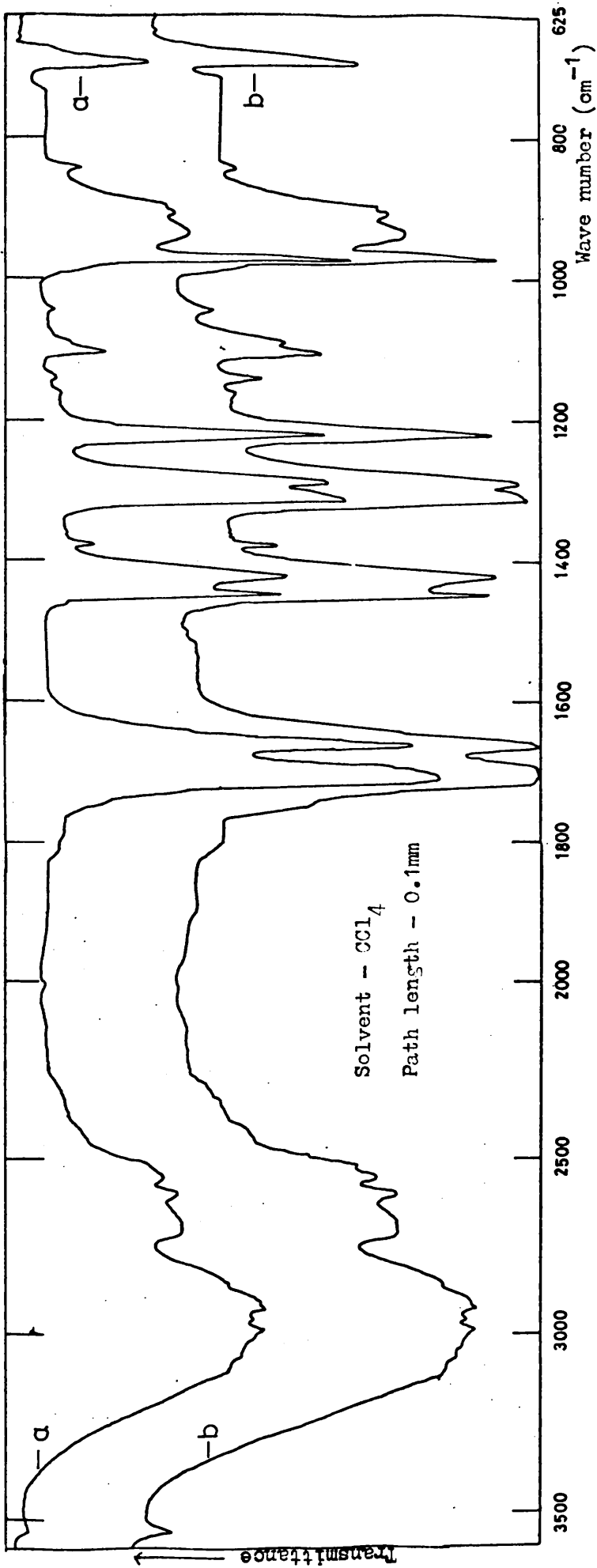


FIGURE 3.13

IR SPECTRA OF (a) THE PRODUCT OF PEAK F and (b) CROTONIC ACID

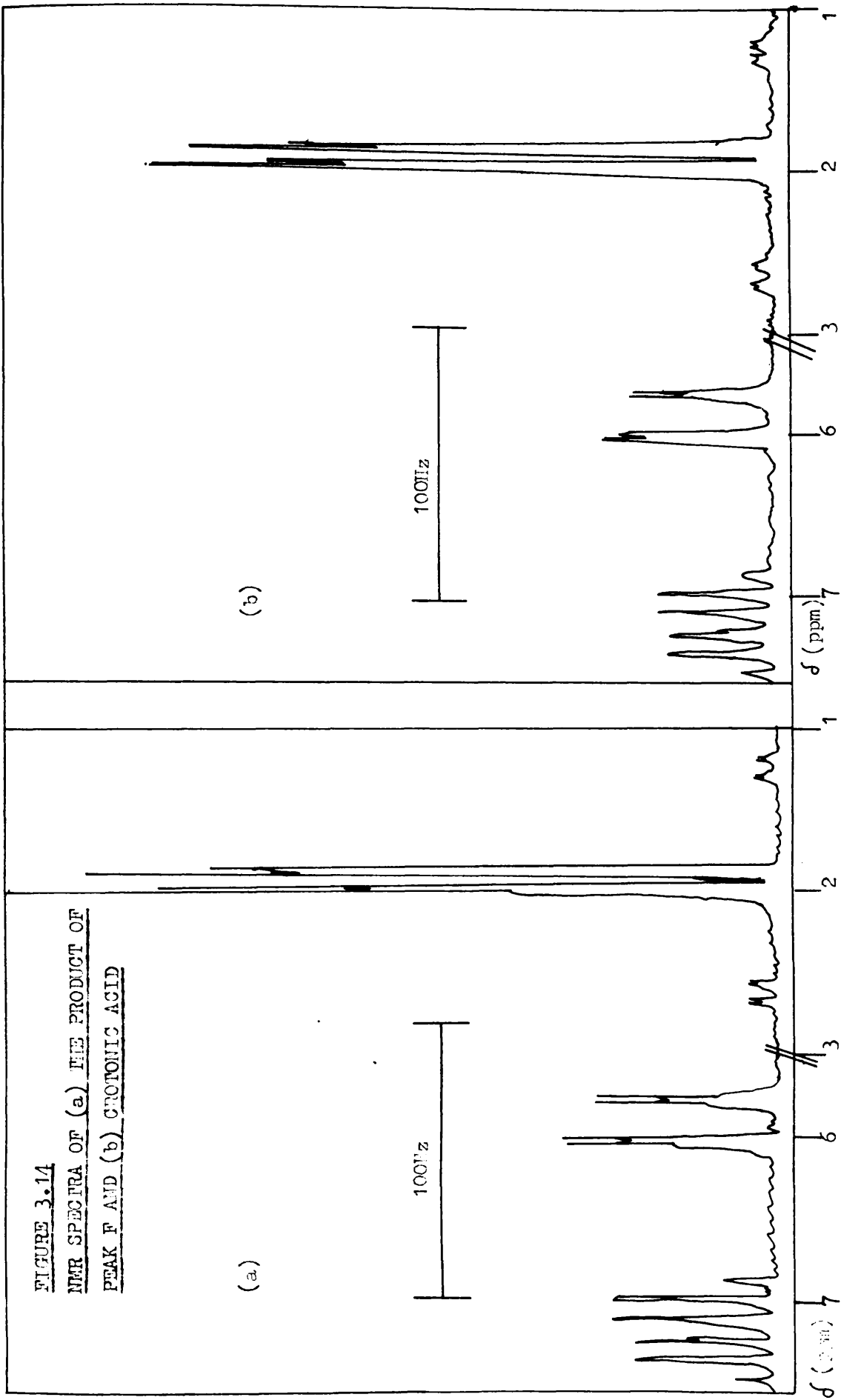


TABLE 3.C

COMPARISON OF THE NMR OF PEAK F
WITH THAT OF PURE CROTONIC ACID

P E A K F			CROTONIC ACID				
δ ppm	J Hz	Int	δ ppm	J Hz	Int		
1.84	1.8	1)	1.85	1.2	1)		
1.87			6.6			1.87	6.9
1.95						1.97	
1.98	1.8	1)	1.98	0.6	1)		
5.72	1.8	1)	5.73	1.8	1)		
5.75			15.6			5.76	15.3
5.98						5.98	
6.01	1.8	1)	6.02	2.4	1)		
6.82	7.8	1)	6.85	7.8	1)		
6.95			4)			6.98	6
7.08						7.08	
7.22	8.4	4)	7.23	9	4)		
7.32	6.0		7.35	7.2			
7.44	7.2		4)	7.45		6	
		1)			1)		

Key δ = chemical shift ppm.
 J = coupling constant Hz.
 Int = integral of peak area.

Errors: Estimated absolute errors in δ and J due to measurements from Spectra alone are:

$$\delta = \pm 0.02 \text{ ppm}$$

$$J = \pm 1 \text{ Hz}$$

Instrument: Spectra were run on a 60 MHz NMR in CDCl_3
 (Chapter 2.5)

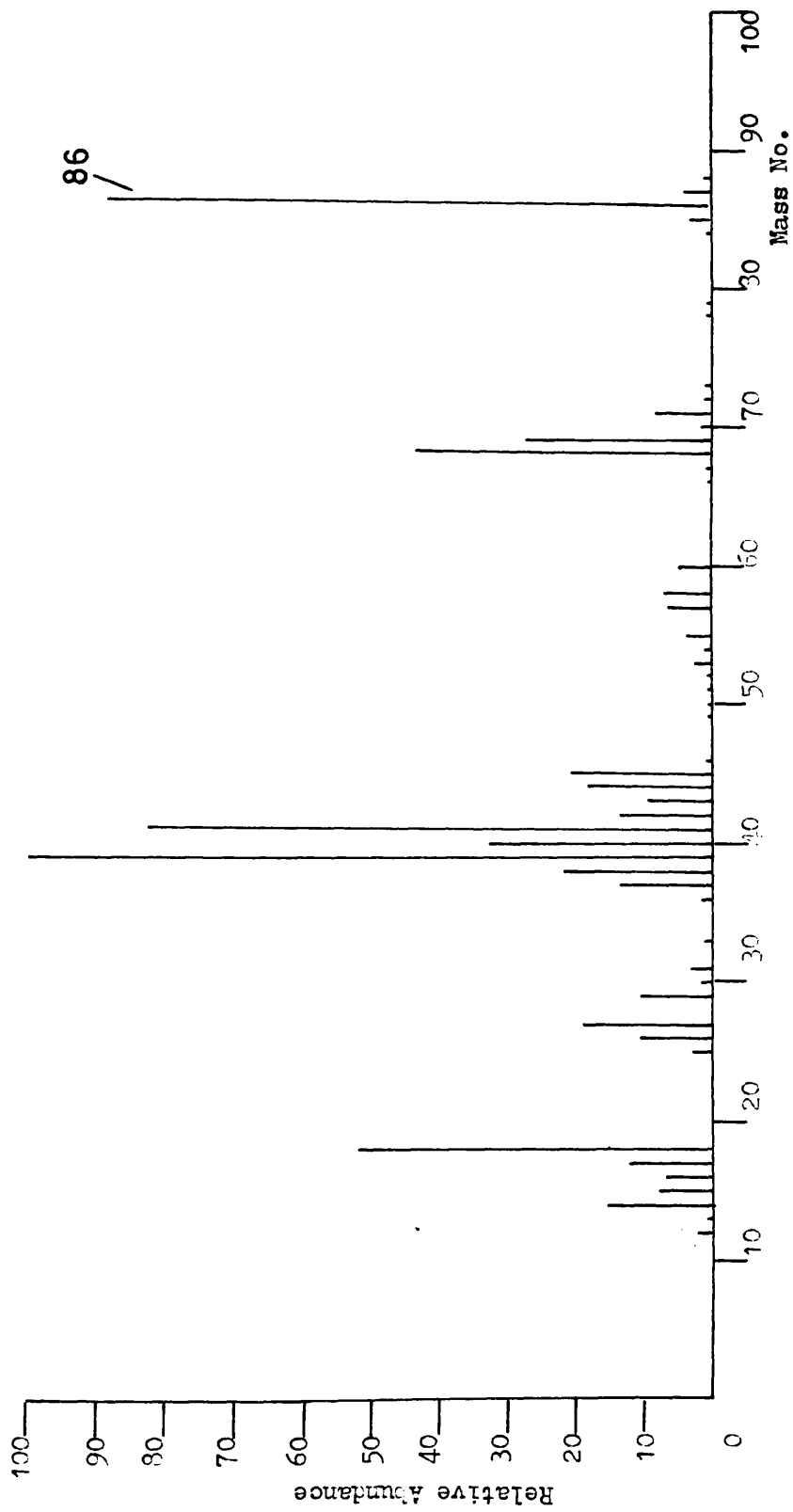


FIGURE 3.15
MASS SPECTRUM OF THE PRODUCT OF PEAK E

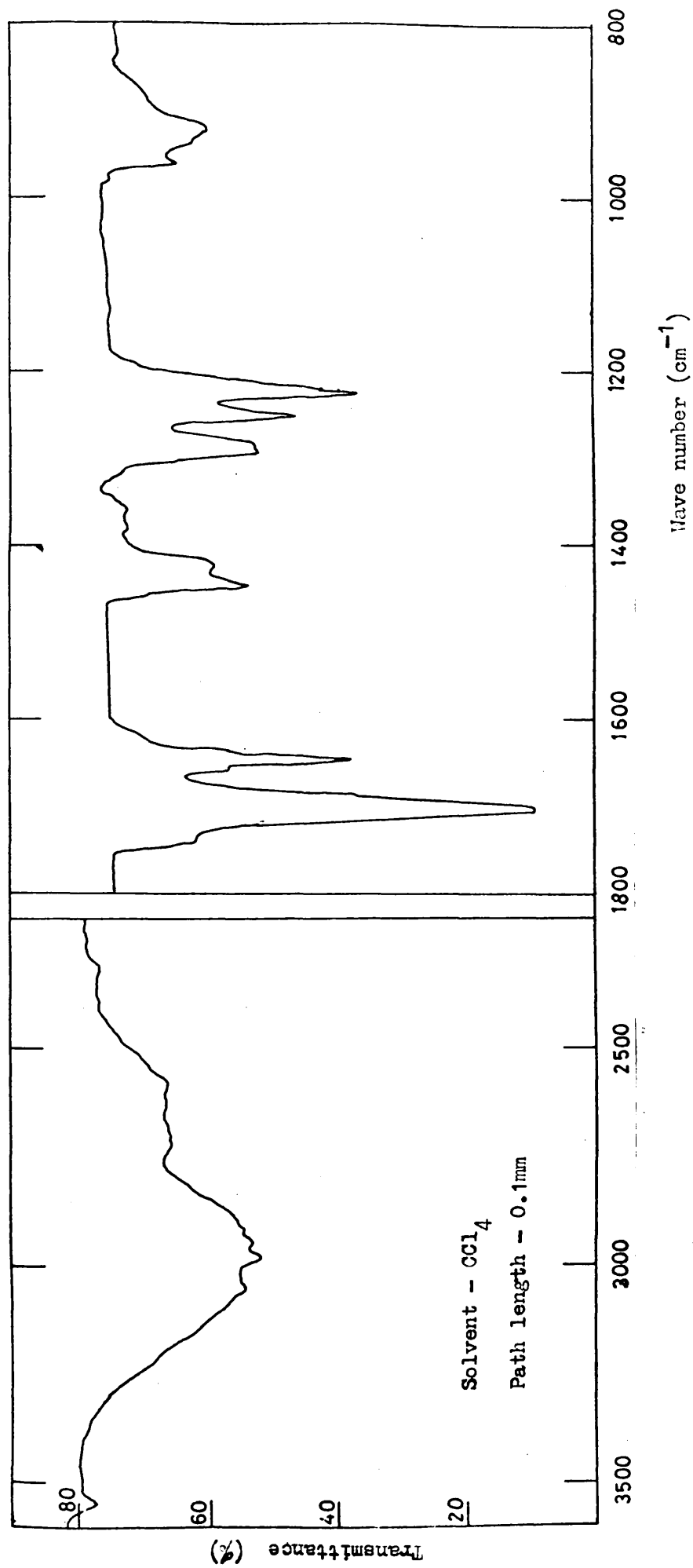


FIGURE 3.16
IR SPECTRUM OF THE PRODUCT OF PEAK K

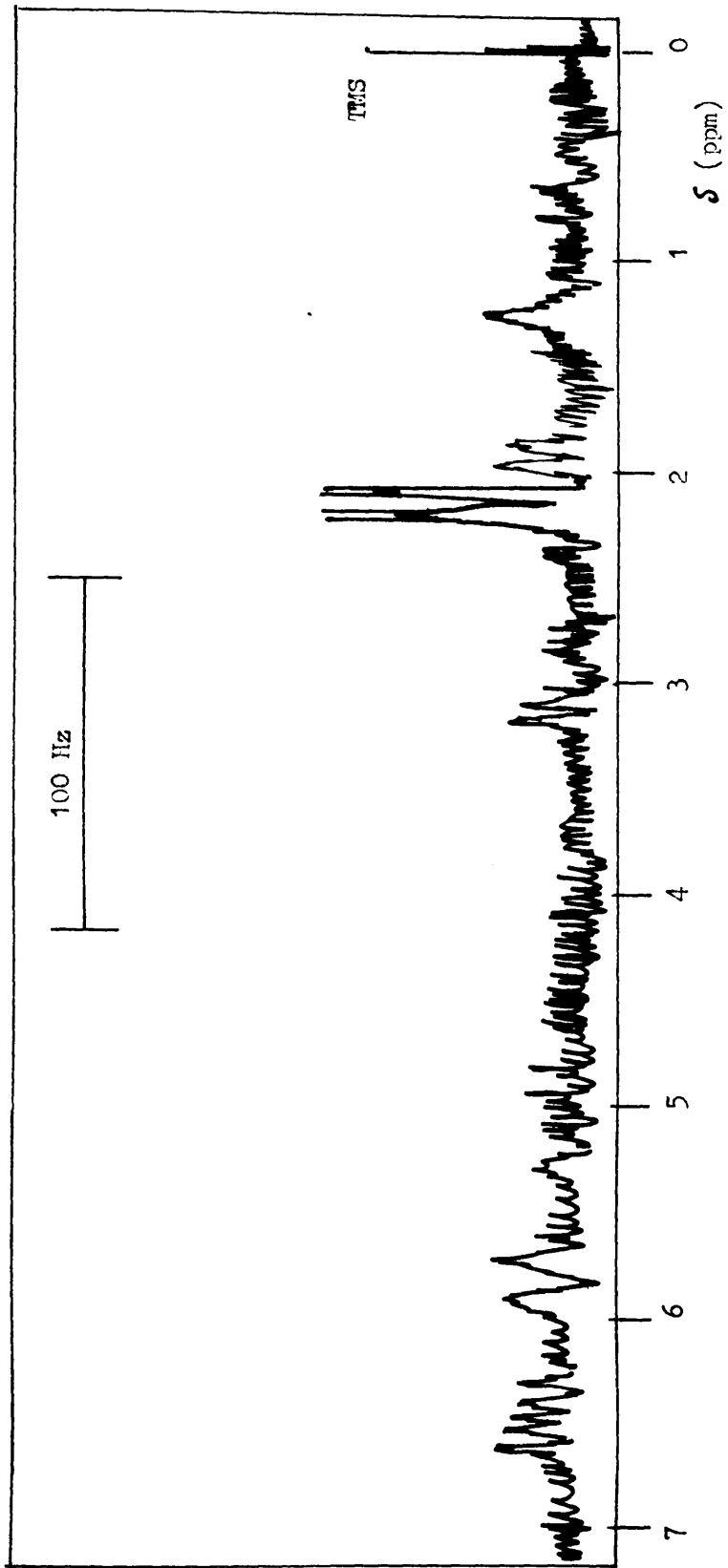
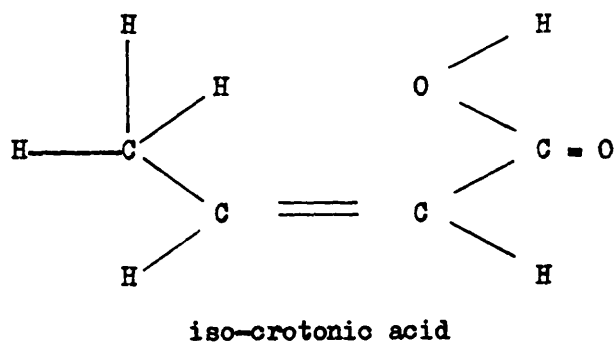


FIGURE 3.17

NMR SPECTRUM OF THE PRODUCT OF PEAK E

- (b) The IR spectra are similar, the main difference being in the position of the C=O and C=C stretching frequencies. The C=O and C=C stretching frequencies at 1705cm^{-1} and 1645cm^{-1} for the product of peak E compared with 1709cm^{-1} and 1660cm^{-1} for crotonic acid imply a lower bond energy or higher conjugation for the product of peak E than for crotonic acid.
- (c) On comparison (Table 3.D) of the methyl proton chemical shifts in the NMR of the material of peak E with those for crotonic acid, the similarity in the spin-spin coupling constants is obvious. However the methyl protons of the product due to peak E are less shielded, more down field, than for the corresponding methyl protons of crotonic acid.

All the above data are consistent with peak E being due to isocrotonic acid (cis but-2-enoic acid).



The closer spatial proximity of the CO₂H group to the methyl protons, with the possibility of intramolecular hydrogen bonding, in isocrotonic acid, would tend to deshield these protons compared with the methyl protons in crotonic acid. Similarly the stretching frequency of the C=O and C=C bonds would be expected to

TABLE 3.D

COMPARISON OF THE METHYL PROTON CHEMICAL SHIFT IN THE
NMR OF PEAK E and CROTONIC ACID

P E A K E			CROTONIC ACID		
δ ppm	Hz ^J	Int	δ ppm	Hz ^J	Int
2.20	1.2	1	1.98	1.2	1
2.18			6.6		
2.09	1.2	1		1.87	0.6
2.07			6.9	1.85	

Key: δ = chemical shift ppm.
 J = coupling constant Hz.
 Int = integral of peak area.

Errors: Estimated absolute errors in δ and J due to measurements from Spectra alone are:

$$\delta = \pm 0.02 \text{ ppm}$$

$$J = \pm 1 \text{ Hz}$$

Instrument: - 60 MHz (See Chapter 2.5)

be at a lower frequency in isocrotonic acid.

From the respective boiling points of isocrotonic acid (169.3°C) and crotonic acid (185°C) (Ref. 96) it is further expected that the former would distil over first under the conditions of SATVA.

Other possible compounds were discounted by comparison with standard IR spectra.

To summarise, the following condensable volatile products produced during the thermal degradation of PHB to 500°C under the conditions outlined above were identified as carbon dioxide, propene, ketene, acetaldehyde, water, β -butyrolactone, isocrotonic acid and crotonic acid. From the shape of the SATVA trace, crotonic acid is the most abundant of these products.

3.8 THE COLD RING FRACTION (ambient to 500°C)

The cold ring fraction (CRF) (Chapter 2.4(iv) p 25) formed upon degrading a 60mg sample of PHB under vacuum as above was a clear viscous liquid, grainy in parts. It was shown to consist of crotonic acid and oligomers of PHB with an unsaturated and an acidic end group. The nature of these species is illustrated in Figure 3.18.

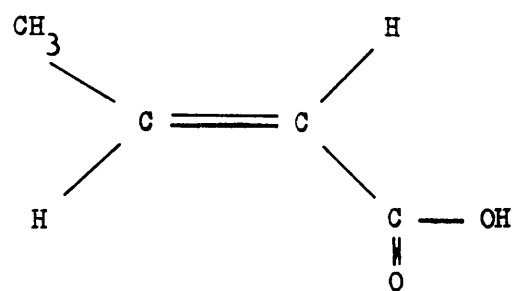
The evidence is as follows:

The solution phase IR spectra of the CRF and that of undegraded PHB are compared in Figure 3.19. They are very similar especially at wavelengths lower than 1400cm^{-1} . The significant points are as follows:

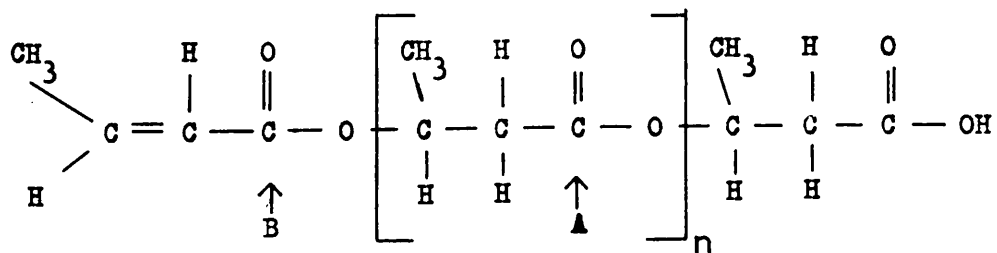
- (a) Two carbonyl stretching frequencies at 1745cm^{-1} (CCl_4) 1739cm^{-1} (CHCl_3) and 1722cm^{-1} (CCl_4) are observed in the CRF spectra, compared with one at 1739cm^{-1} (CHCl_3) in PHB.

FIGURE 3.18

DIAGRAMMATICAL REPRESENTATION OF THE COMPOUNDS
FORMING THE COLD RING FRACTION



and



where $n = 0, 1$ and 2 .

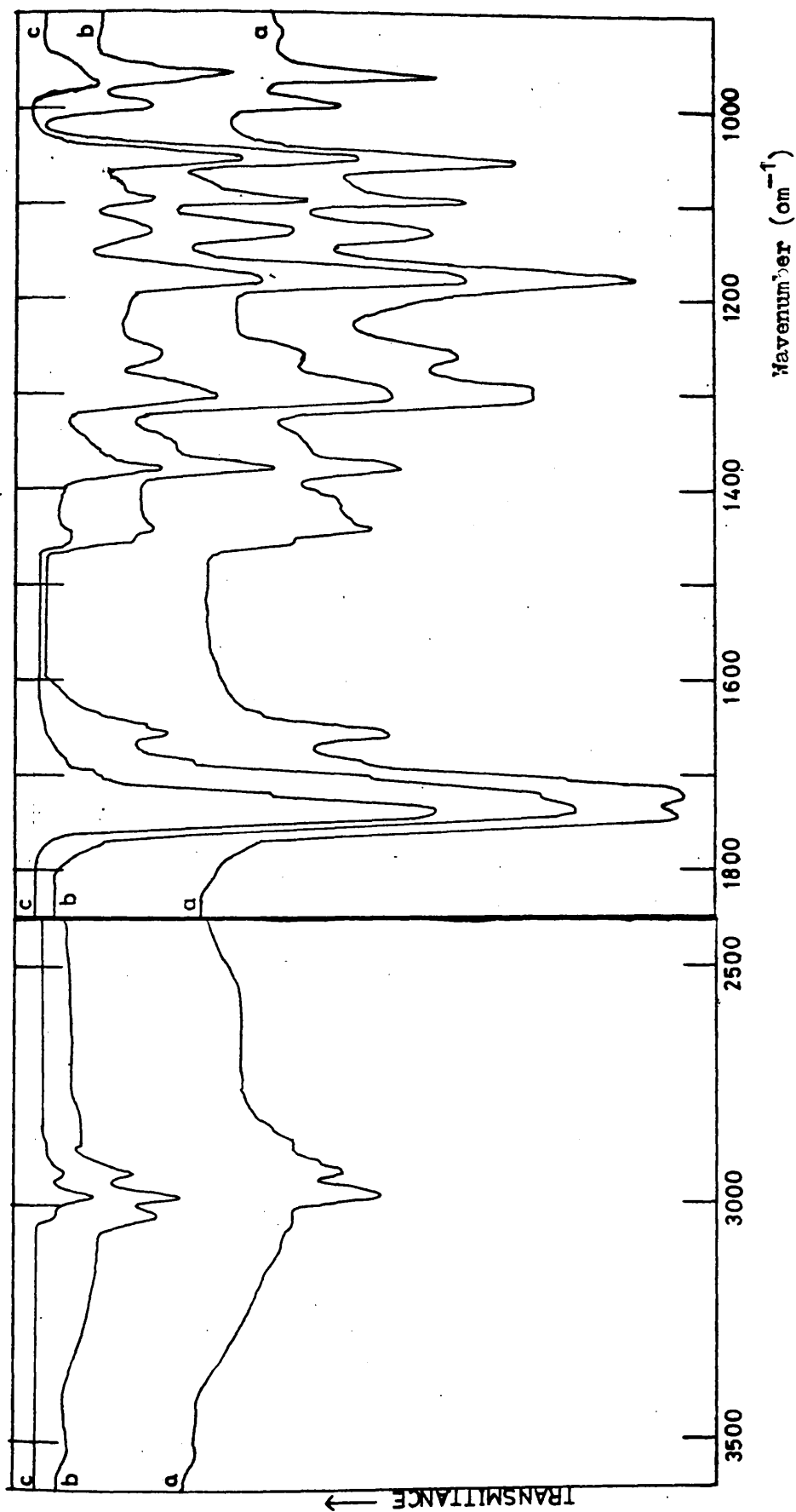


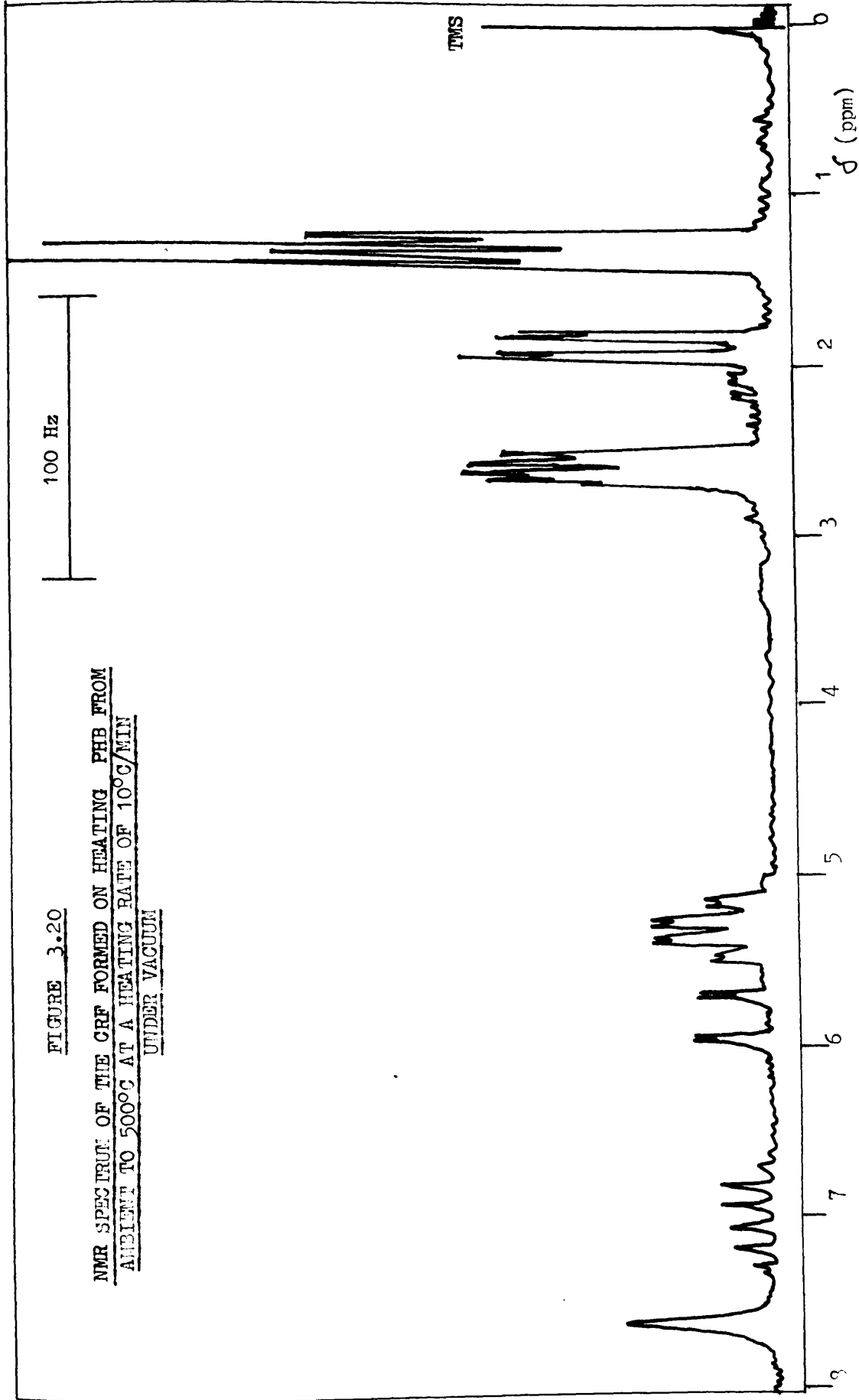
FIGURE 3.19

IR SPECTRA OF

(a) CRF Dissolved in CCl₄ : (b) CRF dissolved in CHCl₃ : (c) Undegraded PHB dissolved in CHCl₃

FIGURE 3.20

NMR SPECTRUM OF THE CRF FORMED ON HEATING PHB FROM
AMBIENT TO 500°C AT A HEATING RATE OF 10°C/MIN
UNDER VACUUM



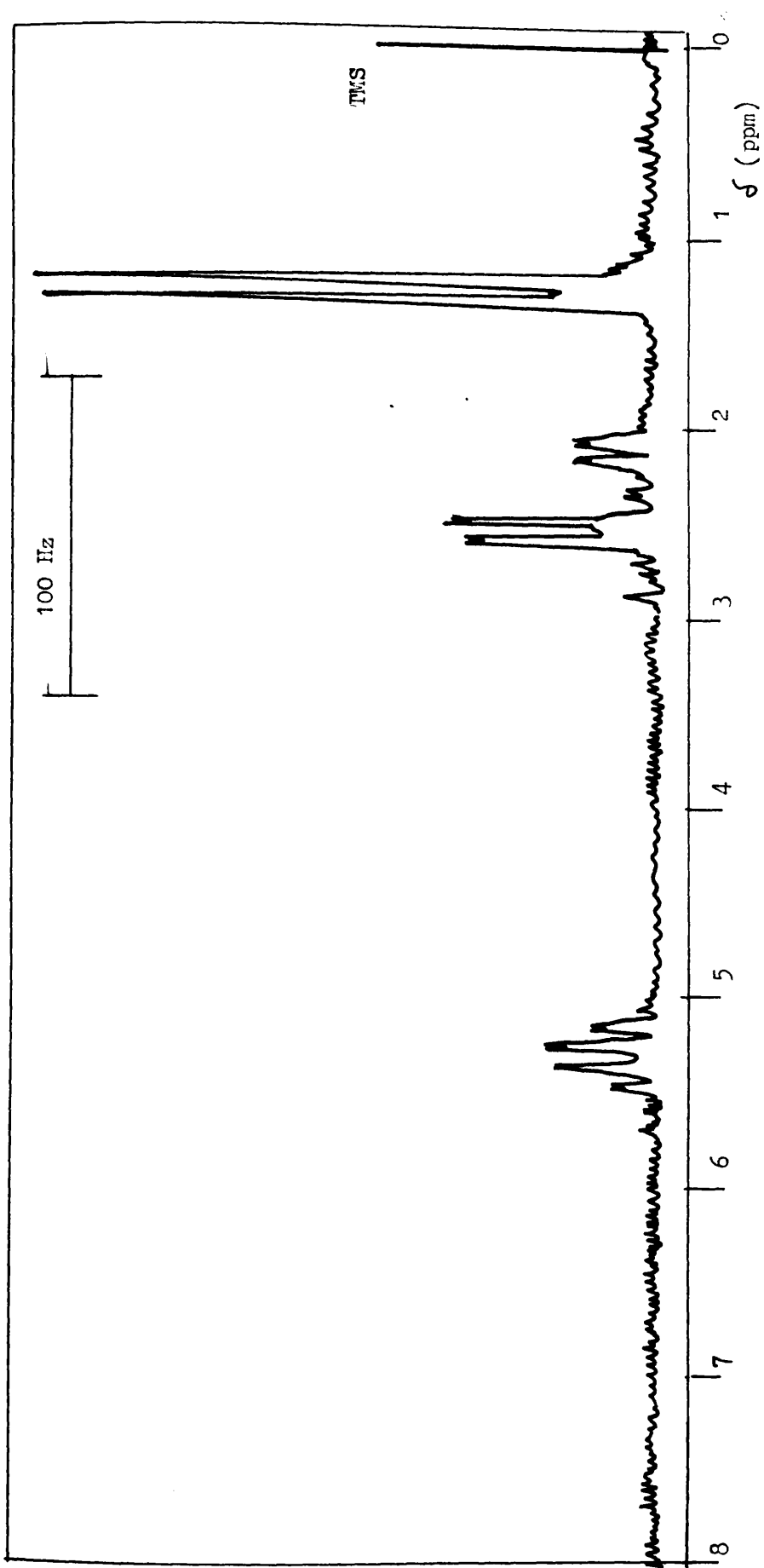


FIGURE 3.21
NMR SPECTRUM OF PIB

TABLE 3.E

COMPARISON OF THE NUCLEAR MAGNETIC RESONANCE SPECTRAS
OF THE COLD RING FRACTION, PHB AND CROTONIC ACID

COLD RING FRACTION			PHB			CROTONIC ACID		
δ ppm	J Hz	Int	δ ppm	J Hz	Int	δ ppm	J Hz	Int
1.23	1.2	1	1.23	6.6				
1.25			6.3					
1.33	1.2	1	1.34					
1.36								
1.80	1.8	1				1.85	1.2	1
1.83			7.2		1.87	6.9		
1.92	1.8	1				1.97	0.6	1
1.95					1.98			
2.06	2.4	1	2.08	6.6	1			
2.10			7.2					
2.18	2.4	1	2.19					
2.22								
2.52	3.6	1	2.48	2.4	1			
2.58			5.1			2.52	6.9	
2.62	1.8	1	2.60	1.8	1			
2.65						2.63		
5.15	1.8	1	5.17	6	1			
5.18			6					
5.25	1.8	3	5.27	6	3			
5.28			6.6					
5.36	1.8	3	5.37	7.2	3			
5.39			6					
5.47	1.8	1	5.49		1			
5.50								

KEY/ERRORS/INSTRUMENT - at foot of table continued overleaf

TABLE 3.E (continued)

COMPARISON OF THE NUCLEAR MAGNETIC RESONANCE SPECTRAS
OF THE COLD RING FRACTION, PHB AND CROTONIC ACID

COLD RING FRACTION			PHB			CROTONIC ACID		
δ ppm	J Hz	Int	δ ppm	J Hz	Int	δ ppm	J Hz	Int
5.63	1.8	1				5.73	1.8	1
5.71			15.3			5.76		
5.94	1.3	1				5.98	2.4	1
5.96						6.02		
6.72	6	1				6.85	7.8	1
6.82	6.6	4				6.98		4
6.93	9	4				7.08	9	4
7.08	6.6	4				7.23	9	4
7.19	5.4	4				7.35	7.2	4
7.28		1				7.45	6	1

KEY: δ = Chemical shift ppm.
 J = Coupling constant Hz
 Int = Relative peak area of separate peaks within each group.

ERRORS: Estimated absolute errors in δ and J due to measurements from spectra alone are as follows:-

$$\delta = \pm 0.02 \text{ ppm}$$

$$J = \pm 1 \text{ Hz}$$

INSTRUMENT: Spectra were run on a 60 MHz NMR machine in CDCl_3 as outlined in Chapter 2.

is illustrated in Figure 3.22 and possible assignments of the major peaks are listed in Table 3.F. The molecular ion of highest mass observed had $m/e = 344$ which would correspond to a tetramer $(M_4)^+$ of PHB having acidic and unsaturated end groups. The more intense peak at $m/e = 345$, the $(M_4 + 1)^+$ ion, was formed by an ion molecule reaction common to this class of compound (Ref. 97-99). Similar peaks were observed which could correspond to trimer (258, 259), dimer (172, 173) and crotonic acid (36). Equivalent fragmentation patterns followed each of these oligomer peaks.

TLC and GLC were used to confirm the existence of a mixture of compounds in the CRF. The CRF was separated by two-dimensional TLC by the method outlined in Chapter 2.5(vi). This showed the existence of at least 3 compounds (Figure 3.23) with R_f values of 0.24, 0.26 and 0.29. This method would not detect trace quantities of closely related compounds and GLC was used to support these results.

GLC was carried out on the CRF under the conditions outlined in Chapter 2.5(vii). The resultant trace, Figure 3.24, showed 4 separate peaks, the first of which was positively identified as crotonic acid. The fourth peak was in such small quantity relative to the others that it would not be expected to be observed in the TLC. The relative retention time for these peaks plotted against the integers 1 to 4, Figure 3.25, gave a straight line relationship, indicating an incremental increase in the number of units from one peak to the next as explained in Chapter 2.5(vii) p 37. Thus since Peak 1 was identified as crotonic acid the others can be assigned to the dimer, trimer and tetramer of PHB respectively as in Figure 3.18. The broad peak from 22 minutes to 40 minutes was

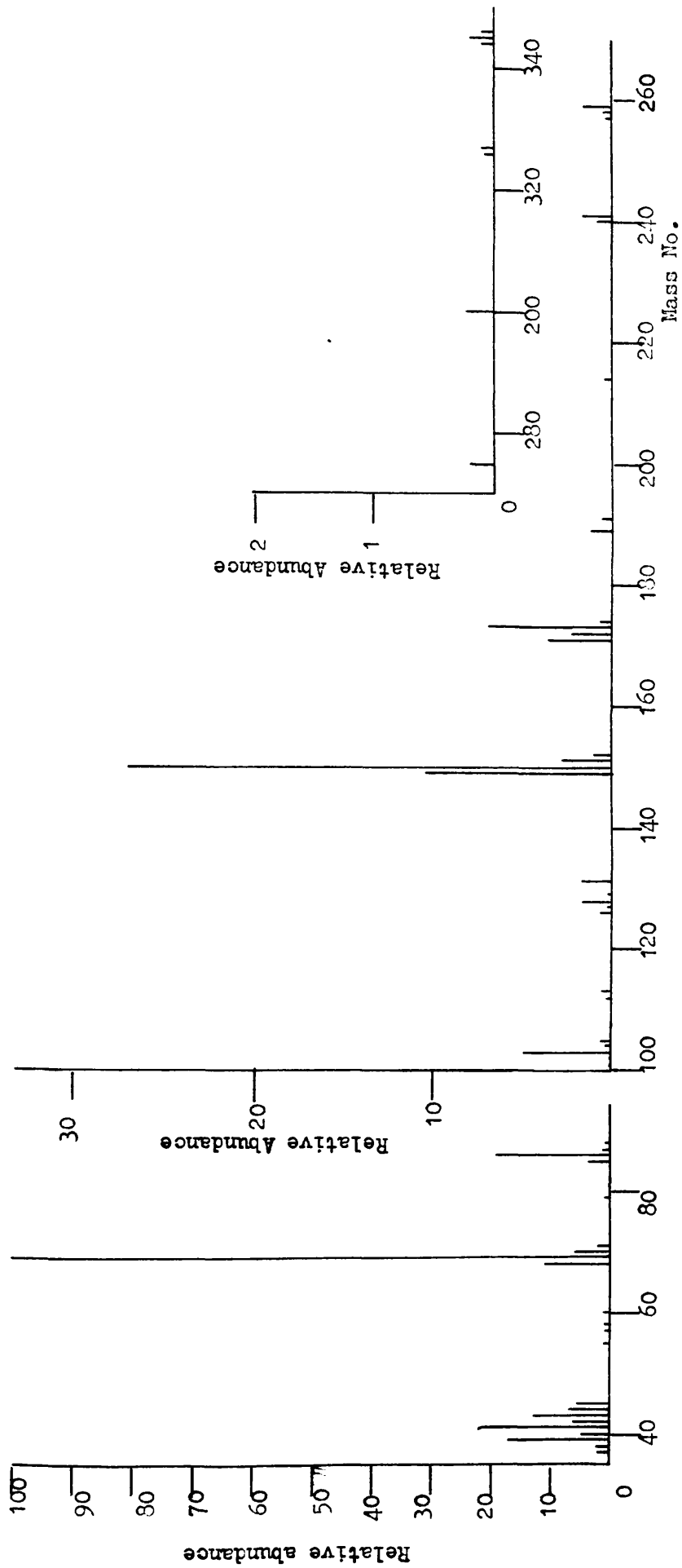


FIGURE 3.22
MASS SPECTRA OF THE CRF FORMED ON HEATING PHB FROM AMBIENT
TO 500°C AT A HEATING RATE OF 100°C/MIN UNDER VACUUM

TABLE 3.F

ASSIGNMENT OF THE MAIN PEAKS IN THE MASS SPECTRA
OF THE CRF FORMED UPON HEATING PEB TO 500°C UNDER VACUUM

m/e	Assignment	
345	tetramer + 1	(M ₄ + 1)
344	tetramer	(M ₄)
327	(M ₄ - OH)	
326	(M ₄ - H ₂ O)	
300	(M ₄ - CO ₂)	(M ₄ + 1 - CO ₂ H)
259	trimer + 1	(M ₃ + 1)
258	trimer	(M ₃)
241	(M ₃ - OH)	
240	(M ₃ - H ₂ O)	
214	(M ₃ - CO ₂)	(M ₃ + 1 - CO ₂ H)
173	dimer + 1	(M ₂ + 1)
172	dimer	(M ₂)
155	(M ₂ - OH)	
154	(M ₂ - H ₂ O)	
128	(M ₂ - CO ₂)	(M ₂ + 1 - CO ₂ H)
86	crotonic acid	(M ₁)
69	(M ₁ - OH)	
68	(M ₁ - H ₂ O)	
42	(M ₁ - CO ₂)	
41	(M ₁ - CO ₂ H)	

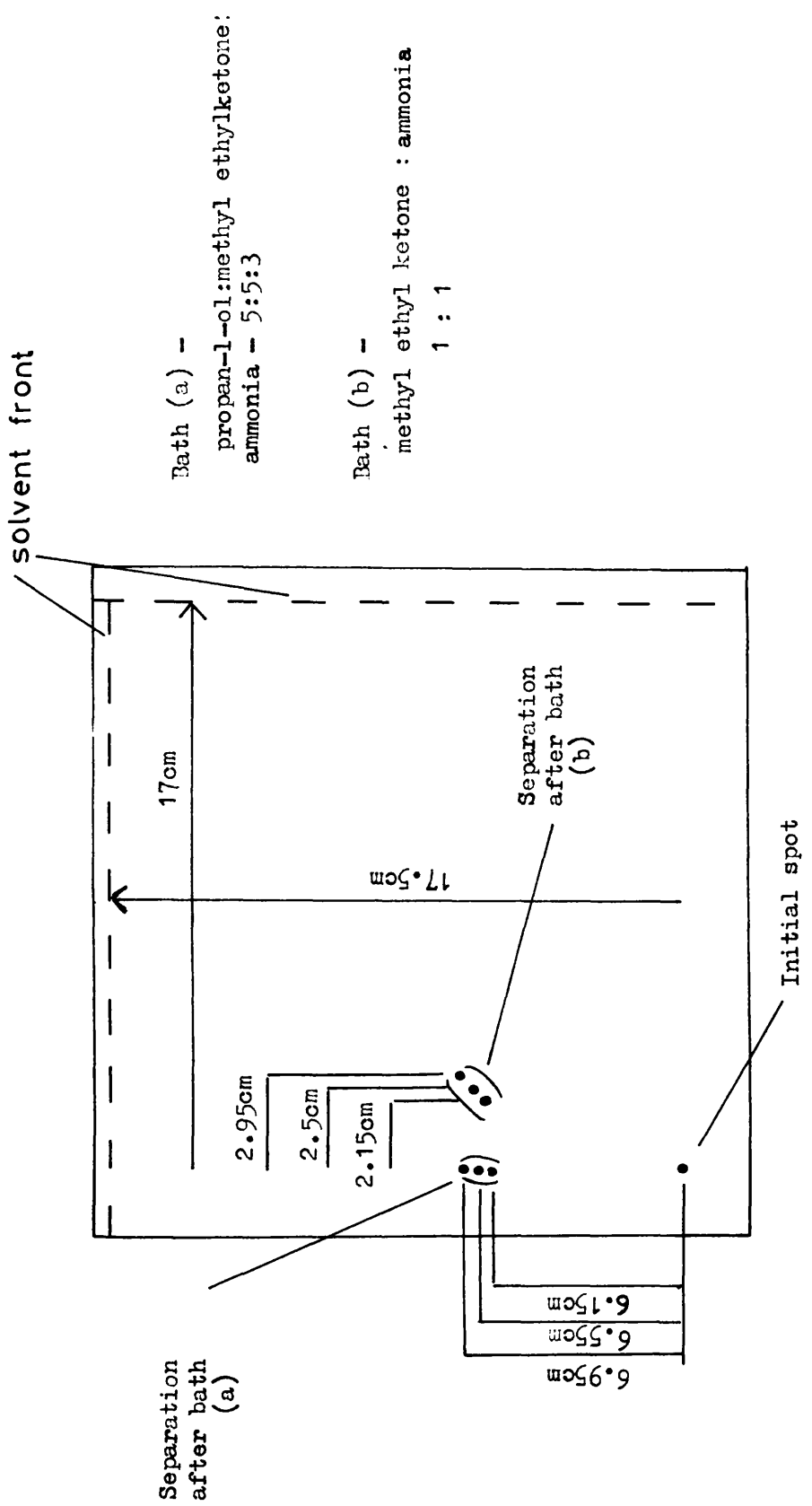


FIGURE 3.23

REPRESENTATION OF THE RESULTS OF TLC ANALYSIS OF THE CRF BY THE METHOD OUTLINED IN CHAPTER 2.5(vi)

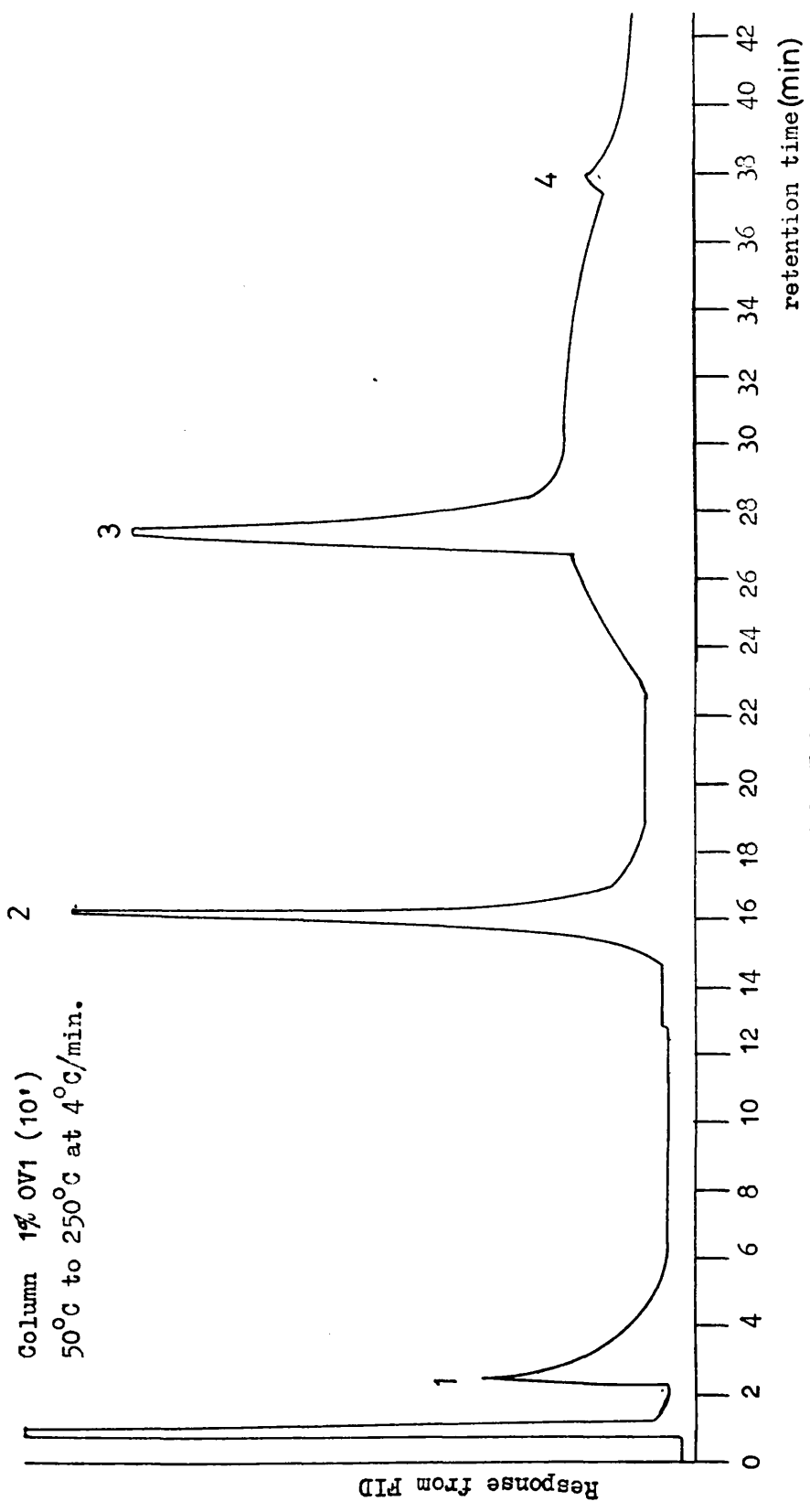


FIGURE 3.24

GLC TRACE OF THE CRF FORMED BY 500°C DURING A TVA OF PHB

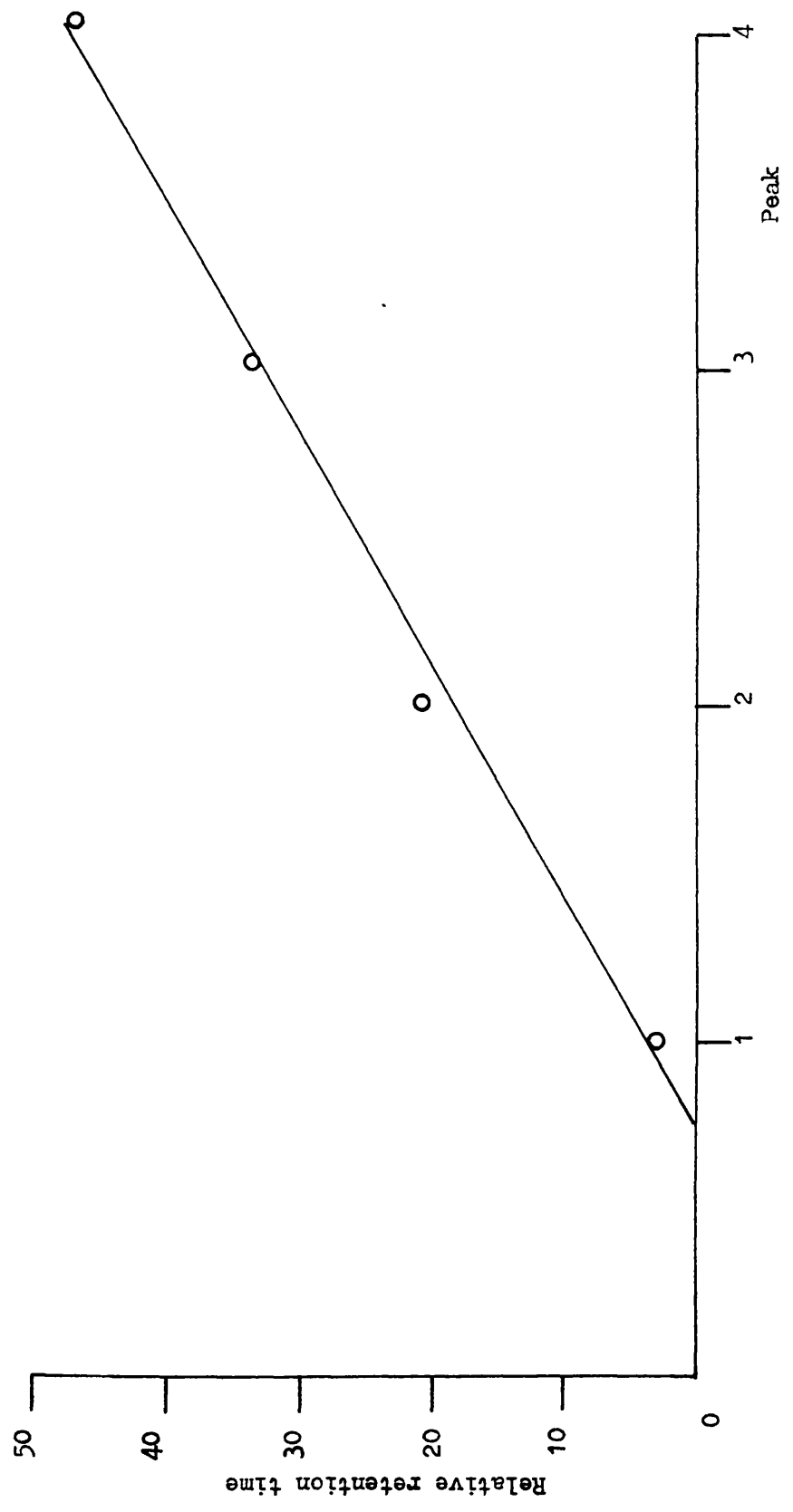


FIGURE 3.25

THE RELATIONSHIP BETWEEN THE RELATIVE RETENTION TIMES OF THE PEAKS
IN THE GLC TRACE (FIG. 3.24) OF THE CRF FORMED ON HEATING PHB TO 500°C UNDER VACUUM

thought to be due to impurity from the original PHB sample.

Therefore the CRF has been shown to consist of the compounds in Figure 3.18.

3.9 RESIDUE (ambient to 500°C)

A slight discolouration on the base of the degradation tube (brown-black) was all that was observed as a residue after degrading PHB from ambient to 500°C at a heating rate of 10°C/min under vacuum as in Chapter 3.8.

3.10 AN INVESTIGATION OF THE PRODUCTS FORMED UPON A PROGRAMMED DEGRADATION OF PHB UNDER VACUUM FROM (i) AMBIENT TO 388°C, (ii) THE RESULTANT RESIDUE OF (i) FROM AMBIENT TO 500°C AND (iii) AMBIENT TO 500°C IN A HORIZONTAL DEGRADATION TUBE

The four previous sections have identified all the products formed and to some extent related the quantity and temperature of their formation by their differing condensabilities in cold traps at different temperatures. The main purpose of this section was to initiate an investigation into the origins of some of these volatile products, especially those formed at temperatures above 340°C which do not register in TG, DTA and DSC traces.

(i) Ambient to 338°C

The degradation products responsible for Stage 1 (240°C to 338°C) in the TVA of PHB (Chapter 3.5), obtained by terminating the heating at 338°C, were examined by SATVA. The resultant trace, illustrated in Figure 3.26, shows 3 main peaks. The products due to Peaks I, II and III were identified by a combination of IR, NMR and MS and gave an identical analysis to those

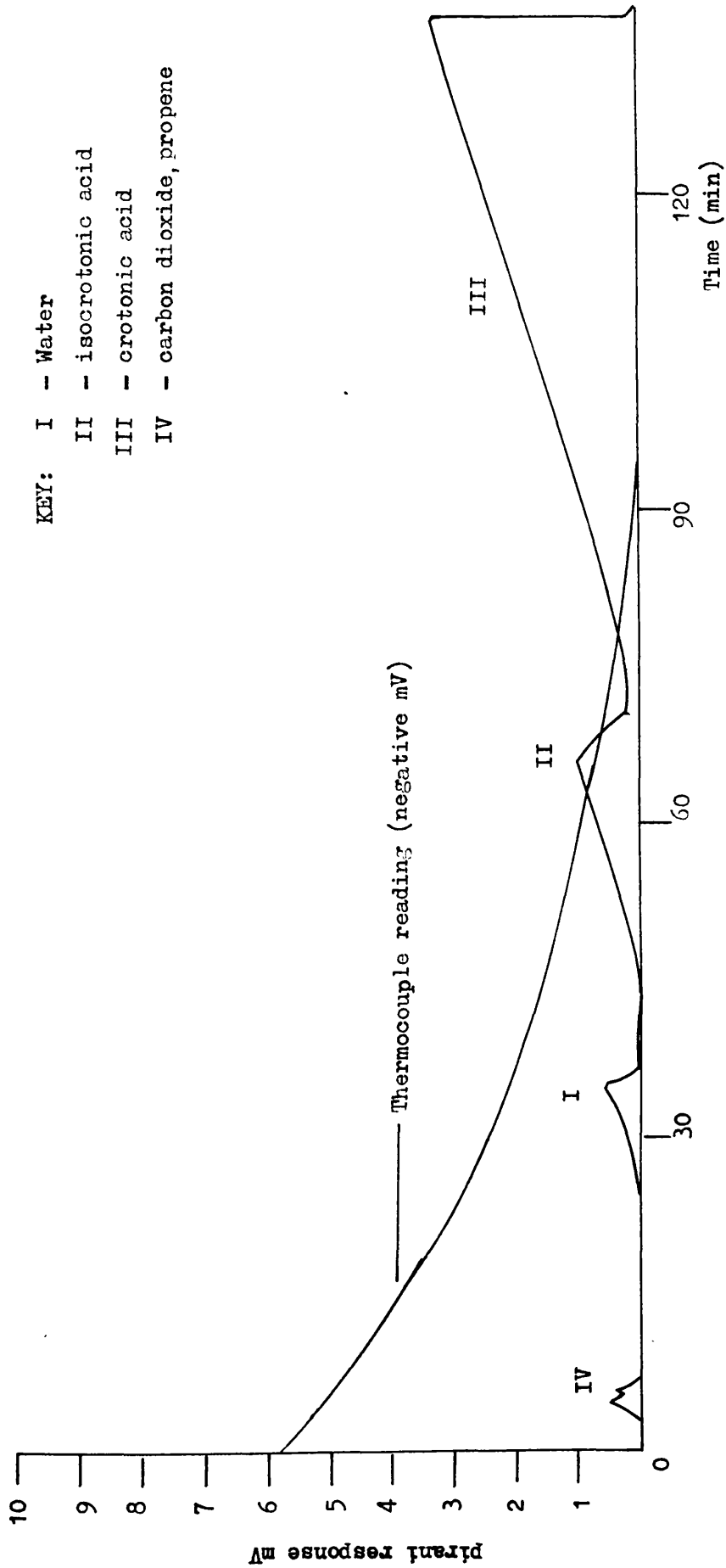


FIGURE 3.26
SATVA TRACE OF THE PRODUCTS OBTAINED ON HEATING PHB TO
338°C AT 10°C/MIN UNDER VACUUM

due to Peaks C, E and F respectively, of Chapter 3.7.

Therefore they can be assigned as follows:

- (a) Peak I was due to water.
- (b) Peak II was due to isocrotonic acid
- (c) Peak III was due to crotonic acid.

Peaks II and III were smaller than the corresponding peaks E and F, obtained on heating to 500°C. No β -butyrolactone and only a trace, Peak IV, of what was identified by its position in the SATVA to correspond to Peak A of Chapter 3.7, could be detected.

The CRF was much heavier (88.5%) of the weight of starting polymer compared with (76.9%) and spread further down the degradation tube, by approximately 1.5cm, than that obtained on heating to 500°C. The IR, NMR, GLC (Figure 3.27(a)) and MS (Figure 3.28) traces gave similar peaks to those obtained in Chapter 3.8 (Figures 3.19, 3.20, 3.23 and 3.22 respectively). A linear relationship existed between the relative retention times of the peaks on the GLC trace and the integers 1 to 4 (Figure 3.27(b)). This showed that the CRF formed up to 338°C consisted of identical species (Figure 3.18) to those formed on heating to 500°C.

(ii) The resultant Residue from (i) Heated from Ambient to 500°C

The residue from (i) above was heated in a clean degradation tube to 500°C under similar conditions to above. No volatiles were observed in either the TVA or SATVA traces obtained.

Therefore the products formed above 338°C during TVA do not originate from the residue present at that temperature.

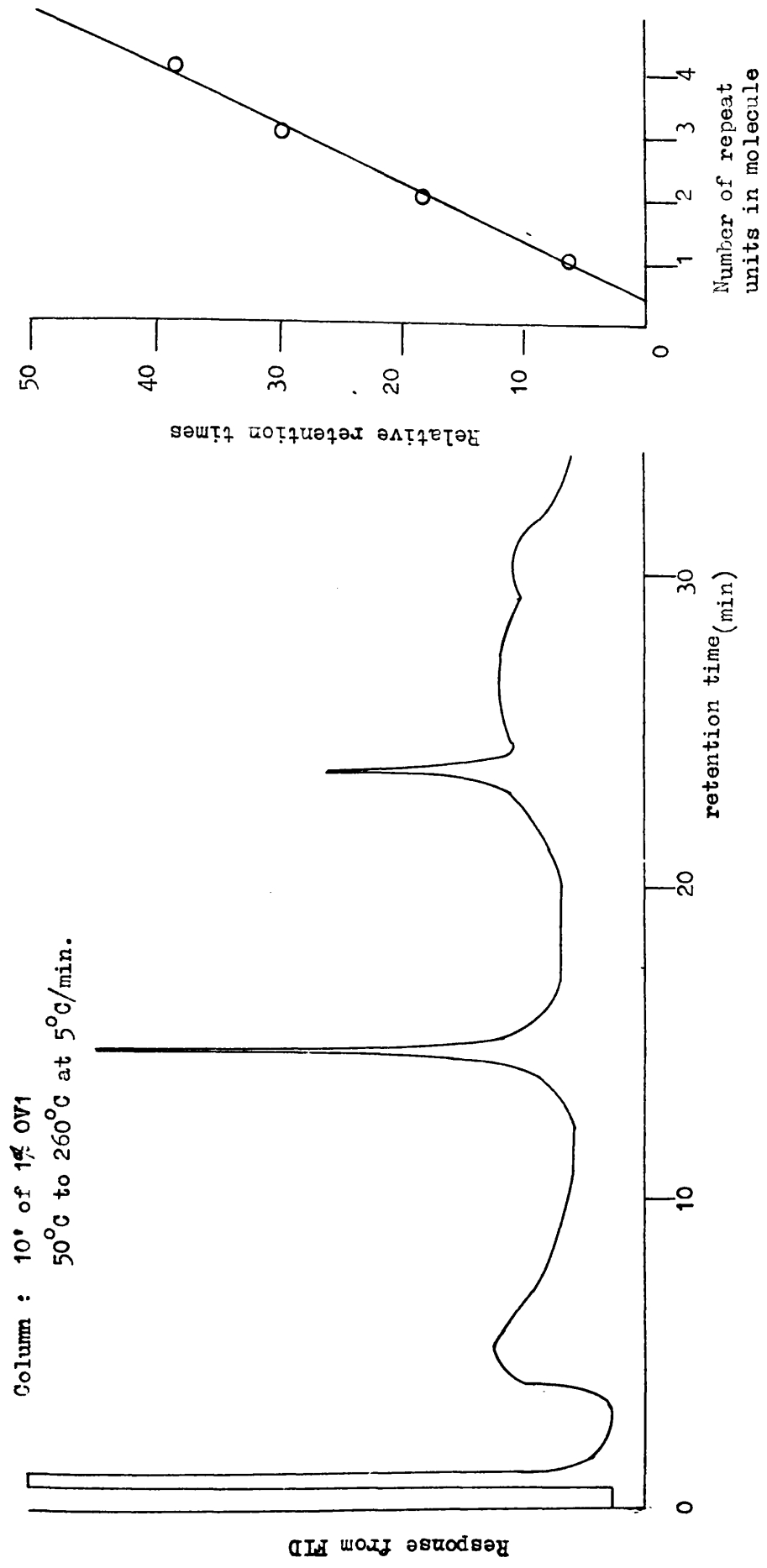


FIGURE 3.27

GLC TRACE OF THE CRF FORMED BY 338°C DURING A TWA OF PFB

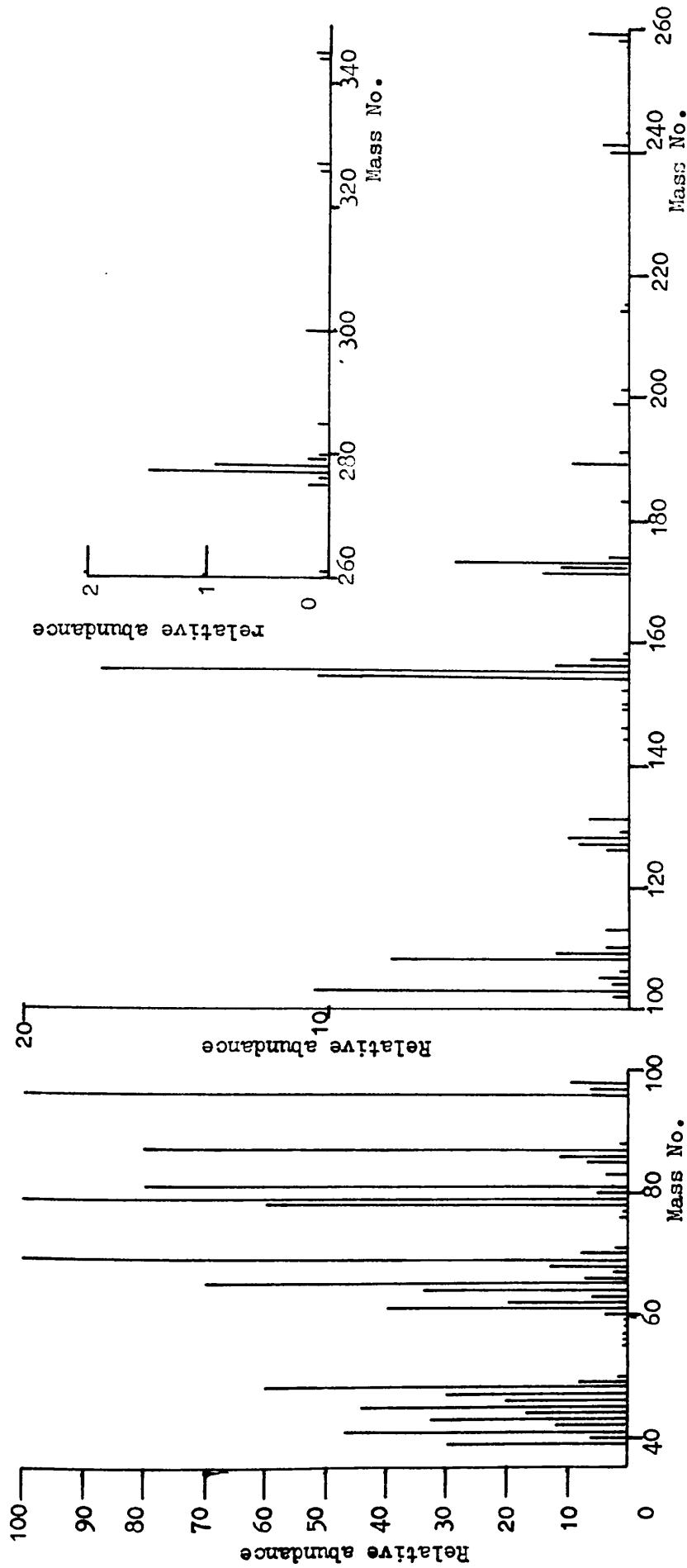


FIGURE 3.28

MASS SPECTRUM OF THE CRF FORMED BY 338°C DURING A TVA OF PHB

(iii) From Ambient to 500°C in a Horizontal Degradation Tube

A SATVA was performed on the products of a TVA of a 60mg sample of PHB heated from ambient to 500°C under vacuum at 10°C/min where the degradation tube and oven assembly were horizontal rather than vertical. The resultant SATVA trace was identical to that in Figure 3.5, implying that any viscous CRF material that ran back into the hot zone when the degradation tube was vertical had negligible effect on the final product distribution.

This information together with the TVA with differential condensation of products (Chapter 3.6) implies that carbon dioxide, propene, ketene, acetaldehyde and β -butyrolactone are essentially formed at elevated temperature ($> 338^\circ\text{C}$), under vacuum, from volatile products either partially or completely decomposing before leaving the hot zone. These volatile products which may undergo further degradation prior to leaving the hot zone can be divided into 3 categories:

- (a) isocrotonic acid and crotonic acid
- (b) β -butyrolactone
- (c) oligomers of PHB

During Stage 1 (Chapter 3.5 p68) of the TVA, compounds of type (a) and (c) are formed. As the temperature rises those of type (c) still in the hot zone decompose to give type (a) and (b) which can further decompose to give CO_2 , CH_2CHCH_3 , CH_2CO and CH_3CHO at the elevated temperature (Stage 2 of the TVA).

3.11 CLOSED SYSTEM DEGRADATION OF CROTONIC ACID

A 40mg sample of crotonic acid was dried under vacuum at -80°C as illustrated in Figure 3.29 prior to being sealed in the tube and placed in an oven at 400°C for 1 hour. The volatile gases formed were transferred via the break seal and a Toepler pump to a gas cell for IR analysis. The resultant spectrum, Figure 3.30, showed peaks due to (a) CO , (b) CO_2 , (c) CH_3CHO , (d) CH_2CHCH_3 , (e) CH_3OH , (f) CH_4 and (g) $\text{CH}_2 = \text{CH}_2$.

From a SATVA trace of the products, water, isocrotonic acid and crotonic acid were identified in addition to (a) to (g).

3.12 CLOSED SYSTEM DEGRADATION OF PHB

Fifty milligram and 300mg samples of PHB were degraded in a closed system under vacuum by heating from ambient to 500°C at a rate of $10^{\circ}\text{C}/\text{min}$ in an oven as described by McNeill (Ref. 76). With the condensable products still trapped in the cold trap any non-condensable products were transferred, as in Chapter 3.11 above, into a gas cell. No non-condensable gases could be detected.

Therefore the rise in the -196°C trace in the TVA with differential condensation of products could not be accounted for by this means, the quantities of the products involved being much too small.

3.13 PRODUCTS FORMED ON HEATING PHB AT 200°C for SIX HOURS

A 200mg sample of PHB was heated for 6 hours under vacuum with continuous pumping at 200°C with an oven set up similar to that for TVA. A very large CRF was formed and analysis of the peaks from SATVA of the condensable products formed, identified

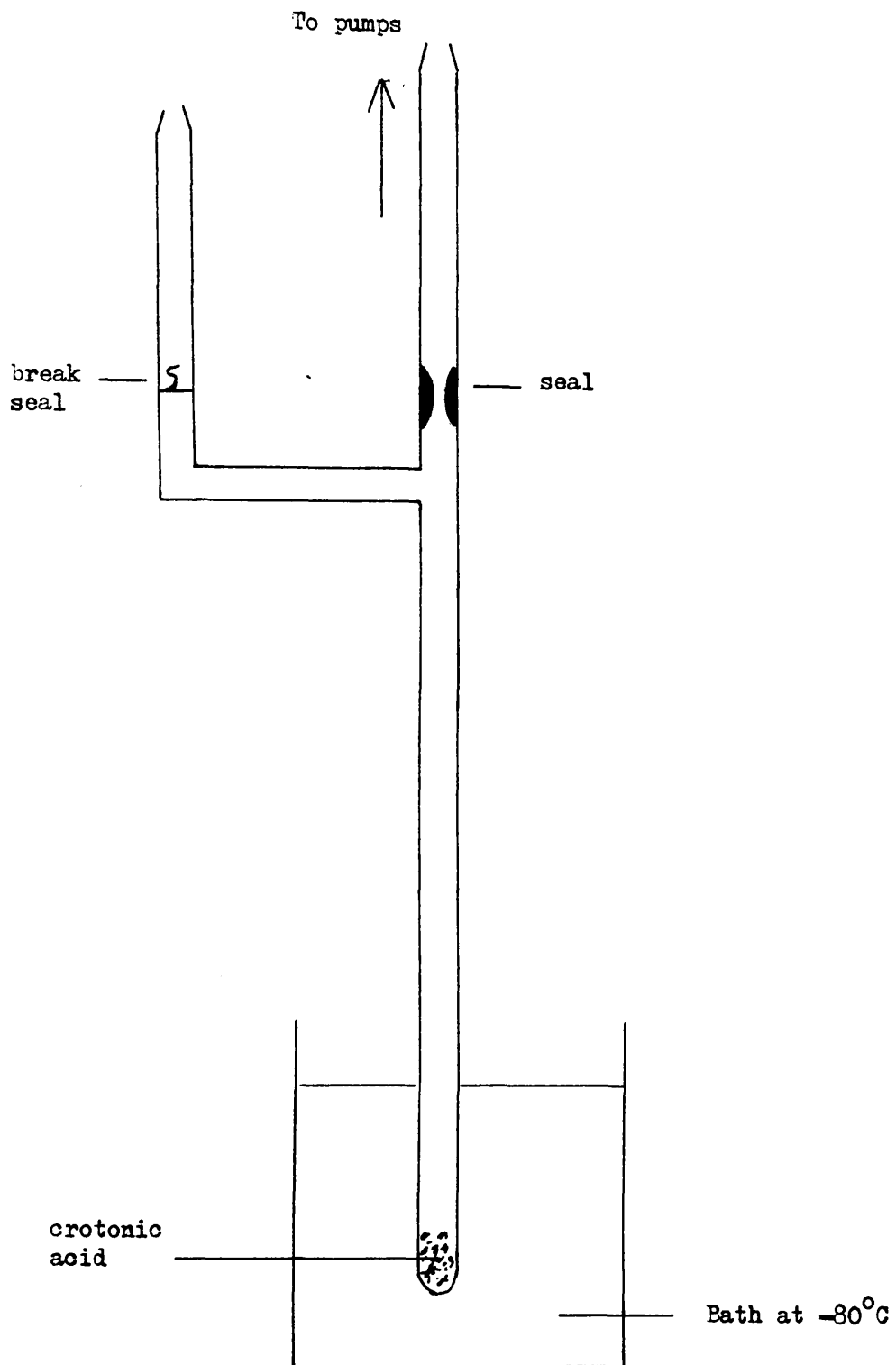


FIGURE 3.29

APPARATUS FOR CLOSED SYSTEM DEGRADATION

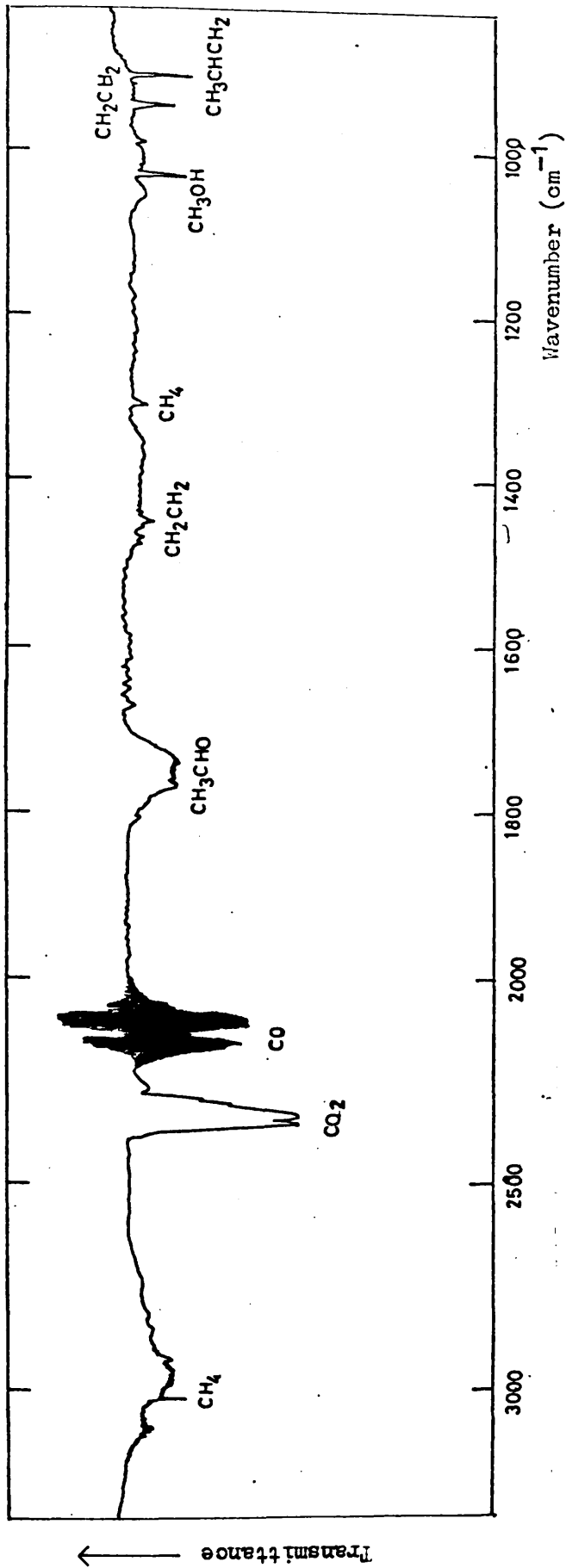


FIGURE 3.30

IR SPECTRUM OF THE PRODUCTS OF A CLOSED SYSTEM DEGRADATION
OF CROTONIC ACID (400°C - 1 hr)

only water, isocrotonic acid and crotonic acid. (Figure 3.31).

It was noted that the quantity of volatiles being evolved rose steadily during the 5th hour until after 6 hours the polymer was completely degraded. No trace of β -butyrolactone was found.

3.14 CONCLUSIONS

The following products have been positively identified from the thermal degradation of PHB under vacuum upon heating to 500°C in an oven at a rate of 10°C/min.

- I tetramer (acidic and unsaturated end groups)
- II trimer (acidic and unsaturated end groups)
- III dimer (acidic and unsaturated end groups)
- IV crotonic acid
- V isocrotonic acid
- VI β -butyrolactone
- VII water
- VIII acetaldehyde
- IX ketene
- X propene
- XI carbon dioxide

The characteristics of the production of I to V from the polymer backbone at temperatures below 340°C was investigated by observing the molecular weight changes which occur on heating PHB isothermally in the temperature range 170°C to 200°C and will be described in Chapter 6.

Products VI, VIII, IX, X and XI were detected only at elevated temperatures ($> 340^\circ\text{C}$).

Some of the I, II and III will still be present in the hot zone as the temperature rises and will undergo further

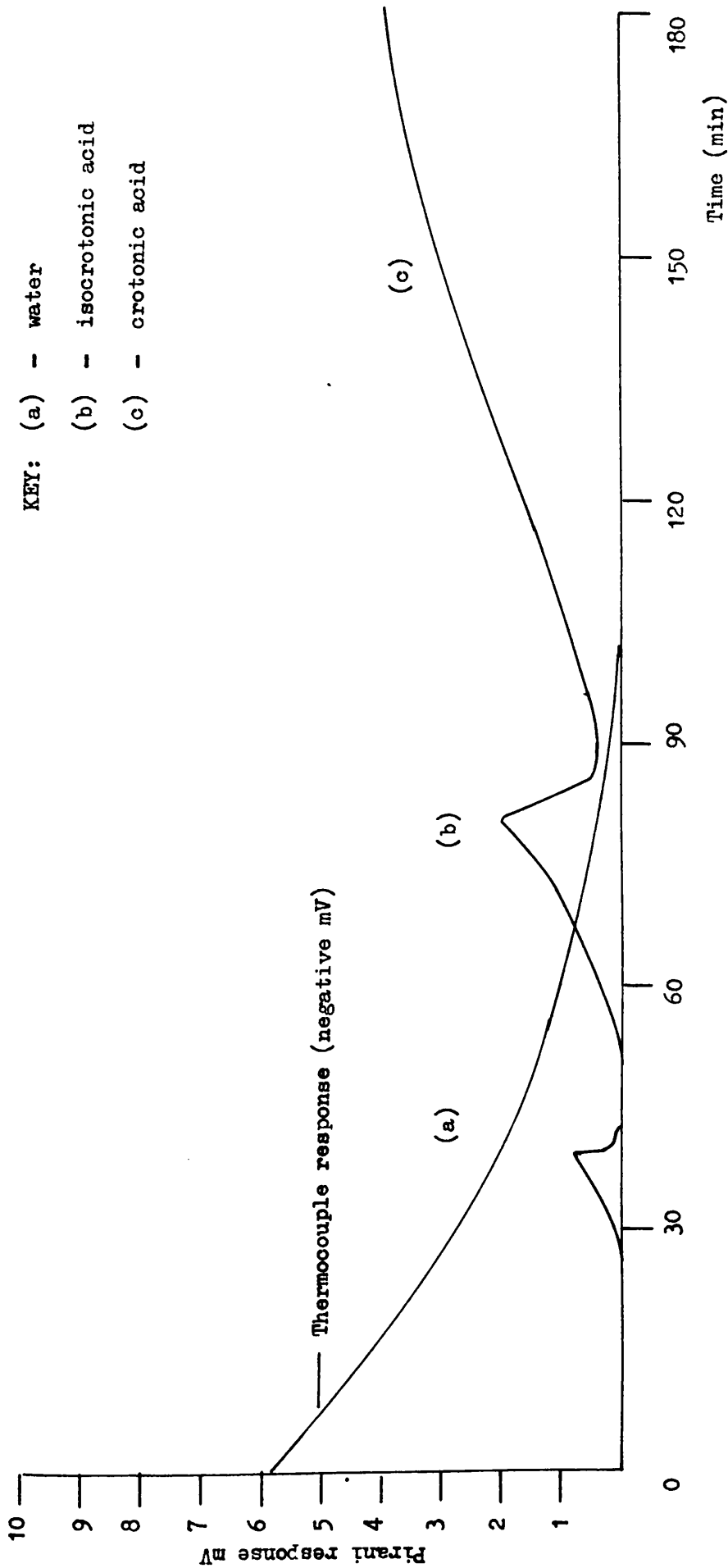
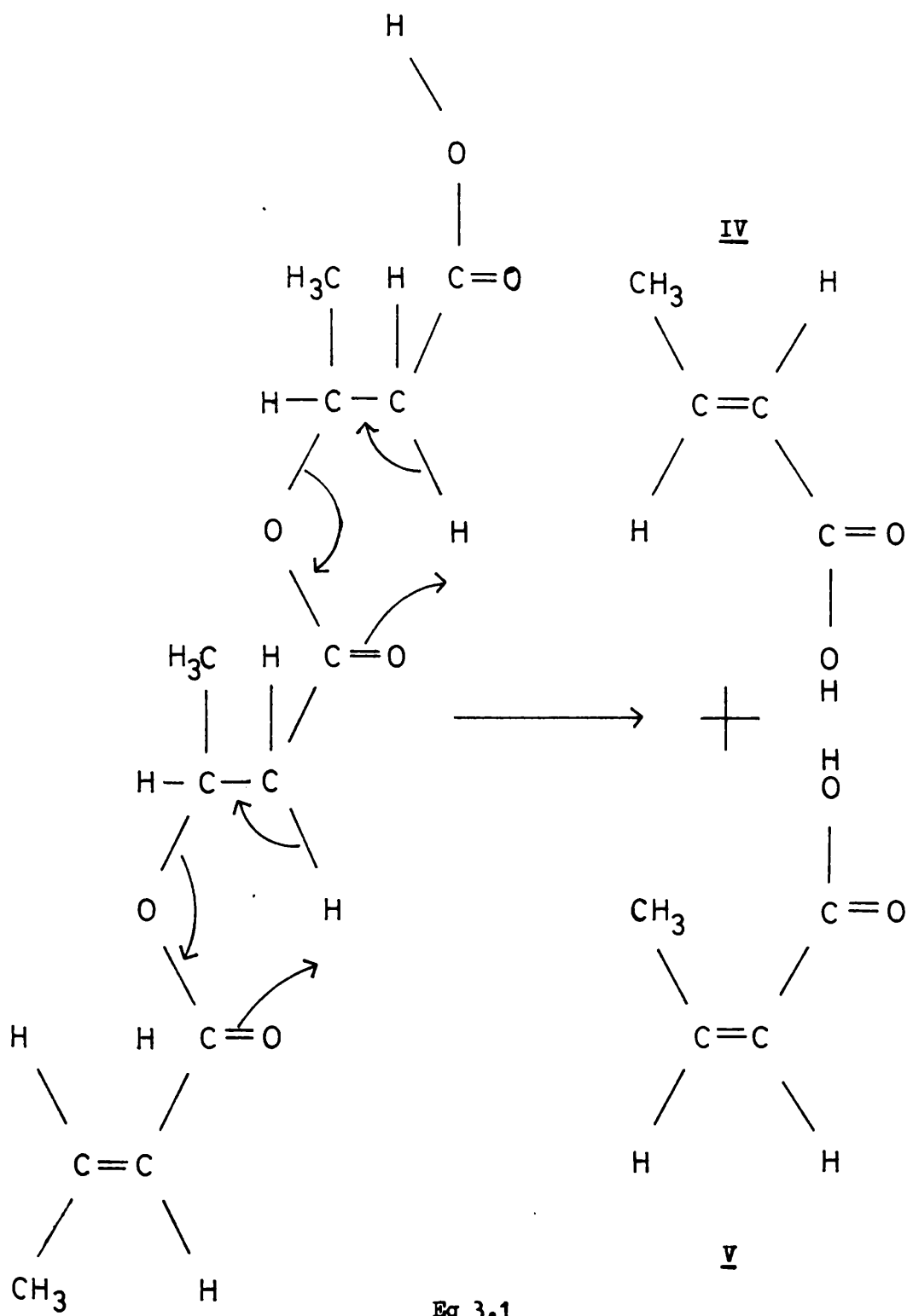


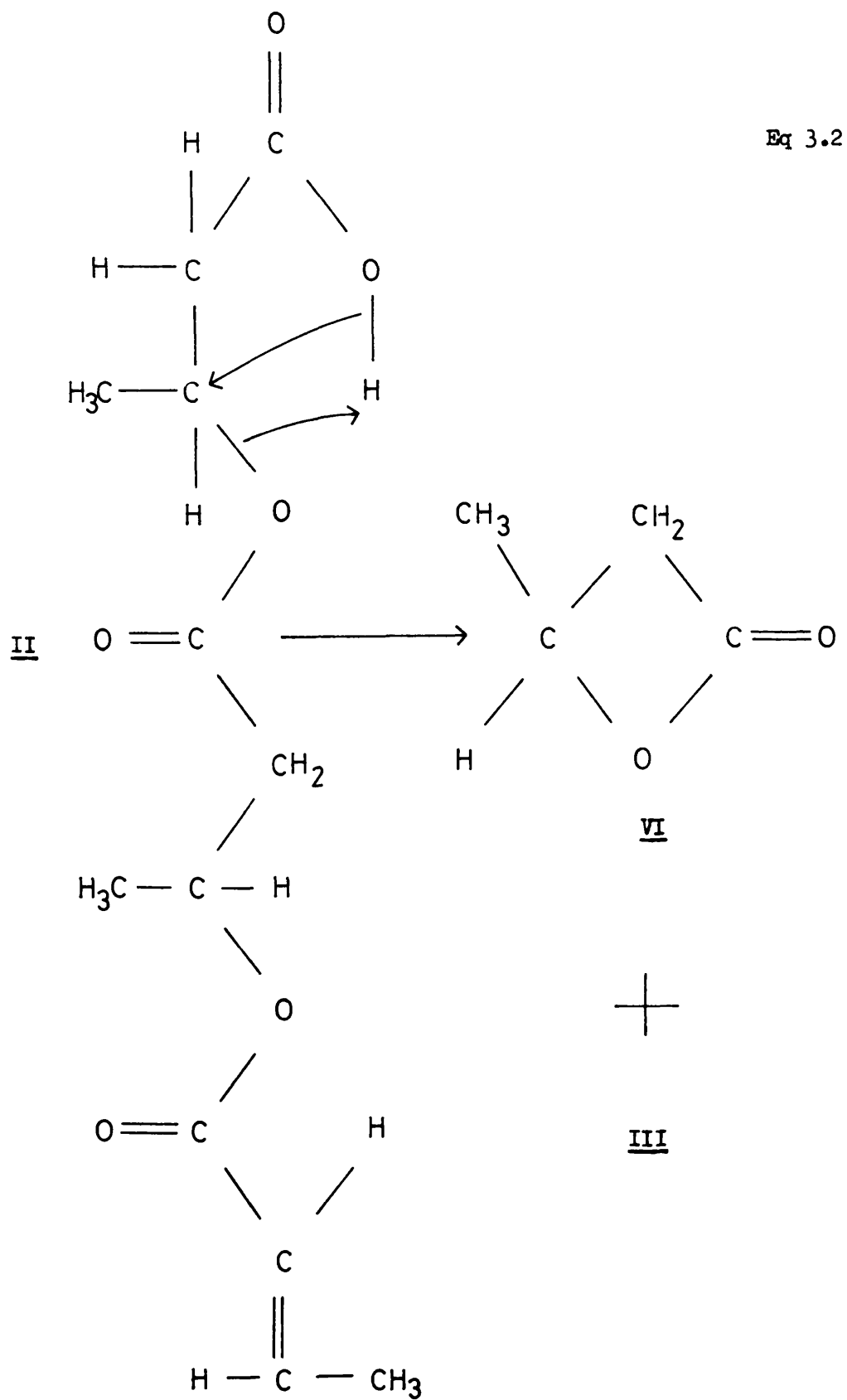
FIGURE 3.31
SATVA TRACE OF THE PRODUCTS FORMED ON HEATING PHB AT 200°C FOR SIX HOURS UNDER VACUUM

decomposition to give IV, V and VI. Likely mechanisms for this are given below.



II

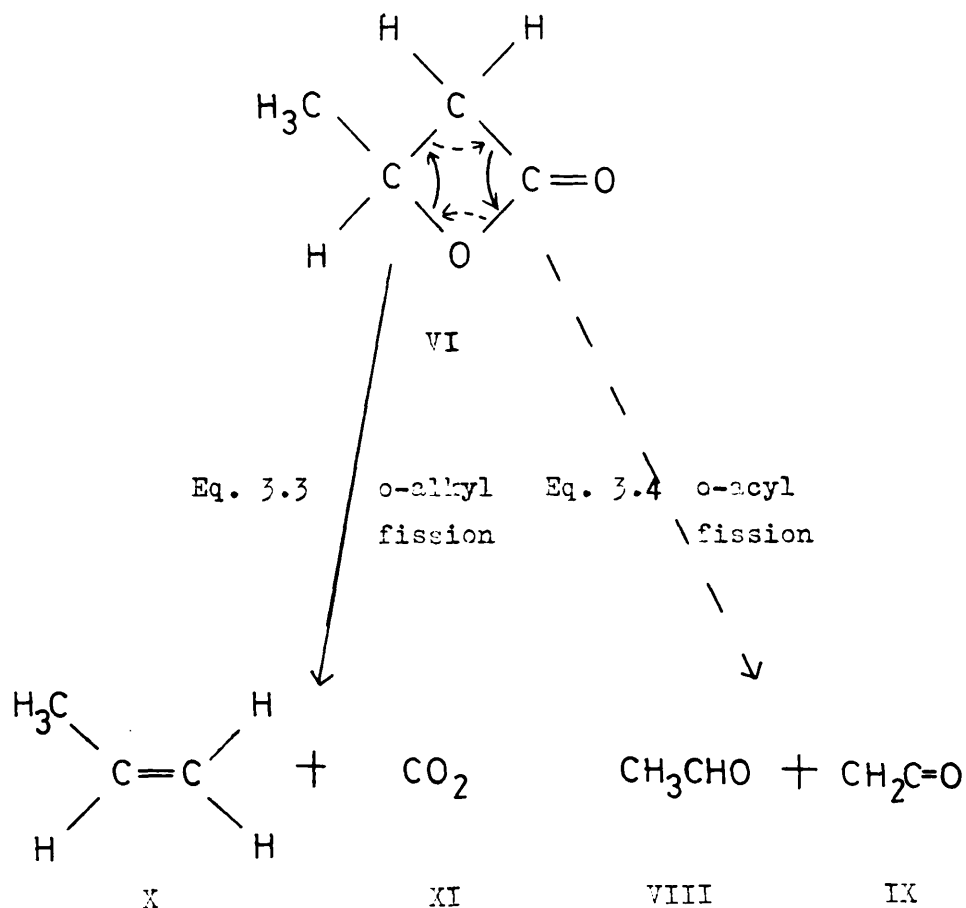
The formation of either IV or V will depend on the conformation of the chiral centres at the time of formation of the double bond. IV would be expected to be most favourable.



Similar reaction sequences can be drawn for I and III.

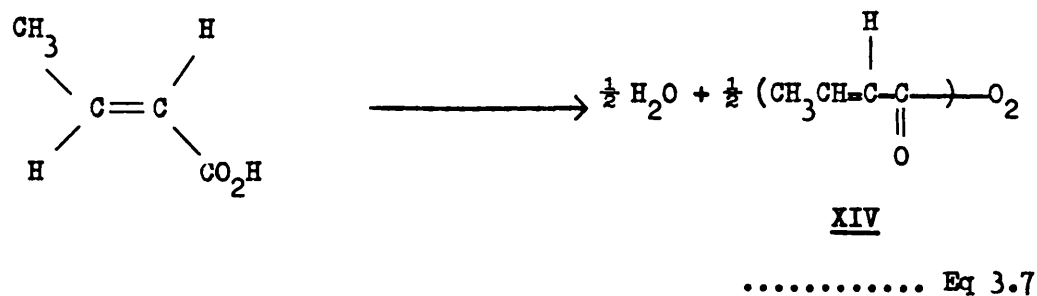
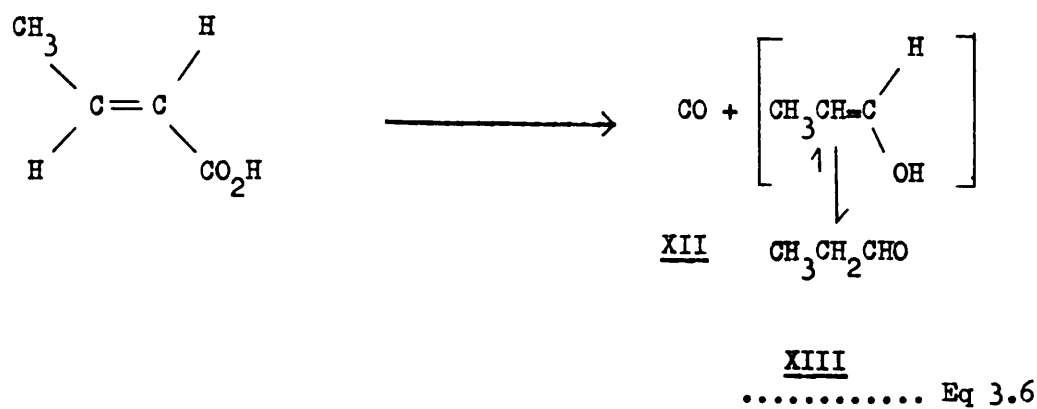
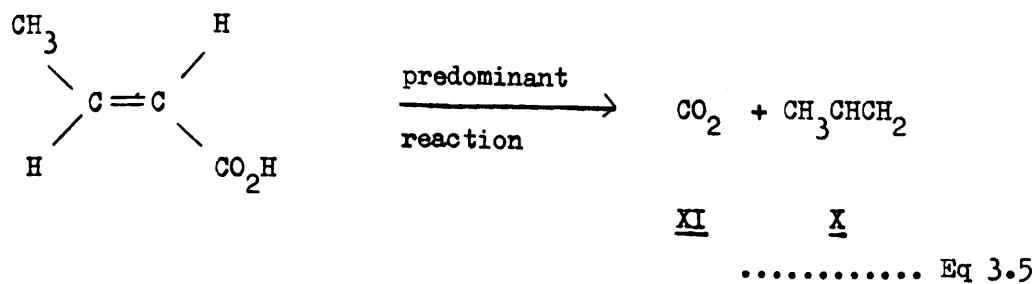
A proportion of IV, V and VI formed by Equations 3.1 and 3.2 would be expected to undergo further degradation at the temperatures of their formation prior to leaving the hot zone.

β -Butyrolactone will decompose via o-alkyl fission to form X and XI and via o-acyl fission to form VIII and IX so relieving the ring strain as in Equations 3.3 and 3.4. (Ref. 100).



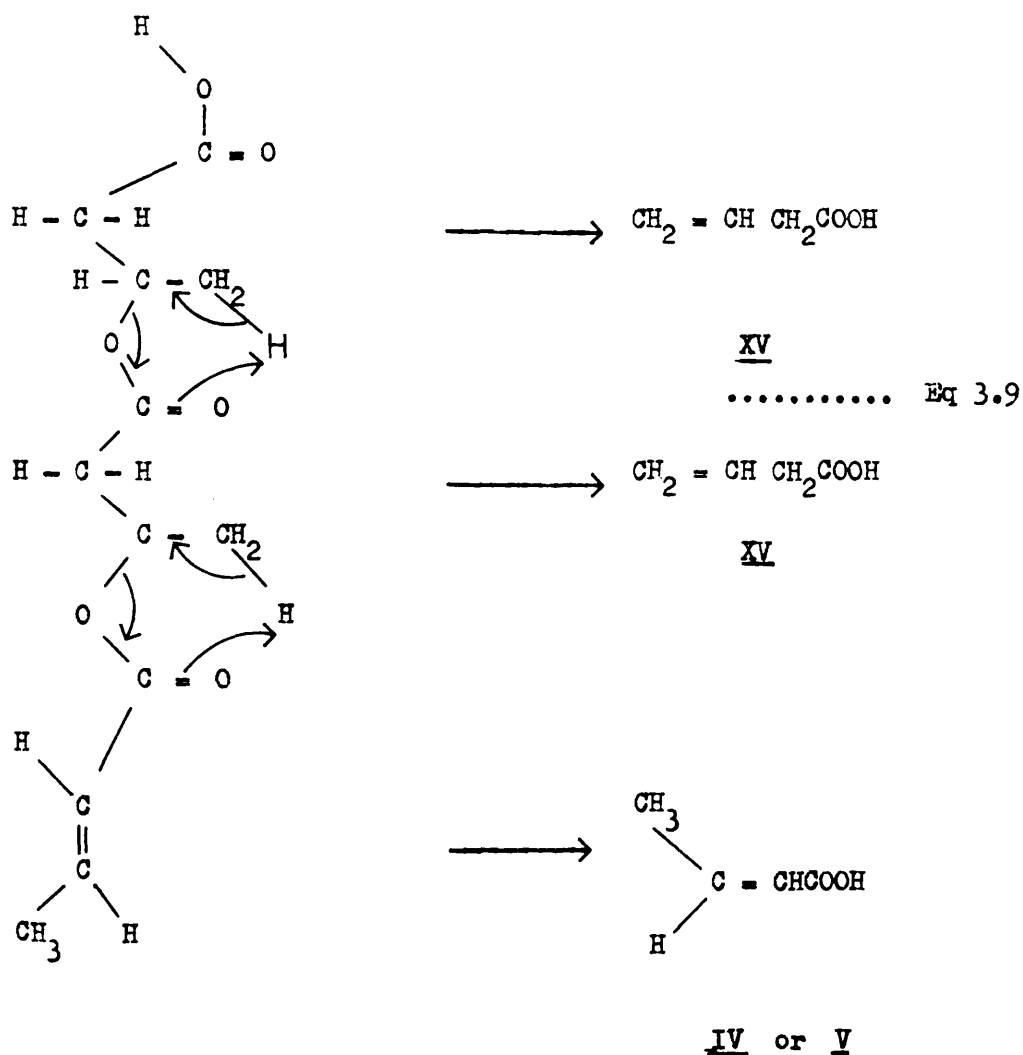
Chapter 3.11 showed that VIII, X and XI could also be formed from the pyrolysis under vacuum of crotonic acid IV at 400°C. It has been shown that under nitrogen IV will undergo pyrolysis to form predominantly XI (61% of carbon content), and X (10.5% of

carbon content), CO XII (28.5% of carbon content) and water (Ref. 101) by the following mechanisms.



Therefore CO XII would appear to be the most likely of the non-condensable gases identified in the pyrolysis of IV, Chapter 3.11, to be responsible for the small rise in the -196°C trace in the TVA with differential condensation of products (Chapter 3.6).

Equation 3.1 dealt with hydrogen P which is obviously the most labile, being α to a carbonyl and β to an etheral oxygen compared with Q which is β to etheral oxygen and γ to the carbonyl. Elimination of the hydrogen Q would lead to 3-butenic acid XV plus either IV or V from the unsaturated terminal grouping as below (IV predominating over V).



XV would be expected to undergo further rapid degradation to X and XI (Ref. 103).

The rate of the reaction represented by Equation 3.1 has been estimated to be 250 to 360 times that of the reaction in Equation 3.9 (Ref. 104, 105, 106).

Therefore it is not surprising that XV has not been observed.

There are three possible sources of the water;

- (1) Water trapped in the polymer which is released when the polymer melts,
- (2) from the degradation of crotonic acid, and
- (3) by an esterification reaction (see Chapter 6).

We are now in a position to explain fully the TVA trace with differential condensation of products (Figure 3.5) The first peak (240°C to 338°C) consists principally of isocrotonic acid and crotonic acid (0°C trace). From 285°C to 340°C water is observed (-45°C) and above 340°C β butyrolactone in addition. A trace of CO₂ and propene is observed between 309°C and 323°C from the degradation of crotonic acid (-100°C trace). Above 351°C a larger -100°C trace was observed due to the degradation of isocrotonic acid, crotonic acid and β butyrolactone to CO₂, CH₂CHCH₃, CH₂C=O and CH₃CHO. A trace of CO is observed above 429°C from the degradation of isocrotonic and crotonic acids (-196°C trace).

The presence of β butyrolactone, with its suspected carcinogenicity (Ref. 107, 108) as a thermal degradation product of PHB will have to be considered in the design of production sites for processing PHB. The lack of detection of β butyrolactone upon heating a 200mg sample of PHB at 200°C for 6 hours does not necessarily imply that while processing larger quantities of PHB no β butyrolactone will be detected.

CHAPTER 4

THE PRODUCTS OF THE THERMAL DEGRADATION OF PHB UNDER A NITROGEN ATMOSPHERE

4.1 INTRODUCTION

Having identified the thermal degradation products formed under vacuum it was thought pertinent to study those formed under a nitrogen atmosphere. A nitrogen atmosphere will be closer to the likely processing conditions of PHB, especially in an extruder where little or no oxygen will be present.

4.2 DIFFERENTIAL THERMAL ANALYSIS AND DIFFERENTIAL SCANNING CALORIMETRY UNDER NITROGEN

The results of these two thermal analysis techniques under a nitrogen flow were fully discussed in Chapter 3.3 and 3.4.

4.3 THE THERMAL DEGRADATION OF PHB UNDER A NITROGEN ATMOSPHERE

A 60mg sample of PHB was degraded under flowing nitrogen ($80\text{cm}^3/\text{min}$) by heating in an oven from ambient to 500°C at a rate of $10^\circ\text{C}/\text{min}$ using the method and apparatus detailed in Chapter 2.4(v).

Copious white fumes were observed coming from the degradation tube at temperatures between 300°C and 450°C . When this subsided, white needle like crystals were observed on the inside of the glass tubing leading from the degradation tube to the cold trap. On completion of the heating programme the degradation tube was allowed to cool prior to the nitrogen flow being terminated and the system opened to the vacuum pumps. The white needle like crystals were pumped into the cold trap leaving traces of a viscous oil on the glass surfaces.

4.4 SUBAMBIENT TVA OF THE PRODUCTS ISOLATED IN THE COLD TRAP

The products in the cold trap were separated by SATVA.

The resultant trace, Figure 4.1 displayed 5 peaks the products from each of which were removed from the vacuum system separately and identified by the methods described in Chapter 2.5.

Products from Peak G were isolated in a gas cell and identified from their IR spectra, Figure 4.2 as carbon dioxide, ketene (trace) and propene, by comparison with standard gaseous phase IR spectra (Ref. 90 - 92). The material of Peak H was identified from its gaseous phase IR spectrum, Figure 4.3, as acetaldehyde, by comparison with standard gas IR spectra (Ref. 93). The product from Peak I was identified from its MS (molecular ion $m/e = 18$) as water.

The IR spectrum (Figure 4.4) of the product of Peak J, its MS and NMR, all showed identical peaks to those obtained from the product of Peak E, Figures 3.16, 3.15 and 3.17 respectively, and was therefore identified as isocrotonic acid (cis but-2-enoic acid).

The material of Peak K was the major condensable degradation product. By comparison of the IR (Figure 4.5), MS and NMR of this material with those from the product of Peak F (Figures 3.13, 3.12 and 3.14 respectively), the material of Peak K was identified as crotonic acid (trans-but-2-enoic acid).

4.5 THE COLD RING FRACTION OBTAINED BY DEGRADING PHB UNDER A NITROGEN ATMOSPHERE

The cold ring fraction CRF (Chapter 2.4(iv)) formed upon degrading a 60mg sample of PHB under nitrogen as in Chapter 4.2 above was investigated by IR, NMR, MS and GLC.

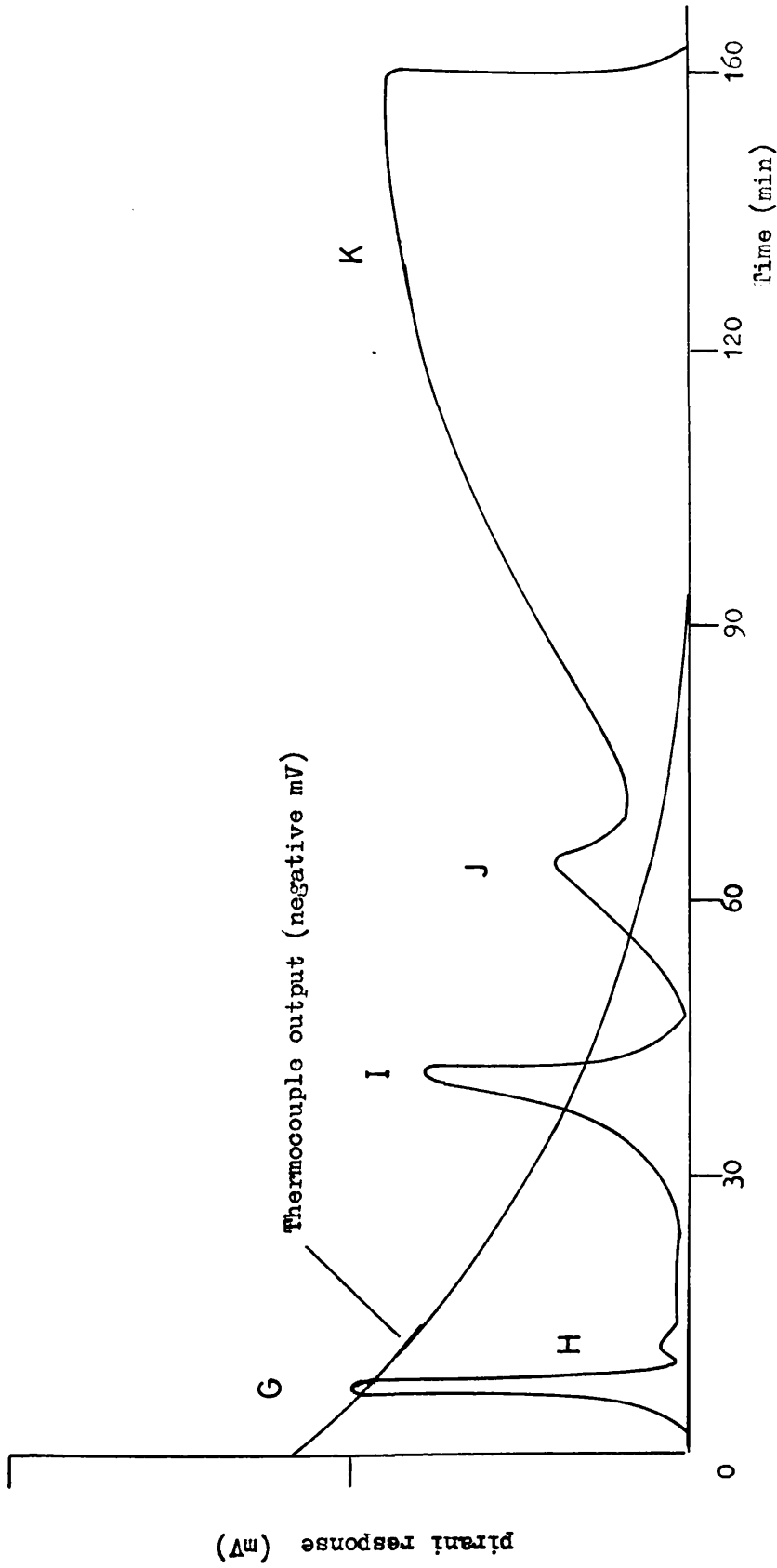


FIGURE 4.1

SATVA TRACE OF THE VOLATILE PRODUCTS COLLECTED DURING A
THERMAL DEGRADATION OF A 60MG SAMPLE OF PIB UNDER NITROGEN
FROM AMBIENT TO 500°C AT 10°C/MIN

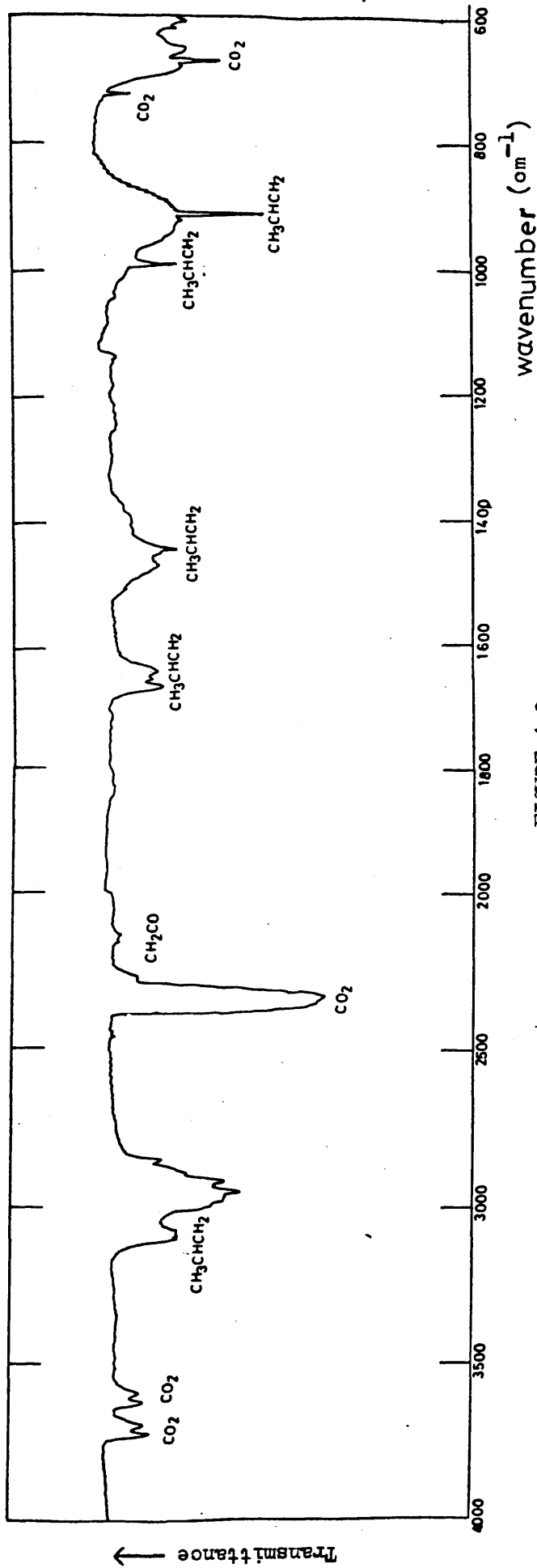


FIGURE 4.2
IR SPECTRUM OF THE PRODUCTS OF PEAK G

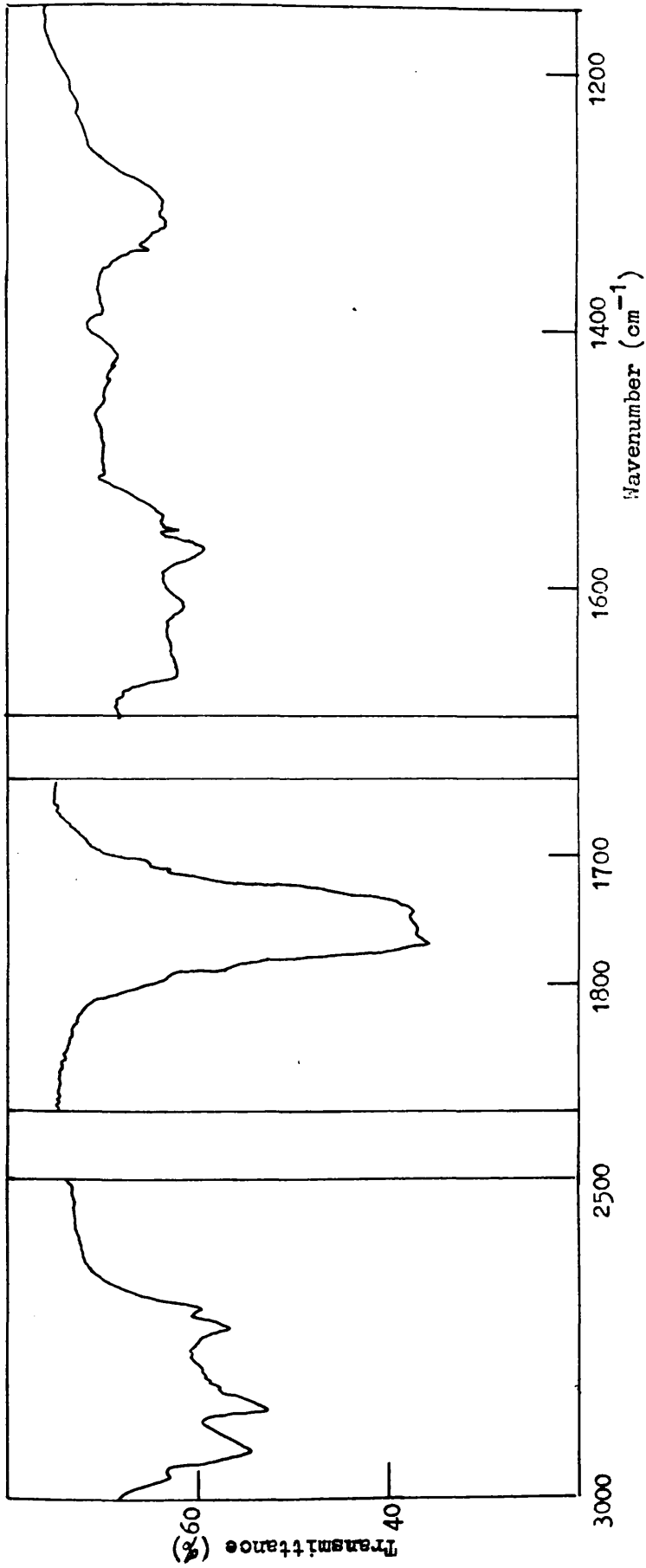


FIGURE 4.3
IR SPECTRUM OF THE PRODUCT OF PEAK H

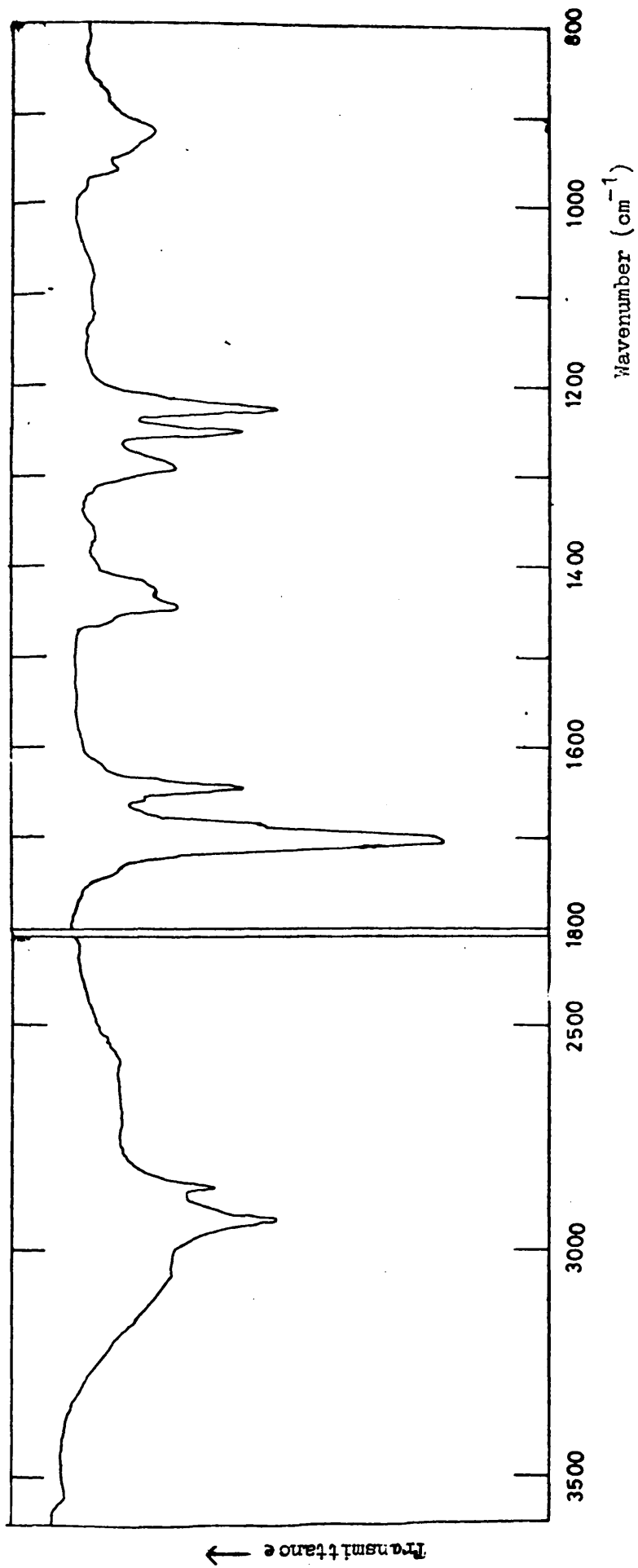


FIGURE 4.4
IR SPECTRUM OF THE PRODUCT OF PEAK J

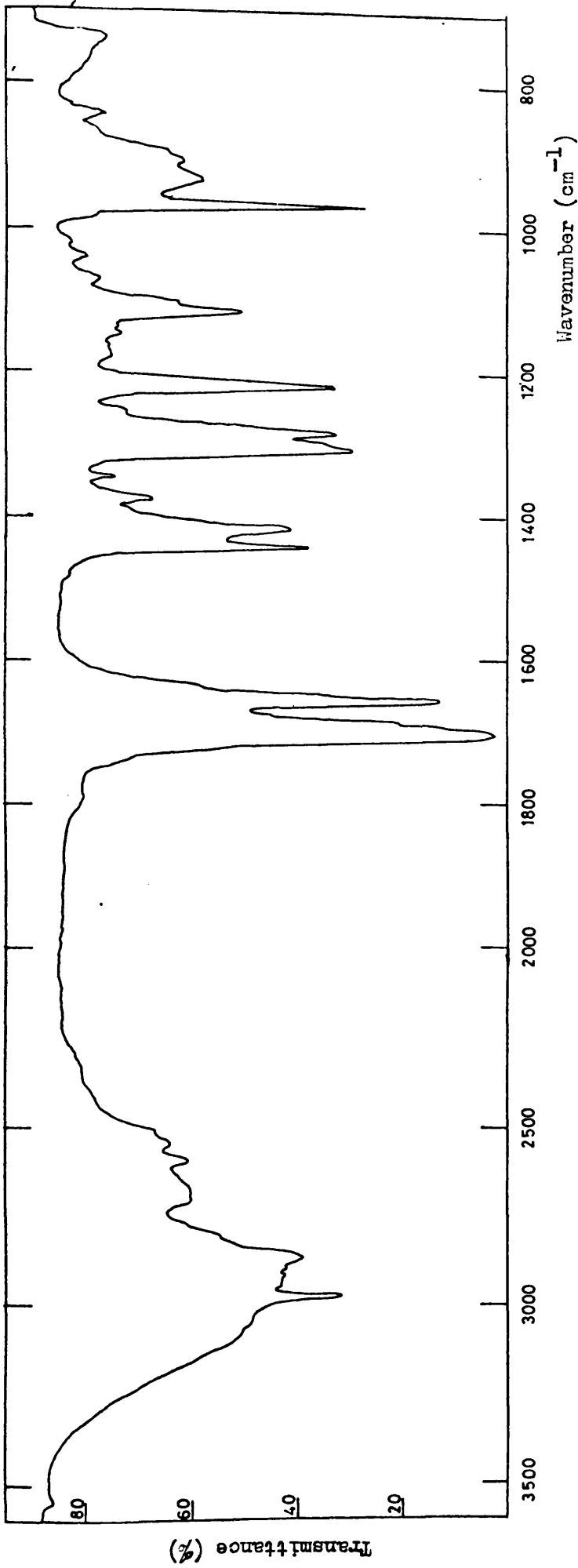
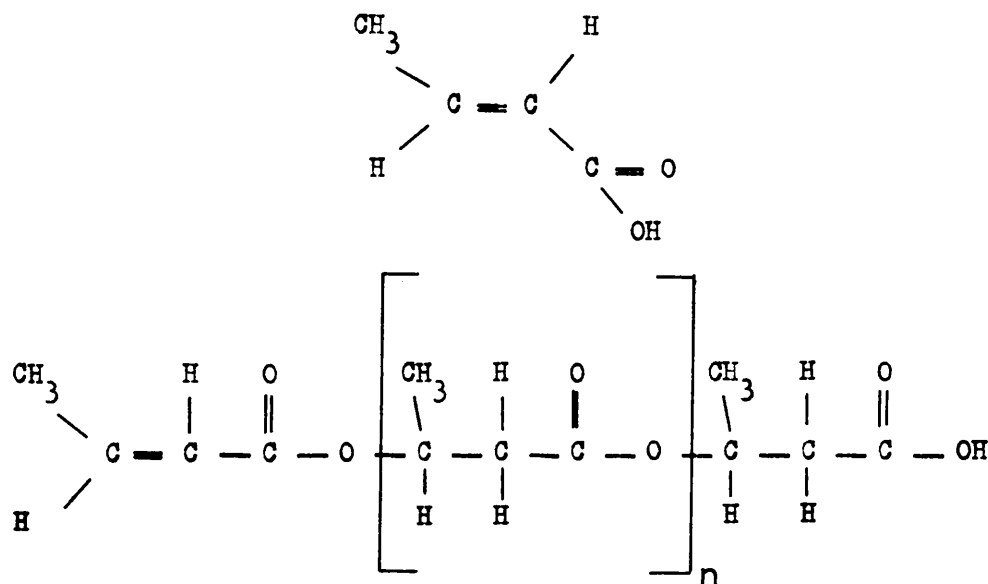


FIGURE 4.5
IR SPECTRUM OF THE PRODUCT OF PEAK K

The IR and NMR spectra were identical to those in Figures 3.19 and 3.20. The GLC trace, Figure 4.6, displayed peaks with similar relative retention times to that obtained from the CRF formed under vacuum (Figure 3.24), and a plot of relative retention time for these peaks versus the integers 1 to 4 again gave a straight line. (Figure 4.7). The MS (Figure 4.8, Table 4.A) also showed peaks due to the tetramer, trimer, dimer of PHB and crotonic acid as reported in Chapter 3.8 (Figure 3.22, Table 3.F)

Thus by an identical argument to that set out in Chapter 3.8 the CRF formed during a degradation of PHB under nitrogen to 500°C at a rate of 10°C/min consists of the following species.



where $n = 0, 1$ or 2 .

4.6 THE RESIDUE FORMED UPON HEATING PHB TO 500°C UNDER NITROGEN

There was only slight discolouration to the base of the degradation tube (brown-black) after degradation under nitrogen to 500°C.

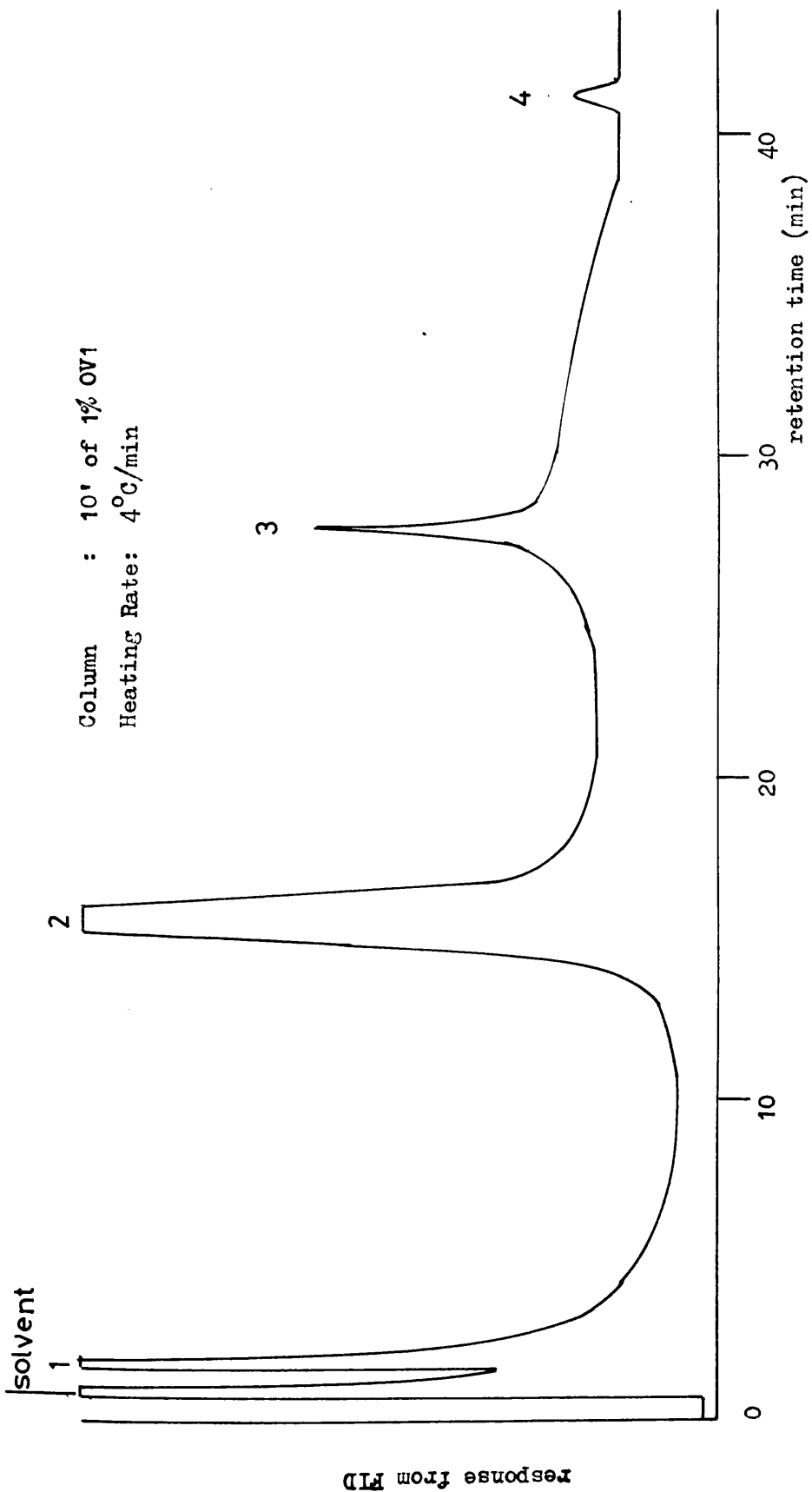


FIGURE 4.6
GLC TRACE OF THE CRF OBTAINED DURING THE THERMAL DEGRADATION
OF PFB TO 500°C UNDER NITROGEN

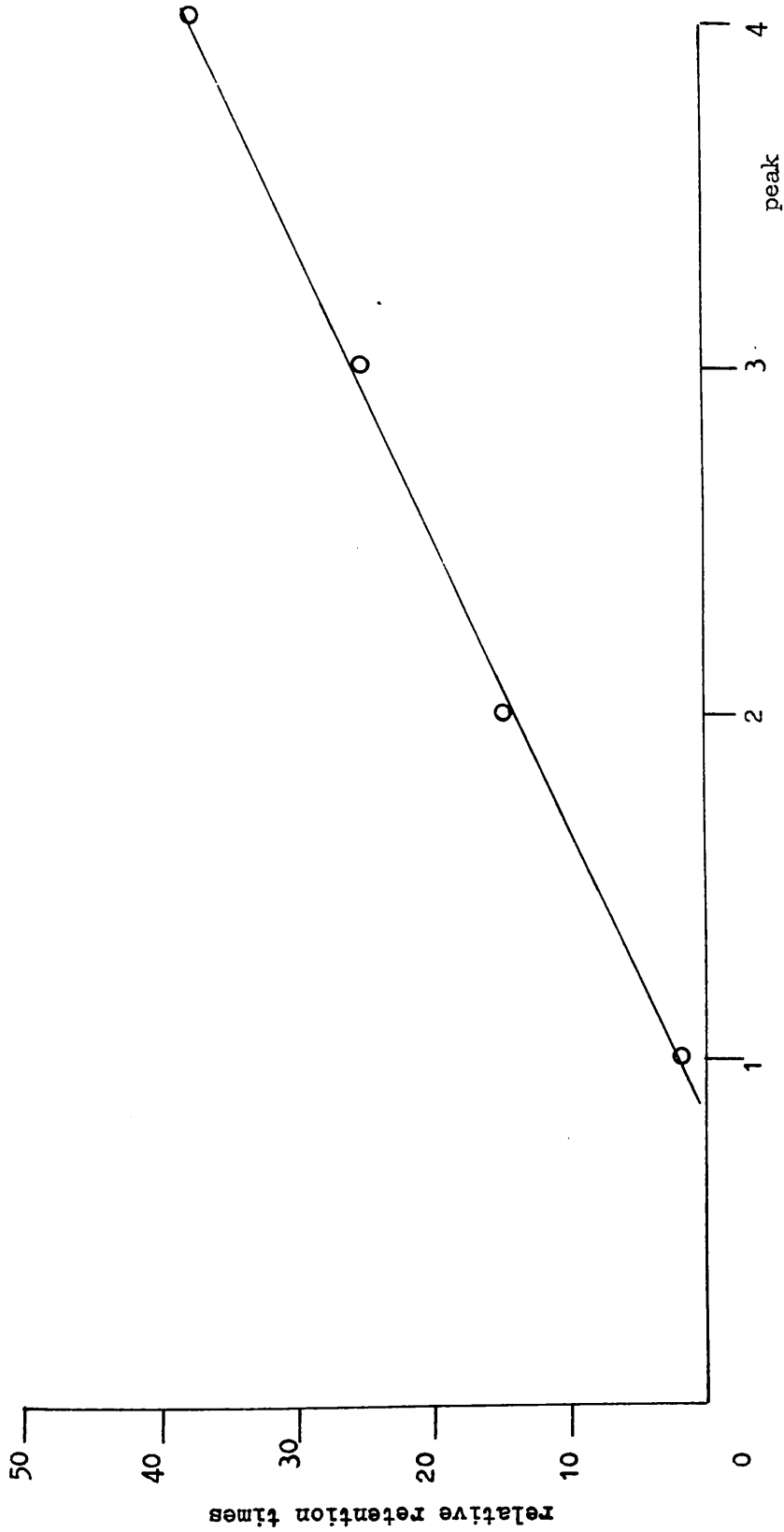


FIGURE 4.7

THE RELATIONSHIP BETWEEN THE RELATIVE RETENTION TIMES OF THE PEAKS
IN THE GLC TRACE (FIG. 4.6) OF THE CRF FORMED ON HEATING PHB
TO 500°C UNDER VACUUM

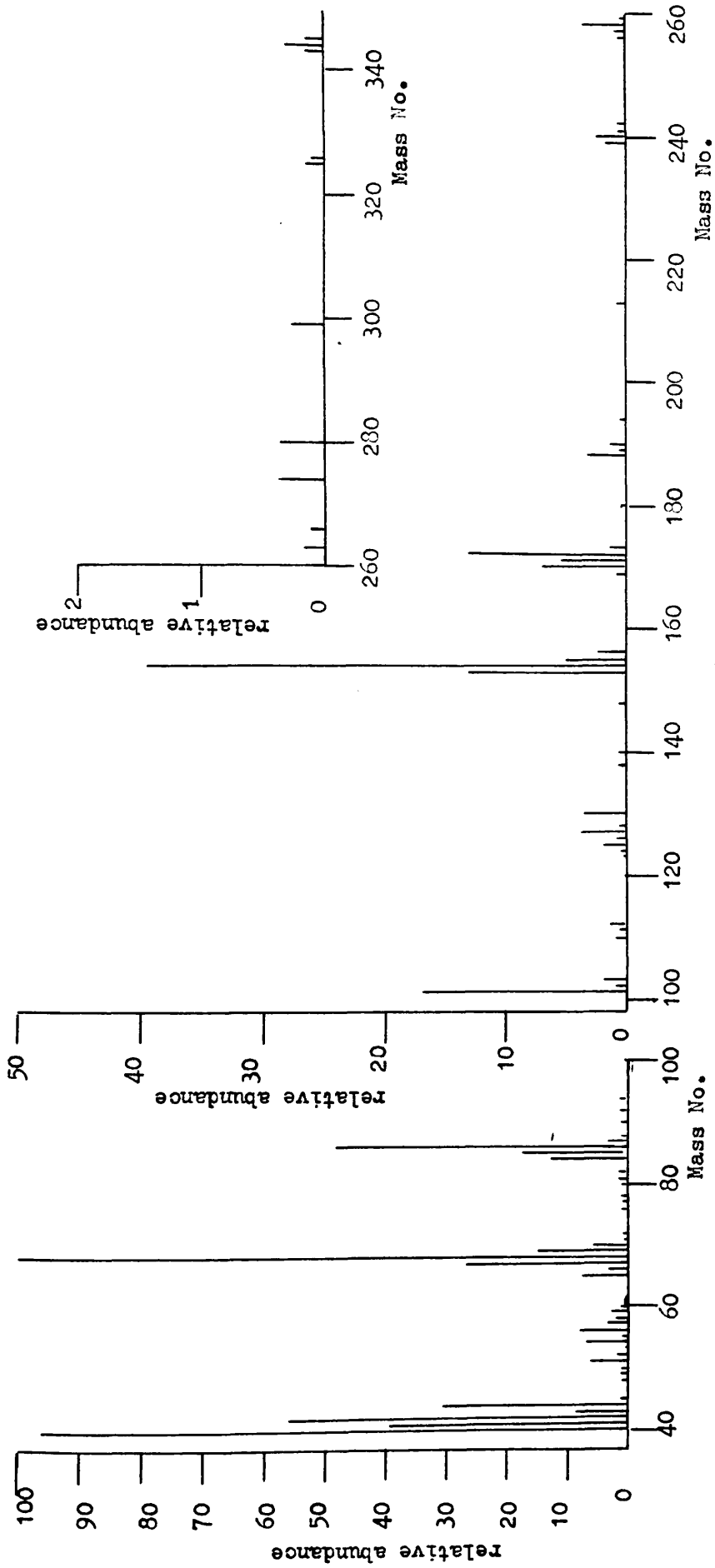


FIGURE 4.8

**MASS SPECTRUM OF THE CRF FORMED ON HEATING FHB FROM
 AMBIENT TO 500°C AT 10°C/MIN UNDER NITROGEN**

TABLE 4.A

ASSIGNMENT OF THE MAIN PEAKS IN THE MASS SPECTRUM OF THE CRF
FORMED UPON HEATING PHB TO 500°C UNDER A NITROGEN FLOW

m/e	Assignment	
345	tetramer + 1	(M ₄ + 1)
344	tetramer	(M ₄)
327	(M ₄ - OH)	
326	(M ₄ - H ₂ O)	
300	(M ₄ - CO ₂)	(M ₄ + 1 - CO ₂ H)
259	trimer + 1	(M ₃ + 1)
258	trimer	(M ₃)
241	(M ₃ - OH)	
240	(M ₃ - H ₂ O)	
214	(M ₃ - CO ₂)	(M ₃ + 1 - CO ₂ H)
173	dimer + 1	(M ₂ + 1)
172	dimer	(M ₂)
155	(M ₂ - OH)	
154	(M ₂ - H ₂ O)	
128	(M ₂ - CO ₂)	(M ₂ + 1 - CO ₂ H)
86	crotonic acid	(M ₁)
69	(M ₁ - OH)	
68	(M ₁ - H ₂ O)	
42	(M ₁ - CO ₂)	
41	(M ₁ - CO ₂ H)	

4.7 CONCLUSIONS

The following species were identified as products of the thermal degradation of PHB, under nitrogen, to 500°C.

- I tetramer of PHB (acidic and unsaturated end groups)
- II trimer of PHB (acidic and unsaturated end groups)
- III dimer of PHB (acidic and unsaturated end groups)
- IV crotonic acid (trans-but-2-enoic acid)
- V isocrotonic acid (cis-but-2-enoic acid)
- VI water
- VII acetaldehyde
- VIII ketene (trace)
- IX propene
- X carbon dioxide

Although no β butyrolactone (β BL) was identified the presence of VII and VIII, which are thermal degradation products of β BL, are strong evidence for its formation probably by the mechanism of Equation 3.2

The fact that β BL was not seen is hardly surprising as it will not be removed from the hot zone as quickly under a nitrogen flow as under vacuum and would be expected to degrade further to give VII and VIII by α -acyl fission and IX and X by α -alkyl fission as in Equations 3.4 and 3.5 respectively. (Ref. 100).

Thus the products formed during the thermal degradation of PHB under an atmosphere of nitrogen are identical, though in different quantities, to those formed under vacuum. The discussion of the products of the thermal degradation of PHB under vacuum and likely mechanisms for their formation contained within Chapter 3.14 (pp112-120) is also valid for the thermal

degradation of PHB under a nitrogen atmosphere and therefore shall not be repeated here. One important point to be noted, however, is that acetaldehyde will not be expected to be a degradation product of crotonic acid under nitrogen as it was under vacuum. (Ref. 101).

The formation of I to III from the polymer backbone will be discussed (Chapter 6) after the molecular weight changes which occur on heating PHB have been investigated.

CHAPTER 5

QUANTITATIVE ANALYSIS OF THE PRODUCTS OF THERMAL DEGRADATION OF PHB UNDER VACUUM AND NITROGEN

5.1 INTRODUCTION

In the previous two chapters the nature of the products formed during the thermal degradation of PHB under vacuum and nitrogen was discussed. In this chapter the results of their quantitative analysis are recorded.

5.2 CONDITIONS OF MEASUREMENT AND CALIBRATION CURVES FOR DEGRADATION PRODUCTS

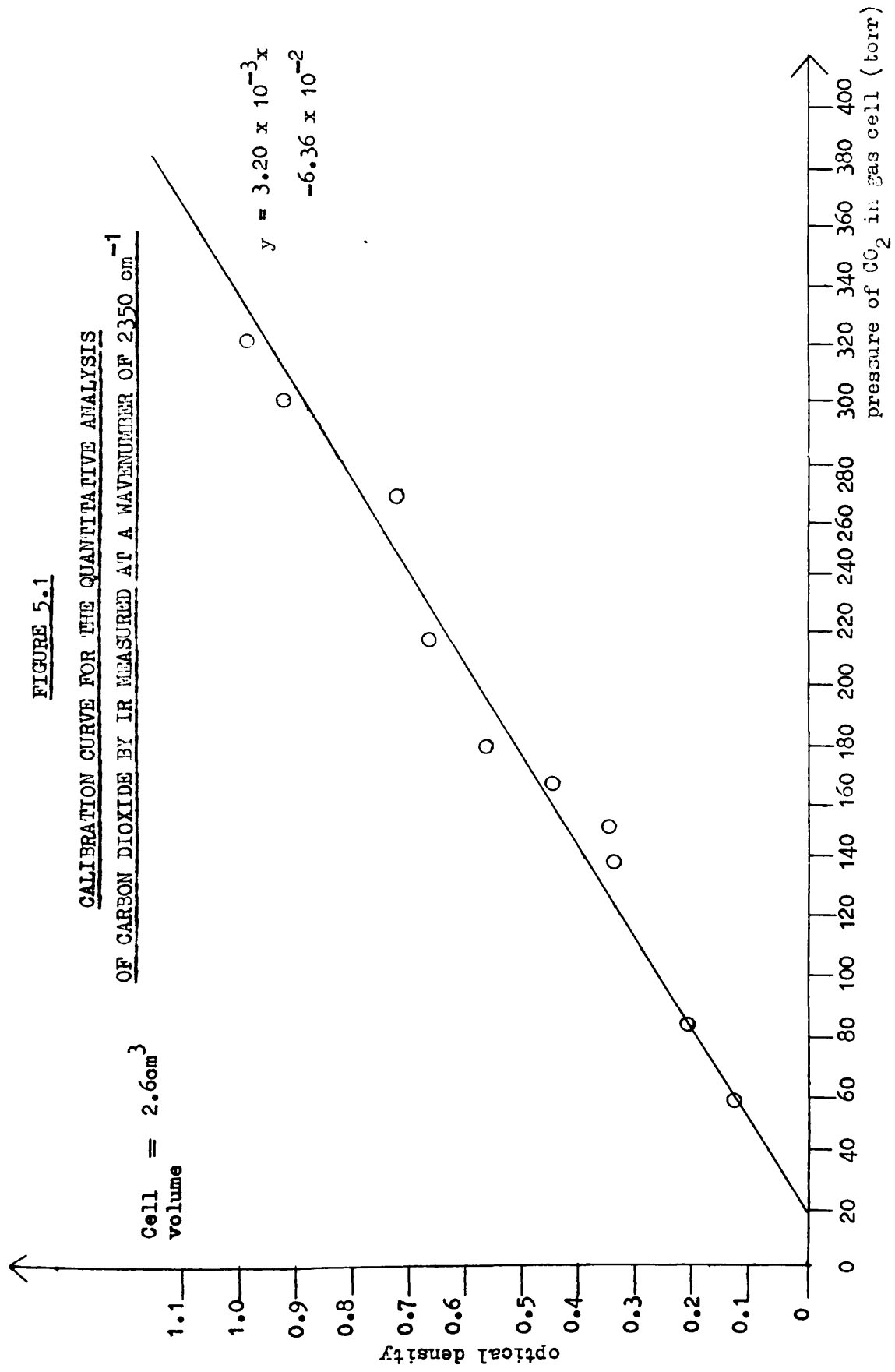
Calibration curves for carbon dioxide and propene were obtained by the method outlined in Chapter 2.5 (ii)(a). The optical densities (OD) of IR spectra of CO_2 were measured at 2350 cm^{-1} and plotted against pressure of CO_2 as shown in Figure 5.1. The curve represents a least squares fit of the points. Similar calibration curves were obtained for propene using the wavenumbers, 910 cm^{-1} , 917 cm^{-1} , and 990 cm^{-1} , (Figure 5.2). The quality of ketene formed was measured as outlined in Chapter 2.5(ii)(a), by subtracting the pressure of all other gases present, CO_2 and CH_2CHCH_3 in this case, from the total pressure.

Calibration curves for acetaldehyde in chloroform (OD at 1724 cm^{-1}), β -butyrolactone in carbon tetrachloride (OD at 1840 cm^{-1}) and crotonic acid in carbon tetrachloride (OD at 1709 cm^{-1} and 1660 cm^{-1}) were obtained by the method outlined in Chapter 2.5(ii)(b) and are illustrated in figures 5.3, 5.4 and

FIGURE 5.1

CALIBRATION CURVE FOR THE QUANTITATIVE ANALYSIS
OF CARBON DIOXIDE BY IR MEASURED AT A WAVENUMBER OF 2350 cm⁻¹

Cell volume = 2.60m³



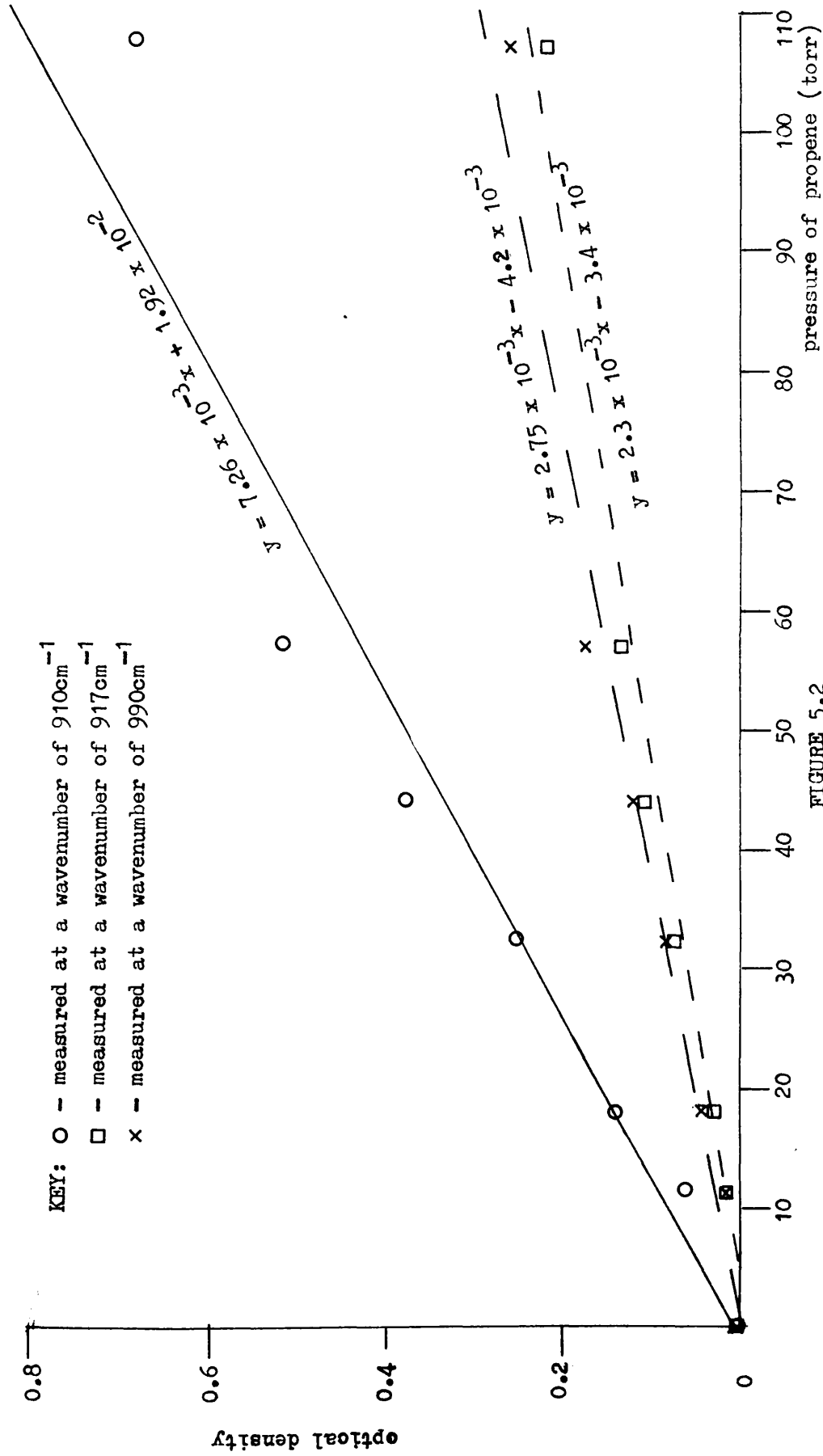
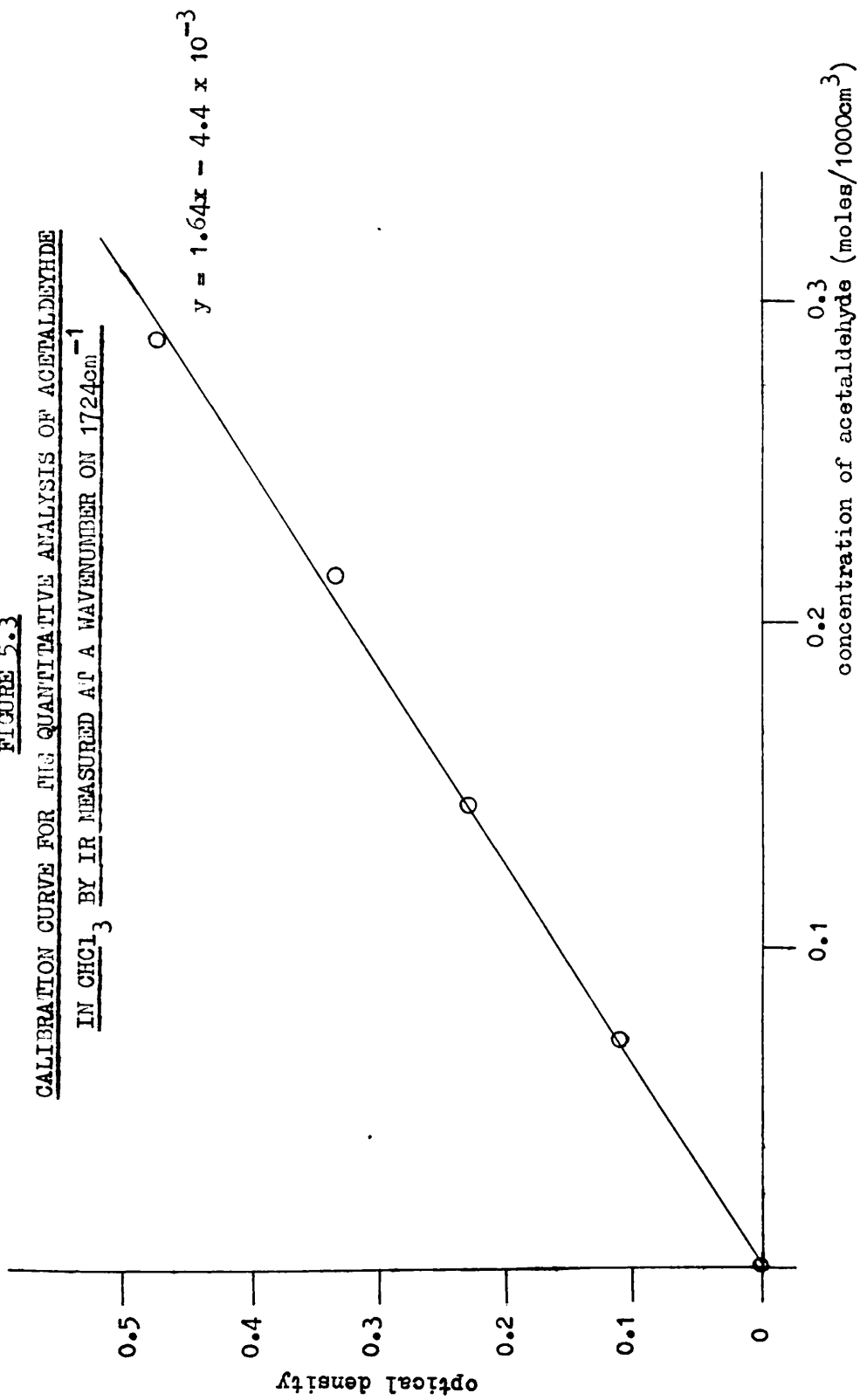


FIGURE 5.2

CALIBRATION CURVES FOR THE QUANTITATIVE ANALYSIS OF PROPENE BY IR

FIGURE 5.3

CALIBRATION CURVE FOR THE QUANTITATIVE ANALYSIS OF ACETALDEHYDE
IN CHCl₃ BY IR MEASURED AT A WAVELENGTH OF 1724cm⁻¹



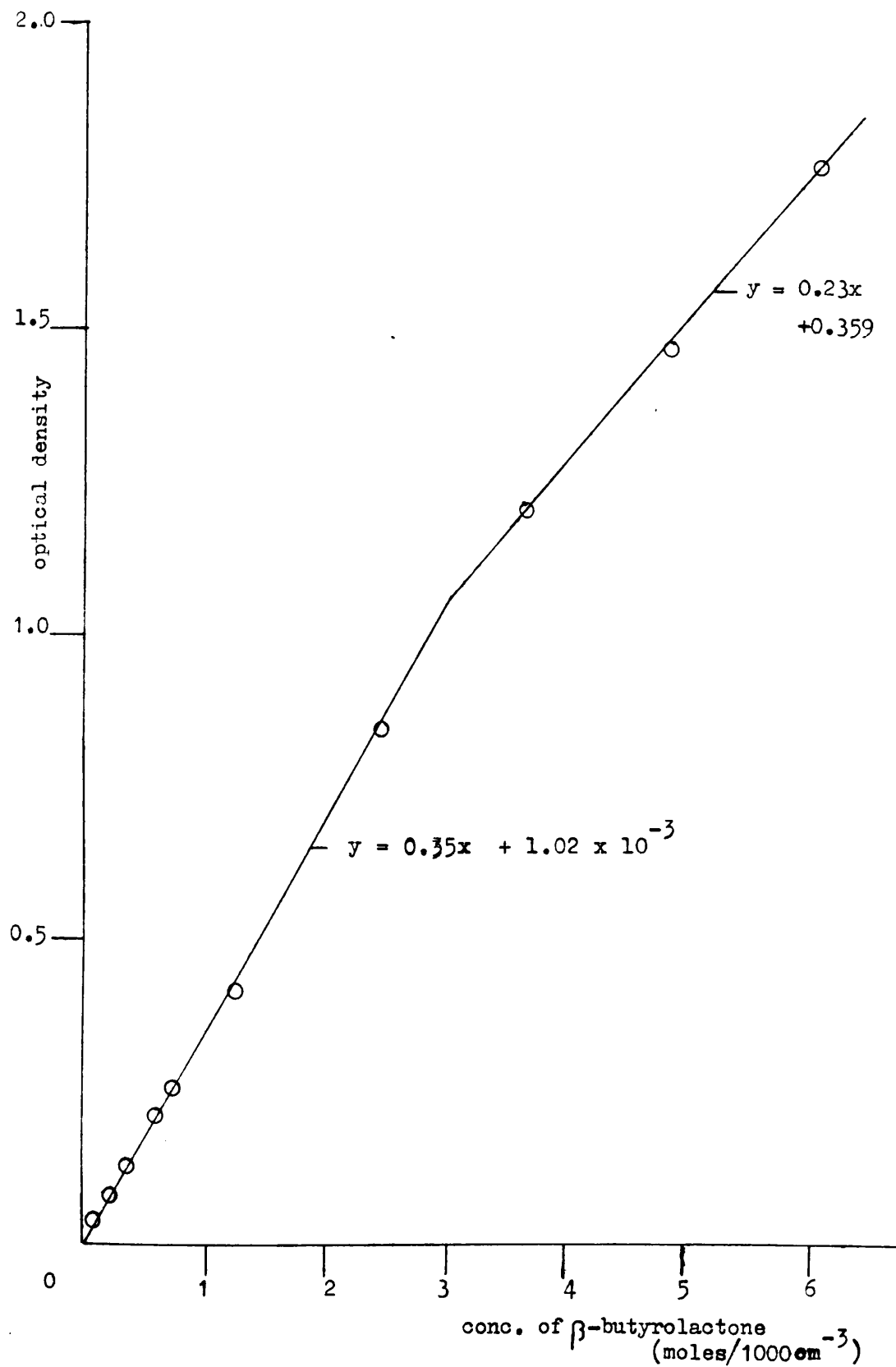


FIGURE 5.4

**CALIBRATION CURVE FOR THE QUANTITATIVE ANALYSIS
OF β -BUTYROLACTONE IN CCl_4 SOLUTION BY IR AT A
WAVENUMBER OF 1840cm^{-1}**

5.5. The gradient of the curve for β BL changes at a concentration of $3\text{mol}/1000\text{cm}^3$ probably due to increased hydrogen bonding between β BL molecules at higher concentrations. For this reason all quantitative measurements of β BL were made using solutions with concentrations well below $3\text{mol}/1000\text{cm}^3$.

As pure isocrotonic acid was not available, the calibration curve obtained for carbonyl stretch in crotonic acid, in carbon tetrachloride, at 1709cm^{-1} (Figure 5.5) was used for the estimation of isocrotonic acid through its carbonyl stretch at 1705cm^{-1} .

All solution spectra were run in matched 0.1mm NaCl cells. Where more than one calibration wavenumber was available an average of the results obtained, using each wavenumber, was quoted.

Carbon dioxide, propene and ketene were measured together in one gas cell as were β butyrolactone and isocrotonic acid in a solution cell.

Since the weight of the residue after degradation is negligible, the weight of the volatiles and of the CRF were calculated from the weight of the degradation tube empty and with the polymer before the experiment and with the CRF afterwards.

The composition of the CRF was determined by GLC using the method outlined in Chapter 2.5 (vii).

5.3 QUANTITATIVE ANALYSIS OF THE PRODUCTS FORMED IN THE THERMAL DEGRADATION OF PHB UNDER VACUUM

The quantitative analysis of the products formed on heating PHB from ambient to 500°C at a heating rate of $10^\circ\text{C}/\text{min}$ under vacuum, and measured by the methods outlined in the previous section, are tabulated in Tables 5.A, 5.B and 5.C. All results

FIGURE 5.5
CALIBRATION CURVE FOR THE IR QUANTITATIVE ANALYSIS OF CROTONIC ACID
DISSOLVED IN CCl₄

KEY: O - calibration curve for C=O stretch at 1709cm⁻¹
 □ - " " C=C " " 1660cm⁻¹

$y = 8.36 \times 10^{-2} x - 1.75 \times 10^{-2}$

$y = 3.69 \times 10^{-2} x - 6.9 \times 10^{-3}$

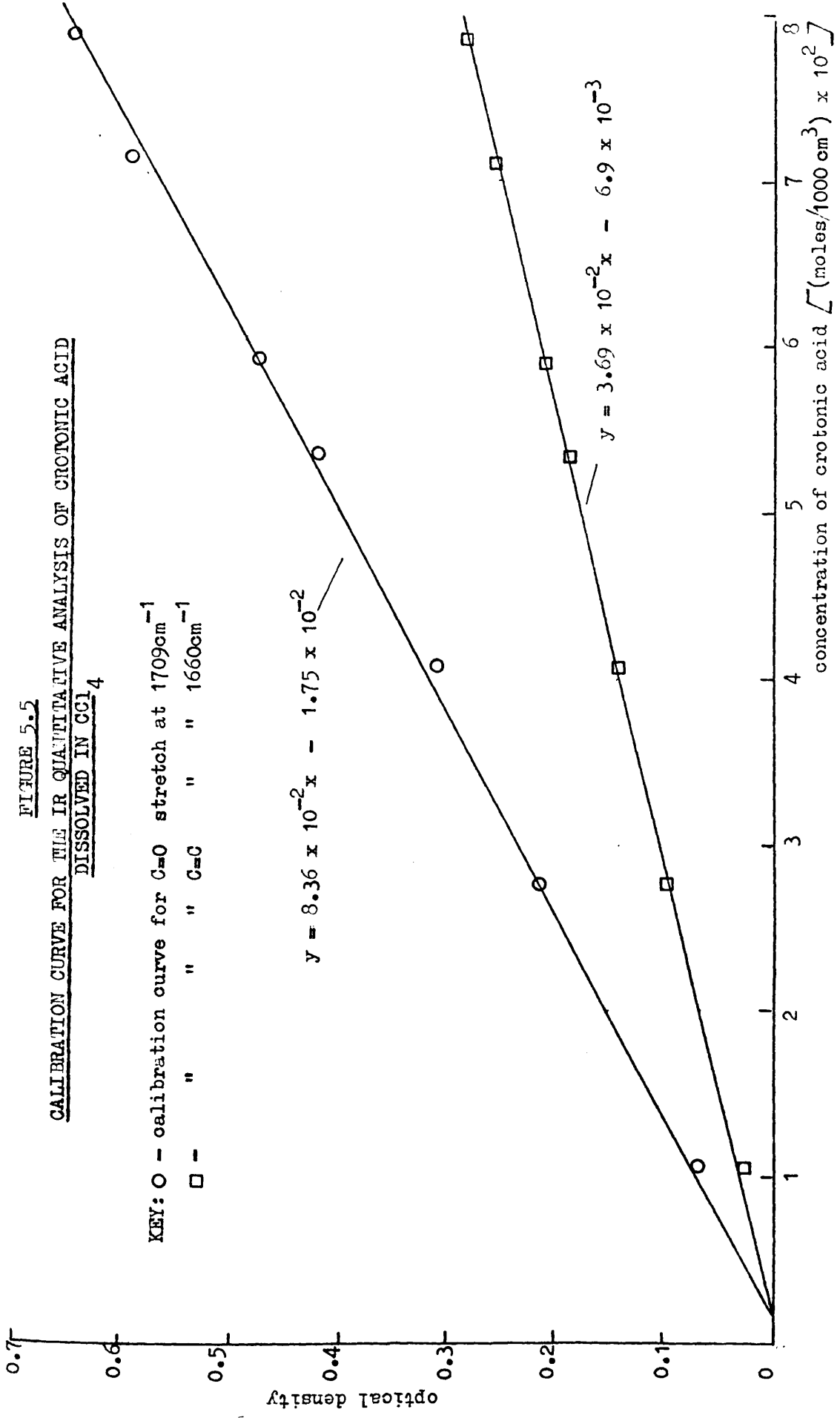
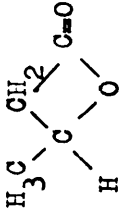
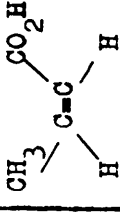
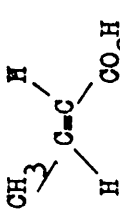


TABLE 5.A

QUANTITATIVE ANALYSIS OF THE CONDENSABLE PRODUCTS OF THERMAL DEGRADATION OF PHB
(0-500°C, 10°C min⁻¹ UNDER VACUUM)

P R O D U C T U N I T S	CO ₂	CH ₂ =CHCH ₃	CH ₂ =C=O	CH ₃ CHO			
Moles/gram of initial polymer	3.7 x 10 ⁻⁴	1.7 x 10 ⁻⁴	8.5 x 10 ⁻⁵	1.2 x 10 ⁻⁴	4.7 x 10 ⁻⁴	1.3 x 10 ⁻⁴	2.2 x 10 ⁻³
Moles of product / Mole of monomer unit	3.2 x 10 ⁻²	1.5 x 10 ⁻²	7.3 x 10 ⁻³	1.0 x 10 ⁻²	4.0 x 10 ⁻²	1.1 x 10 ⁻²	0.189
Weight % of initial polymer	1.6	0.71	0.36	0.53	4.0	1.1	18.9

NOTE: 1. All measurements were made by quantitative IR analysis.

2. No measurement was made of water formed.

TABLE 5.B

QUANTITATIVE ANALYSIS OF THE CRF FROM PHB
(0-500°C, 10°C min⁻¹ UNDER VACUUM)

U n i t s / P r o d u c t	Crotonic acid	Dimer of PHB	Trimer of PHB	Tetramer of PHB
Mole % of CRF	36.9	47.8	14.4	0.9
Weight % of CRF	20.6	53.4	24.1	2.0
$\frac{\text{Moles of product}}{\text{Mole of monomer unit}}$	0.158	0.205	6.2×10^{-2}	3.85×10^{-3}
Weight % of initial polymer	15.8	41.1	18.5	1.5

NOTE: Measurements made by GLC.

TABLE 5.C

MASS BALANCE TABLE FOR DEGRADATION OF PHB
TO 338°C and 500°C UNDER TVA CONDITIONS

Products	Weight % of Initial Polymer	
	to 338°C	to 500°C
Carbon Dioxide	trace	1.6
Propene	trace	0.7
Ketene	—	0.4
Acetaldehyde	—	0.5
Water	No measurement	No measurement
β Butyrolactone	—	4.0
Isocrotonic Acid	0.9	1.1
Crotonic Acid { in cold trap	3.4	18.9
{ in CRF	31.9	15.8
	35.3	34.7
Dimer of PHB	41.2	41.1
Trimer of PHB	12.5	18.5
Tetramer of PHB	2.9	1.5
Residue	trace	trace
Total	92.8	104.1

quoted are average values obtained over at least four experiments.

The results in Table 5.A show that crotonic acid is the major condensable volatile, accounting for 18.9% by weight of the initial polymer. The value quoted for β -butyrolactone, 4.7×10^{-4} moles/g, takes no account of any further degradation of β BL to $\text{CO}_2 + \text{CH}_2\text{CHCH}_3$ and $\text{CH}_2\text{CO} + \text{CH}_3\text{CHO}$, which was discussed in Chapter 3.14. Degradation of β BL to CH_2CO and CH_3CHO would account for a further 1×10^{-4} moles of β BL/g of PHB. Isocrotonic acid and crotonic acid are similar to β BL in undergoing further degradation reactions prior to leaving the hot zone. Therefore the quantities quoted in Table 5.A should be considered as lower limits for the formation of these products.

The composition of the CRF, which accounted for 76.9% by weight of the original polymer, is given in Table 5.B. Clearly the dimer of PHB is the major constituent.

The percentage composition by weight of the initial polymer, for each degradation product analysed, is tabulated in Table 5.C. No measurement for water was obtained and the major absolute error in the results can be attributed to the measurement of the weight of the CRF, estimated as $\pm 3\%$. From these data it can be seen that the most abundant products of thermal degradation are dimer (41.1%), followed by crotonic acid (34.7%) and trimer (18.5%).

Quantitative analysis of the products formed when the heating programme was terminated at 338°C are summarised in Tables 5.C, 5.D and 5.E. The results quoted are average values over at least four experiments.

The CRF accounted for 88.5% of the original weight of undegraded polymer and from the data in Table 5.C the most abundant products formed up to 338°C are, dimer (41.2%)

TABLE 5.D

QUANTITATIVE ANALYSIS OF THE CONDENSABLE PRODUCTS
OF THERMAL DEGRADATION OF PHB
(0-338°C, 10°C min⁻¹ under vacuum)

P r o d u c t U n i t s	$\begin{array}{c} \text{CH}_3 \quad \text{CO}_2\text{H} \\ \diagdown \quad / \\ \text{C} = \text{C} \\ / \quad \diagdown \\ \text{H} \quad \text{H} \end{array}$	$\begin{array}{c} \text{CH}_3 \quad \text{H} \\ \diagdown \quad / \\ \text{C} = \text{C} \\ / \quad \diagdown \\ \text{H} \quad \text{CO}_2\text{H} \end{array}$
Moles/gram of initial polymer	1.1×10^{-4}	3.9×10^{-4}
$\frac{\text{Moles of product}}{\text{Mole of monomer unit}}$	9×10^{-3}	3.4×10^{-2}
Weight % of initial polymer	0.9	3.4

TABLE 5.E

QUANTITATIVE ANALYSIS OF THE CRF FROM PHB
(0-338°C, 10°C min⁻¹, UNDER VACUUM)

U n i t s / P r o d u c t	Crotonic acid	Dimer of PHB	Trimer of PHB	Tetramer of PHB
Mole % of CRF	66.2	27.3	5.5	1.0
Weight % of CRF	36.1	46.5	14.1	3.3
<u>Moles of product</u> Mole of monomer unit	0.319	0.206	4.17×10^{-2}	7.25×10^{-3}
Weight % of initial polymer	31.9	41.2	12.5	2.9

followed by crotonic acid (35.3%) and trimer (12.5%). No measurement was made of the quantity of water formed and as before the major absolute error was in the measurement of the weight of the CRF, estimated to be $\pm 2\%$.

From the data in Table 5.C a comparison of the quantities of each product formed up to 338°C and up to 500°C can be made. Although the percentage of crotonic acid at both temperatures is similar, a far higher proportion was present in the CRF at 338°C than at 500°C . Although no quantitative measurement was made of the water formed it is clear from the heights of the water peaks in the SATVA traces (Figures 3.6 and 3.26) that there is no significant difference.

A comparison of the weight ratio of tetramer:trimer:dimer:crotonic acid, 1:4.3:14.2:12.2 formed up to 338°C to that formed up to 500°C , 1:12.3:27.4:23.1 is interesting. It indicates a tendency to form lower oligomers at higher temperatures during the TVA experiment. This is strong evidence for the breakdown of the oligomers at temperatures greater than 338°C to form lower oligomers, β butyrolactone, isocrotonic acid and crotonic acid as discussed in Chapter 3.14.

5.4 QUANTITATIVE ANALYSIS OF THE PRODUCTS FORMED FROM THE THERMAL DEGRADATION OF PHB UNDER NITROGEN

Quantitative analysis of the products of thermal degradation of PHB obtained by heating from ambient to 500°C at a rate of $10^{\circ}\text{C}/\text{min}$ under a flow of $80\text{ cm}^3/\text{min}$ of nitrogen was measured as outlined in Chapter 5.2. The results, summarised in Tables 5.F and 5.G, are the average of at least four experiments.

TABLE 5.F

QUANTITATIVE ANALYSIS OF THE CONDENSABLE PRODUCTS FROM PHB
 (0-500°C, 10°C⁻¹, under nitrogen)

Products	CO ₂	CH ₂ =CHCH ₃	CH ₂ =C=O	CH ₃ CHO	$\begin{array}{c} \text{CO}_2\text{H} \\ \\ \text{CH}_3-\text{C}=\text{C}-\text{H} \\ \\ \text{H} \end{array}$	$\begin{array}{c} \text{H} \\ \\ \text{CH}_3-\text{C}=\text{C}-\text{CO}_2\text{H} \\ \\ \text{H} \end{array}$
Moles/gram of initial polymer	2.2 x 10 ⁻⁴	1.0 x 10 ⁻⁴	trace	5.0 x 10 ⁻⁵	1.6 x 10 ⁻⁴	1.0 x 10 ⁻³
Moles of product / Mole of monomer unit	1.9 x 10 ⁻²	8.6 x 10 ⁻⁴	trace	4.3 x 10 ⁻³	1.4 x 10 ⁻²	8.6 x 10 ⁻²
Weight % of initial polymer	1.0	0.4	trace	0.2	1.4	8.6

TABLE 5.GQUANTITATIVE ANALYSIS OF THE CRF FROM PHB(0-500°C, 10°C min⁻¹, under nitrogen)

P r o d u c t U n i t s	Crotonic Acid	Dimer of PHB	Trimer of PHB	Tetramer of PHB
Mole % of CRF	53.4	41.1	4.9	0.5
Weight % of CRF	35.0	53.9	9.7	1.4

The major product collected in the cold trap was crotonic acid. The presence of acetaldehyde and ketene, which are products of decomposition of β butyrolactone (see Equation 3.4), give an indication of the lower limit of formation of β BL as 5×10^{-5} moles/gm of PHB under nitrogen. β Butyrolactone also degrades to give carbon dioxide and propene as does crotonic and isocrotonic acid.

Since the species making up the cold ring fraction condensed on the tube delivering the nitrogen (see Figure 2.19), the glassware connecting the degradation tube to the vacuum system and in the cold trap, as well as on the walls of the degradation tube, no complete quantitative measurement of the weight of CRF could be made. However the weight of CRF on the walls of the degradation tube alone was in the range 70% to 80% by weight of the original undegraded polymer. This value is similar to that obtained for the whole CRF under vacuum (76.9%). This, combined with the observation that the volatiles condensed in the cold trap accounted for 27.2% of the weight of undegraded PHB under vacuum compared to 11.6% under nitrogen suggests the formation of a much heavier CRF under nitrogen. The data in Table 5.G shows that the ratio of oligomers measured from that portion of CRF material condensing on the walls of the degradation tube is similar to that obtained under vacuum, with the dimer of PHB accounting for the greatest portion by weight of the CRF.

Assuming that the CRF, formed under nitrogen, accounts for that portion of the initial weight of polymer not contained within the data of Table 5.F, and has the same composition to that noted in Table 5.G, then a mass balance table for the degradation can be constructed as in Table 5.H. From these data, it can be

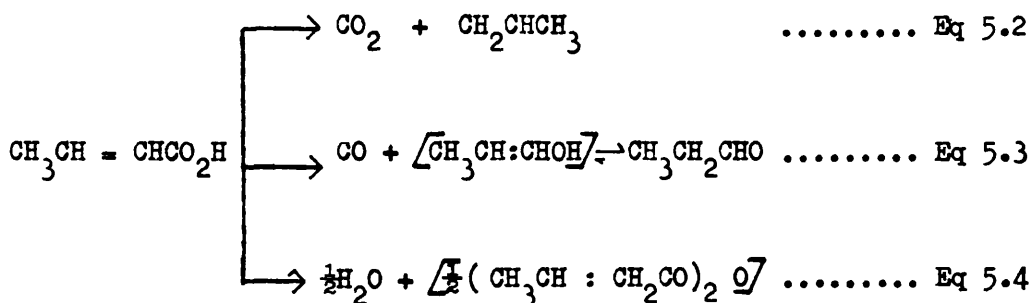
TABLE 5.H

MASS BALANCE TABLE FOR DEGRADATION OF PHB
TO 500°C UNDER NITROGEN (HEATING RATE 10°C min⁻¹)

Products	Weight % of Initial Polymer
Carbon Dioxide	1.0
Propene	0.4
Ketene	trace
Acetaldehyde	0.2
Water	No measurement
β Butyrolactone	Nil
Isocrotonic Acid	1.4
Crotonic Acid (in cold trap in CRF)	8.6 } 30.9 } 39.5
Dimer of PHB	47.6
Trimer of PHB	8.6
Tetramer of PHB	1.2
Residue	trace
Total	99.9

The highly unsaturated residue, A, will rapidly undergo further reaction leading to the formation of the char (or residue) observed on the base of the degradation tube. Since carbon dioxide is only a minor product formed during the thermal decomposition of PHB, accounting for only 2% to 3% of the available carbonyl groups, the formation of a light carbonatious residue, as observed, could account for the observed molar excess of carbon dioxide over propene.

In support of this proposal, it is of interest to consider the thermal decomposition of crotonic acid under nitrogen which has been comprehensively studied by Ritchie et al (Ref. 101) who proposed that, although the reaction reported by Equation 5.2 predominates, the following two reactions also occur.



Propionaldehyde (Equation 5.3) undergoes rapid decomposition at 500°C giving a molar ratio of carbon dioxide : propene of unity (Ref. 102). Only very small quantities of acid anhydride will be formed (Ref. 109) due to a minor intramolecular dehydration (Ref. 109). Therefore from the above one would expect a molar ratio of carbon dioxide to propene of approximately one. In fact Ritchie observed that crotonic acid underwent thermal decomposition at 510°C in a flow reaction vessel giving

molar ratios of carbon dioxide : propene : carbon monoxide of 5.8 : 1 : 2.7. This result and the observed shortage of alkyne in the thermal degradation products of acid anhydrides (Ref. 109) is due to the formation of a highly unsaturated char or residue.

CHAPTER 6

MOLECULAR WEIGHT IN PHB ON ISOTHERMAL HEATING

6.1 INTRODUCTION

The work described in this chapter was carried out to investigate the effect on the molecular weight of samples of poly(-(D)- β -hydroxybutyric acid) (PHB) of heating, at temperatures in the range 170°C to 200°C, for differing lengths of time and under various atmospheres. From this study it was hoped to develop an understanding of the nature of the depolymerisation reaction, whether random or chain end initiating, and to measure the kinetic parameters, such as rate constants and energies of activation, under the various experimental conditions.

The experimental errors quoted were calculated by the method described in Chapter 2.8, and are expressed as (\pm) one standard deviation.

6.2 WEIGHT LOSS ON ISOTHERMAL HEATING OF PHB

Ten milligram samples of PHB were heated at temperatures of 200°C, 190°C, 180°C and 170°C for 2 hours in an isothermal TG analysis in (a) vacuum, (b) a dynamic nitrogen flow and, (c) static air, by the method outlined in Chapter 2.4(i). The results are illustrated in Figures 6.1, 6.2 and 6.3. Below 190°C weight loss is always negligible and begins to become significant at 200°C.

6.3 MOLECULAR WEIGHT CHANGES UNDER VACUUM

The changes in molecular weight during isothermal heating of

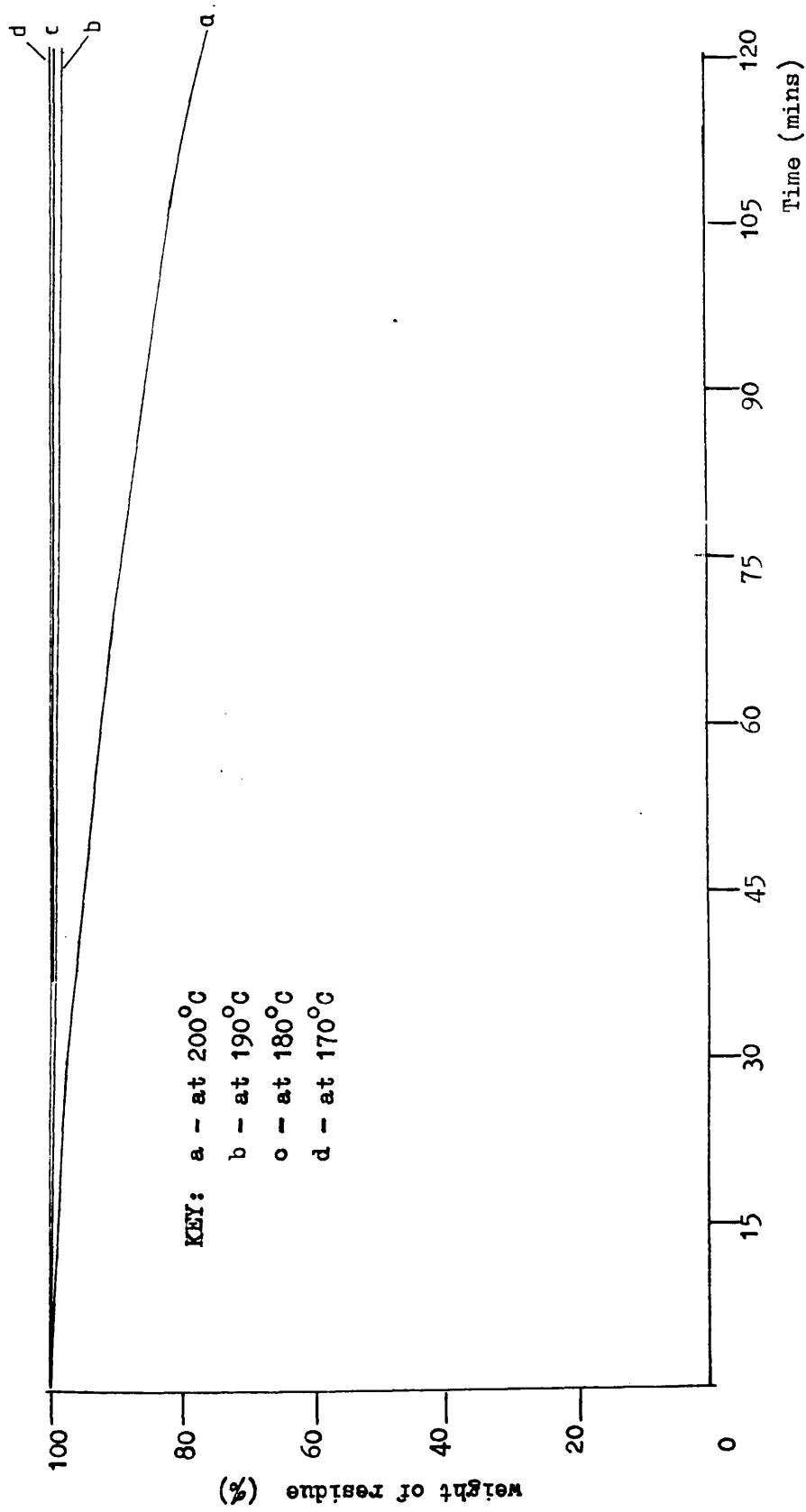


FIGURE 6.1

ISOTHERMAL THERMOGRAVIMETRIC ANALYSIS TRACES OF PHB UNDER VACUUM

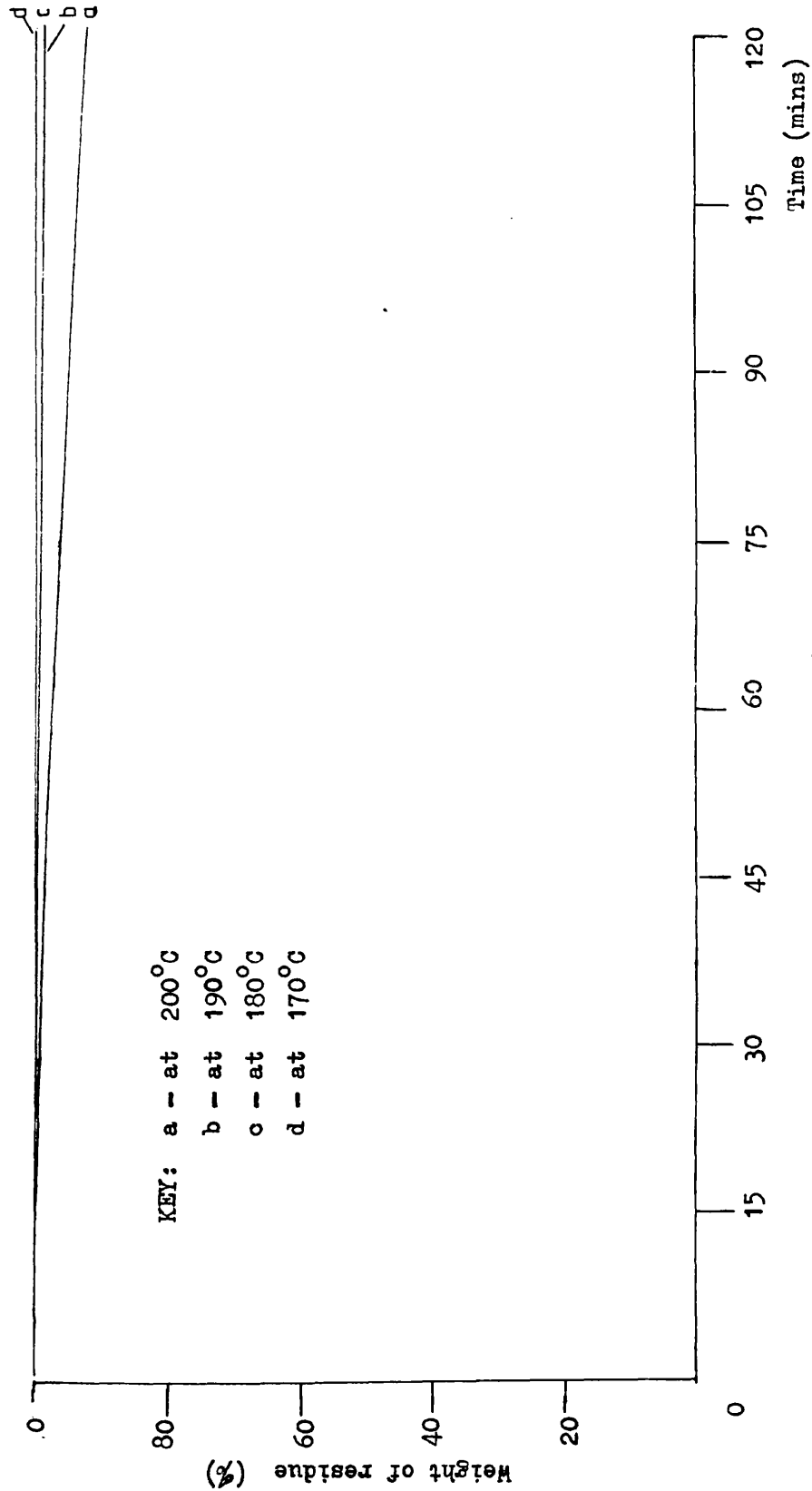


FIGURE 6.2

ISOTHERMAL THERMOGRAVIMETRIC ANALYSIS TRACE OF PHB UNDER NITROGEN
 (flow rate of nitrogen = 50cm²/min)

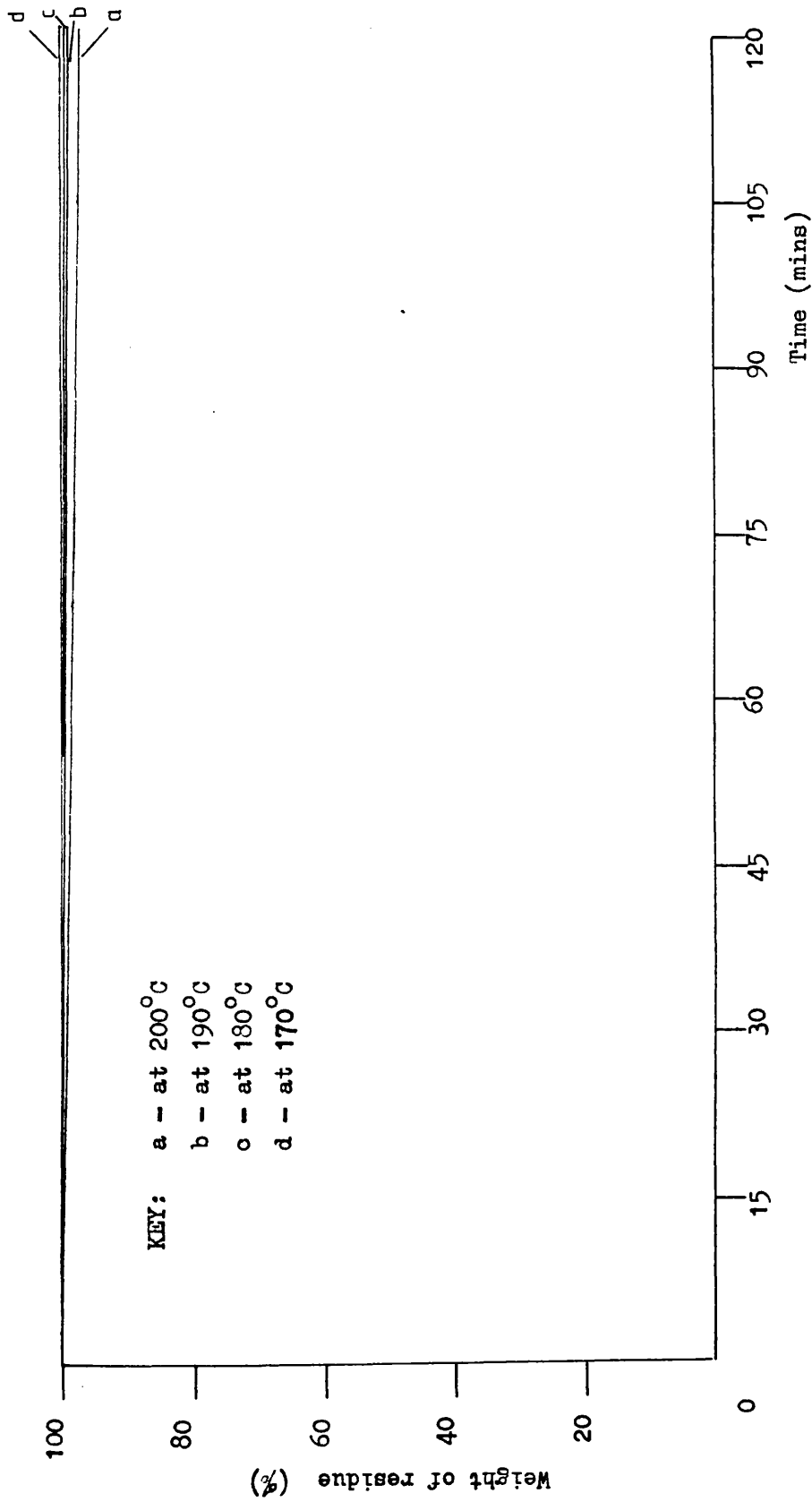


FIGURE 6.3

ISOTHERMAL THERMOGRAVIMETRIC ANALYSIS TRACE OF PHB UNDER STATIC AIR

polymer S1 (Chapter 2.11) under vacuum at various temperatures were investigated by the method outlined in Chapter 2.9(i). Plots of number average molecular weight (\bar{M}_n) versus time of heating, solid trace, at temperatures of 200°C, 190°C, 180°C and 170°C are recorded in Figures 6.4, 6.5, 6.6 and 6.7 respectively. From these figures it is clear that there is either an initial increase in \bar{M}_n followed by a sharp decrease or an increase in \bar{M}_n preceded and followed by a sharp decrease.

The relationships between molecular weight and extent of volatilisation in the temperature range 170–200°C are illustrated in Figures 6.8 and 6.9. The extents of volatilisation were measured by weighing the polymer sample prior to and after heating. The results obtained from the isothermal TG analysis described in Chapter 6.2 were included in Figures 6.8 and 6.9. The rapid decrease in molecular weight at small extents of volatilisation is evidence that the degradation reaction involves a random chain scission mechanism (Ref. 110) but the tendency to increase early in the reaction is quite reproducible and must be accounted for.

It is proposed that it is associated with condensation of terminal hydroxyl and carboxyl groups on the polymer molecules and a correction must be made for this if the true rate of chain scission is to be deduced from molecular weight measurements. The original polymer sample (number average molecular weight = $\bar{M}_{n(o)}$) consists of molecules terminated by hydroxyl and carboxyl groups.



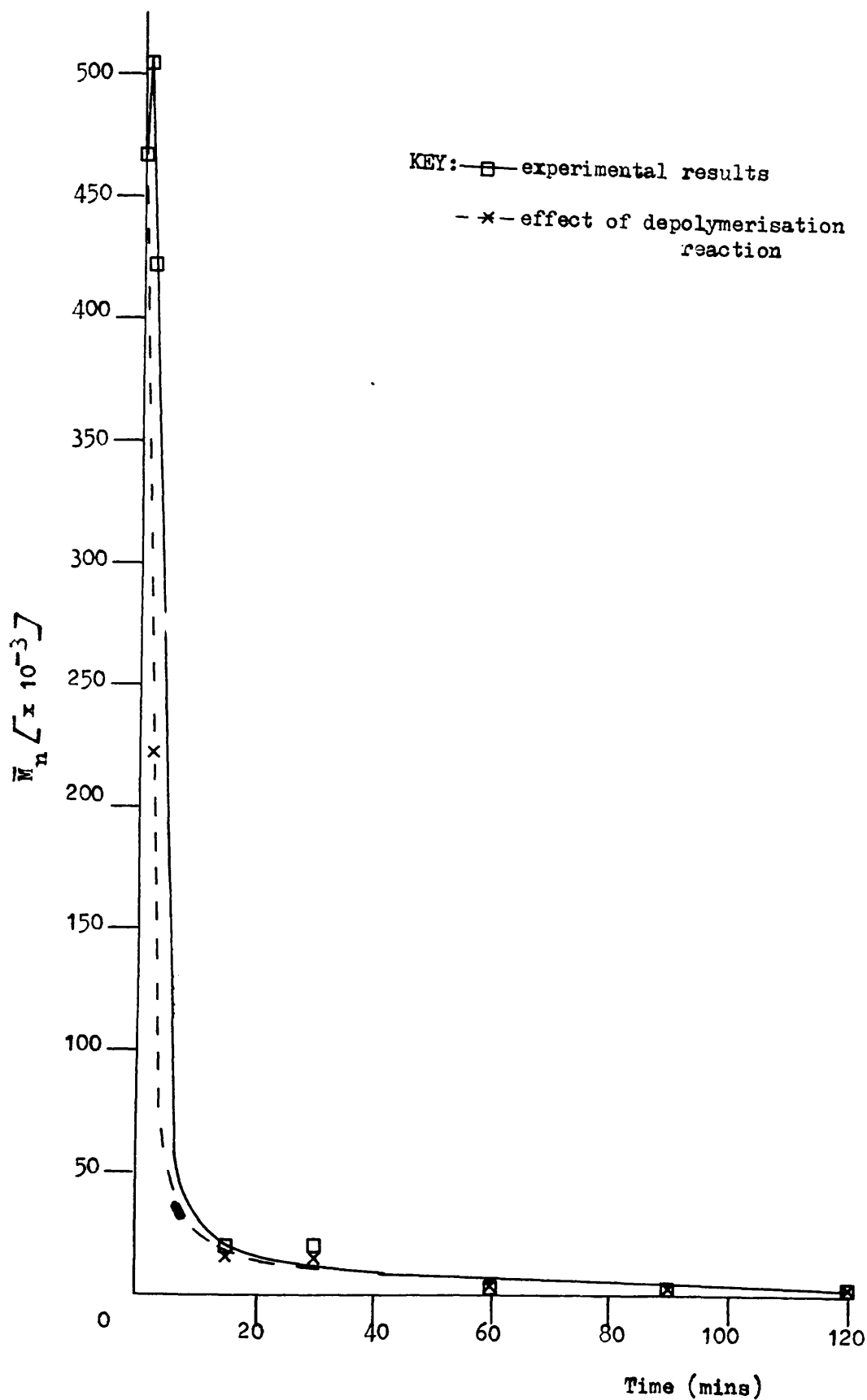


FIGURE 6.4

CHANGES IN MOLECULAR WEIGHT (\bar{M}_n) WITH TIME OF HEATING OF
PHB AT 200°C UNDER VACUUM

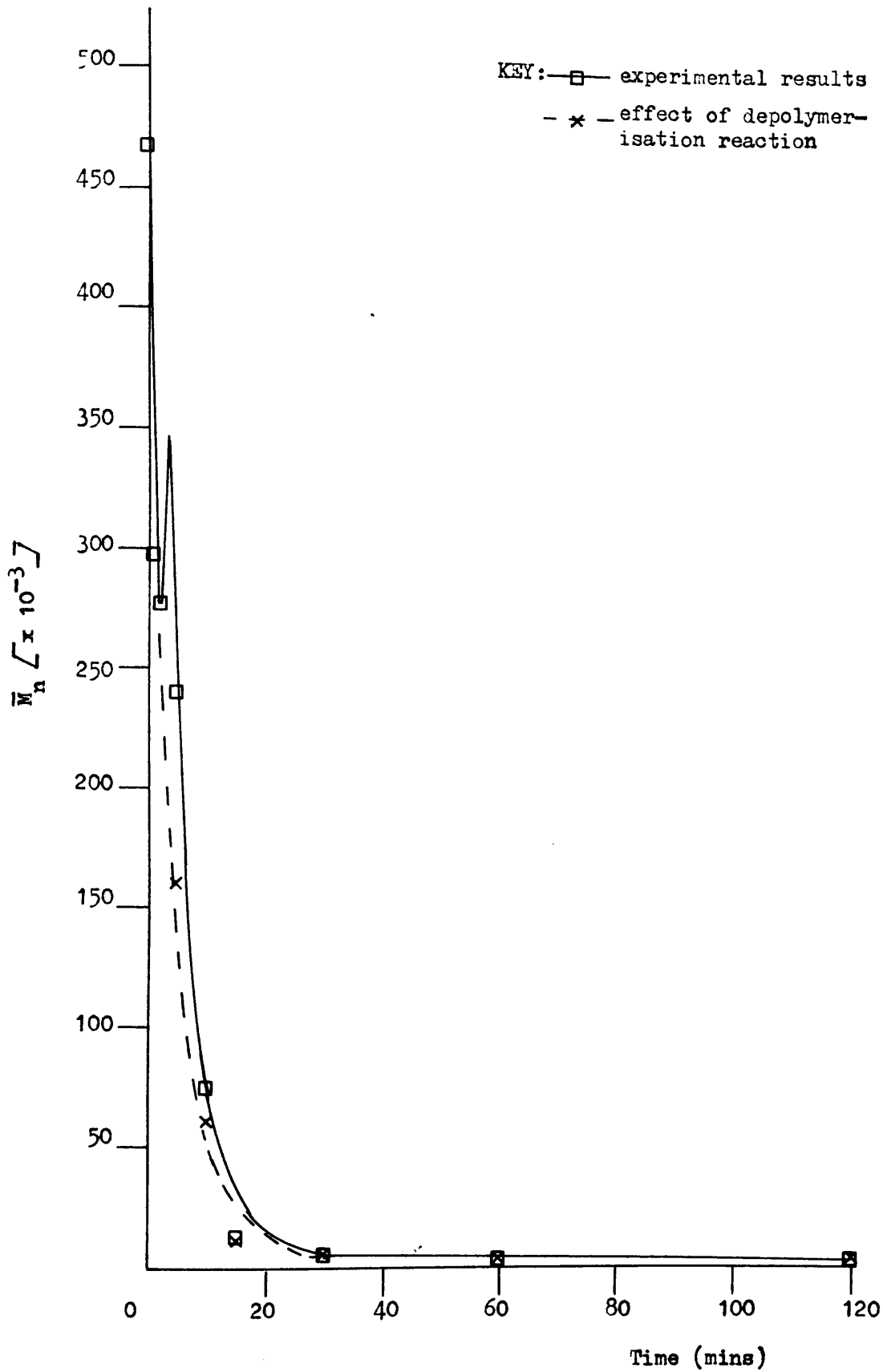


FIGURE 6.5

CHANGES IN MOLECULAR WEIGHT (\bar{M}_n) WITH TIME OF HEATING OF
PHB AT 190°C UNDER VACUUM

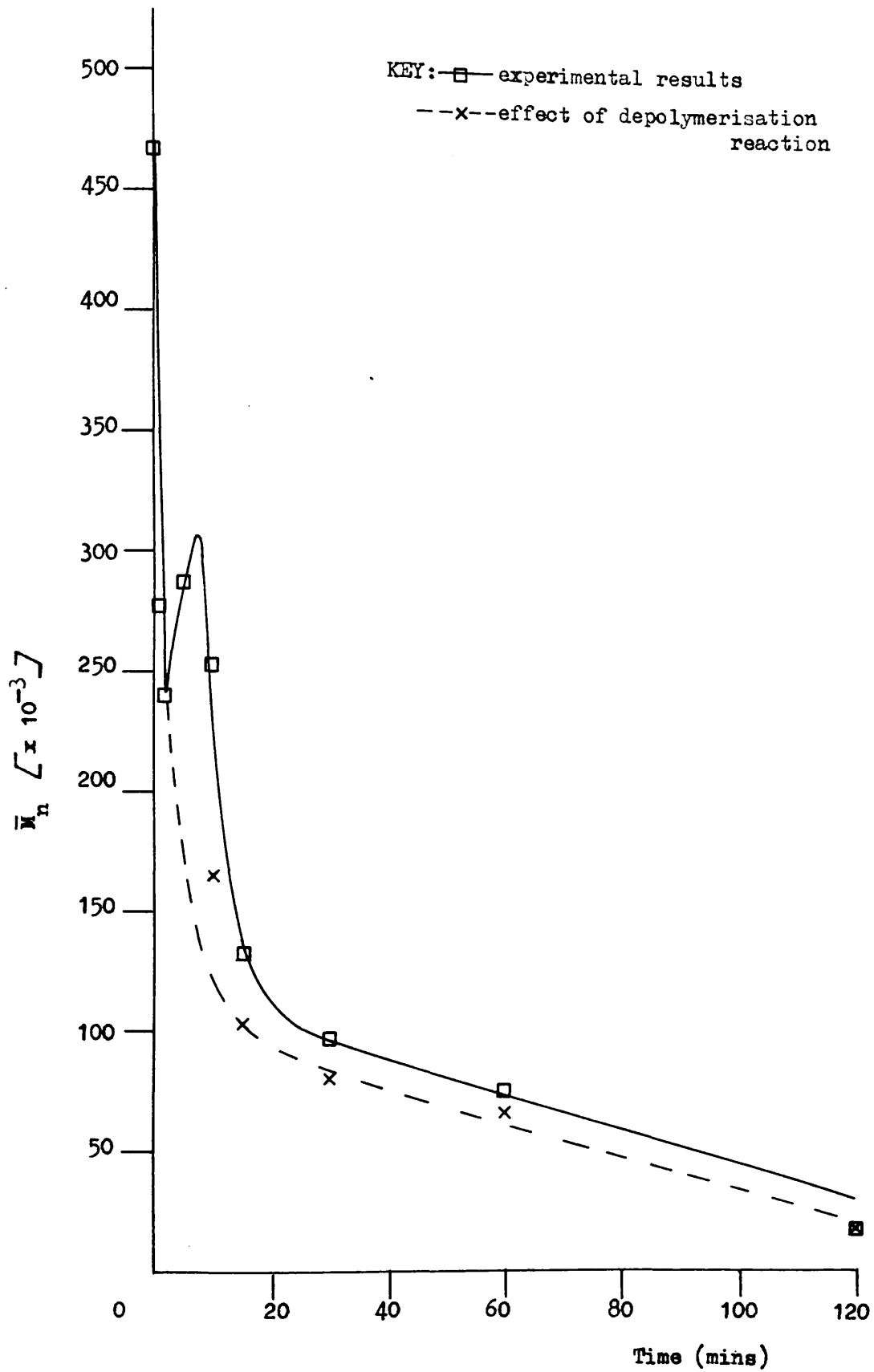


FIGURE 6.6

**CHANGES IN MOLECULAR WEIGHT (\bar{M}_n) WITH TIME OF HEATING OF
PHB AT 180°C UNDER VACUUM**

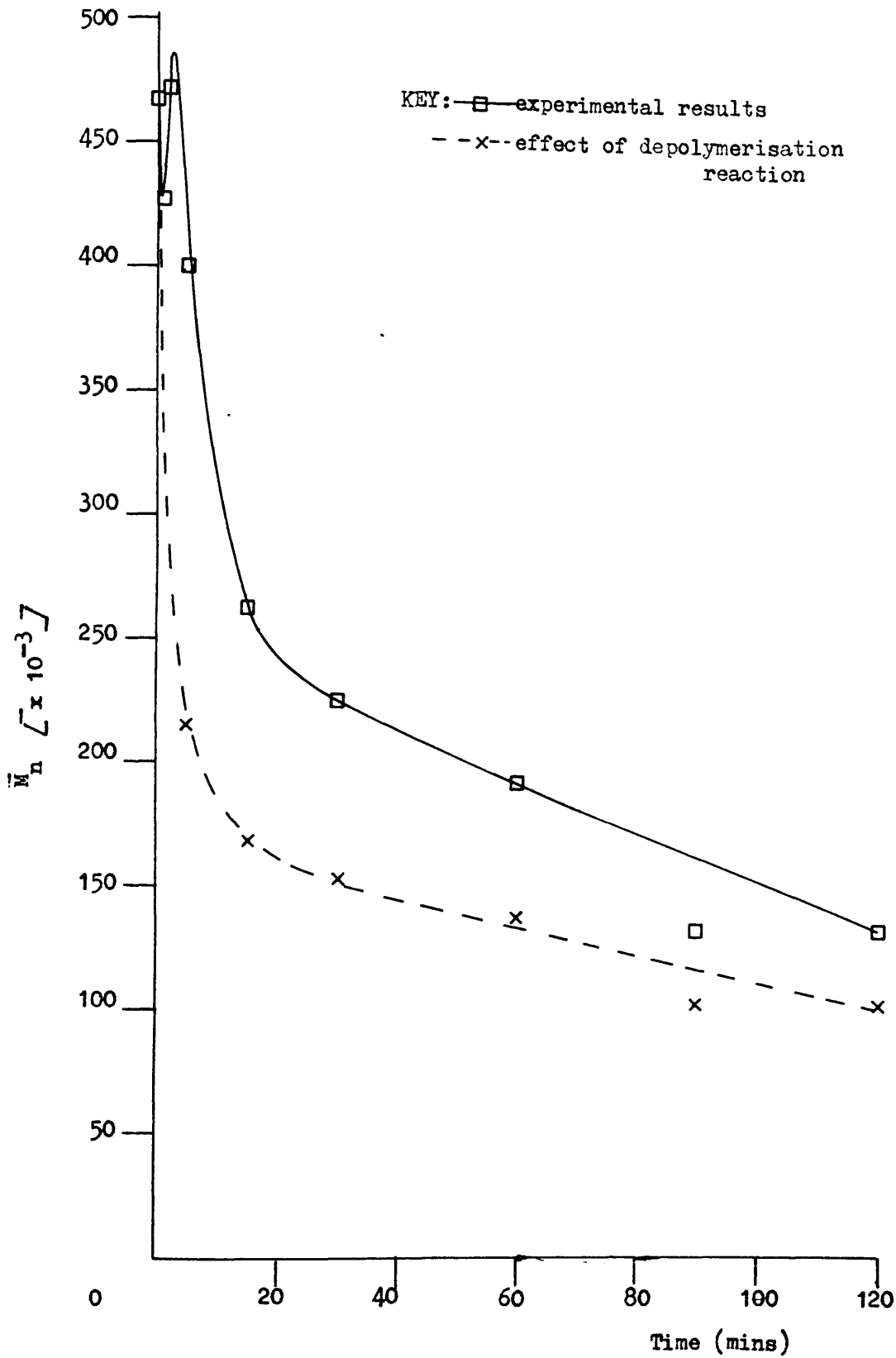


FIGURE 6.7

CHANGES IN MOLECULAR WEIGHT (\bar{M}_n) WITH TIME OF HEATING OF
PHB AT 170°C UNDER VACUUM

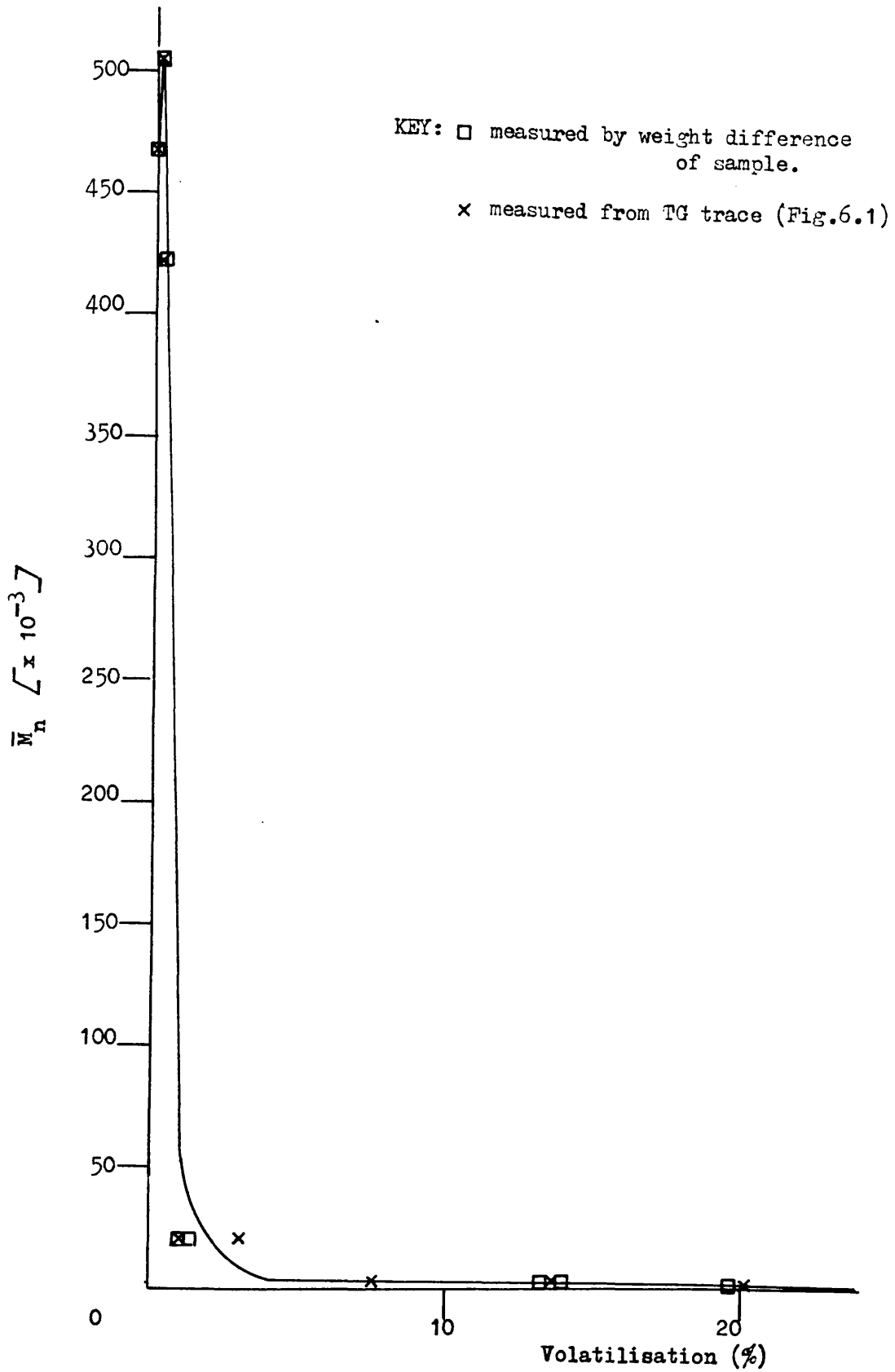


FIGURE 6.8

CHANGES IN \bar{M}_n WITH VOLATILISATION OF PEB AT 200°C

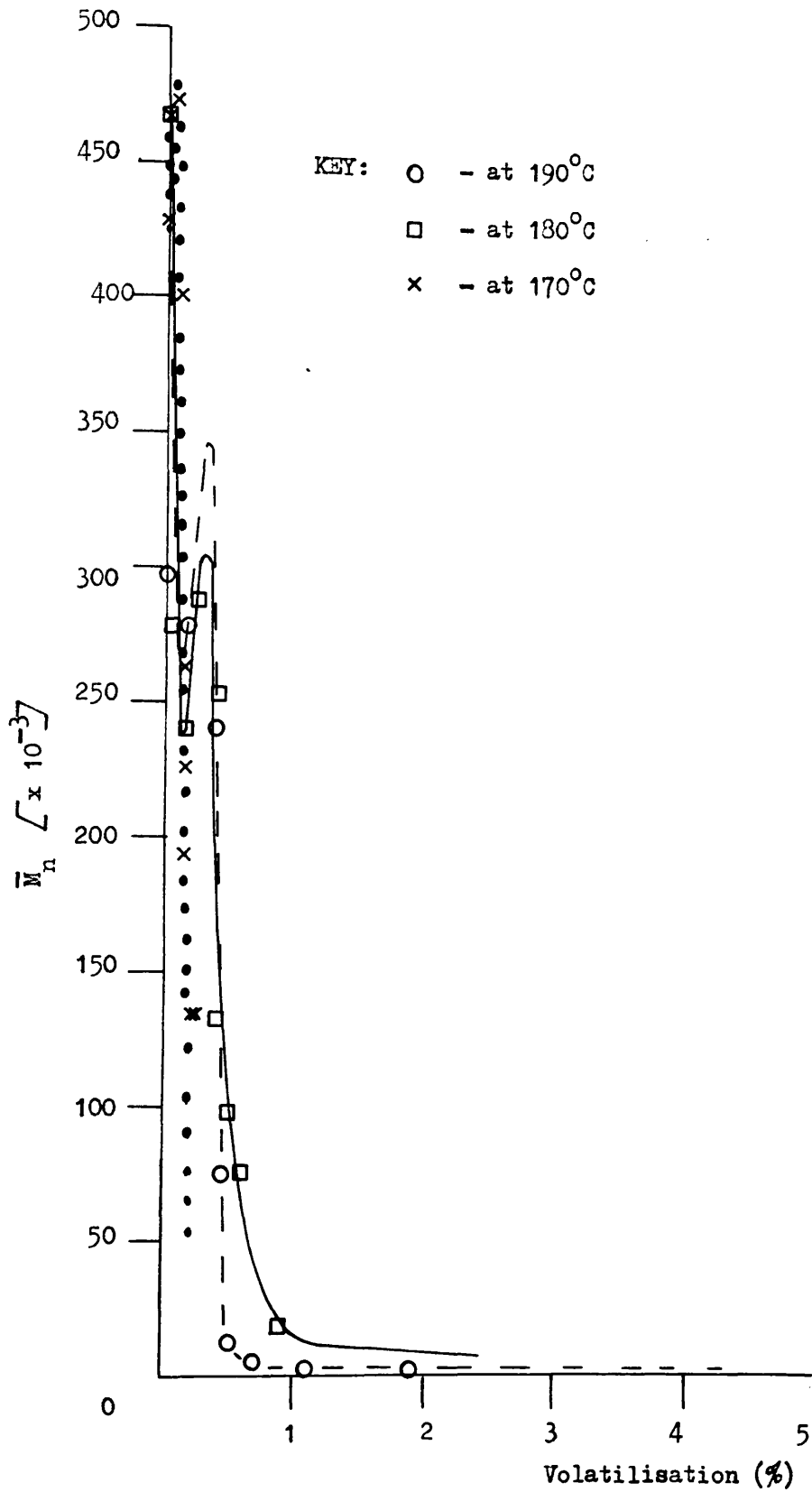


FIGURE 6.9

CHANGES IN \bar{M}_n WITH VOLATILISATION OF PHB AT SEVERAL
TEMPERATURES UNDER VACUUM

(Volatilisation measured from the data of Figure 6.1)

If chain scission occurs by the six centred elimination mechanism represented by Equation 3.1 then each chain scission will result in the formation of a carboxyl and vinyl (crotonate ester) group (V). S chain scissions per original molecule will result in S+1 molecules in the degraded sample.



A gradual increase in the crotonate ester group during the thermal degradation of PHB has indeed been reported (Ref. 23).

It is suggested that at the degradation temperature the residual hydroxyl groups are relatively quickly consumed by condensation with the gradually increasing concentration of carboxyl groups. Since there was only one hydroxyl group per original molecule this means that in the degraded polymer each original molecule will be represented by one less chain fragment than if chain scission only had occurred. If the measured molecular weight of the degraded polymer at time t is $\bar{M}_n(t)$ and $\bar{M}_n(t^1)$ is the molecular weight in the absence of hydroxyl/carboxyl condensation then,

$$\bar{M}_n(t^1) = \frac{\bar{M}_n(o)}{S + 1} \quad \text{and} \quad \bar{M}_n(t) = \frac{\bar{M}_n(o)}{S}$$

Thus,

$$\bar{M}_n(t^1) = \frac{\bar{M}_n(o)}{\frac{\bar{M}_n(o)}{\bar{M}_n(t)} + 1} \dots \dots \dots \text{Eq 6.1}$$

Using this equation the values of molecular weight which would have been observed as a result of chain scission in absence of hydroxyl/carboxyl condensation ($\bar{M}_{n(t^1)}$) may be calculated from separate measurements of $\bar{M}_{n(t)}$ and $\bar{M}_{n(o)}$.

An esterification reaction of this kind could be one possible source of the water, reported in Chapters 3 and 4 as a product of degradation, and could be responsible, in part, for the small amount of volatilisation reported in the early stages of heating (Chapter 6.2).

The correction of the experimental results to describe chain scission only, using Equation 6.1 is represented by the broken lines in Figures 6.4 - 6.7.

The number average chain length during the course of a random chain scission reaction is given by,

$$CL_t = \frac{CL_o}{S + 1} \dots\dots\dots \text{Eq 6.2}$$

where CL_o is the original number average chain length and CL_t is the number average chain length after, on average S links per original chain length have been broken. The degree of degradation, α , at any stage of the degradation process is defined by,

$$\alpha = \frac{S}{CL_o - 1} \dots\dots\dots \text{Eq 6.3}$$

which reduces to

$$\alpha = \frac{S}{CL_o} \dots\dots\dots \text{Eq 6.4}$$

if CL_o is large.

If it is assumed that the rate of chain scission is proportional to the number of chain units, n , present in the system at time t , then

$$\frac{-dn}{dt} = kn \dots\dots\dots \text{Eq 6.5}$$

Let n_0 be the number of links present at the start of the degradation, then

$$n = n_0 - \alpha n_0 = n_0 (1 - \alpha) \dots\dots\dots \text{Eq 6.6}$$

and hence

$$\frac{-dn_0 (1 - \alpha)}{dt} = kn_0 (1 - \alpha)$$

$$\text{or } -\ln (1 - \alpha) = kt \dots\dots\dots \text{Eq 6.7}$$

for small values of α ,

$$\ln (1 - \alpha) \approx -\alpha$$

and therefore Equation 6.7 becomes

$$\alpha = kt \dots\dots\dots \text{Eq.6.8}$$

or, by substituting for α , by using Equation 6.4,

$$\frac{s}{CL_0} = kt \dots\dots\dots \text{Eq 6.9}$$

Rearranging Equation 6.2 gives

$$\frac{s}{CL_0} = \frac{1}{CL_t} - \frac{1}{CL_0} \quad \text{which when substituted into}$$

Equation 6.9 gives

$$\frac{1}{CL_t} - \frac{1}{CL_0} = kt \quad \dots\dots\dots \text{Eq 6.10}$$

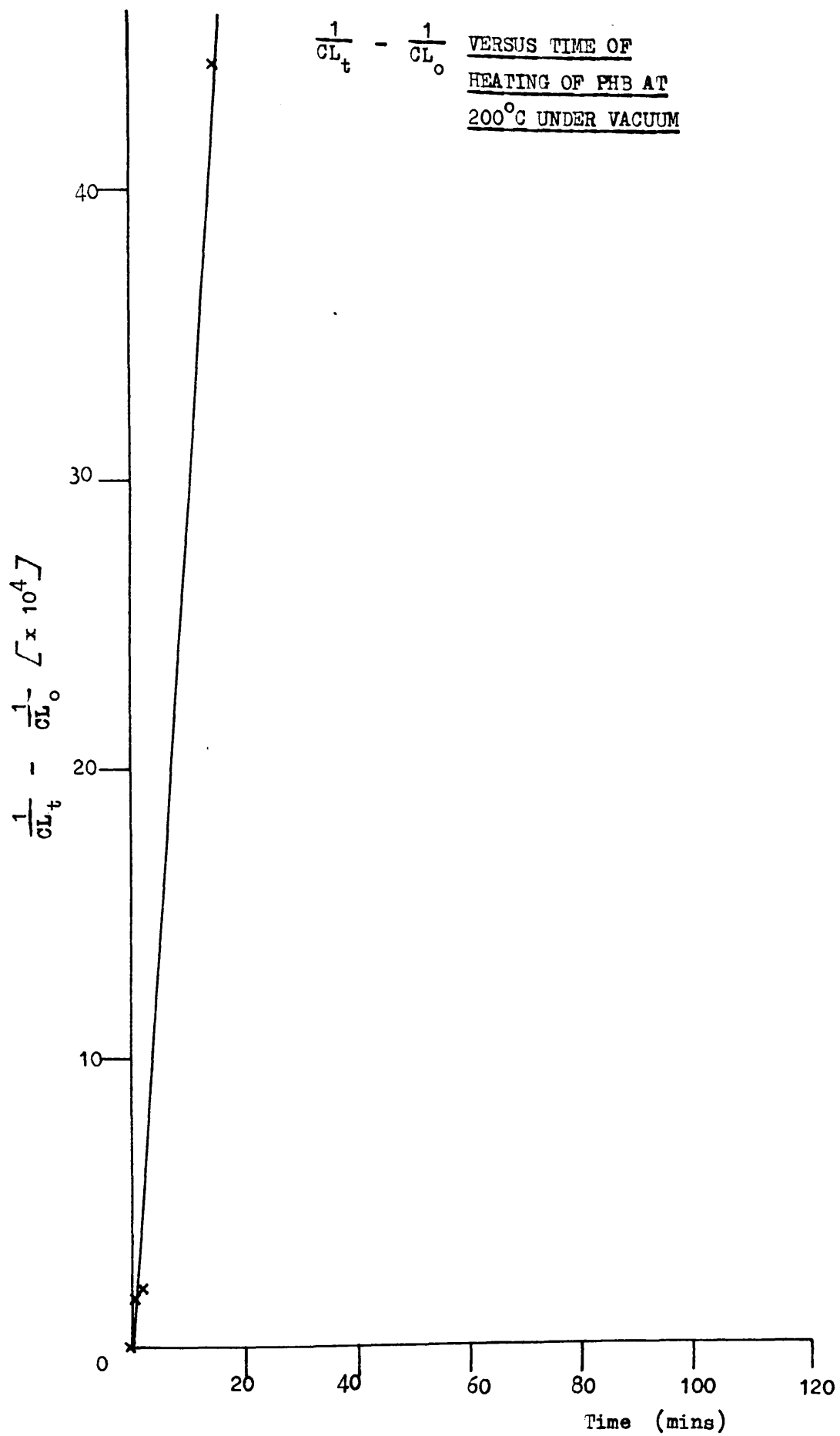
Equation 6.10 holds quite generally for random scission processes, at low conversions, regardless of the chemical nature or cause of degradation, provided little or no volatilisation occurs. (Ref. 111-113).

Figures 6.10-6.13 demonstrate that Equation 6.10 applies to the corrected data in Figures 6.4-6.7, since a linear relationship between $\frac{1}{CL_t} - \frac{1}{CL_0}$ and t is obtained at least at low conversions. It is thus confirmed that the depolymerisation reaction proceeds via a random chain scission mechanism. Since the left hand side of Equation 6.10 represents the number of bonds broken per monomer unit, the slopes of the lines in Figures 6.10-6.13 are a measure of the rates of the depolymerisation reaction at the respective temperatures. These are recorded in Table 6.A. From these values the Arrhenius plot shown in Figure 6.14 was obtained from which an energy of activation of $247 \pm 19 \text{ kJ mol}^{-1}$ was calculated.

Plots of \bar{M}_w versus time of heating, at temperatures of 170°C , 180°C , 190°C , and 200°C are shown in Figure 6.15. It can be seen that there is a rise in \bar{M}_w at approximately the same time as that recorded for \bar{M}_n in Figures 6.4-6.7.

FIGURE 6.10

$\frac{1}{CL_t} - \frac{1}{CL_0}$ VERSUS TIME OF
HEATING OF PHB AT
200°C UNDER VACUUM



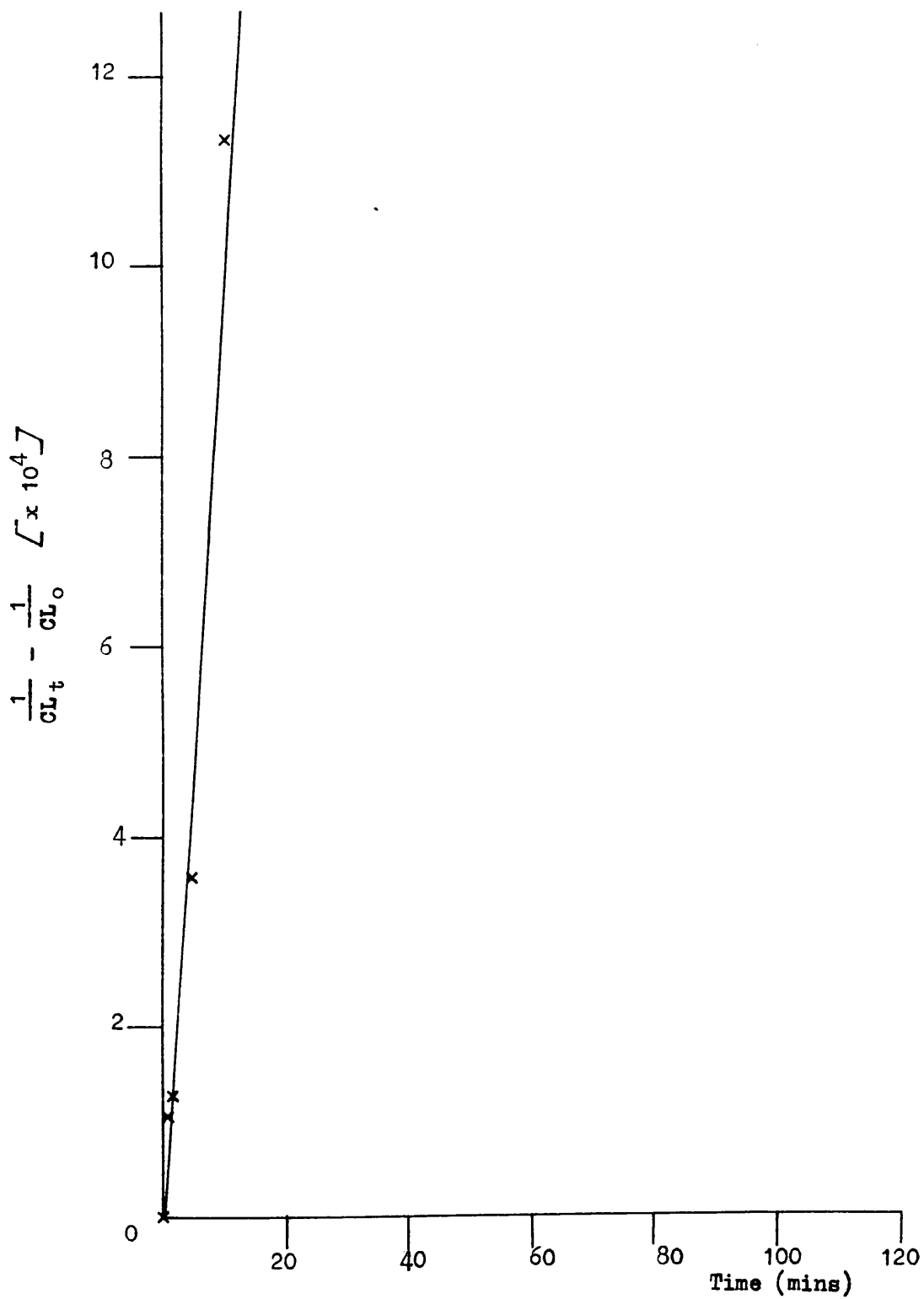


FIGURE 6.11

$\frac{1}{CL_t} - \frac{1}{CL_o}$ VERSUS TIME OF HEATING OF PHB
at 190°C UNDER VACUUM

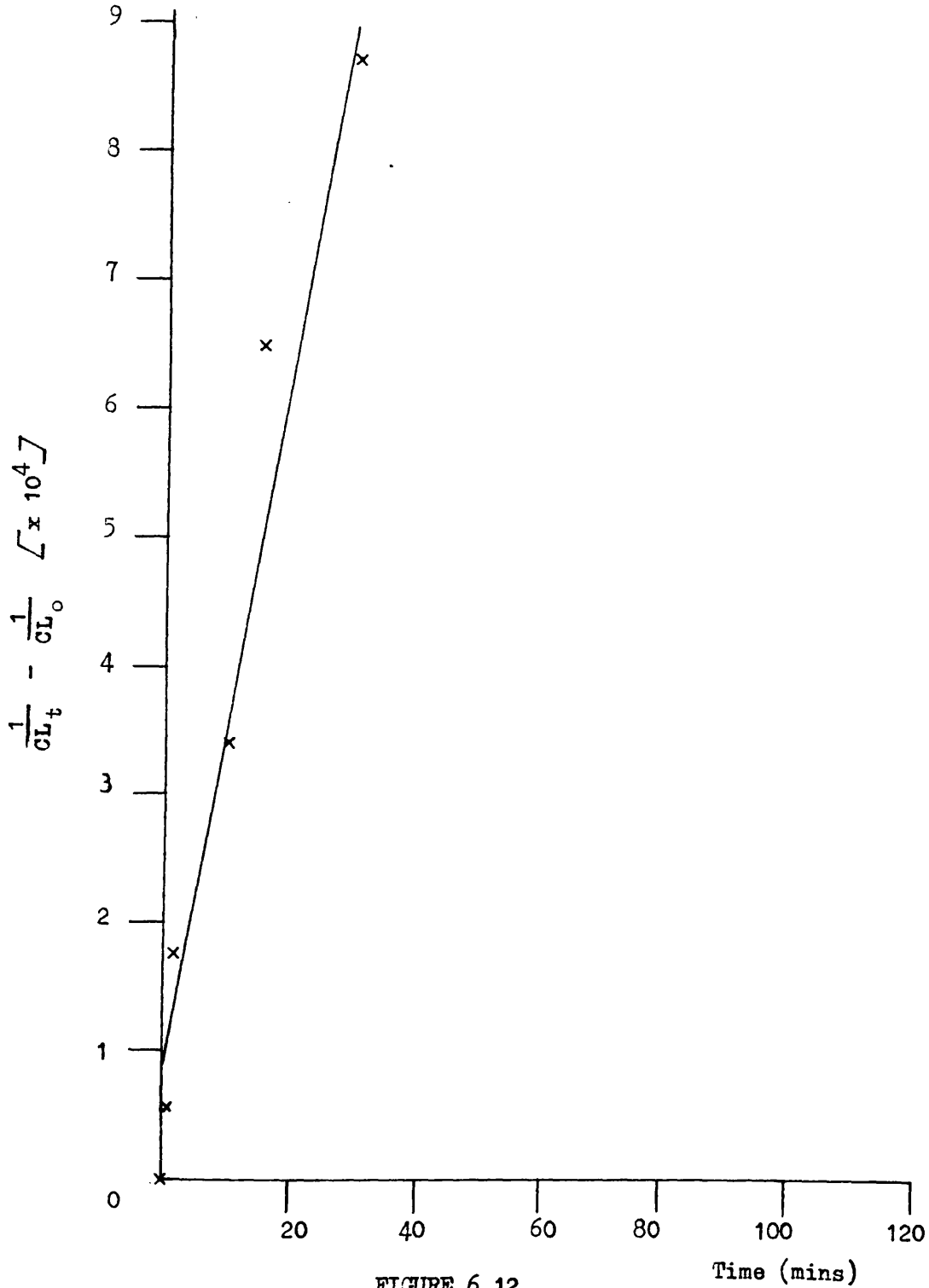


FIGURE 6.12

$\frac{1}{CL_t} - \frac{1}{CL_o}$ VERSUS TIME OF HEATING OF PHB
AT 180°C UNDER VACUUM

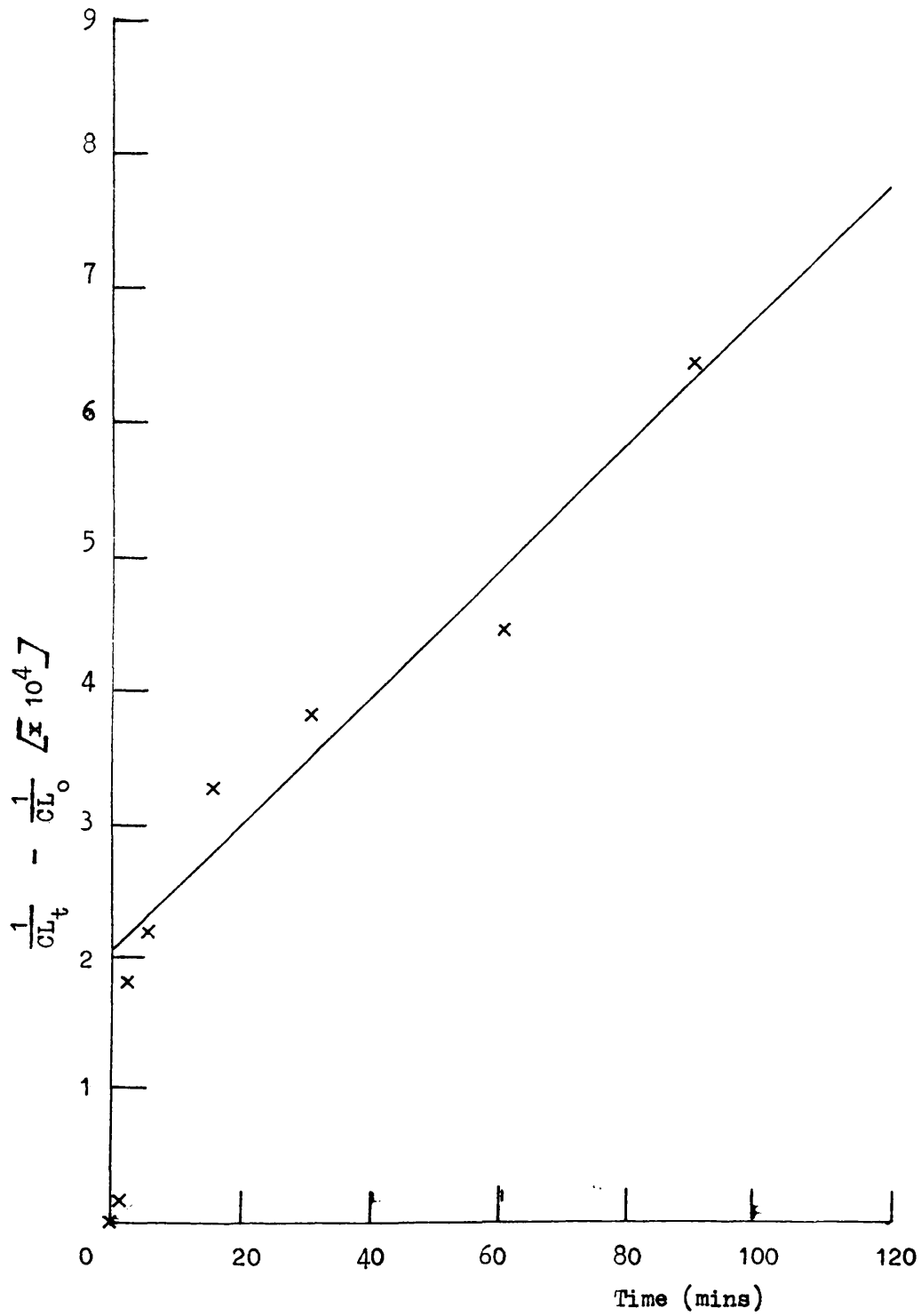


FIGURE 6.13

$\frac{1}{CL_t} - \frac{1}{CL_o}$ VERSUS TIME OF HEATING OF PHB AT 170°C
UNDER VACUUM

TABLE 6.A

RATES OF CHAIN SCISSION
IN PHB AT VARIOUS TEMPERATURES UNDER VACUUM

Temperature °C	Rate of random chain scission (bonds broken/monomer unit/sec)	Intercept on $\frac{1}{CL_t} - \frac{1}{CL_0}$ axis
170	$(7.99 \pm 0.9) \times 10^{-8}$	2.06×10^{-4}
180	$(4.72 \pm 0.6) \times 10^{-7}$	8.72×10^{-5}
190	$(1.86 \pm 0.2) \times 10^{-6}$	-5.71×10^{-5}
200	$(4.99 \pm 0.3) \times 10^{-6}$	-1.66×10^{-4}

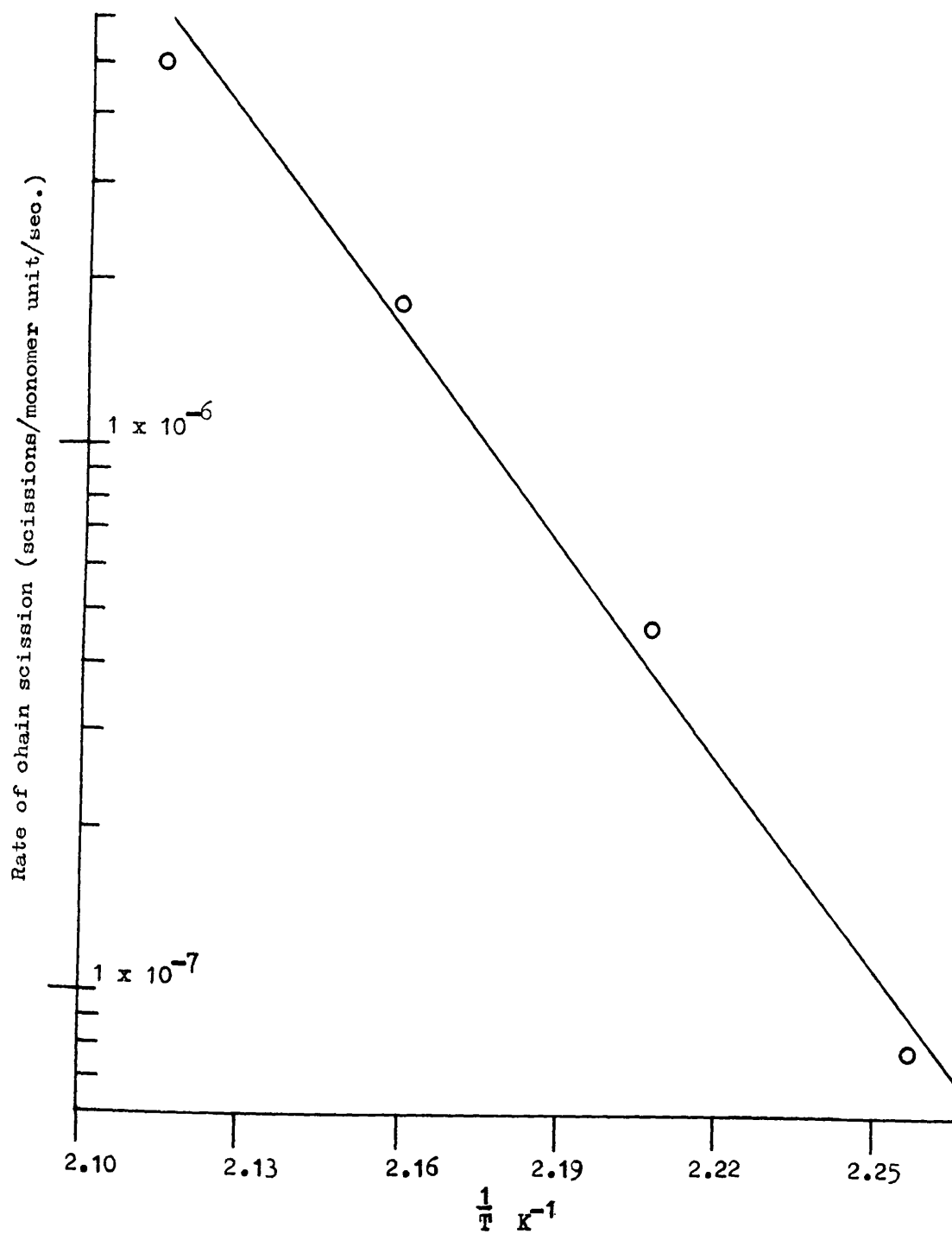


FIGURE 6.14

ARRHENIUS PLOT FOR THE DEGRADATION OF PBE
UNDER VACUUM (170°C to 200°C)

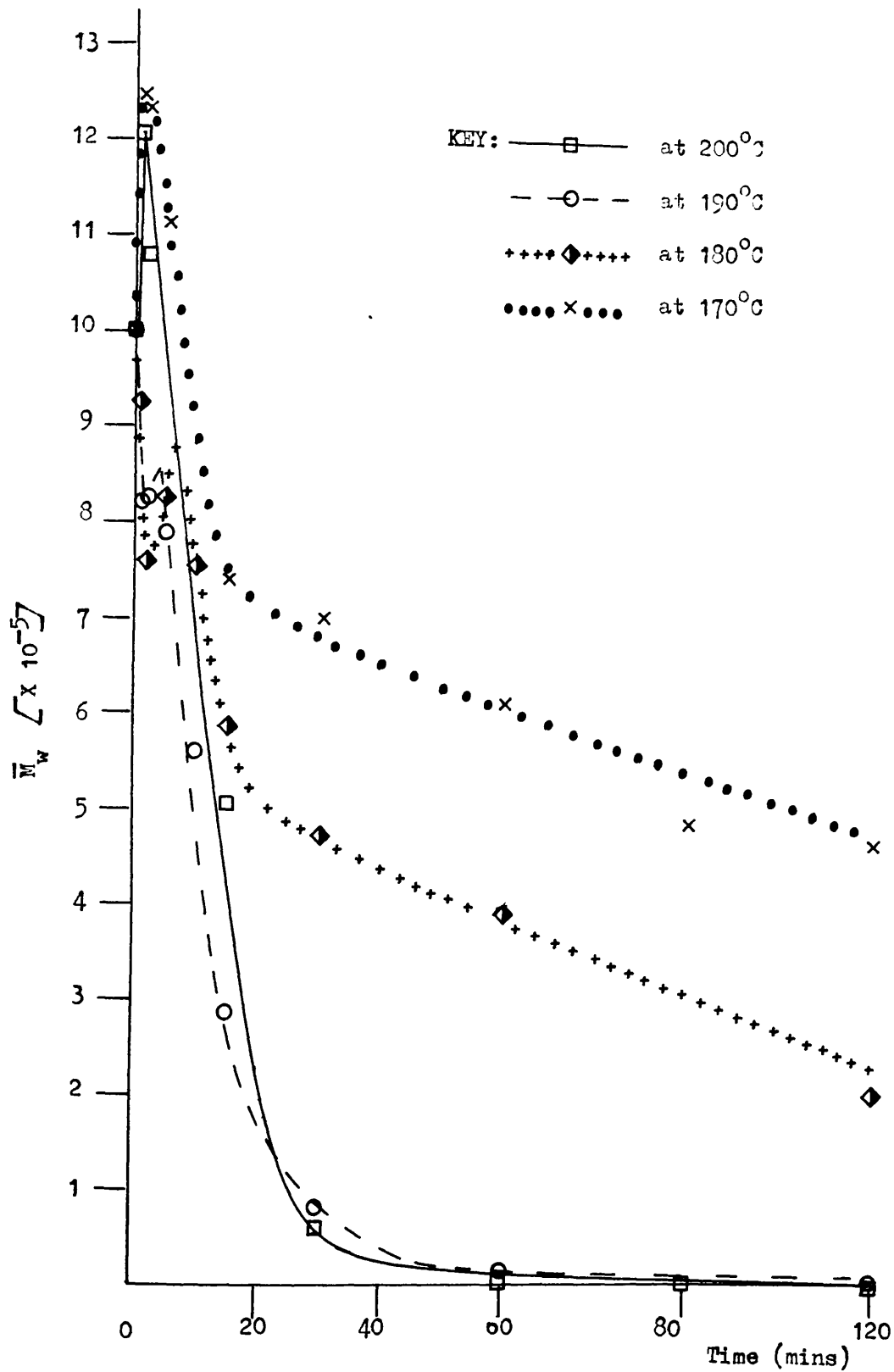


FIGURE 6.15

CHANGES IN MOLECULAR WEIGHT (\bar{M}_w) WITH TIME OF HEATING OF PHB AT SEVERAL TEMPERATURES UNDER VACUUM

6.4 MOLECULAR WEIGHT CHANGES UNDER NITROGEN

The changes in molecular weight during isothermal heating of polymer S1 (Chapter 2.11) under a dynamic nitrogen flow were investigated by the method outlined in Chapter 2.9(ii).

Plots of number average molecular weight versus time of heating (solid trace) at temperatures of 200°C, 190°C, 180°C and 170°C are recorded in Figures 6.16, 6.17, 6.18 and 6.19 respectively. These traces are similar in shape to the traces obtained under vacuum, Figures 6.4 - 6.7, and show the effect on \bar{M}_n of the two competing reactions, chain scission and esterification. The effect of the chain scission reaction only on \bar{M}_n is illustrated in Figures 6.16 - 6.19 by the broken line trace, obtained by applying Equation 6.1 to the experimentally measured \bar{M}_n values that occur after the maximum on the \bar{M}_n versus time traces, as in Chapter 6.3.

The relationships between molecular weight and extent of volatilisations at 170-200°C are illustrated in Figures 6.20 and 6.21. The shapes of these curves are similar to those obtained by heating PHB under vacuum, Figures 6.8 and 6.9 and are evidence that the degradation reaction also proceeds via a random chain scission mechanism (Ref. 110) under nitrogen.

The dependences of $\frac{1}{CL_t} - \frac{1}{CL_0}$ on the time of heating at 200°C, 190°C, 180°C and 170°C, under a nitrogen atmosphere, were calculated for the data of Figures 6.16 - 6.19 (broken line trace) and are illustrated in Figures 6.22 - 6.25. From these figures it can be seen that Equation 6.10 holds, at least at low conversions, which is indicative of a random chain scission process. The gradients of the traces in Figures 6.22 - 6.25,

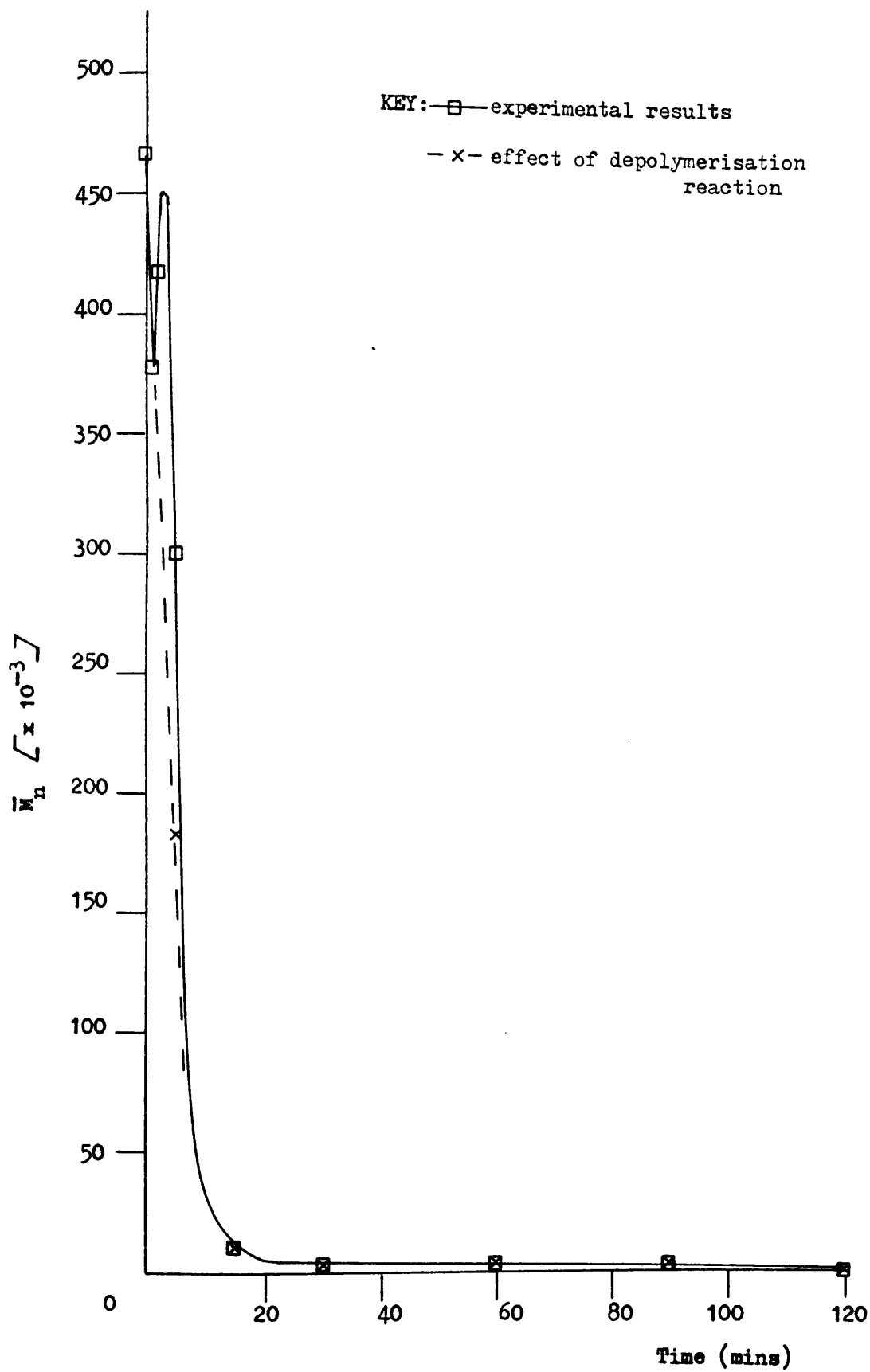


FIGURE 6.16

CHANGES IN MOLECULAR WEIGHT (\bar{M}_n) WITH TIME OF HEATING OF
PHB AT 200°C UNDER NITROGEN

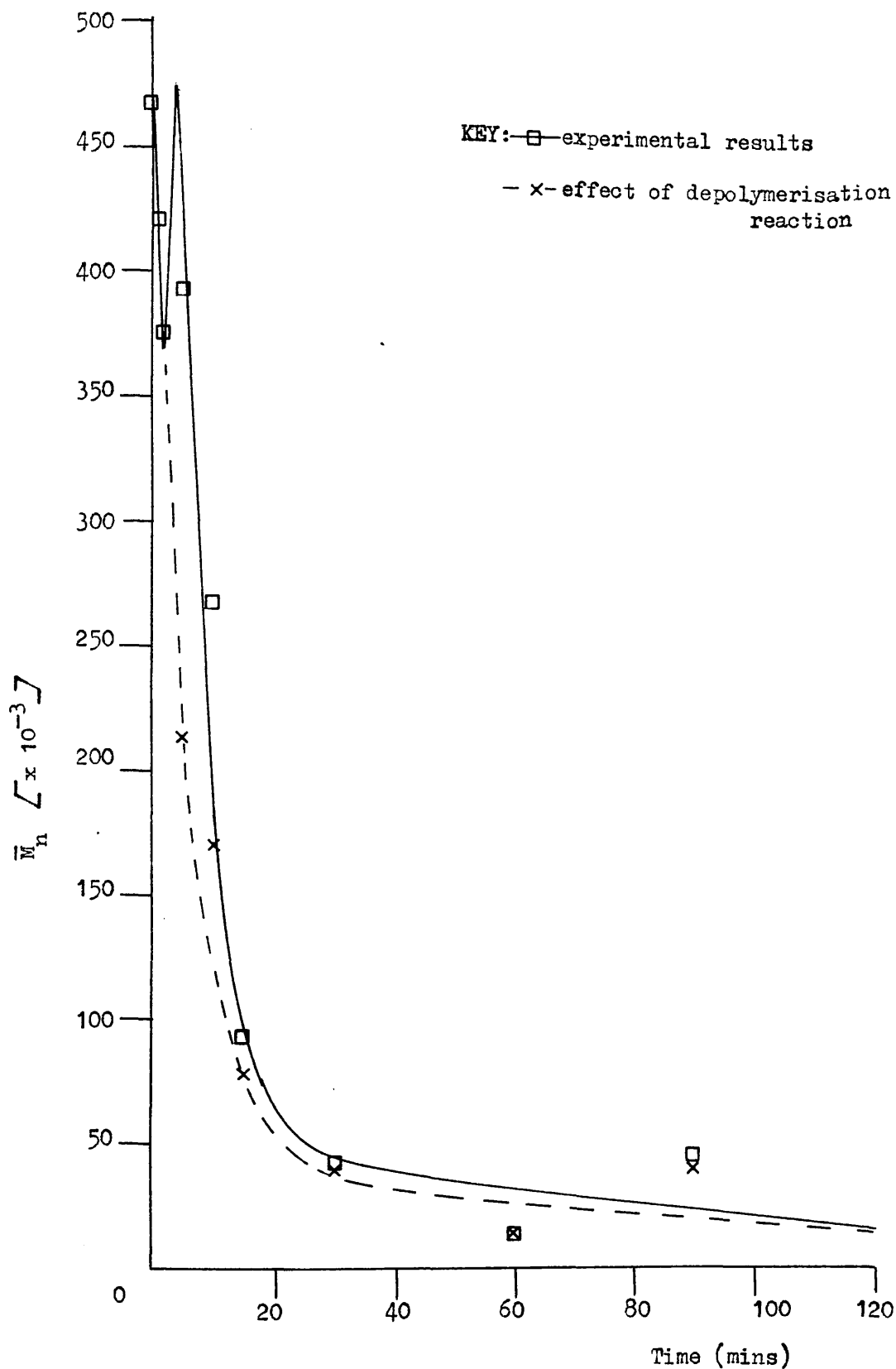


FIGURE 6.17

CHANGES IN MOLECULAR WEIGHT (\bar{M}_n) VERSUS TIME OF HEATING OF
PHB AT 190°C UNDER NITROGEN

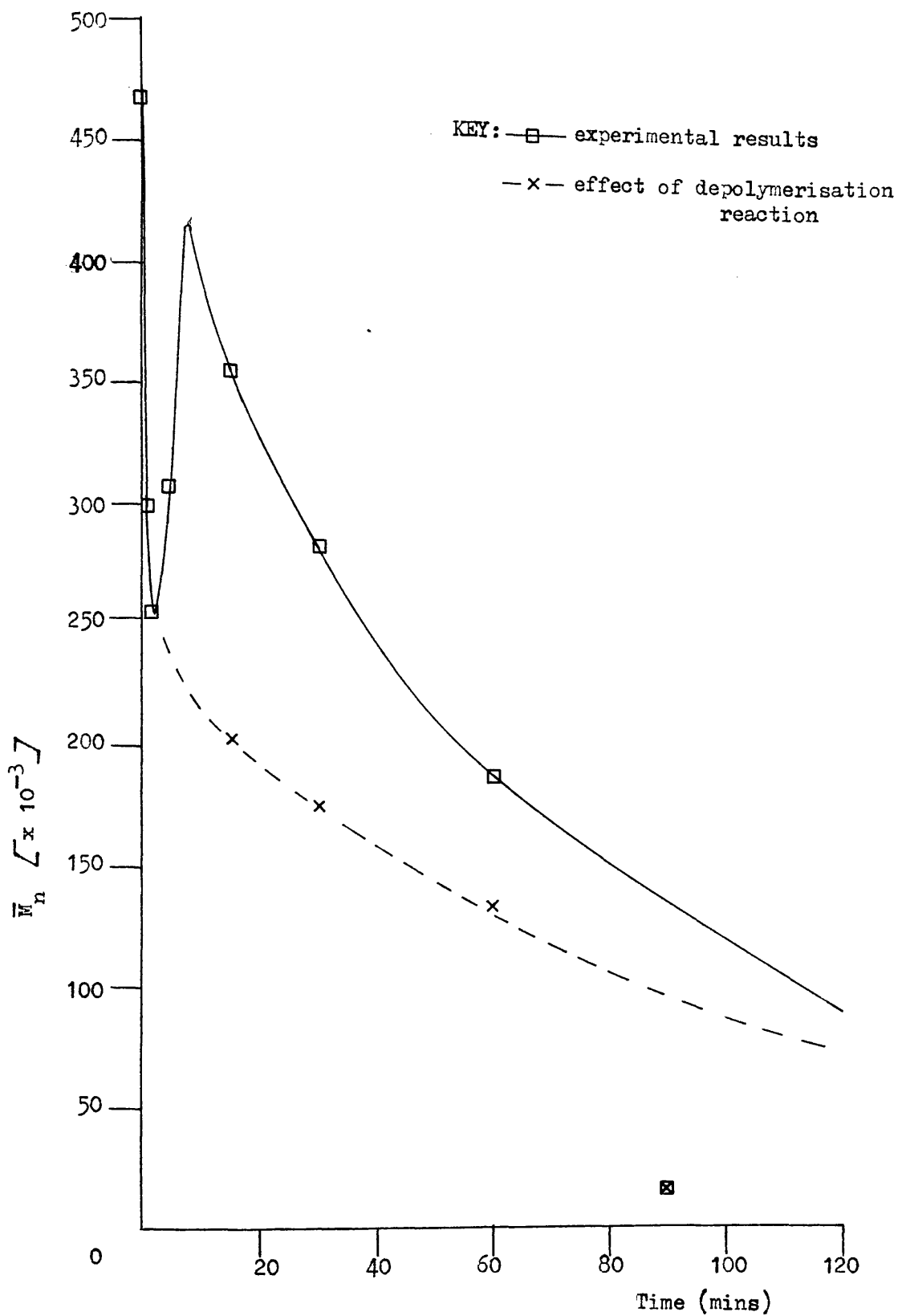


FIGURE 6.18

CHANGES IN MOLECULAR WEIGHT (\bar{M}_n) WITH TIME OF HEATING OF PHB AT 180°C UNDER NITROGEN

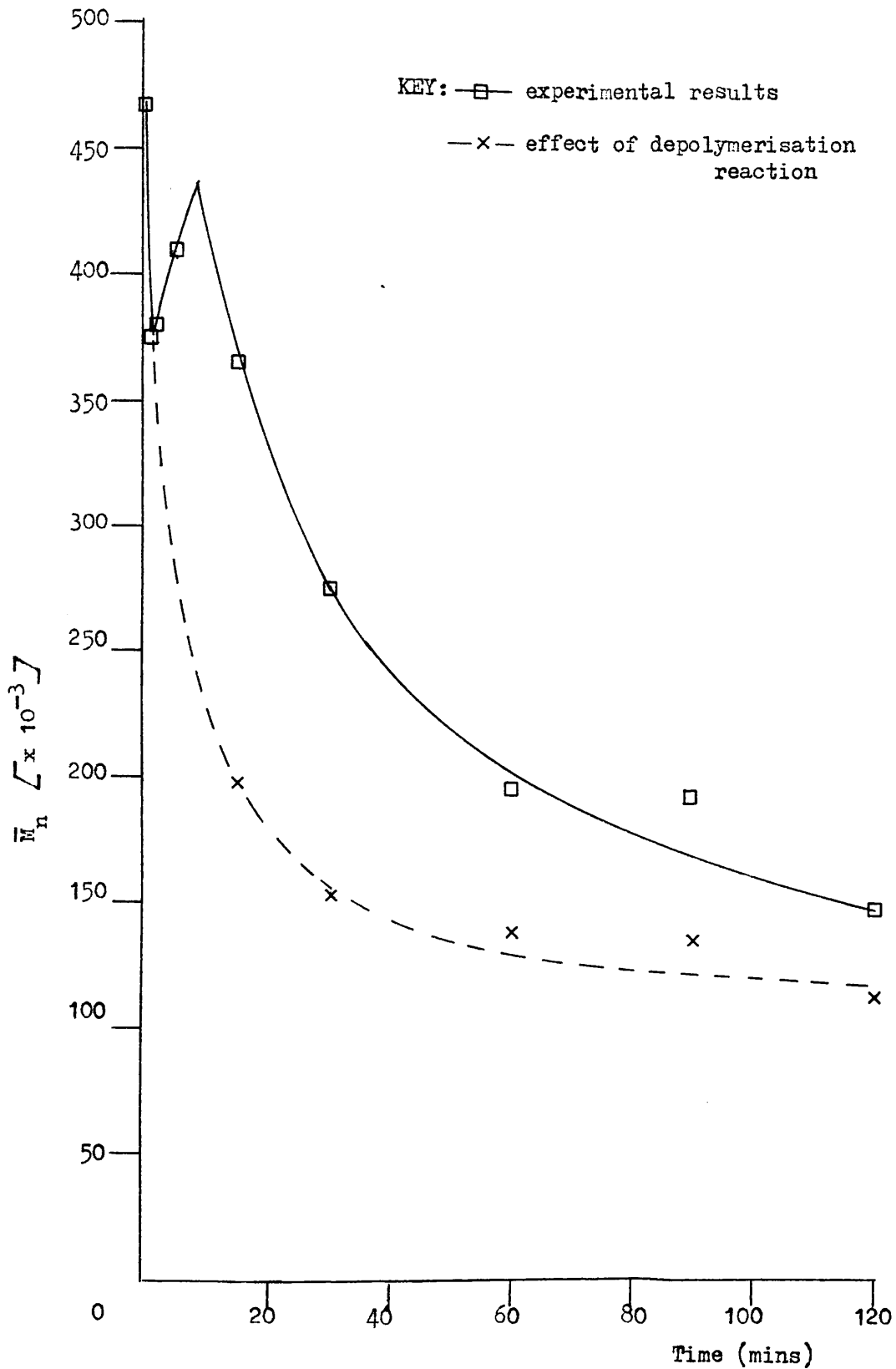


FIGURE 6.19
CHANGES IN MOLECULAR WEIGHT (\bar{M}_n) VERSUS TIME OF HEATING
OF PHB AT 170°C UNDER NITROGEN

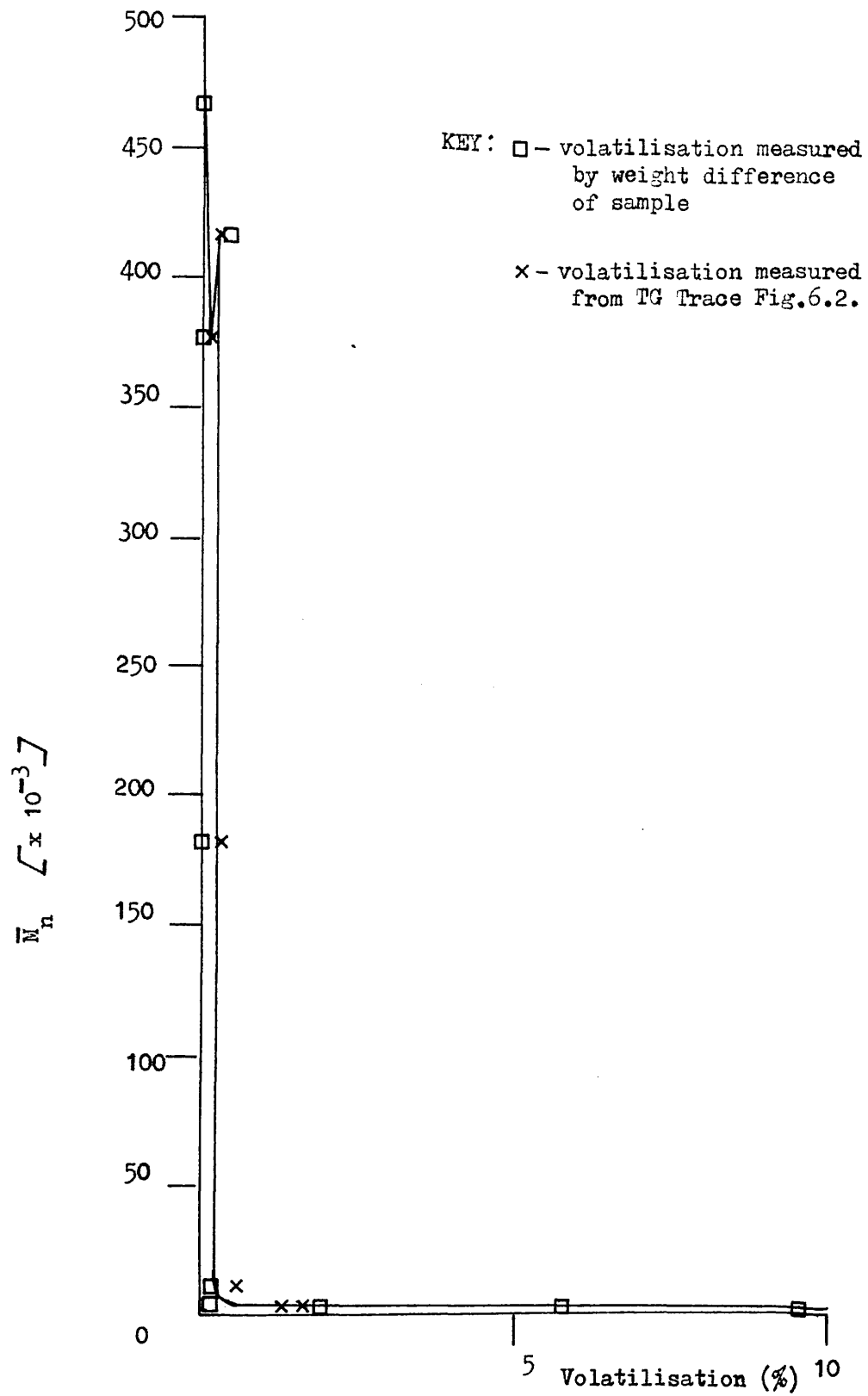


FIGURE 6.20
CHANGES IN \bar{M}_n WITH VOLATILISATION OF
PHB AT 200°C UNDER NITROGEN

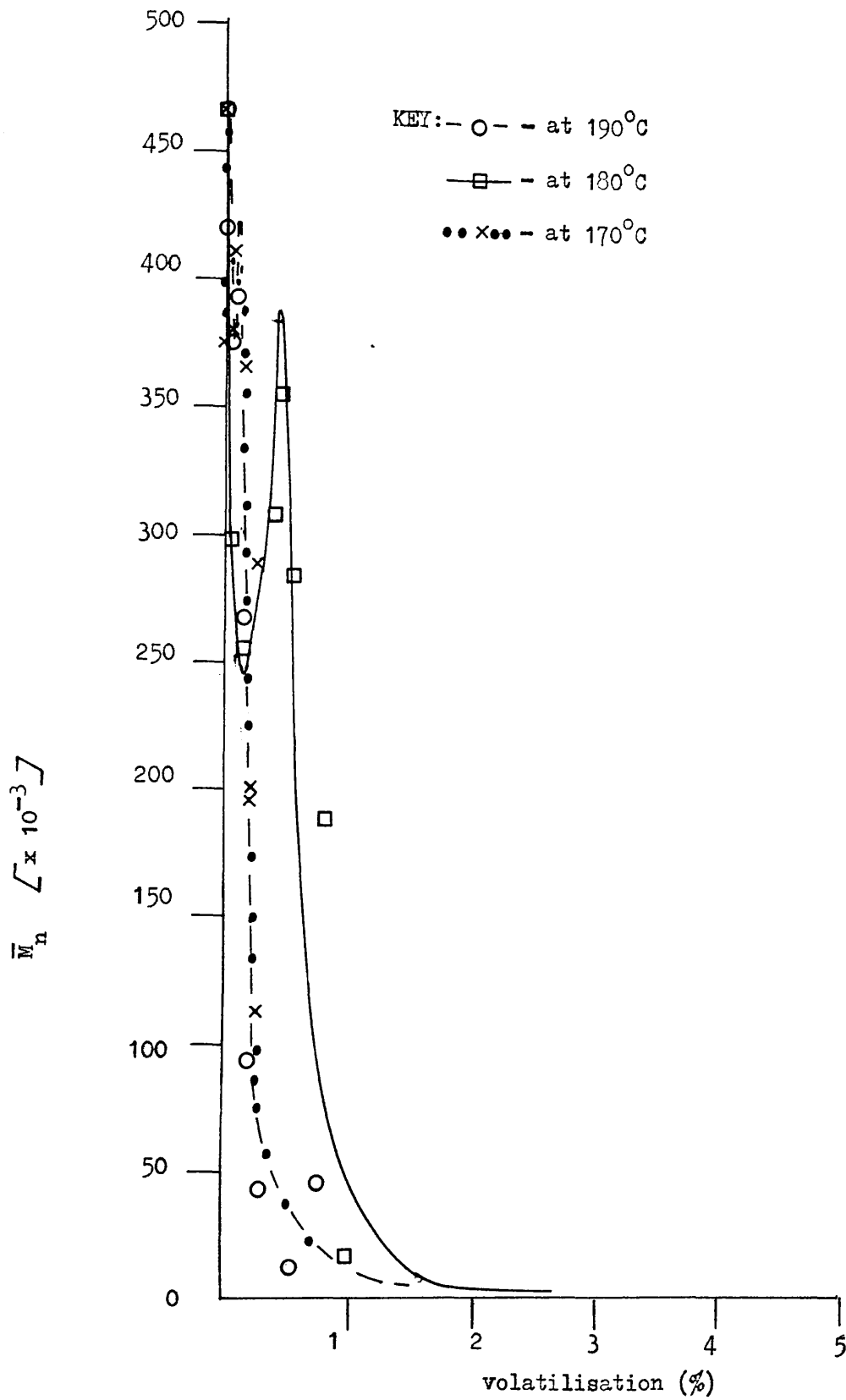


FIGURE 6.21

**CHANGES IN \bar{M}_n WITH VOLATILISATION OF PHB AT
 SEVERAL TEMPERATURES, UNDER NITROGEN**

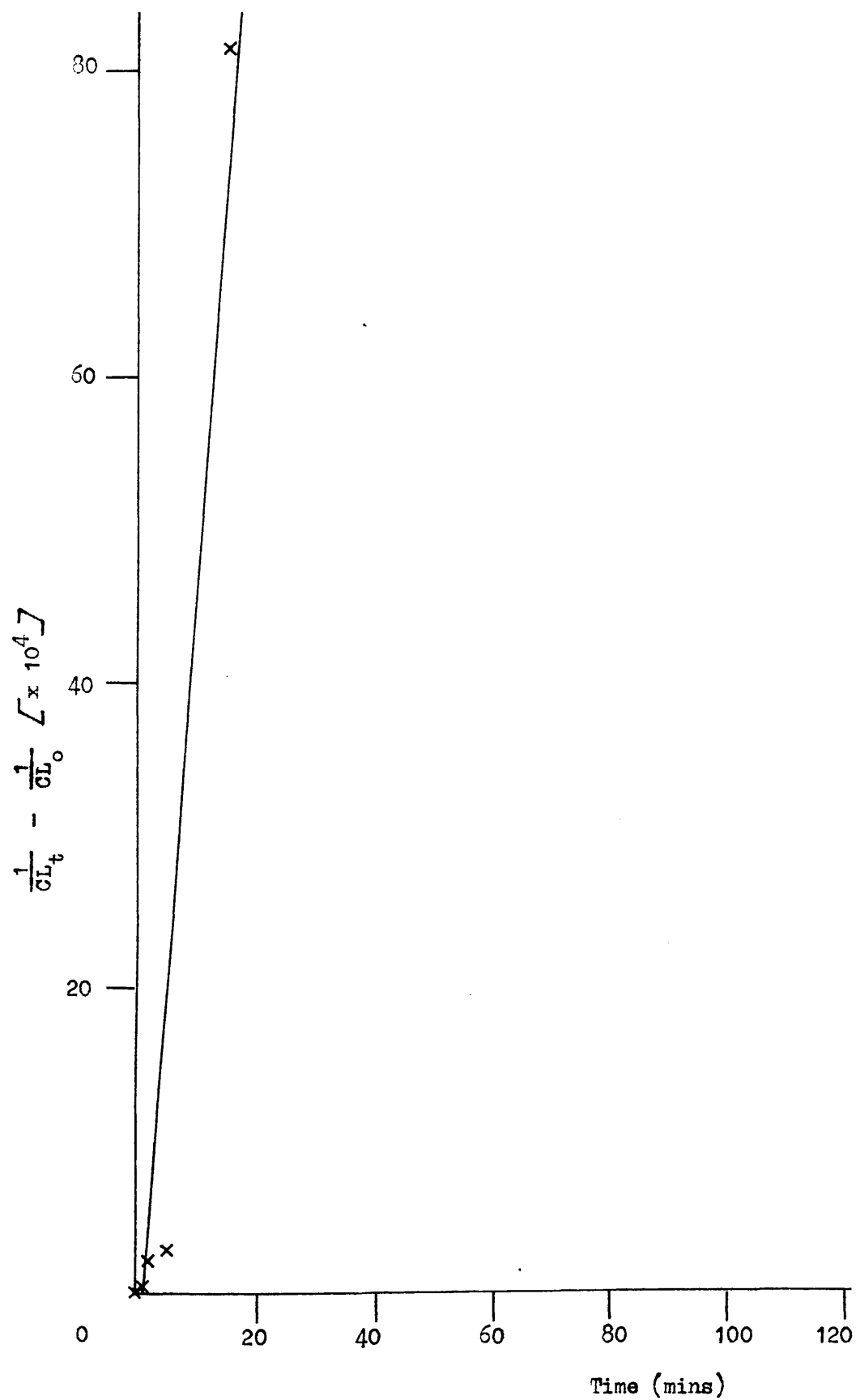


FIGURE 6.22

$\frac{1}{CL_t} - \frac{1}{CL_0}$ VERSUS TIME OF HEATING OF PHB
AT 200°C UNDER NITROGEN

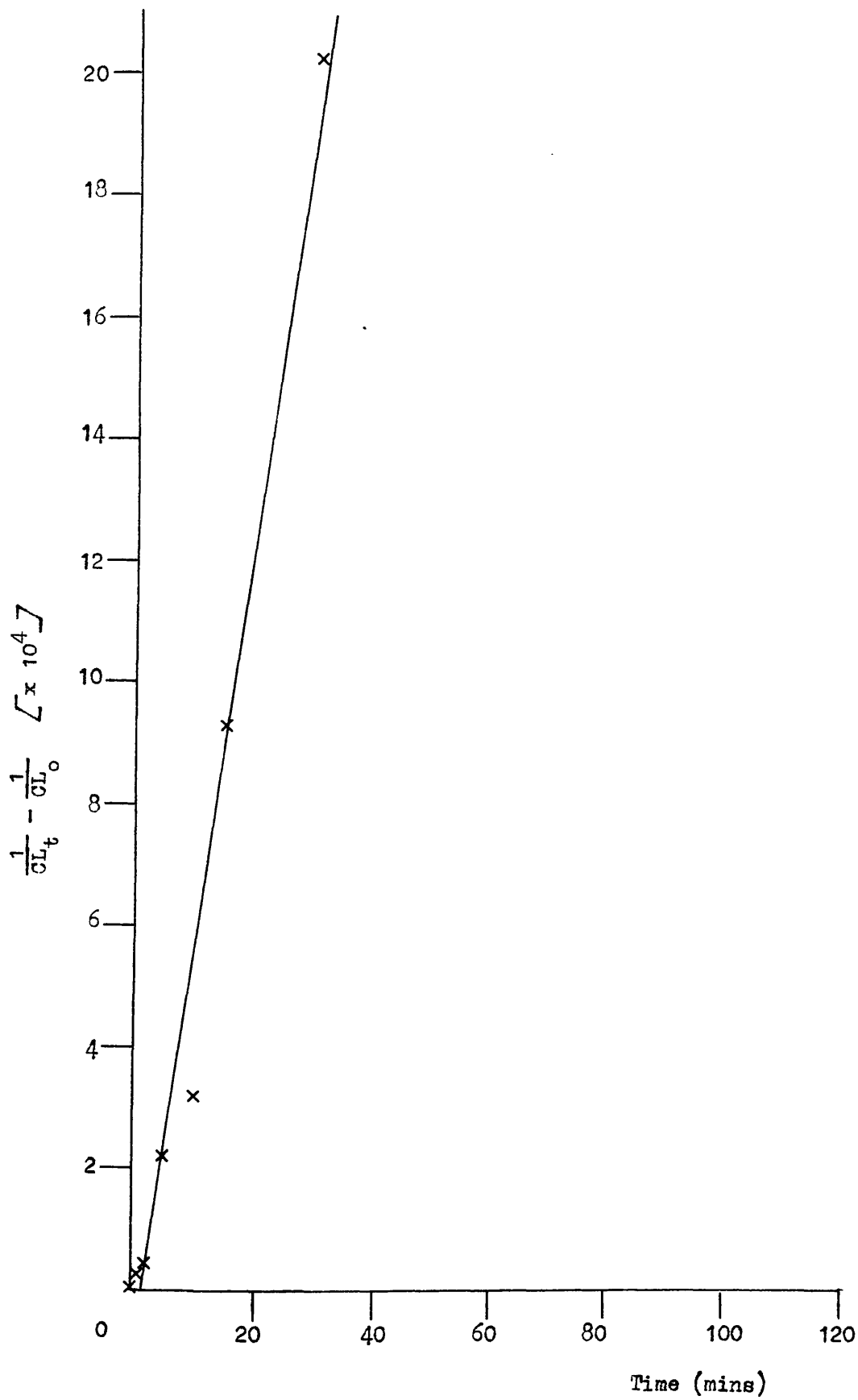


FIGURE 6.23

$\frac{1}{CL_t} - \frac{1}{CL_0}$ VERSUS TIME OF HEATING OF PHB
AT 190°C UNDER NITROGEN

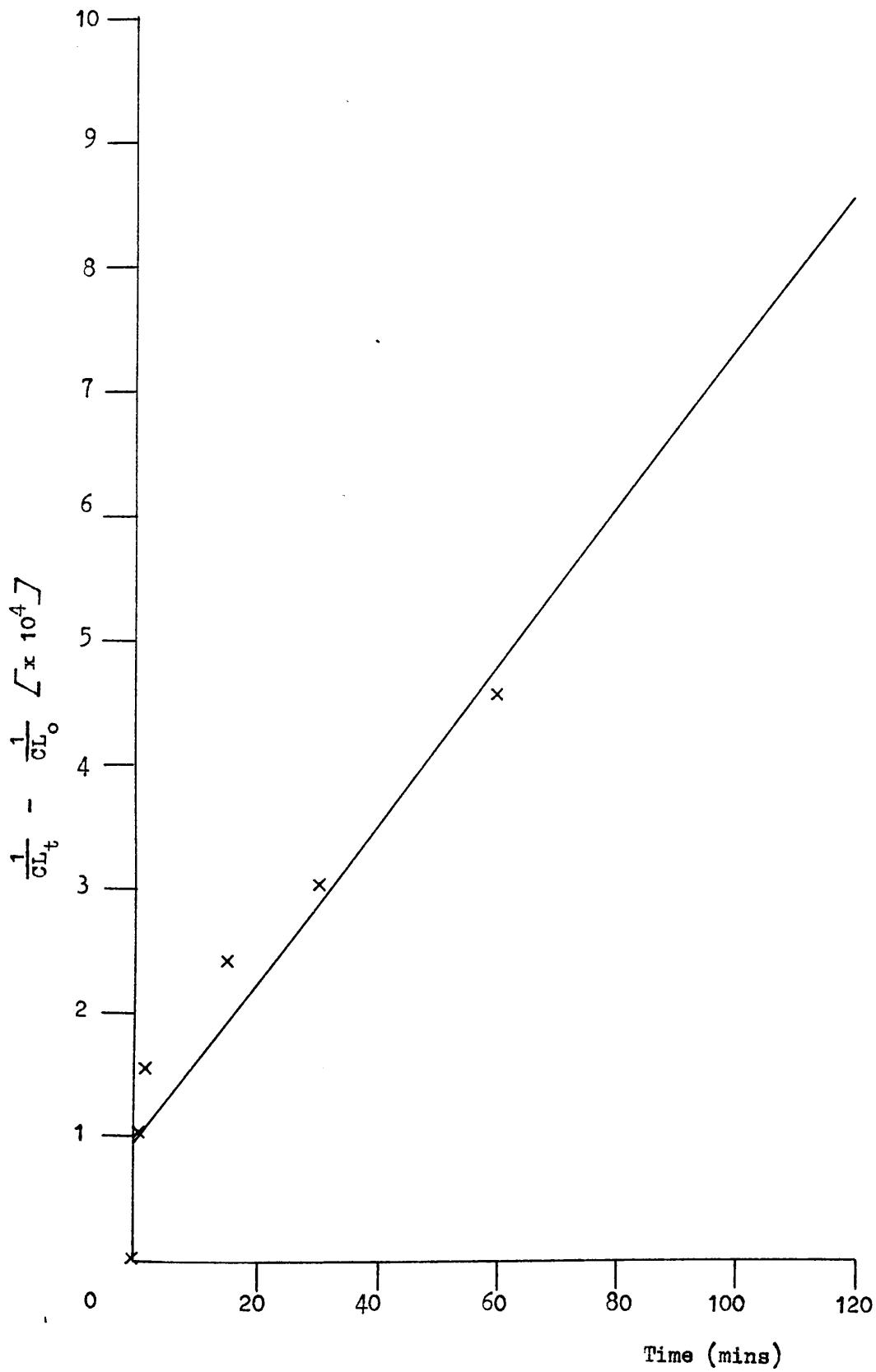


FIGURE 6.24

$\frac{1}{CL_t} - \frac{1}{CL_0}$ VERSUS TIME OF HEATING OF PHB
AT 180°C UNDER NITROGEN

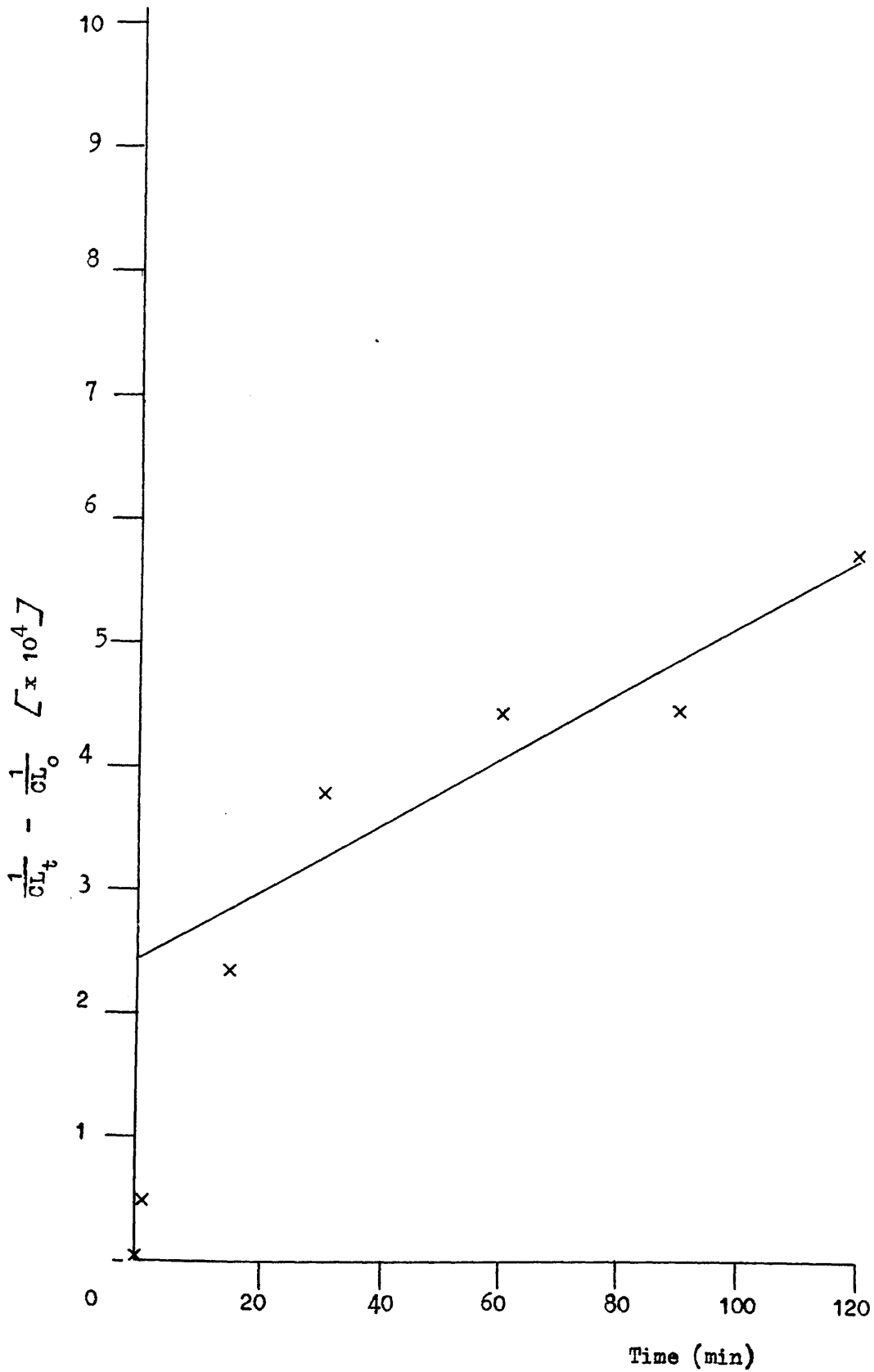


FIGURE 6.25

$\frac{1}{CL_t} - \frac{1}{CL_o}$ VERSUS TIME OF HEATING OF PHB
AT 170°C UNDER NITROGEN

obtained by the least squares method, give a measure of the rate of chain scission and are recorded in Table 6.3.

An energy of activation of $326 \pm 45 \text{ kJ mol}^{-1}$ was obtained from the Arrhenius plot of these results which is shown in Figure 6.26.

Plots of \bar{M}_w versus time of heating at the various temperatures are shown in Figure 6.27.

6.5 MOLECULAR WEIGHT CHANGES UNDER STATIC AIR

The changes in molecular weight which occur during isothermal heating of polymer S1 (Chapter 2.11) under static air were investigated by the method outlined in Chapter 2.9(iii).

Plots of number average molecular weight versus time of heating, (solid trace), at 200°C , 190°C , 180°C and 170°C are shown in Figures 6.28–6.31. The shapes of these traces are obviously similar to those in Figures 6.4–6.7 (Chapter 6.3) and Figures 6.16–6.19 (Chapter 6.4) and again reflect the competition between esterification and depolymerisation reactions. The measured values of \bar{M}_n were corrected using Equation 6.1, and the \bar{M}_n versus time traces considering only the depolymerisation reaction are illustrated by the broken lines in Figures 6.28–6.31. Using these results, plots of $\frac{1}{CL_t} - \frac{1}{CL_0}$ versus time of heating at the four different temperatures, were obtained and are illustrated in Figures 6.32–6.35. The linear relationships obtained imply a random chain scission mechanism for the degradation process, (Ref. 111, 112). As explained in Chapter 6.4 the slopes of these straight lines are a measure of the rate of bond scission and the results obtained in the least squares fit are presented in Table 6.C. Using these data the Arrhenius plot in Figure 6.36

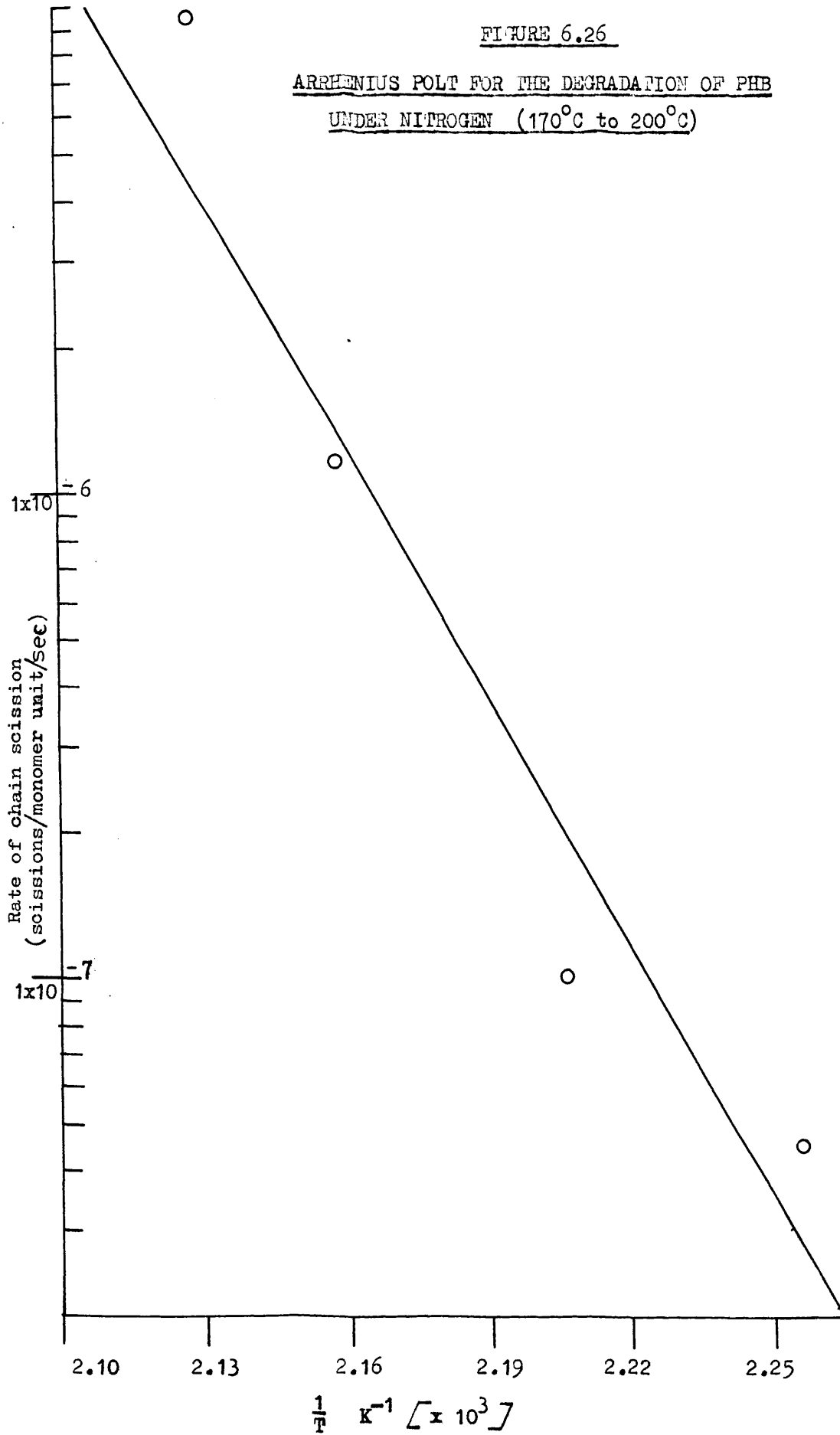
TABLE 6.B

RATES OF CHAIN SCISSION
IN PHB AT VARIOUS TEMPERATURES UNDER NITROGEN

Temperature °C	Rate of Random Chain Scission (bonds broken/monomer unit/sec)	Intercept on $\frac{1}{CL_t} - \frac{1}{CL_0}$ axis
170	$(4.51 \pm 1) \times 10^{-8}$	2.47×10^{-4}
180	$(1.08 \pm 0.2) \times 10^{-7}$	9.46×10^{-5}
190	$(1.15 \pm 0.08) \times 10^{-6}$	-1.07×10^{-4}
200	$(9.42 \pm 2) \times 10^{-6}$	-8.6×10^{-4}

FIGURE 6.26

ARRHENIUS PLOT FOR THE DEGRADATION OF PHB
UNDER NITROGEN (170°C to 200°C)



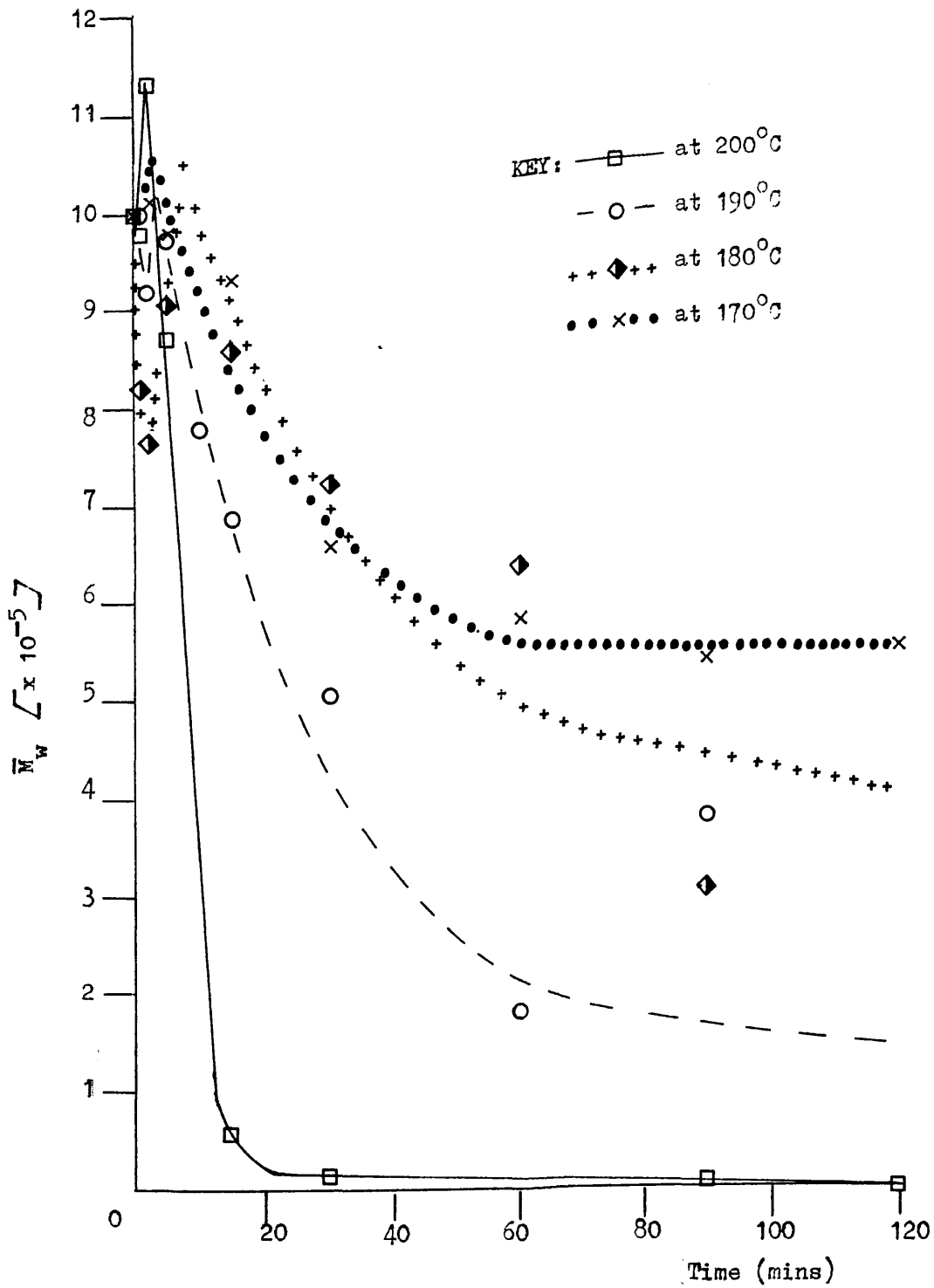


FIGURE 6.27

CHANGES IN MOLECULAR WEIGHT (\bar{M}_w) WITH TIME OF HEATING OF PHB AT SEVERAL TEMPERATURES UNDER NITROGEN

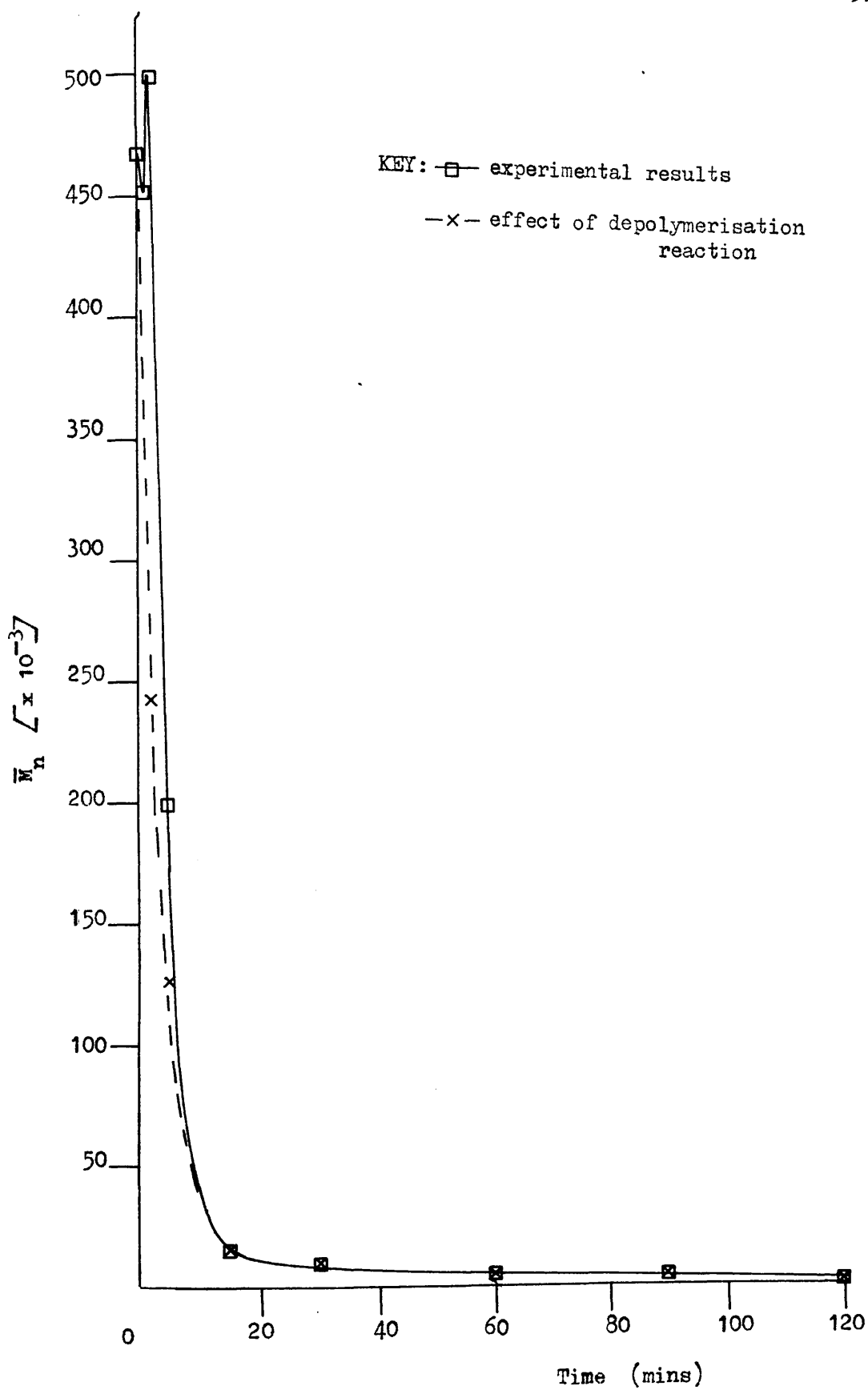


FIGURE 6.28

CHANGES IN MOLECULAR WEIGHT (\bar{M}_n) WITH TIME OF HEATING OF
PHB AT 200°C UNDER AIR

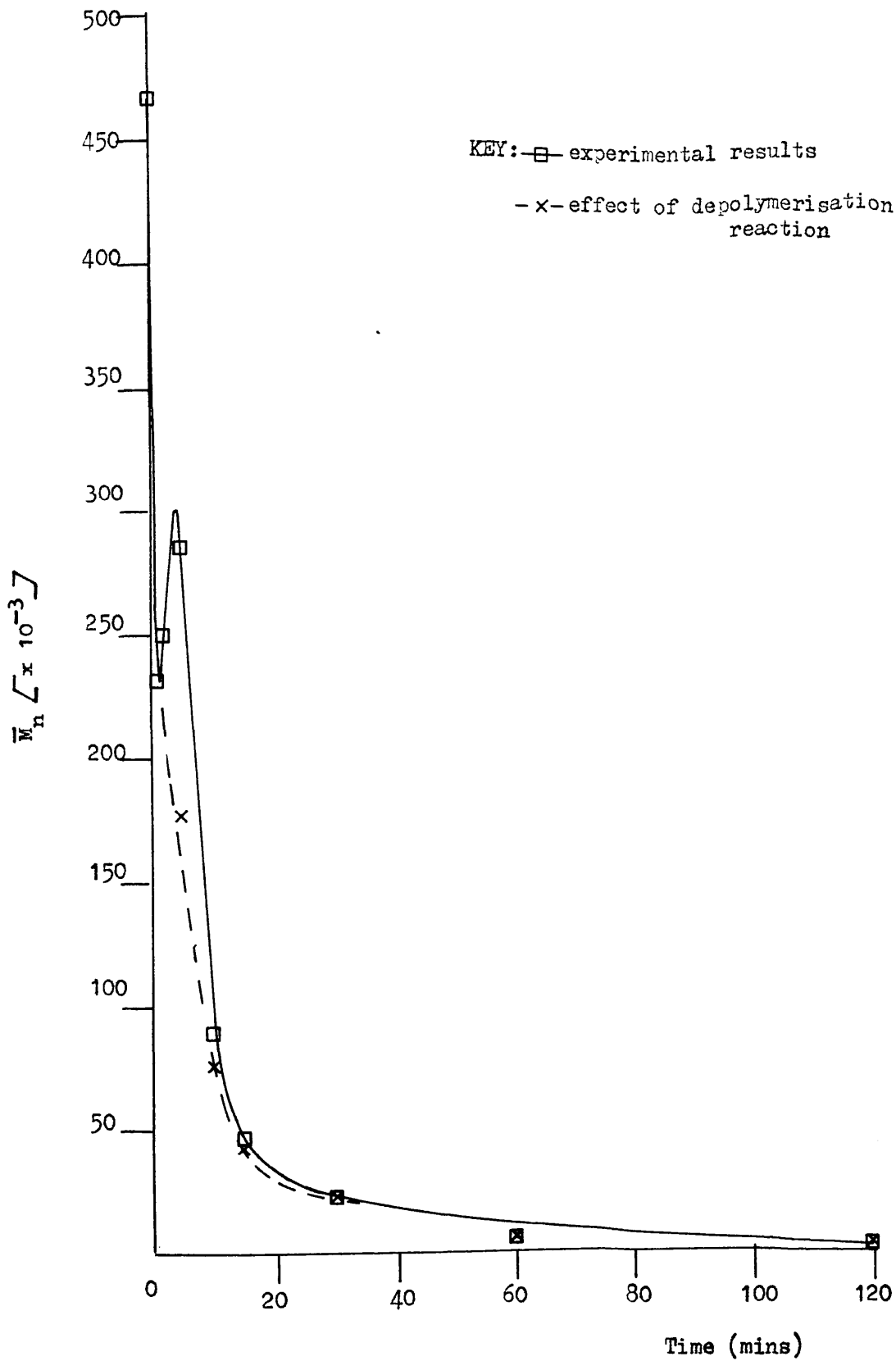


FIGURE 6.29

CHANGES IN MOLECULAR WEIGHT (\bar{M}_n) WITH TIME OF HEATING OF
 PHB AT 190°C UNDER AIR

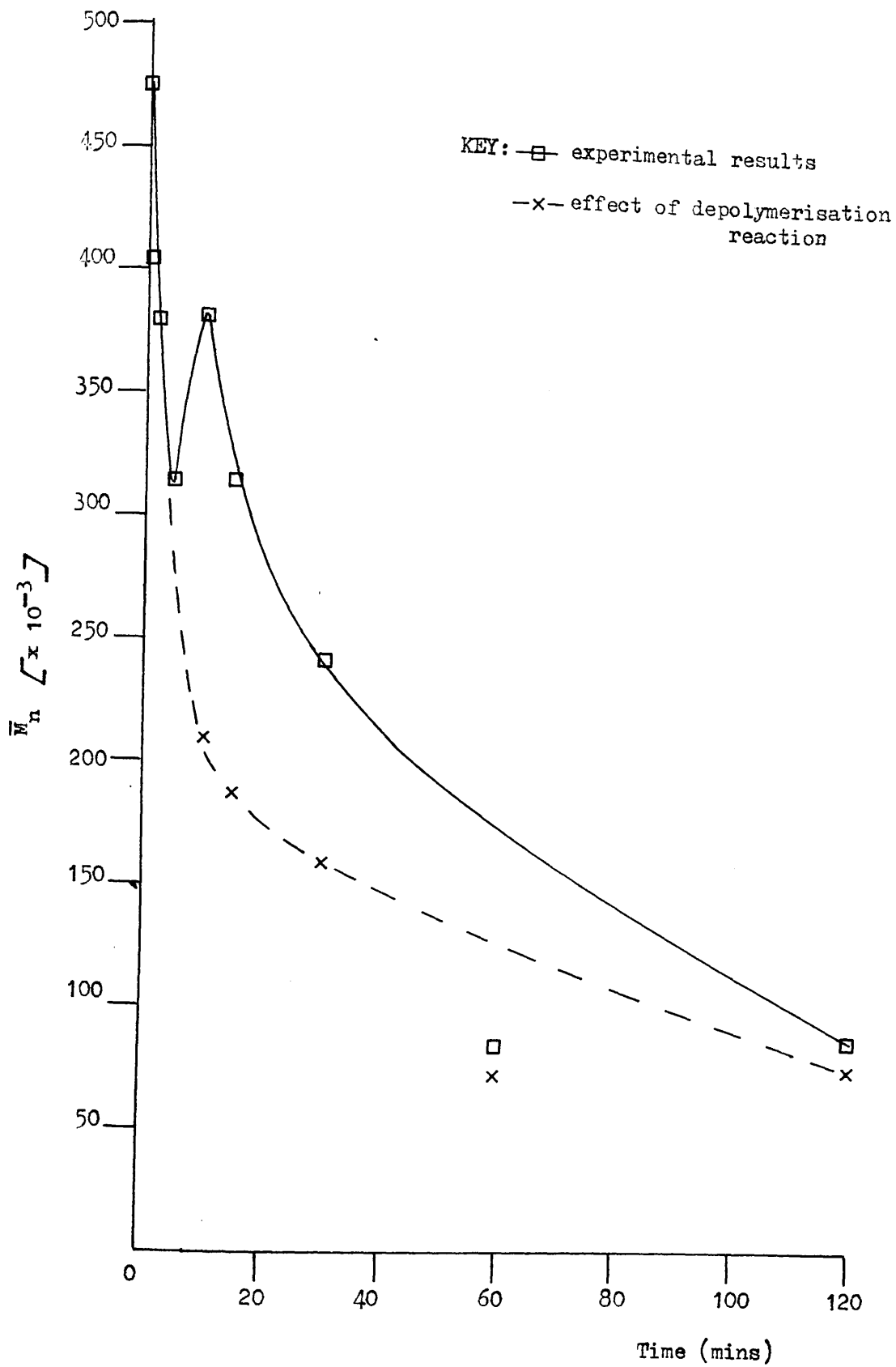


FIGURE 6.30

CHANGES IN MOLECULAR WEIGHT (\bar{M}_n) WITH TIME OF HEATING OF
PFB AT 180°C UNDER AIR

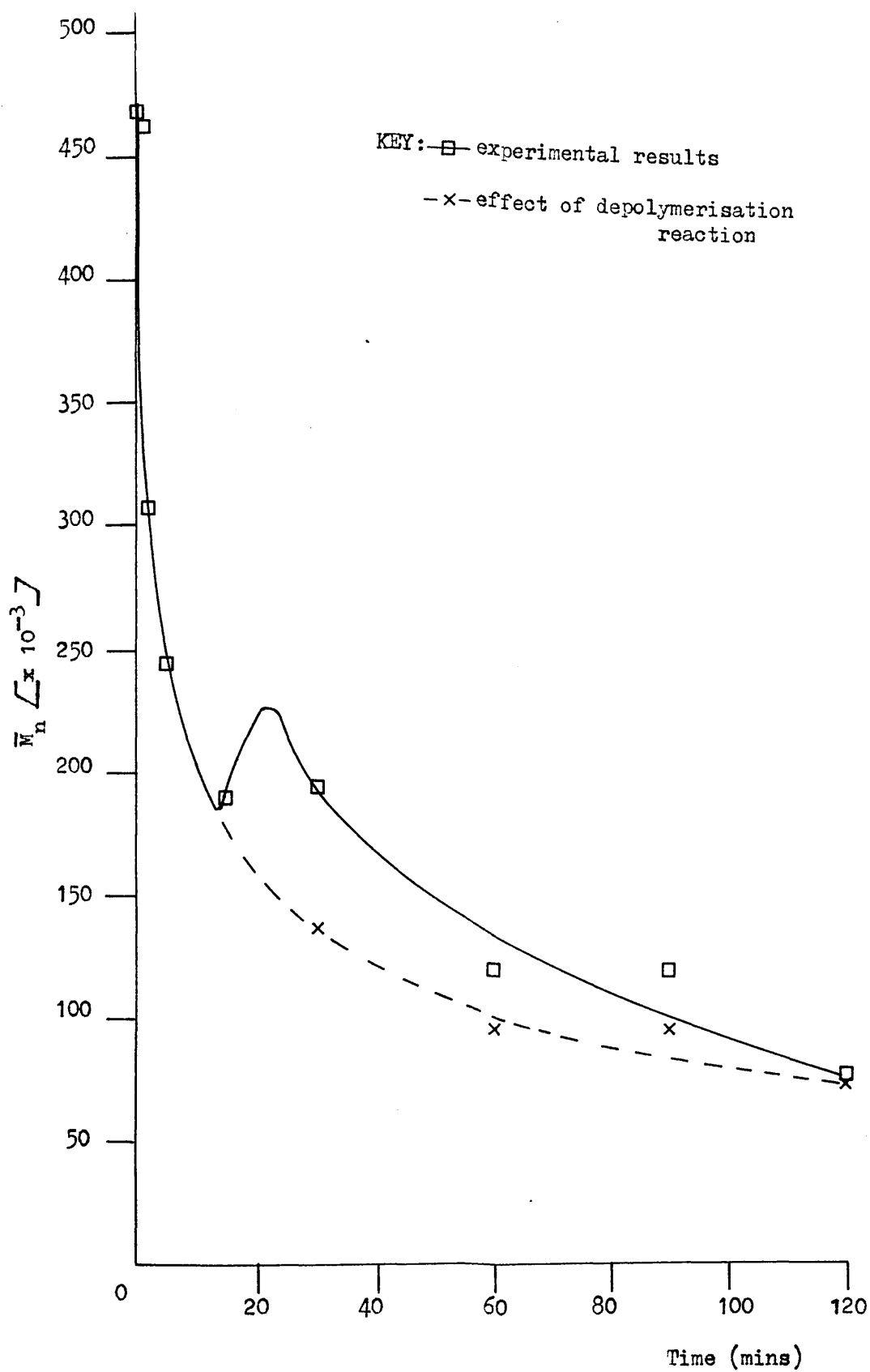


FIGURE 6.31

CHANGES IN MOLECULAR WEIGHT WITH TIME OF HEATING OF
PHB AT 170°C UNDER AIR

FIGURE 6.32

$\frac{1}{CL_t} - \frac{1}{CL_0}$ VERSUS TIME OF HEATING OF PHB
AT 200°C UNDER AIR

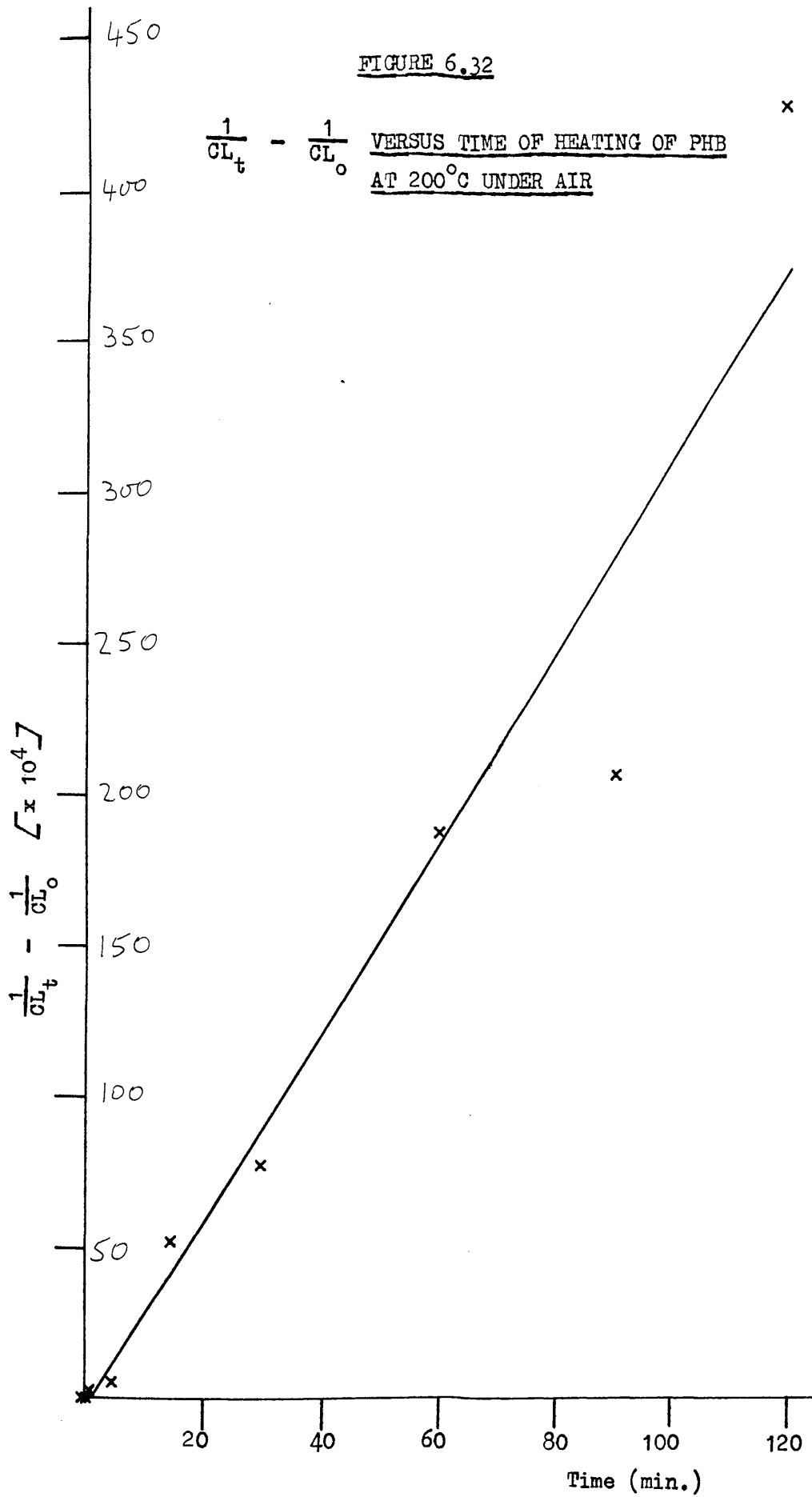
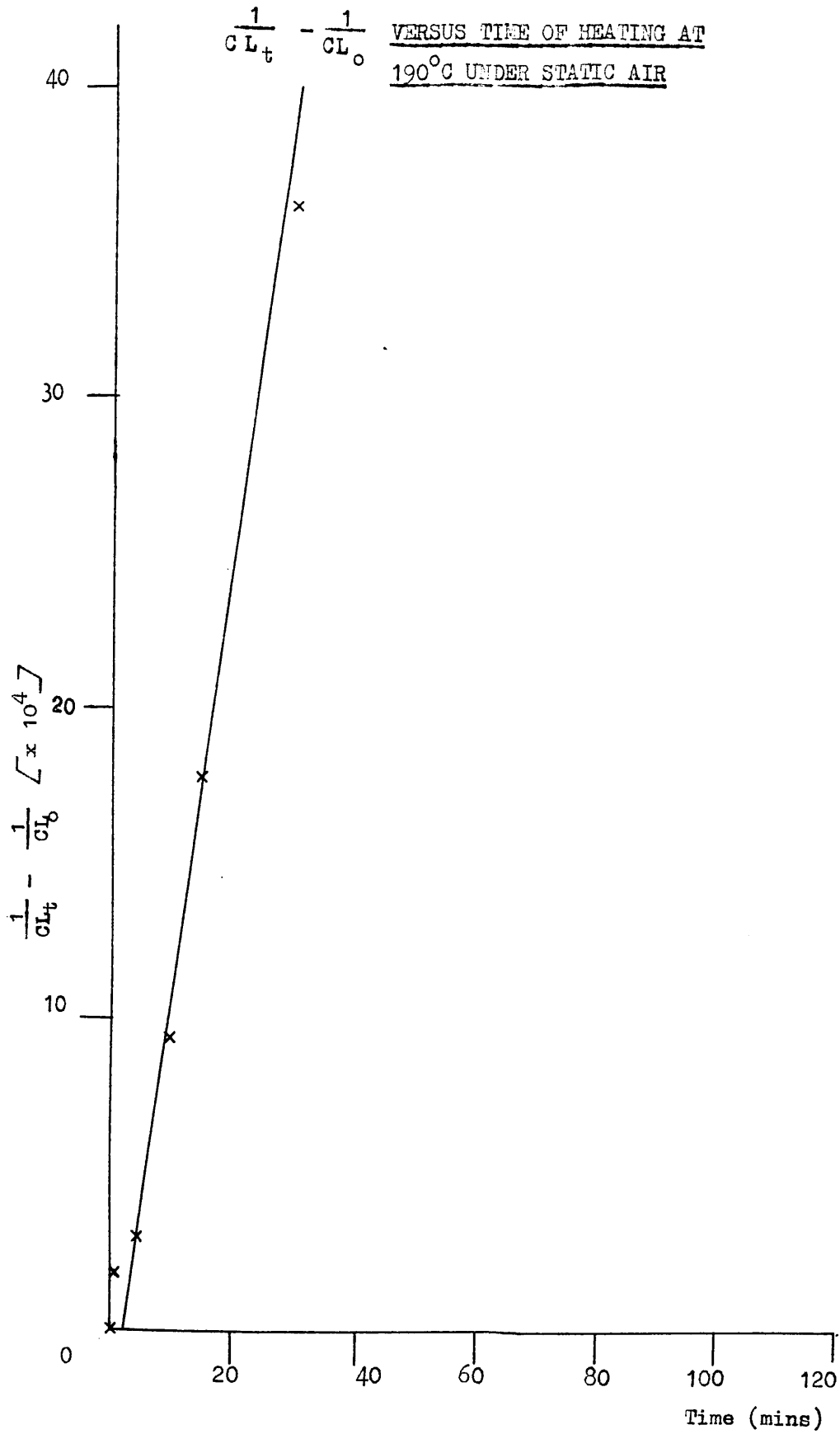


FIGURE 6.33

VERSUS TIME OF HEATING AT
190°C UNDER STATIC AIR



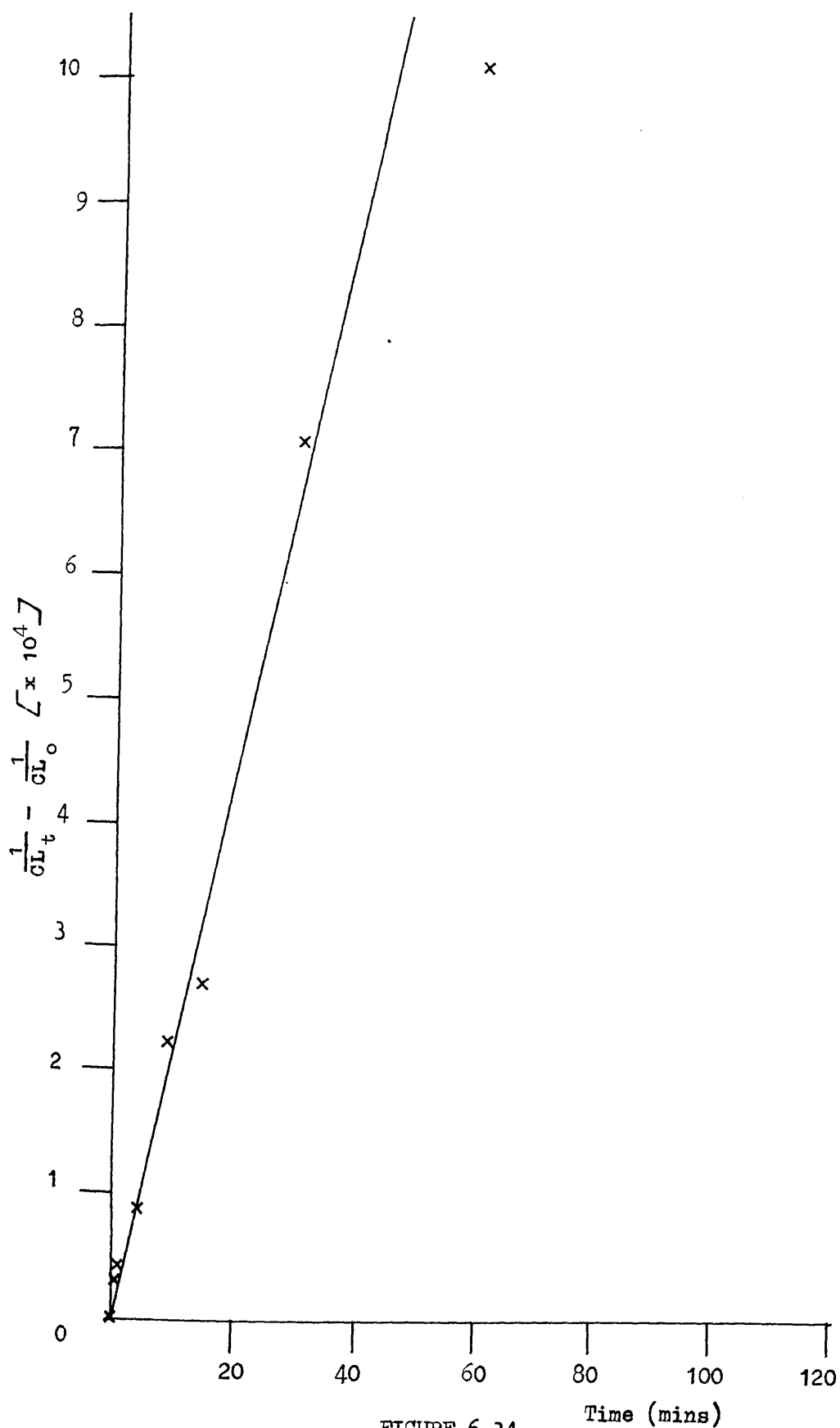


FIGURE 6.34

$\frac{1}{CL_t} - \frac{1}{CL_o}$ VERSUS TIME OF HEATING OF PHB AT
180°C UNDER STATIC AIR

FIGURE 6.35
 $\frac{1}{CL_t} - \frac{1}{CL_0}$ VERSUS TIME OF HEATING
 OF PHB AT 170°C UNDER
 STATIC AIR

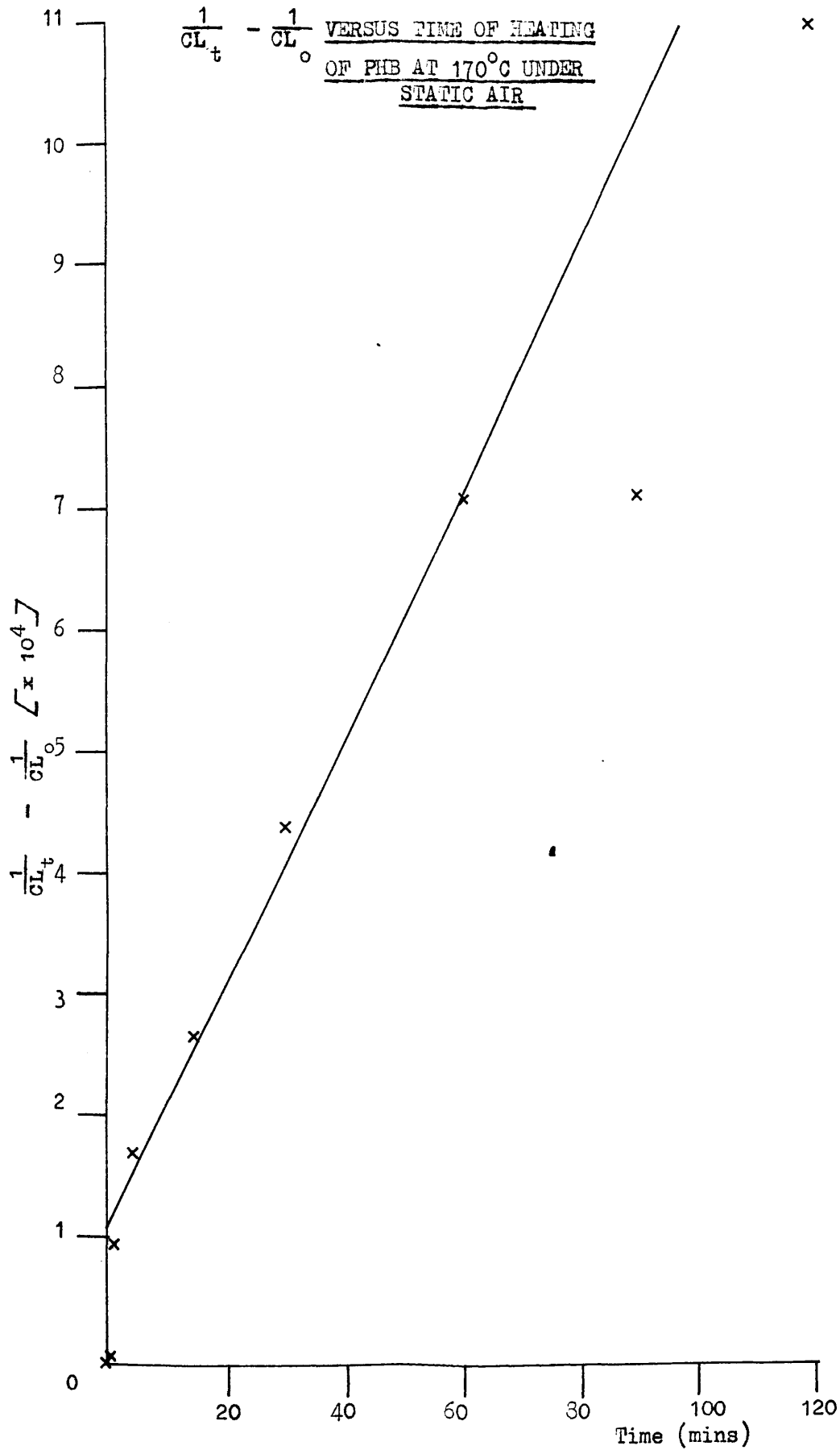


TABLE 6.C

RATES OF CHAIN SCISSION
IN PHB AT VARIOUS TEMPERATURES UNDER VACUUM

Temperature °C	Rate of Random Chain Scission (bonds broken/monomer unit/sec)	Intercept on $1/c_{L_t} - 1/c_{L_0}$ axis
170	$(1.72 \pm 0.09) \times 10^{-7}$	1.06×10^{-4}
180	$(3.86 \pm 0.2) \times 10^{-7}$	1.43×10^{-4}
190	$(2.42 \pm 0.2) \times 10^{-6}$	-3.38×10^{-4}
200	$(5.26 \pm 0.2) \times 10^{-6}$	-4.21×10^{-4}

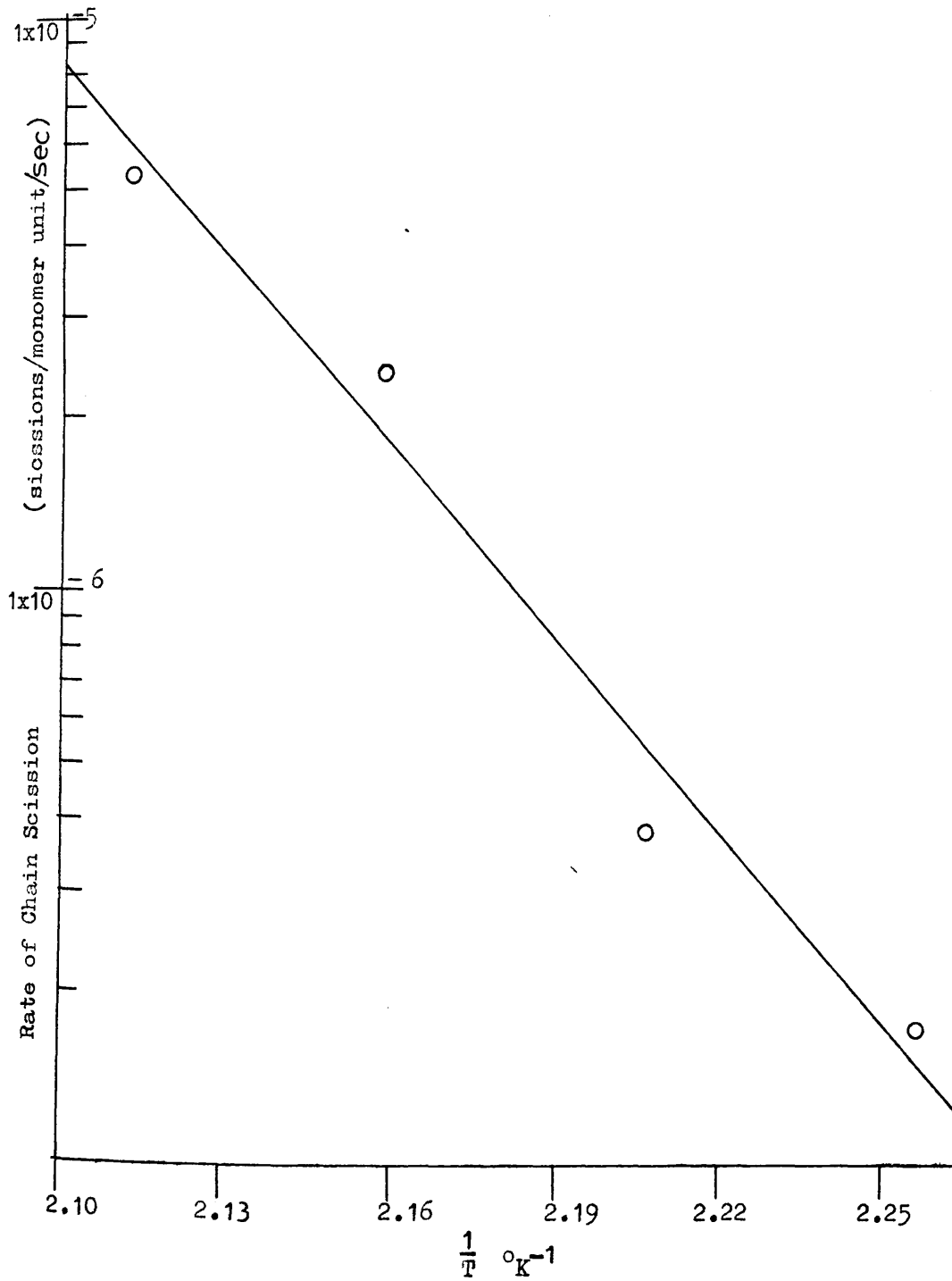


FIGURE 6.36

ARRHENIUS PLOT FOR THE DEGRADATION OF PHB
UNDER STATIC AIR (170°C - 200°C)

was obtained and by means of a least squares fit the energy of activation for the chain scission process calculated at $215 \pm 43 \text{ kJ mol}^{-1}$.

The effect of different times of heating under static air at various temperatures on the \bar{M}_w of a PHB sample is illustrated in Figure 6.37. These data correspond closely to those in Figures 6.28-6.31.

The relationships between molecular weight and extent of volatilisation in the temperature range $170-200^\circ\text{C}$ are illustrated in Figures 6.38 and 6.39. The rapid decrease in molecular weight with little volatilisation, is characteristic of a random chain scission process.

6.6 EFFECT OF A CYCLIC HEATING PROGRAMME ON MOLECULAR WEIGHT

The experimental set up described for the experiments discussed in Chapter 6.3 was used to heat five, 200mg samples of PHB (S1 - of Chapter 2.11), rapidly under vacuum, from ambient to 200°C , where the temperature was held constant for 60 seconds, prior to the sample being allowed to cool to ambient temperatures. The intrinsic viscosity of each sample was measured by the method outlined in Chapter 2.6(ii), after completion of 1 to 5 of the above heating cycles. Experimental data is presented in Figure 6.40 while Figure 6.41 presents a plot of intrinsic viscosity, \bar{M}_w (calculated from $[\eta]$ via Equation 2.5) and \bar{M}_v (calculated from $[\eta]$ via Equation 2.6), versus number of heating cycles. From the data in Figure 6.41 it can be seen that the combined effect of the esterification and the random chain scission reactions on the molecular weight of the PHB sample, are effectively negligible after 3 such heating cycles. Only on subsequent heating

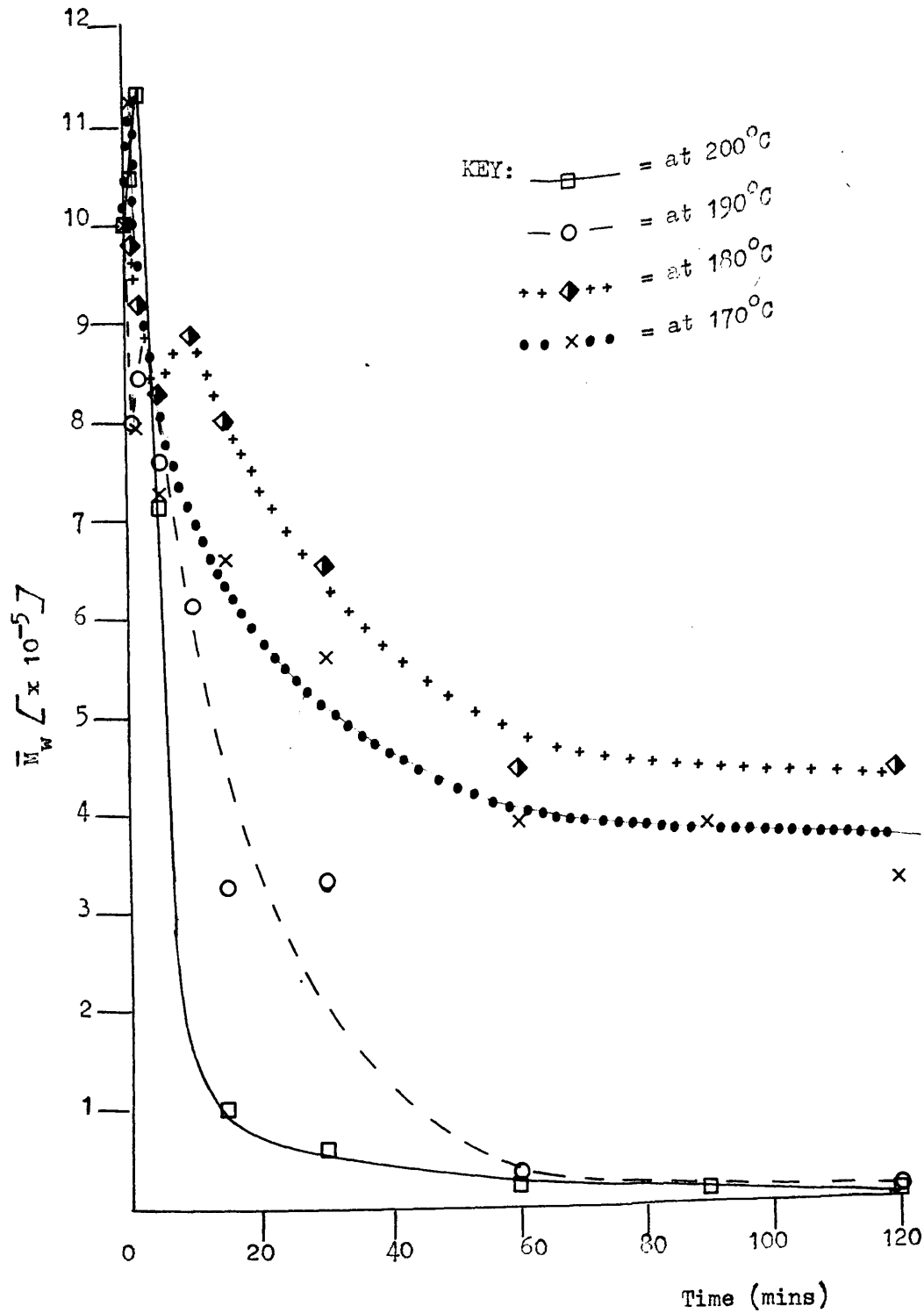


FIGURE 6.37

CHANGES IN MOLECULAR WEIGHT (\bar{M}_w) WITH TIME OF HEATING OF
 PHB AT SEVERAL TEMPERATURES UNDER STATIC AIR

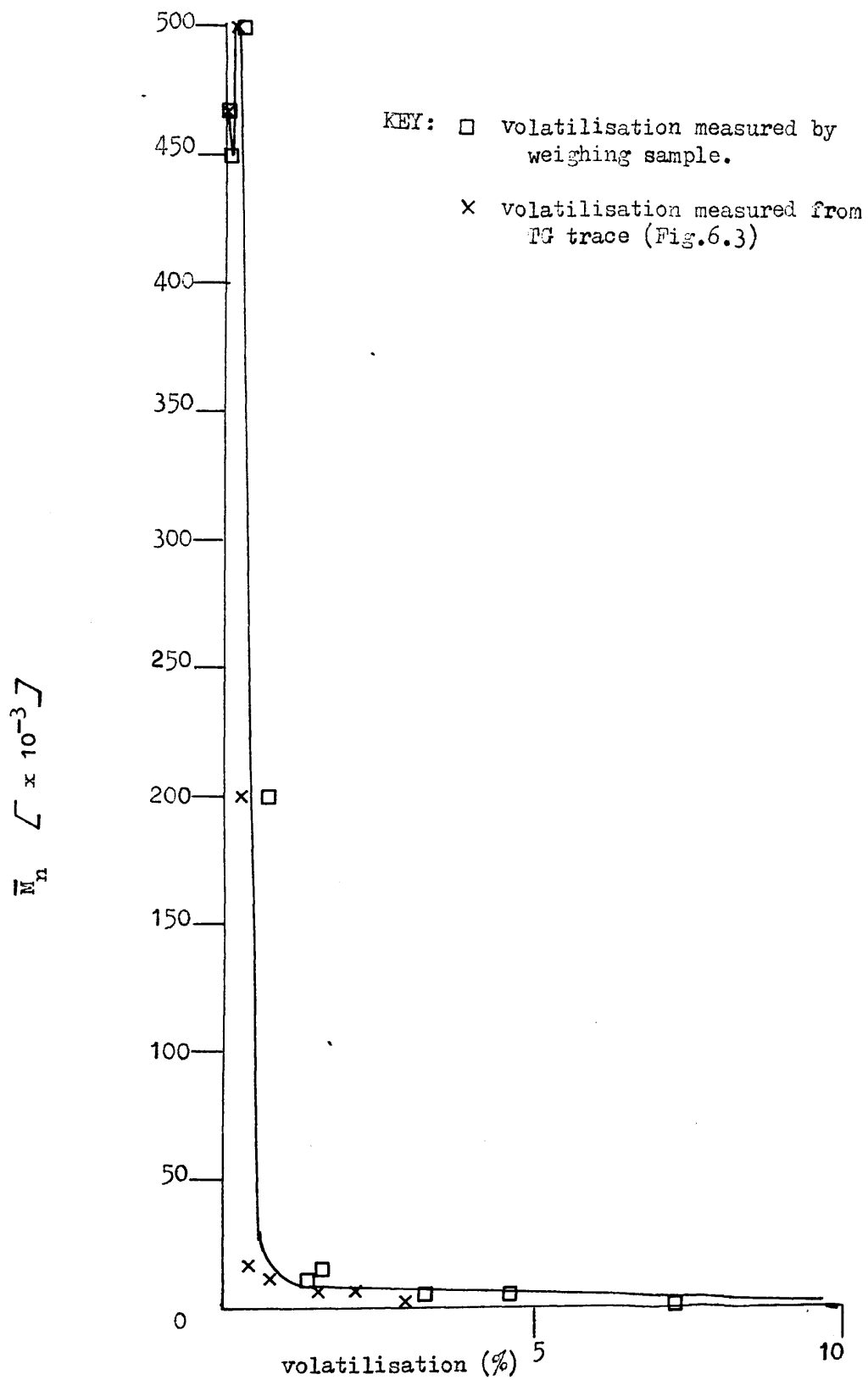


FIGURE 6.38

CHANGES IN \bar{M}_n WITH VOLATILISATION OF PHB AT 200°C IN STATIC AIR

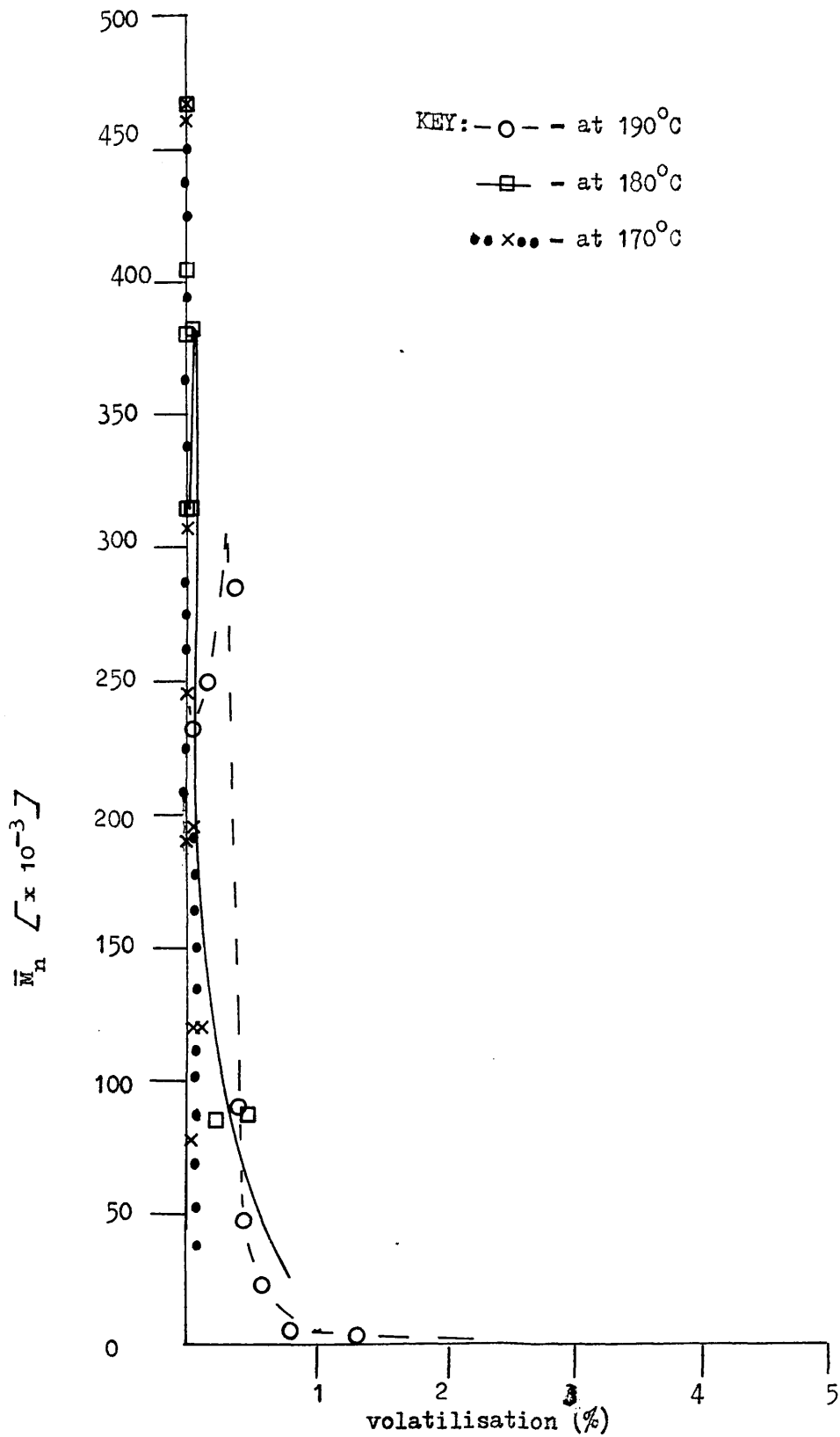
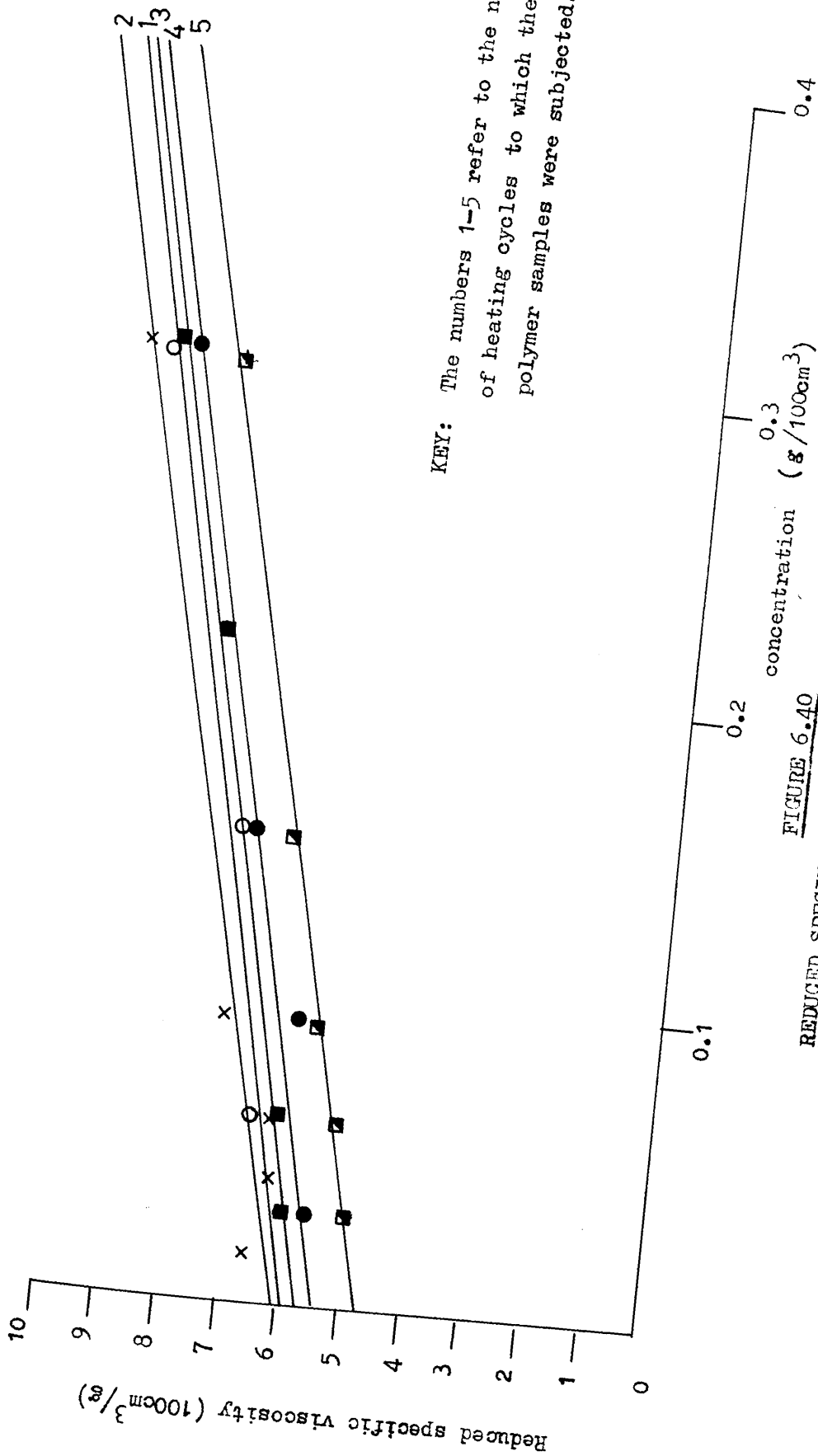


FIGURE 6.39

CHANGES IN \bar{M}_n WITH VOLATILISATION OF PHB
AT SEVERAL TEMPERATURES UNDER STATIC AIR



KEY: The numbers 1-5 refer to the number of heating cycles to which the polymer samples were subjected.

FIGURE 6.40
REDUCED SPECIFIC VISCOSITY VERSUS CONCENTRATION
OF POLYMER SOLUTION

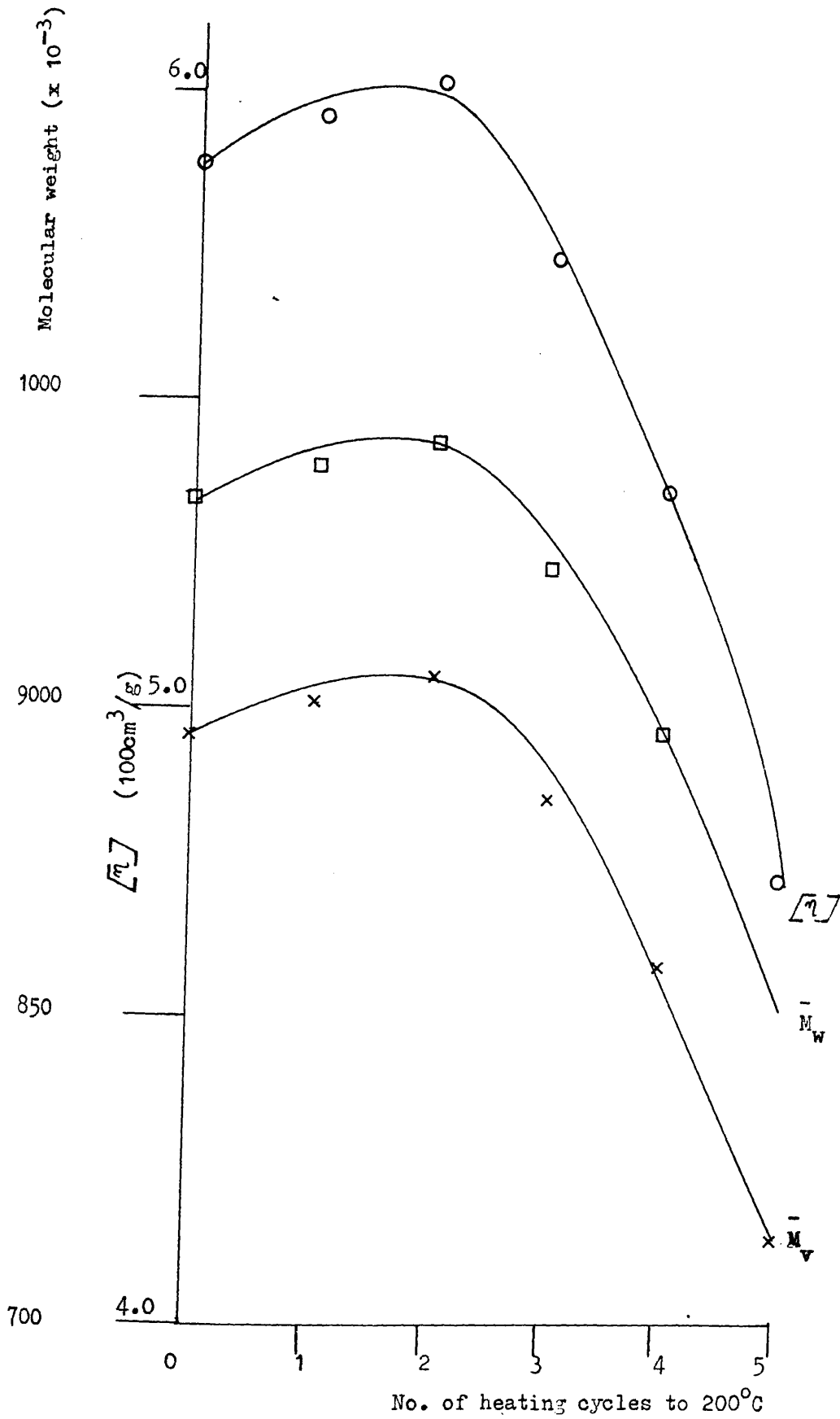


FIGURE 6.41
 $[\eta]$, \bar{M}_w , \bar{M}_v VERSUS NUMBER OF HEATING CYCLES
 TO 200°C

cycles does the random chain scission reaction predominate and the molecular weight fall significantly, presumably since most of the available hydroxyl end groups on the polymer have reacted.

6.7 CORRELATION BETWEEN MELT FLOW INDEX AND MOLECULAR WEIGHT

It is well established that melt viscosity, of which melt flow index (MFI) is a numerical expression, is related to weight average (\bar{M}_w) rather than number average molecular weight (\bar{M}_n) (Ref. 114-116). In many polymer systems the relationship between Newtonian melt viscosity and \bar{M}_w has been shown to be satisfactorily represented by an empirical equation of the form,

$$\log \eta = A \log \bar{M}_w - B_T \dots\dots\dots \text{Eq 6.11}$$

where A generally has a value of 3.4 to 3.5 (Ref. 117-119) and B_T is a temperature dependant constant. Equation 6.11 is valid for values of \bar{M}_w above some critical value at which intermolecular entanglement of the chains determine the flow (Ref. 120-121). Below this value A equals unity.

The work described in this section was an attempt to relate MFI to \bar{M}_w for PHB at 190°C which is a possible processing temperature for PHB. Since MFI measurements are both quick and simple to make, it was proposed that if a relationship of the type found in Equation 6.11 could be defined, it would provide a rapid means of determining the molecular weight or of comparing molecular weights of different batches in an industrial production setting. It would also enable a rapid assessment of molecular weight changes resulting from processing to be made.

The conditions and procedure for the operation of the melt flow indexer are outlined in Chapter 2.4(vi). The molten polymer flow being extruded from the capillary orifice at the base of the melt flow indexer was cut into separate samples as detailed below. The molten polymer leaving the indexer during the following time intervals (see Note at foot of page) (a) 0 to 10 sec., (b) 70 to 80 sec., (c) 140 to 160 sec., (d) 220 to 230 sec., and 290 to 300 sec., were quench cooled, in 8cm^3 of chloroform contained in small sample bottles. The 5 solutions obtained were subjected to GPC analysis, using instrument (b) as detailed in Chapter 2.6(i), by which means the molecular weight of the polymer sections (a) to (e) were determined. Similarly 60 second sections of the polymer flow were taken during the following time intervals, (f) 10 to 70 sec., (g) 80 to 140 sec., (h) 160 to 220 sec., (i) 230 to 290 sec., and (j) 300 to 360 sec. and weighed. The weight measurements obtained for polymer sections (f) to (j) were multiplied by 10 to give a value of MFI, in units of grams of polymer/ten minutes, during each time interval. The molecular weight measurements obtained for polymer sections (a) to (e), and MFI values obtained for polymer sections (f) to (j) correspond to average values over the time interval during which the measurements were taken.

NOTE: The zero value for the times quoted above was taken as the end of the equilibration time for the polymer in the barrel of the melt flow indexer (Chapter 2.4(vi)).

These values were assumed to be the instantaneous values for the polymer sample at the mid point of the time interval during which they were measured. During the six minutes in which sections were cut from the polymer flow the position of the plunger, in the melt flow indexer, was within the scribed rings on the plunger which mark the region within which valid results for MFI may be measured. The values of \bar{M}_w and MFI thus obtained are shown in Table 6.D.

Plots of MFI and \bar{M}_w versus time, using the data in Table 6.D, are illustrated in Figure 6.42. It can be seen from Figure 6.42 that both the MFI and the \bar{M}_w of the PHB sample change rapidly on heating at 190°C. From the data of Figure 6.42 it was possible to tabulate (Table 6.E) corresponding values of \bar{M}_w and MFI, at 20 second intervals during the melt flow index experiment. From the data of Table 6.E a linear plot of log MFI versus log \bar{M}_w was obtained (Figure 6.43). A least squares fit on the points gave the following relationship:

$$\log \text{MFI} = 19.8 - 3.49 \log \bar{M}_w \quad \dots\dots\dots \text{Eq 6.12}$$

which is of the same type to that of Equation 6.11. The value of the exponent to which \bar{M}_w is raised (-3.49) is in excellent agreement with the value of approximately 3.5 reported for many linear polymers (Ref. 117). The negative value is due to the inverse proportionality relationship between $[\eta]$ and MFI.

6.8 GENERAL CONCLUSIONS

The results described in this chapter have shown that two competing reactions occur when PHB is heated in the temperature range 170°C to 200°C. These are a random chain scission

TABLE 6.D

VALUES OF \bar{M}_w AND MFI OBTAINED FROM EXTRUDED POLYMER

Polymer Section	Time Seconds	\bar{M}_w	MFI grams of polymer/ 10 minutes
(a)	5	444,700	—
(f)	40	—	1.331
(b)	75	422,900	—
(g)	110	—	1.624
(c)	150	404,100	—
(h)	190	—	2.074
(d)	225	353,700	—
(i)	260	—	5.108
(e)	295	285,200	—
(j)	330	—	6.608

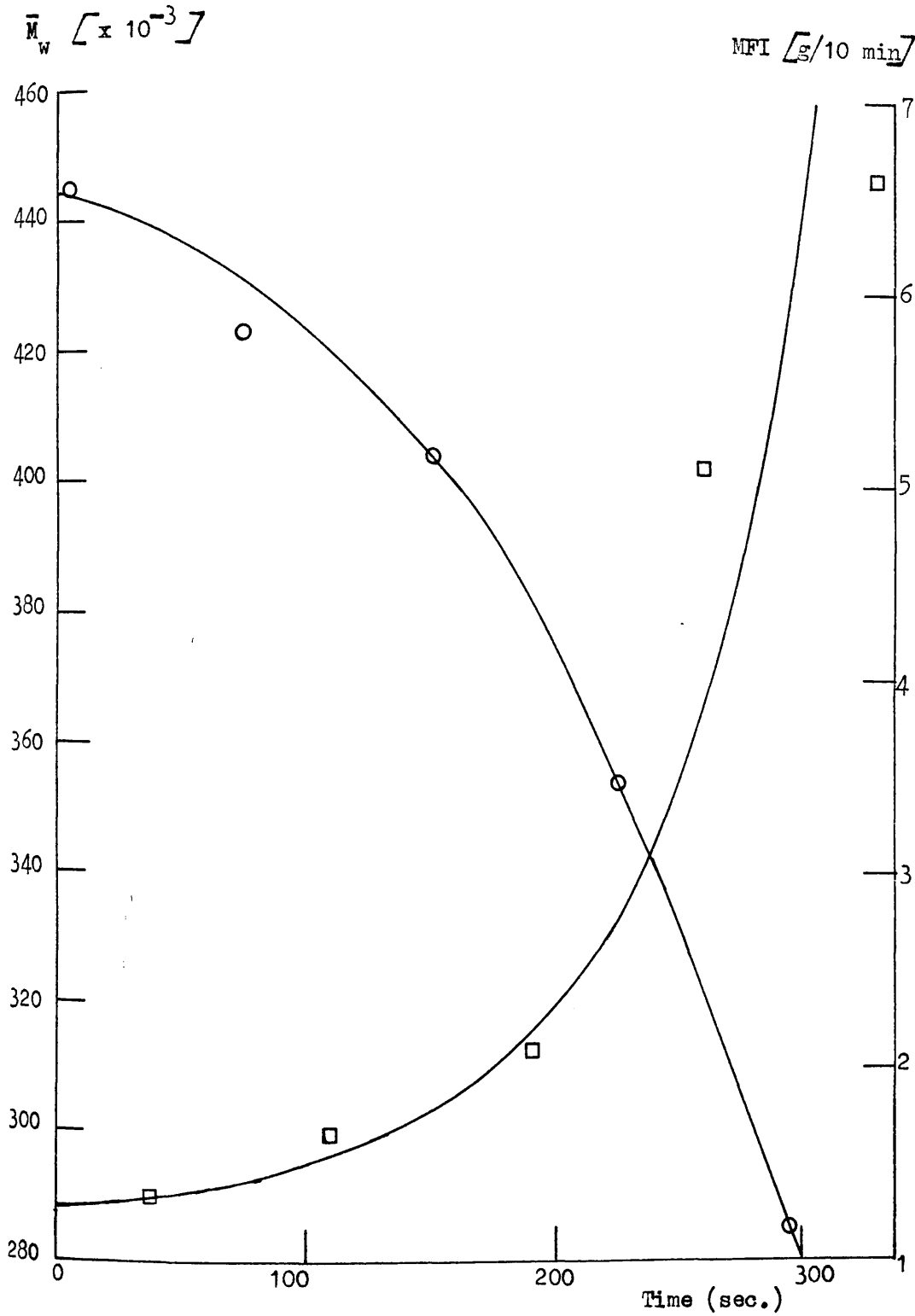


FIGURE 6.14

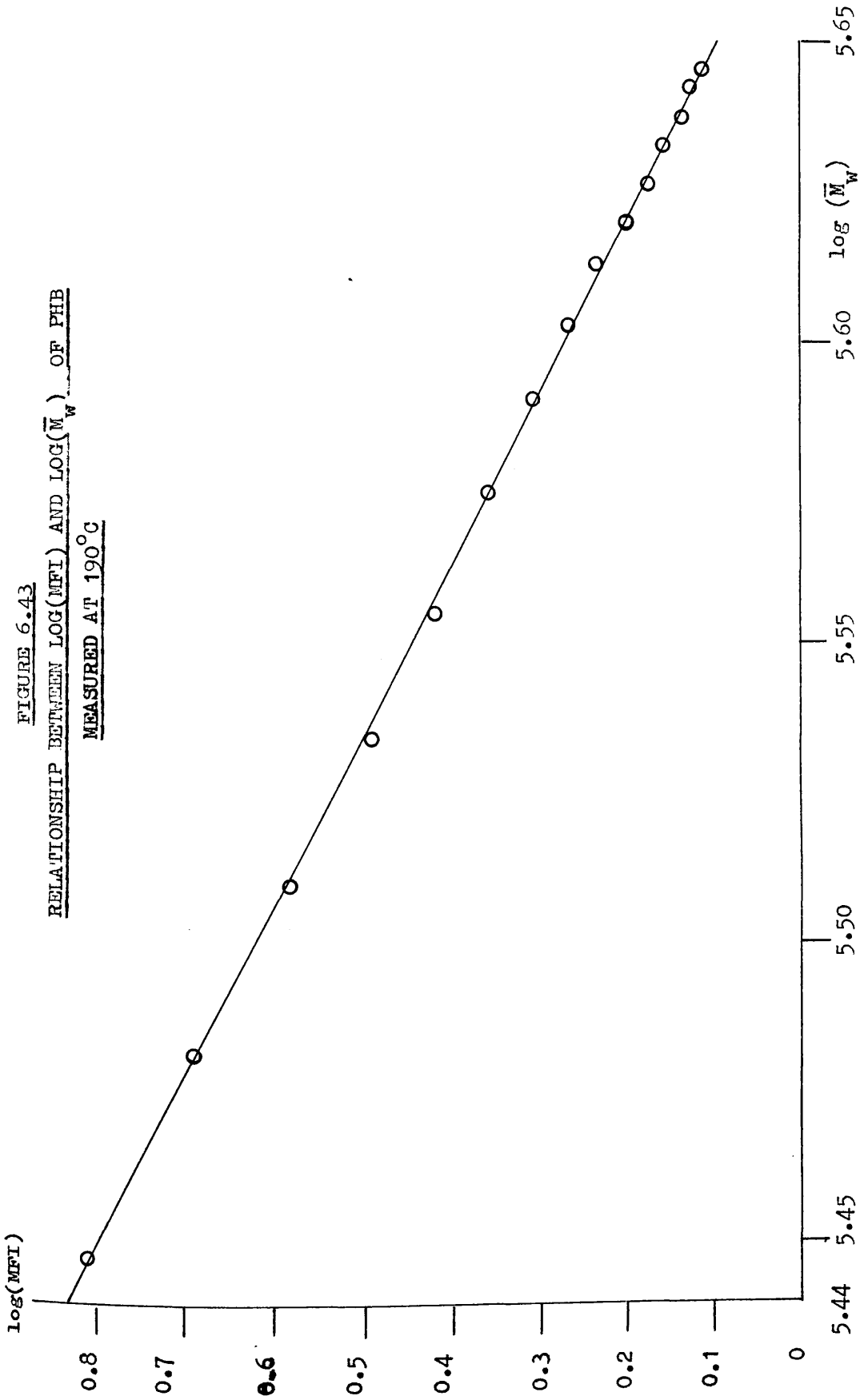
CHANGES IN MFI AND \bar{M}_w WITH TIME OF HEATING
AT 190°C FOR PHB IN A DAVENPORT MELT FLOW INDEXER

TABLE 6.E

CORRESPONDING VALUES OF MFI AND \bar{M}_w OBTAINED FROM
THE DATA OF FIGURE 6.42

Time (seconds)	MFI (grams/10 minutes)	\bar{M}_w	log MFI	log \bar{M}_w
20	1.30	442,000	0.114	5.645
40	1.34	438,100	0.127	5.642
60	1.37	434,000	0.137	5.537
80	1.44	428,500	0.153	5.632
100	1.50	423,000	0.176	5.626
120	1.60	416,200	0.204	5.619
140	1.72	408,900	0.236	5.612
160	1.86	400,000	0.270	5.602
180	2.05	389,000	0.312	5.590
200	2.30	375,000	0.362	5.574
220	2.64	358,000	0.422	5.554
240	3.11	341,000	0.493	5.533
260	3.85	322,500	0.585	5.509
280	4.90	302,800	0.690	5.481
300	6.45	280,000	0.810	5.447

FIGURE 6.43
RELATIONSHIP BETWEEN $\log(\overline{M}_w)$ AND $\log(\overline{M}_n)$ OF PHB
MEASURED AT 190°C



depolymerisation reaction and an esterification reaction which occurs between terminal hydroxyl and carboxyl groups. This latter reaction is of limited duration, stopping when all the hydroxyl groups originally present in the polymer have reacted. It is proposed that it is this esterification reaction which is responsible for the following experimental observations:

- (a) The narrow endotherm observed in the DSC trace of a sample of PHB (Figure 3.3) at a temperature of 280°C. At this time during the heating programme the conditions must be ideal for this reaction to occur.
- (b) A portion of the water identified as a product of thermal degradation of PHB (see Chapters 3 and 4).
- (c) The small amount of volatilisation observed in the early portions of the isothermal TG traces (Chapter 6.2).

Condensation reactions of this type are not uncommon during the thermal degradation of polymers, being previously reported for hydroxyl terminated siloxanes (Ref. 52, 122, 123) and for nylons (Ref.124).

Subsequent experiments have provided further evidence for the occurrence of an esterification reaction. A rise in \bar{M}_n within the time scale of 0.5 to 2.5 minutes, from loading, for PHB in a Davanport Grader at 190°C (Ref. 125) has been observed, and after passing through a Betol 2520 extruder (residence time 2 to 2.25 minutes) at 190°C to 205°C PHB samples have shown relatively minor changes in \bar{M}_w and in some cases an increase. (Ref. 126).

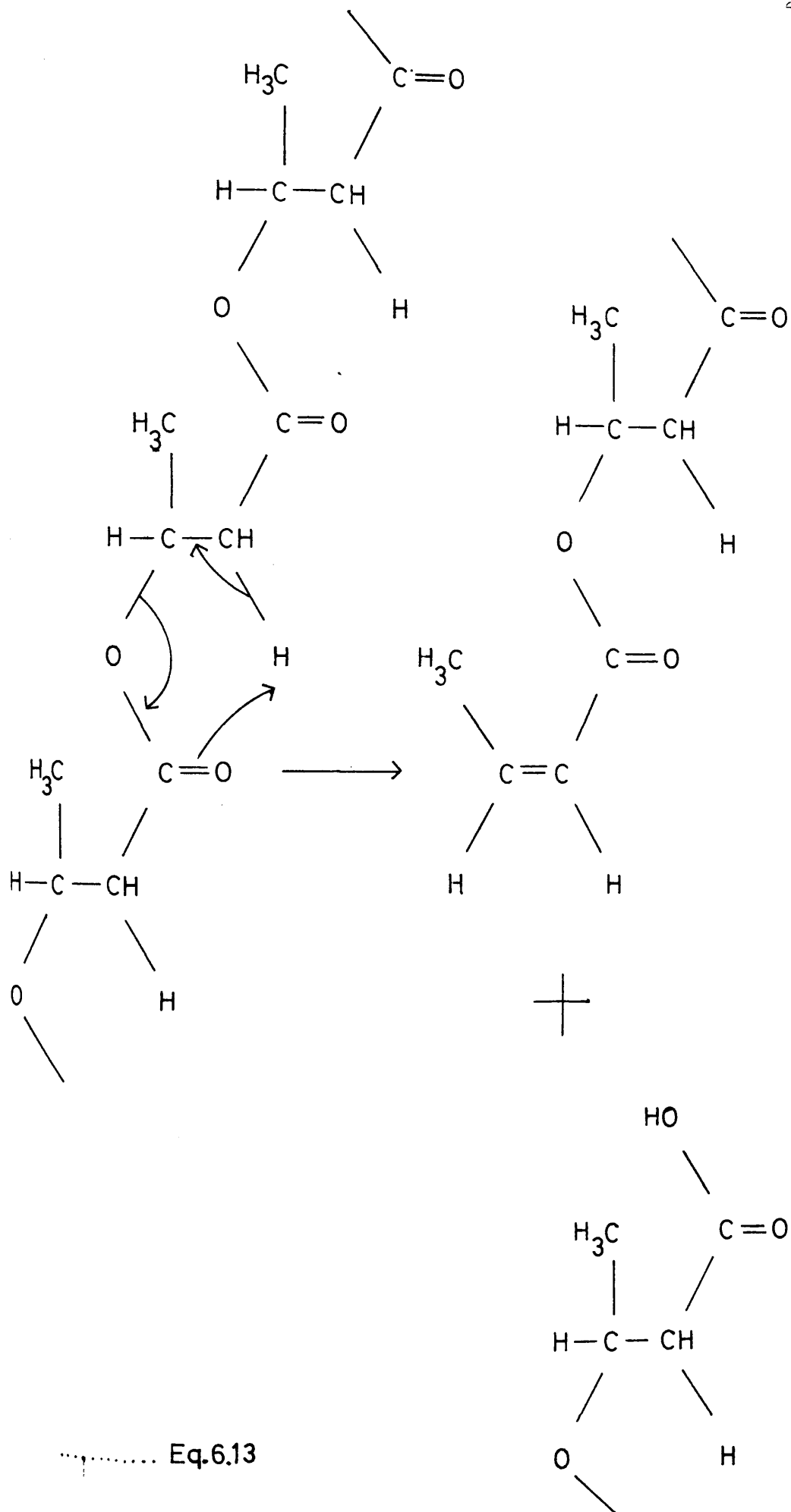
It has been reported that none of the conventional polyolefin chain-breaking antioxidants give any significant improvement, even at high concentrations, in the stability of PHB (Ref.127). Further the addition of free radical producing compounds such as bisdialkylperoxides, has little effect on stability (Ref. 125).

Thus a free radical mechanism can be discounted. This suggests that the random chain scission reaction proceeds via a mechanism analogous to that represented by Equation 3.1, involving a six-centred β -elimination occurring on the folded chain. (Equation 6.13).

A summary of the kinetic data calculated from the experimental results discussed in this chapter are given in Table 6.F. The most accurate control of temperature and experimental conditions can be obtained under vacuum and for this reason this set of results are thought to be the most accurate. The absolute errors in the rates of chain scission increase with increasing temperature for the following reasons:

- (a) The molecular weight of the polymer sample is changing so rapidly at higher temperatures that control over the length of time of heating becomes increasingly important and further,
- (b) at higher temperatures the molecular weight of the polymer sample rapidly falls to values at which there is a large percentage error in the measurement of the molecular weight by GPC and consequently large errors in $\frac{1}{CL_t} - \frac{1}{CL_0}$.

The value for the energy of activation, E_a , obtained under the different atmospheres studied, does not vary significantly and from the three results given can be estimated to be in the region of 250 kJ mol^{-1} . This value can be compared with that reported for various low molecular weight esters which have E_a in the range 153 kJ mol^{-1} for $\text{PhOCO}_2 \text{ Bu}^t$ to 214 kJ mol^{-1} for $\text{CH}_3\text{OCH}_2\text{CH}_2\text{O}_2\text{CCH}_3$ (Ref. 128, 129).



Eq.6.13

TABLE 6.F
SUMMARY OF KINETIC DATA ON PEB

Atmosphere	RATE OF BOND SCISSION (bond scissions/monomer unit/sec)				Energy of Activation for Bond Scission Reaction kJ mol ⁻¹
	at 170°C	at 180°C	at 190°C	at 200°C	
Vacuum	$(7.99 \pm 0.9) \times 10^{-8}$	$(4.72 \pm 0.6) \times 10^{-7}$	$(1.86 \pm 0.2) \times 10^{-6}$	$(4.99 \pm 0.3) \times 10^{-6}$	247 ± 19
Flowing Nitrogen (80cm ³ min ⁻¹)	$(4.51 \pm 1.0) \times 10^{-8}$	$(1.08 \pm 0.2) \times 10^{-7}$	$(1.15 \pm 0.08) \times 10^{-6}$	$(9.42 \pm 2.0) \times 10^{-6}$	326 ± 45
Static Air	$(1.72 \pm 0.09) \times 10^{-7}$	$(3.86 \pm 0.2) \times 10^{-7}$	$(2.42 \pm 0.2) \times 10^{-6}$	$(5.26 \pm 0.2) \times 10^{-6}$	215 ± 43

Within experimental error the intercept in the $\frac{1}{CL_t} - \frac{1}{CL_0}$ versus time of heating plots did not vary significantly from the origin. Thus no indication of weak links being present in the polymer was observed.

There did not appear to be any significant variation in rates measured under the three sets of atmospheric conditions.

CHAPTER 7

CRYSTALLINITY IN PHB AND ITS EFFECT ON THERMAL DEGRADATION

7.1 INTRODUCTION

Crystallisation in high polymers is not only of theoretical interest for understanding polymer morphology but is also of basic importance in such practical operations in plastics fabrication such as extrusion and spinning of molten polymers. The mode of crystallisation of a polymer affects the density and crystallinity of the polymer and consequently its mechanical, thermal and optical properties.

Naturally occurring PHB has a stereoregular isotactic structure and x-ray data have established the fact that the polymer is highly crystalline both in and outside the living cell (Ref. 20, 21). Indeed one of the reasons why PHB is attractive as a commercial polymer is its high crystallinity.

The crystal structure of PHB has been extensively studied and has been shown to consist of an orthorombic unit cell with $a = 5.76 \text{ \AA}$, $b = 13.20 \text{ \AA}$ and the fibre period $c = 5.96 \text{ \AA}$. Furthermore the molecule has a conformation, in the case of a rectus polymer, of a left handed (2/1) helix (Ref. 19, 20, 130). However no study has been carried out to determine the effect of crystallinity on the thermal degradation of PHB at temperatures below its melting point. For this reason a study of the thermal properties of two polymer samples, from the same batch of PHB, but with differing crystallinity was carried out and is described in this chapter.

7.2 PREPARATION OF POLYMER SAMPLES

A single crystal mat form of PHB, labelled SX, was prepared from a sample of PHB, labelled BLDX01, by the method outlined in Chapter 2.10. The impurities present in both these samples were measured by the methods described in Chapter 2.5(vii) and the results are listed in Table 2.B of Chapter 2.11. The data in Table 2.B shows that polymer SX contains a greater level of impurities than polymer BLDX01. The reasons for this and the difficulties involved in purifying PHB were discussed in Chapter 1.3.

7.3 MEASUREMENT OF CRYSTALLINITY

The heat of fusion of a polymer sample is the amount of energy necessary to transform it from a crystalline or partially crystalline state to a completely disordered state. Therefore a measure of percentage crystallinity, x , can be obtained using the following relationship.

$$x = (\Delta H_{\text{fus}}^* / \Delta H_{\text{fus}}) \times 100 \dots\dots\dots \text{Eq 7.1}$$

where ΔH_{fus}^* and ΔH_{fus} are the heats of fusion of a sample of unknown crystallinity and of 100% crystallinity respectively.

This method has been shown to give results comparable to those obtained by other methods (Ref. 131). The heat of fusion of a sample of material can be measured in a DSC which has been calibrated with a substance of known ΔH_{fus} , such as indium, by the use of Equation 7.2.

$$\Delta H = \frac{60EAB \triangle qS}{m} \dots\dots\dots \text{Eq 7.2}$$

where ΔH = heat of fusion J/g
 E = cell calibration coefficient mW/mV
 A = Peak area in cm^2
 B = Time base setting min/cm.
 ΔqS = Y - axis sensitivity setting mV/cm
 m = sample mass mg

The heats of fusion of polymers SX and BLDX01 were measured in this way using a Du Pont 990 thermoanalyser fitted with a calibrated DSC cell. The DSC traces obtained are depicted in Figure 7.1. By measuring the areas under the curve with a planimeter and applying Equation 7.2 the following values were obtained:

$$\Delta H_{\text{fus}} (\text{SX}) = 107.9 \text{ Jg}^{-1}$$

$$\Delta H_{\text{fus}} (\text{BLDX01}) = 80.4 \text{ Jg}^{-1}$$

Thus by converting a sample of PHB, which had been rapidly precipitated from solution, to a single crystal mat form by the experimental procedure described in Chapter 2.10, the crystallinity of the polymer was increased by 34%. If it is assumed that polymer SX is 100% crystalline then by applying Equation 7.1, using the values of ΔH_{fus} recorded above, polymer BLDX01 would be 74.5% crystalline.

From Figure 7.1 it can be seen that there are two endotherms in the DSC trace of polymer SX compared with only one in that of polymer BLDX01. Possible explanations for this will be discussed in Chapter 7.5.

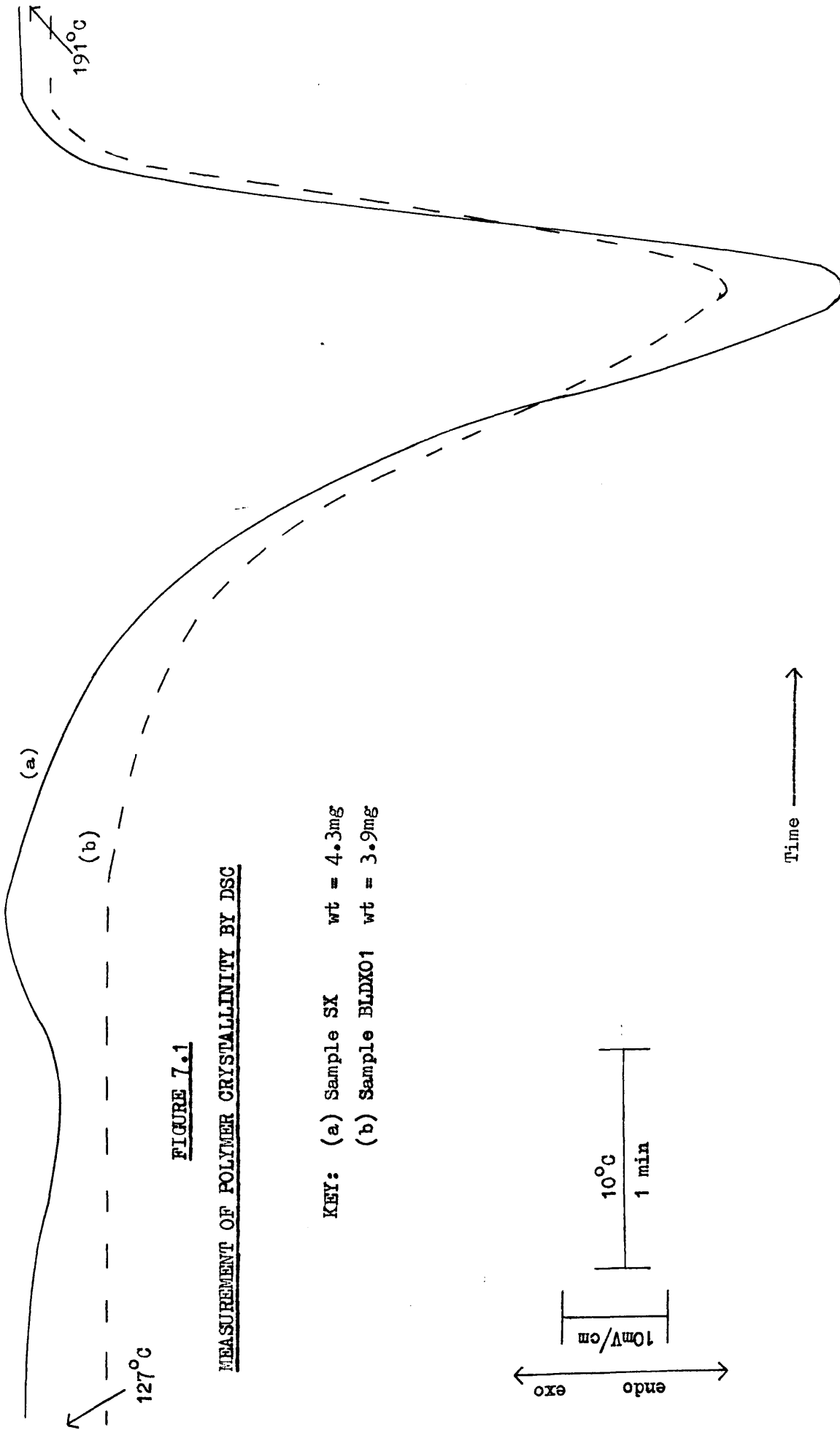


FIGURE 7.1

MEASUREMENT OF POLYMER CRYSTALLINITY BY DSC

KEY: (a) Sample SX wt = 4.3mg
(b) Sample BLDXO1 wt = 3.9mg

7.4 X-RAY POWDER PHOTOGRAPH OF PHB SAMPLE SX

To demonstrate the crystalline nature of sample SX an x-ray powder photograph of a finely ground sample was obtained by the method outlined in Chapter 2.7. From the resultant photograph, of which Figure 7.2 is a contact print, the density of the diffraction rings was measured using a microdensitometer, the trace obtained being depicted in Figure 7.3. The sharpness of the diffraction rings illustrated in Figures 7.2 and 7.3 are characteristic of a highly crystalline polymer sample. The d spacings and their intensities measured from the x-ray powder photograph are recorded in Table 7.A and those d spacings designated (a) to (h) are in close agreement with those reported for PHB by Alper et al (Ref. 20) and by Baptist (Ref.23).

7.5 DIFFERENTIAL SCANNING CALORIMETRY

DSC traces for both polymer samples were obtained on a Du Pont 900 thermoanalyser, under an atmosphere of dynamic nitrogen, by the method outlined in Chapter 2.4(iii) and are illustrated in Figure 7.4. Two endotherms in the trace of sample SX (denoted by \uparrow and $\uparrow\uparrow$) are absent from that of BLDX01.

The endotherm at 140°C (\uparrow), was completely reproducible having already been noted in the previous section (see Figure 7.1) and this was further investigated as follows:

A 4.3mg sample of SX was heated from 122°C to 180°C at a heating rate of $10^{\circ}\text{C}/\text{min}$ in a DSC cell. The resultant trace, obtained on a time base x-axis scan is illustrated in Figure 7.5(a). On reaching a temperature of 180°C the sample was quench cooled in liquid nitrogen prior to a second scan trace (b) Figure 7.5.

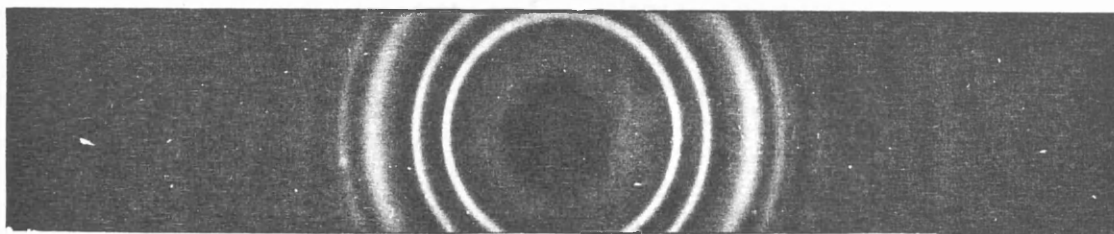


FIGURE 7.2
X-RAY DIFFRACTIOGRAM OF A POWDER SAMPLE OF
PFB, (SX)
(CONTACT PRINT)

Instrument - 3CS
manufactured by Joyce
Loebl Ltd.
For assignment of peaks
see Table 7.A.

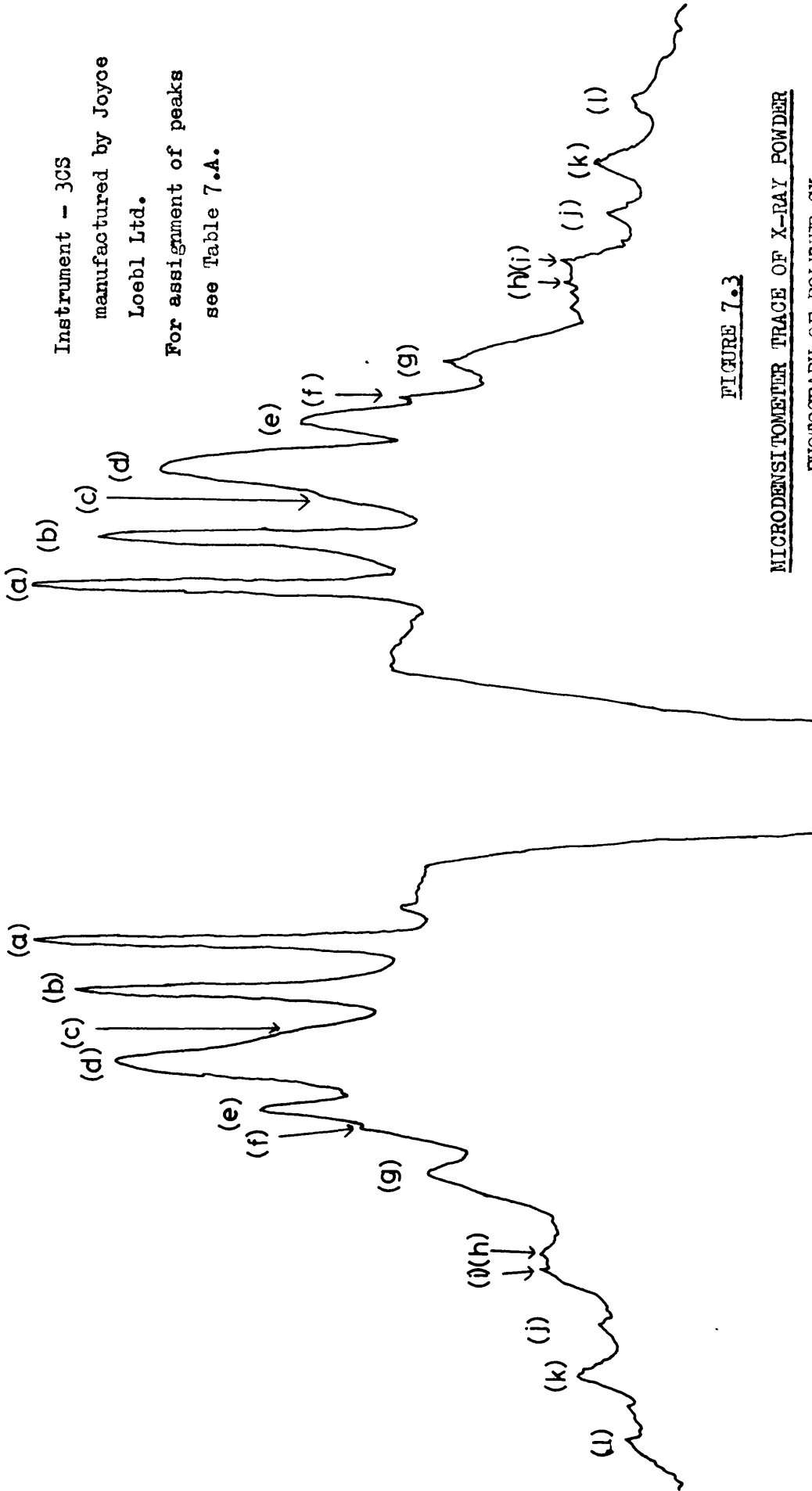


FIGURE 7.3

MICRODENSITOMETER TRACE OF X-RAY POWDER
PHOTOGRAPH OF POLYMER SX

TABLE 7.AX-RAY DATA FROM THE POWDER PHOTOGRAPH OF
POLYMER SAMPLE SX

Ref.	d spacing $\overset{\circ}{\text{A}}$	Intensity
(a)	6.56	Strong
(b)	5.23	Strong
(c)	4.49	Weak
(d)	3.97	Medium
(e)	3.47	Medium
(f)	3.28	Weak
(g)	2.95	Weak
(h)	2.51	Weak
(i)	2.37	Weak
(j)	2.16	Weak
(k)	1.99	Weak
(l)	1.81	Weak

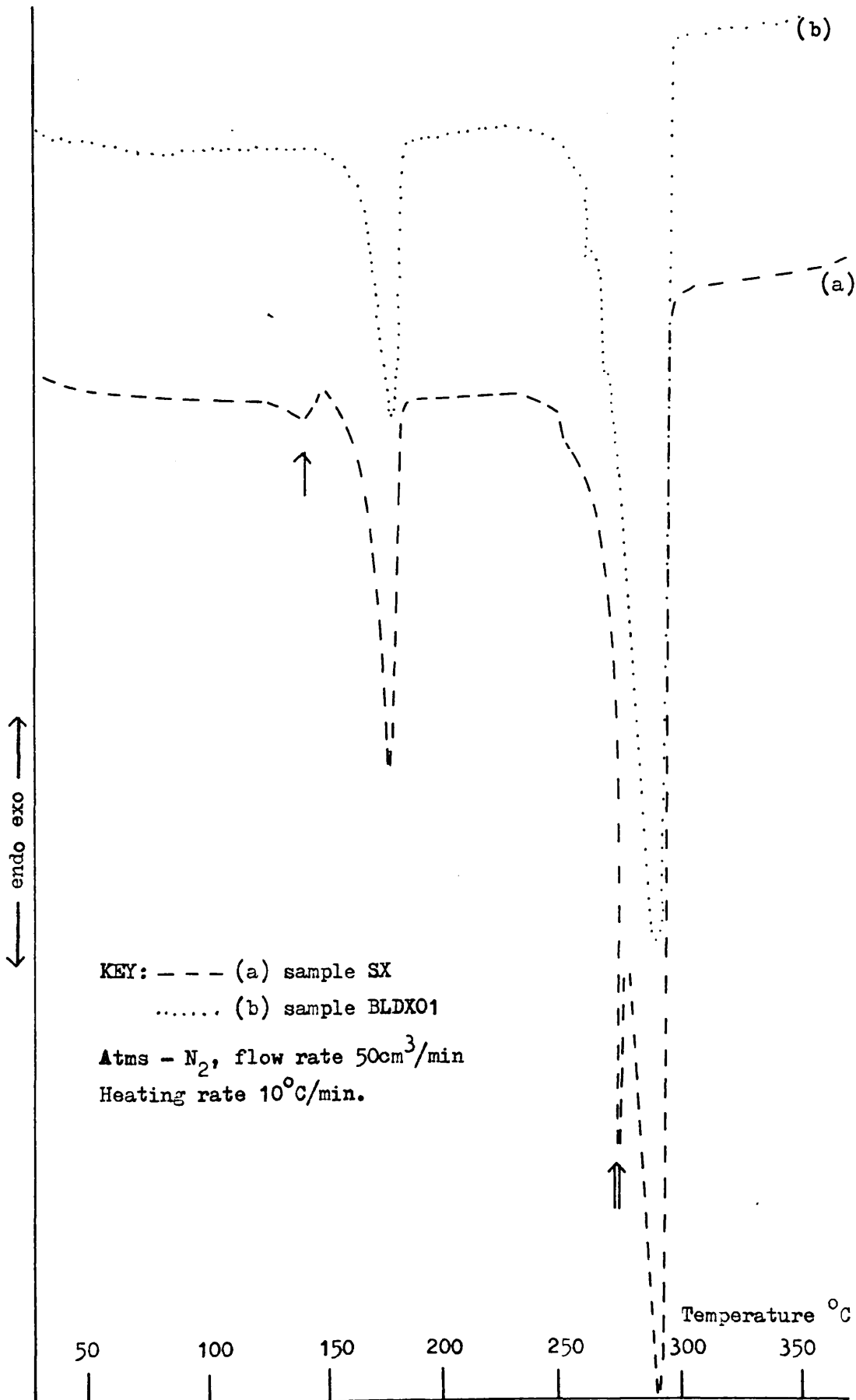


FIGURE 7.4

DSC TRACE OF SX AND BLDX01

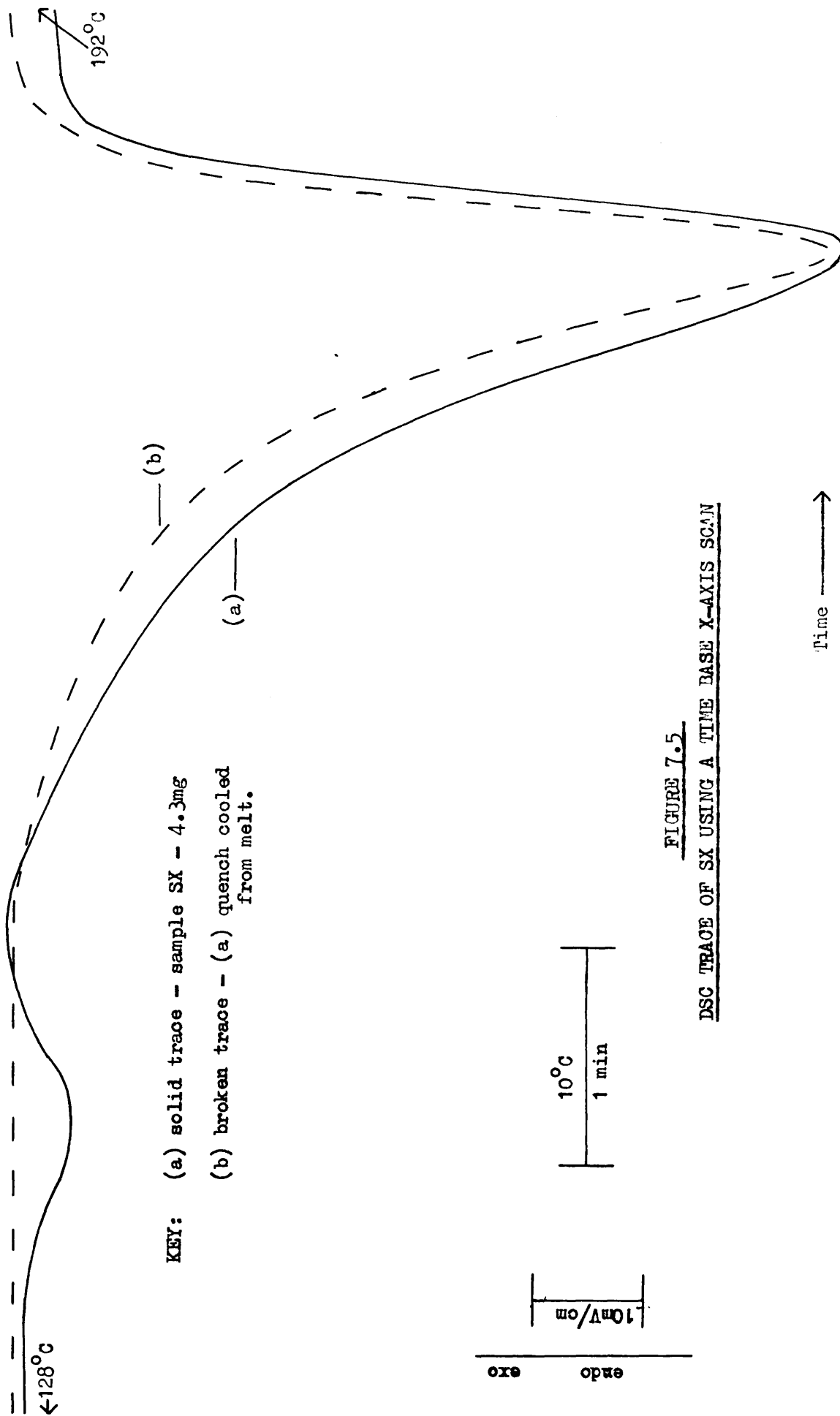


FIGURE 7.5
DSC TRACE OF SX USING A TIME BASE X-AXIS SCAN

The complete lack of an endotherm at 140°C on the second scan implies that the crystallite structure giving rise to this endotherm did not reform upon quench cooling from a temperature of 180°C although the crystallite structure responsible for the larger endotherm obviously did reform.

There are two possible explanations of these experimental results. One explanation for this endotherm at 140°C is that it may be due to the melting of small crystallites in SX which are absent in BLDX01. Such a double melting endotherm has been observed in the TG traces of some samples of isocyanate crosslinked polyurethanes (Ref. 132). Another explanation is that it may be due to a crystal-crystal interaction in which the crystal form changes from one form (PHB I) to another (PHB II) which then melts near 170°C giving rise to the larger endotherm. On quench cooling only form (PHB II) was formed as was evident from the resultant DSC trace (Figure 7.5(b)). Such a phenomenon has been reported for samples of isotactic polybut-1-ene, crystallised from dilute solution, which on heating transforms from a crystal form designated III to form II which then melts at a temperature some 14°C higher (Ref. 133, 134). On close examination of the DSC traces of SX illustrated in Figures 7.1(a) and 7.4(a) the presence of an exothermic peak at a temperature of 150°C , immediately following the endotherm at 140°C , was observed. Such a phenomenon was also observed for the transformation of polybut-1-ene from form III to form II (Ref. 133). This exotherm is explained in terms of a process in which melting of (PHB I) is followed by recrystallisation to (PHB II). It is thus believed that the latter explanation, involving crystal-crystal interaction, best fits the experimental

DSC results.

The sharp, distinct, reproducible endotherm at 275°C (\uparrow) which is observable in the DSC trace of SX (Figure 7.4), appears only as a small shoulder on the DSC trace of BLDX01. It is thought that this may be due to the esterification reaction, discussed fully in Chapter 6, and subsequent evaporation of the eliminated water. The traces in Figure 7.4 suggest that the esterification reaction is more pronounced in SX than in BLDX01, occurring over a shorter time period. Further evidence of this rests in the number average molecular weight versus time of heating (at 170°C under N_2) relationship for SX and BLDX01, (Figure 7.8), which are discussed in Chapter 7.8.

7.6 THERMOGRAVIMETRIC ANALYSIS

Programmed TG traces of both samples were obtained using a Du Pont 951 thermobalance as outlined in Chapter 2.4(i) and are illustrated in Figure 7.6 (traces (a) and (b)). From the traces it can be seen that 50% weight loss occurs at a temperature 5°C lower for BLDX01 than for SX. This small difference in the TG traces may be due to different densities in the samples (see Chapter 8.2) leading to different rates of heat uptake or, most probably due to the effect of different levels of impurities in the samples.

Isothermal TG analysis similar to that described in Chapter 6.2 was carried out on SX and BLDX01 at a temperature of 170°C under flowing nitrogen. Negligible weight loss was recorded for both samples after heating for 2 hours.

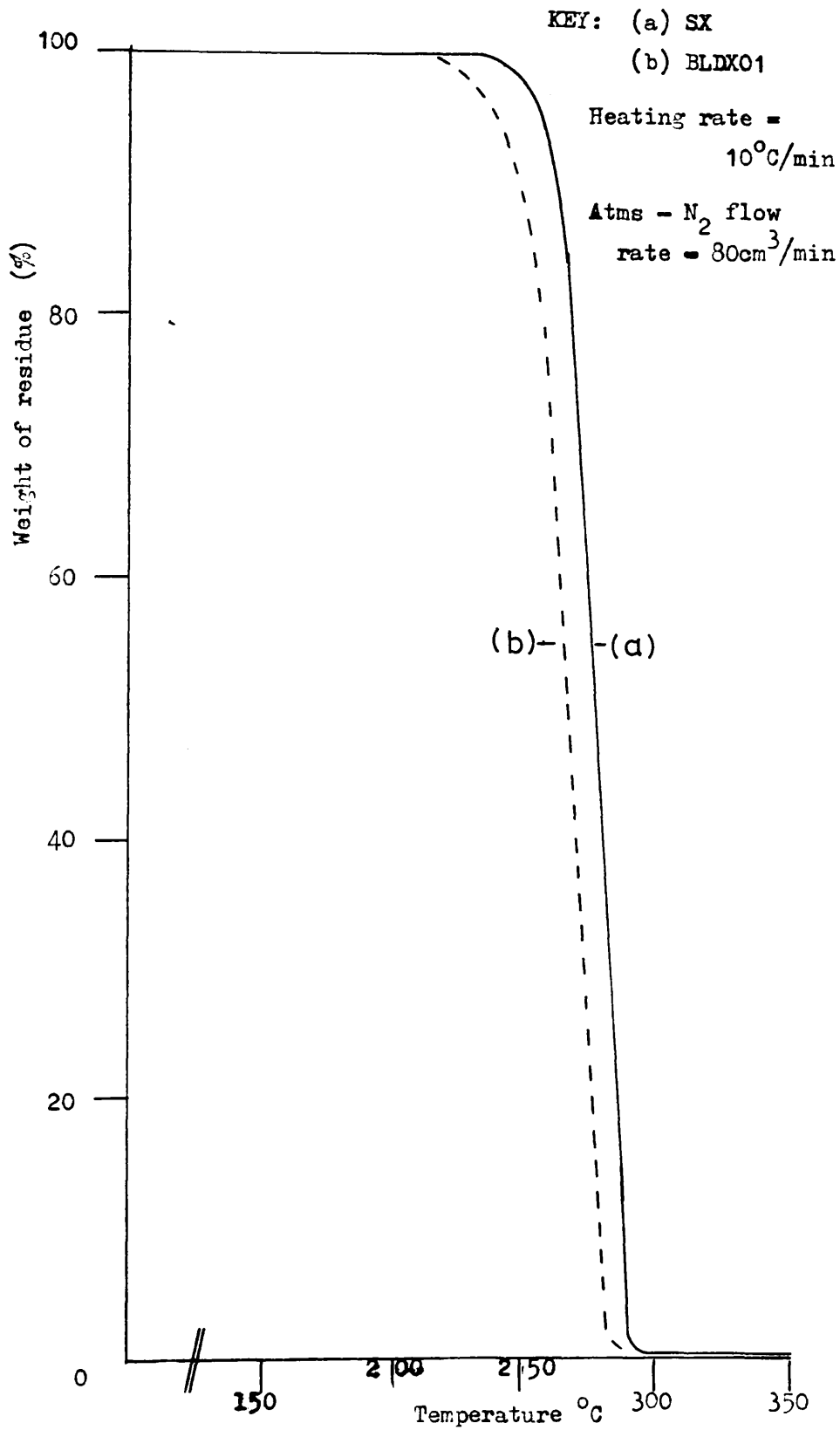


FIGURE 7.6

TG TRACES OF SX AND BLDX01

7.7 TVA WITH DIFFERENTIAL CONDENSATION OF PRODUCTS

TVA with differential condensation of products was carried out on PHB samples SX and BLDX01 using the method described in Chapter 2.4(iv). The resultant traces are illustrated in Figure 7.7. The maximum rate of evolution of volatiles occurs, within experimental error, at the same temperature for both samples (288^oC for BLDX01, 291^oC for SX), the remainder of the trace being virtually identical.

7.8 EFFECT OF CRYSTALLINITY ON THE RATE OF CHAIN SCISSION

The effect of increased crystallinity between BLDX01 and SX on the rate of chain scission was investigated at temperatures below the melting point of either sample.

The changes in molecular weight during isothermal heating of polymers SX and BLDX01 at 170^oC under nitrogen were investigated by the method outlined in Chapter 2.9(ii). Plots of number average molecular weight (\bar{M}_n) versus length of heating, (solid trace), are recorded in Figures 7.8 and 7.9. It is obvious that the effect of the esterification reaction, discussed in Chapter 6, is more pronounced in the single crystal mat sample, SX, (Figure 7.8), bringing about an overall 43.3% increase from the original value of \bar{M}_n after 5 minutes heating. By applying Equation 6.1 to the data of Figures 7.8 and 7.9 it was possible to replot, on the same diagrams (broken traces), the effect on \bar{M}_n of the depolymerisation reaction had no esterification occurred. Using this amended data plots of $\frac{1}{CL_t} - \frac{1}{CL_o}$ versus time of heating, were drawn as in Figure 7.10.

Least squares fits on the data of Figure 7.10 gave the following

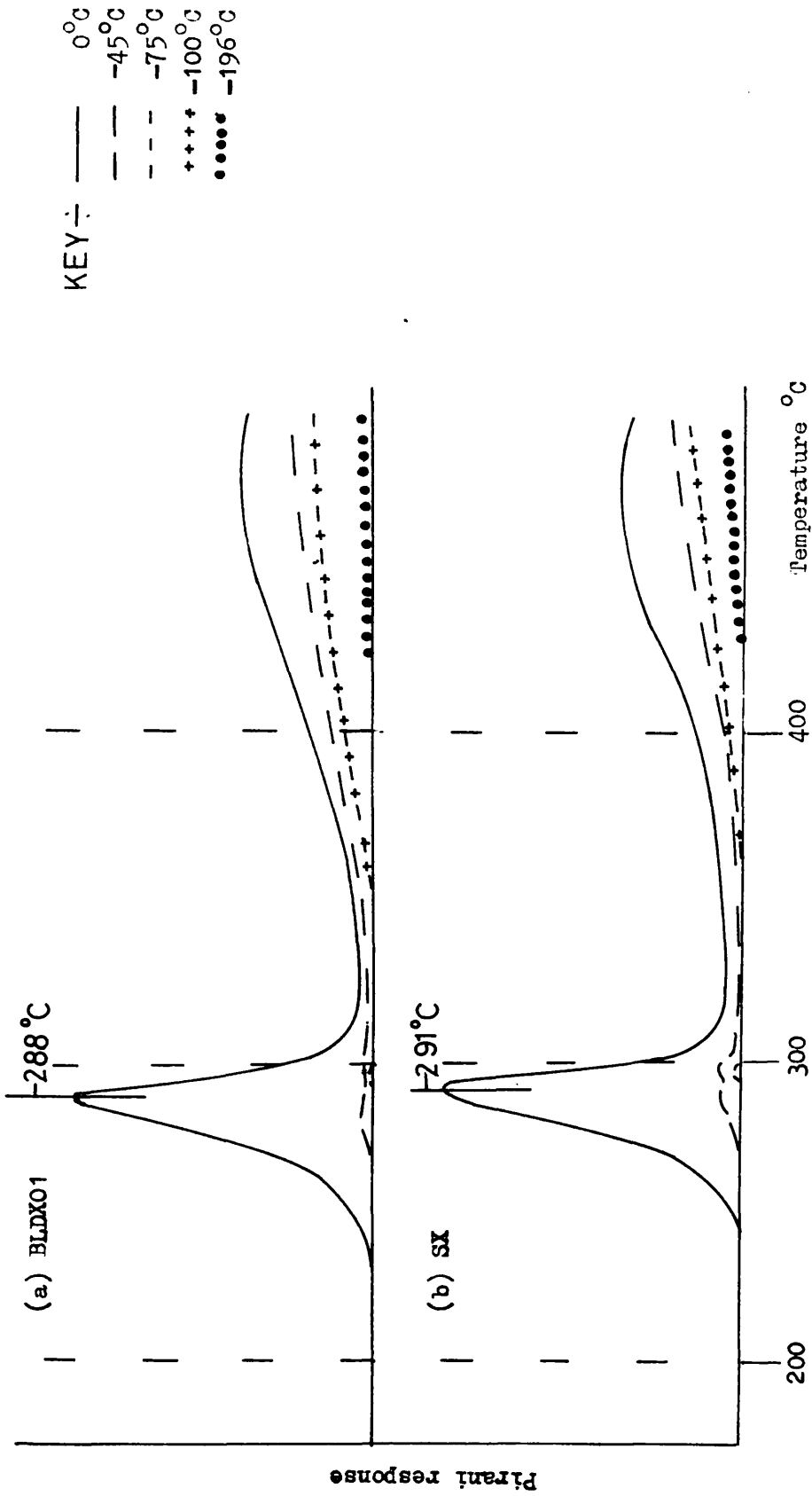


FIGURE 7.7
TVA WITH DIFFERENTIAL CONDENSATION OF PRODUCTS OF SAMPLES BLDX01 AND SX

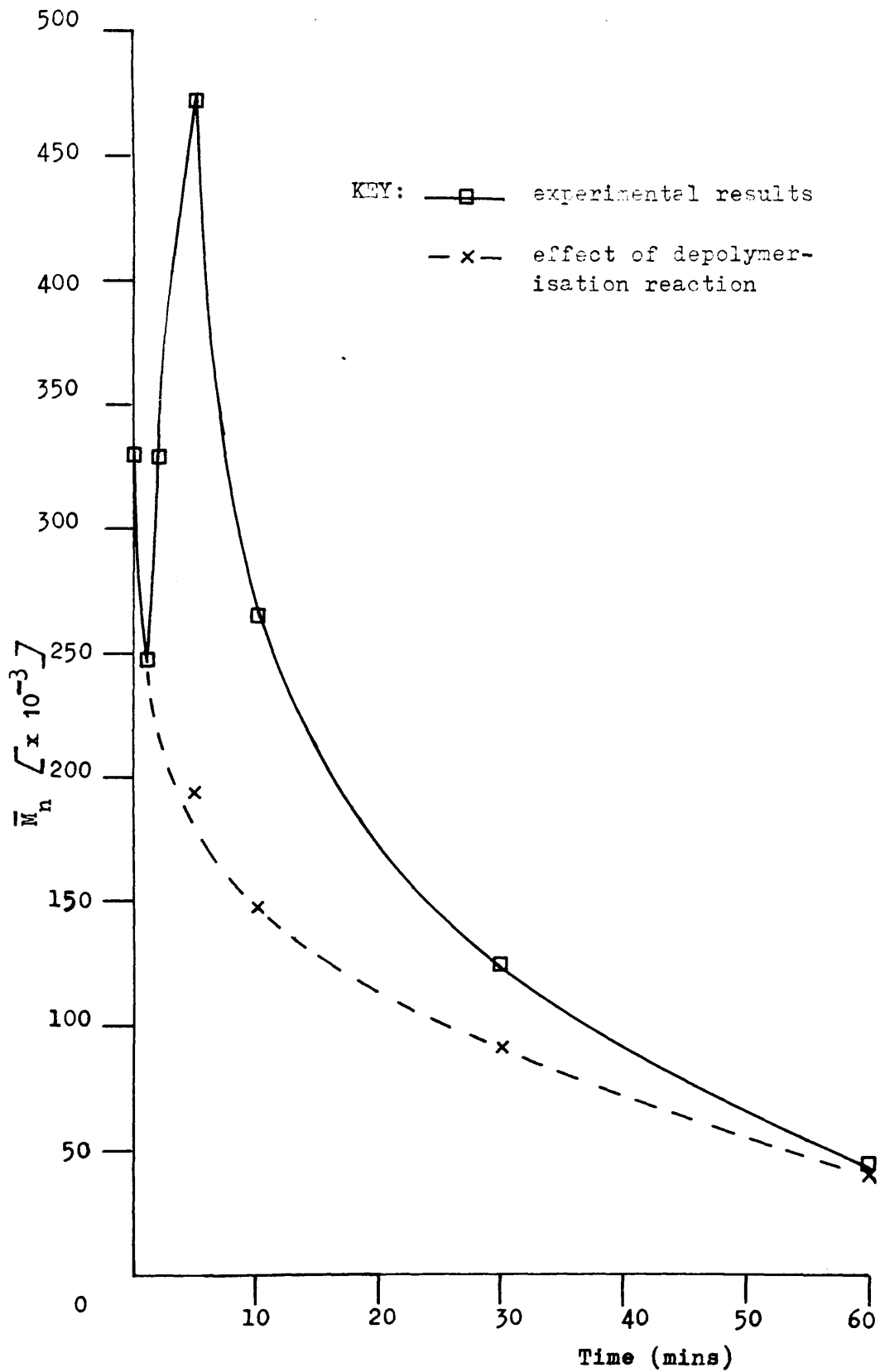


FIGURE 7.8

**CHANGES IN MOLECULAR WEIGHT (\bar{M}_n) WITH TIME
OF HEATING OF SX AT 170°C UNDER NITROGEN**

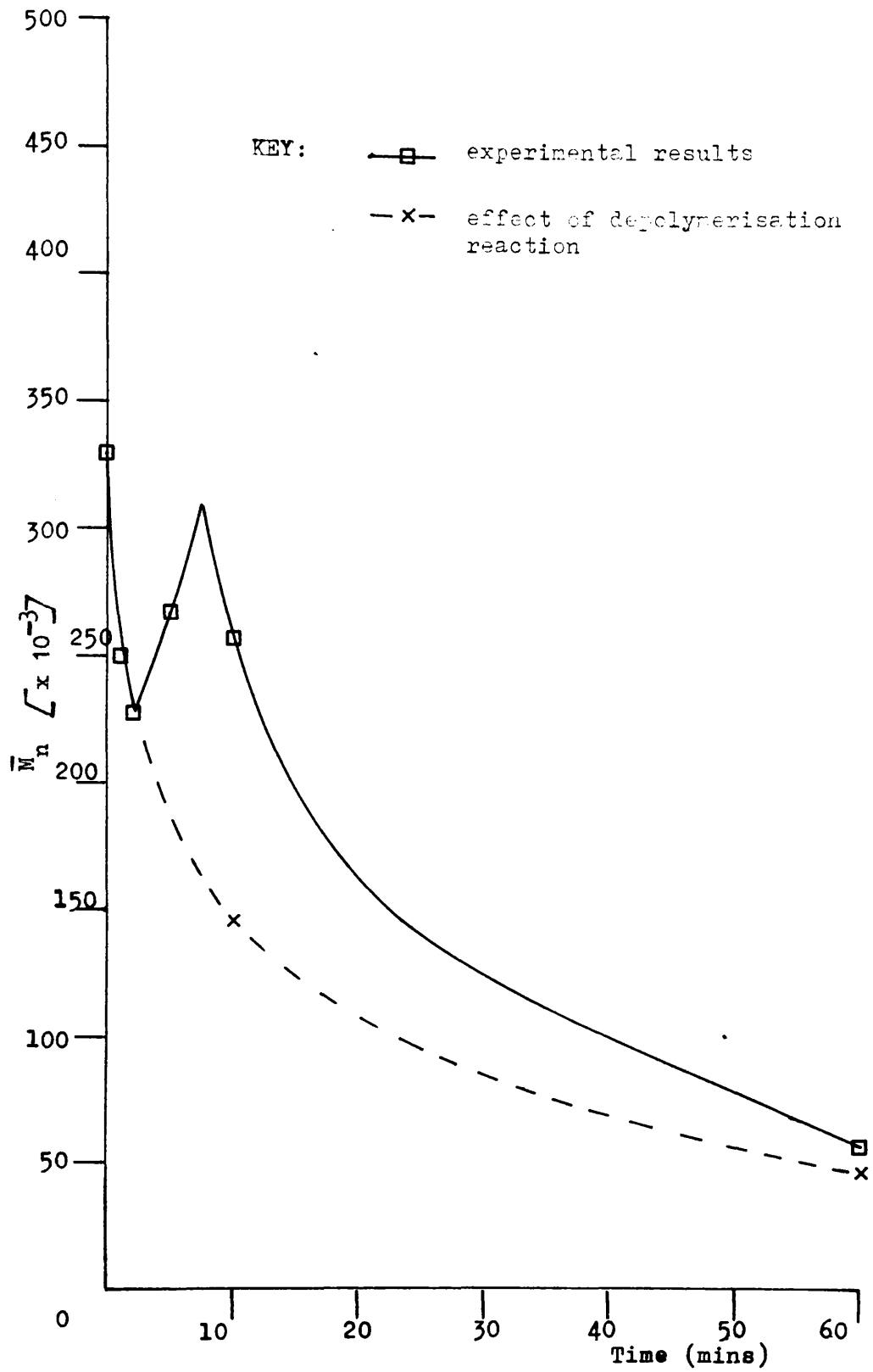


FIGURE 7.9

CHANGES IN MOLECULAR WEIGHT (\bar{M}_n) WITH TIME
OF HEATING OF BLDX01 AT 170°C UNDER NITROGEN

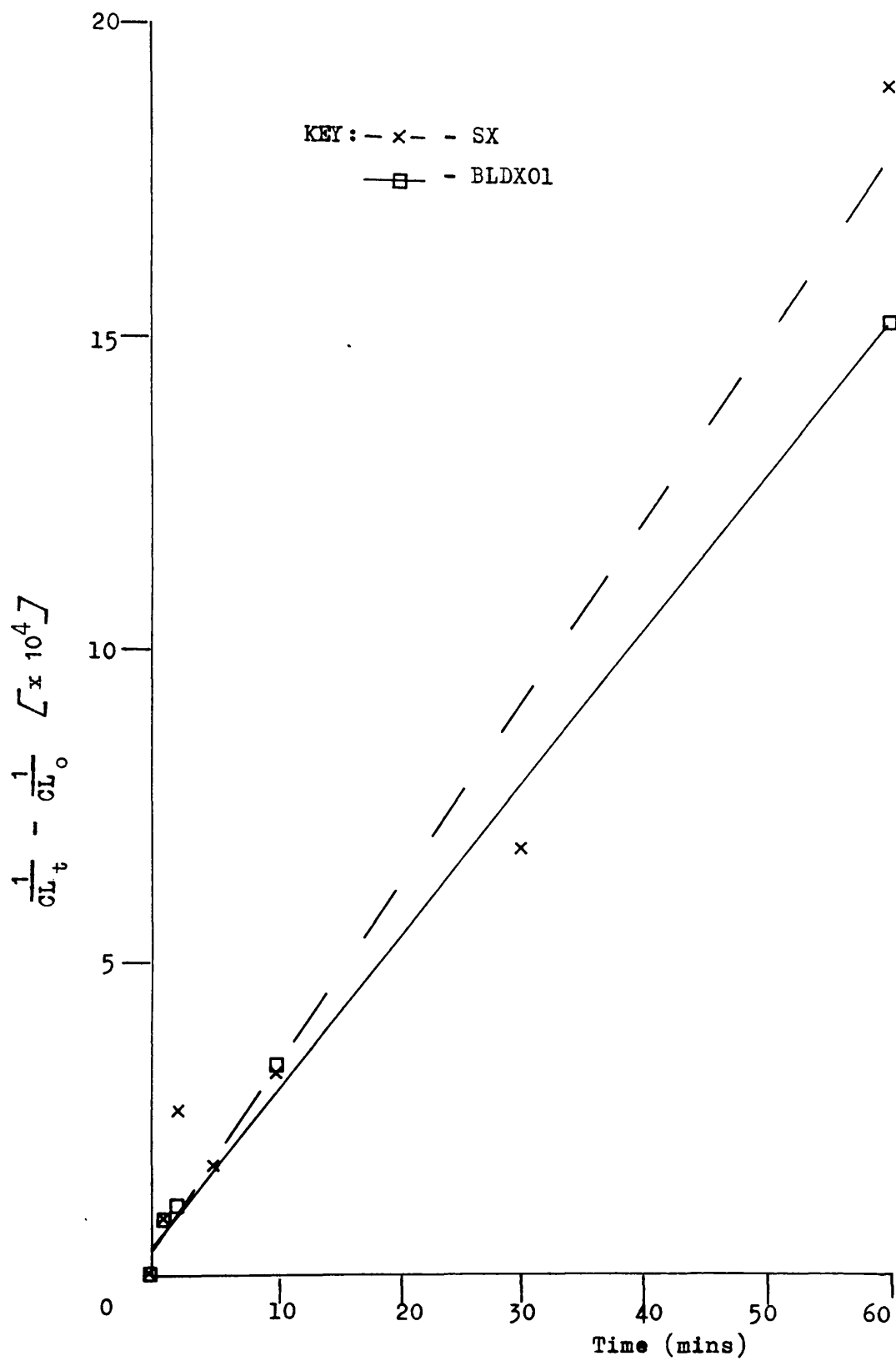


FIGURE 7.10

$\frac{1}{CL_t} - \frac{1}{CL_0}$ VERSUS TIME OF HEATING FOR SX AND BLDX01 AT 170°C UNDER NITROGEN

values of rate of chain scission.

$$\begin{array}{l} \text{Rate of chain} \\ \text{scission (SX)} \end{array} = (4.87 \pm 0.5) \times 10^{-7} \text{ scissions/monomer unit/sec}$$

$$\begin{array}{l} \text{Rate of Chain} \\ \text{scission (BLDX01)} \end{array} = (4.11 \pm 0.1) \times 10^{-7} \text{ scissions/monomer unit/sec}$$

(see Chapter 2.8 for method of error calculation)

A similar study was carried out under static air, by the method outlined in Chapter 2.9(iii). The resultant traces of \bar{M}_n versus time of heating (solid trace) are illustrated in Figures 7.11 and 7.12. This data was replotted, (broken trace), by applying Equation 6.1 to show the effect on \bar{M}_n if only the depolymerisation reaction had occurred. Using this amended data a graph of $\frac{1}{\bar{M}_t} - \frac{1}{\bar{M}_0}$ versus time of heating was plotted for each sample, Figure 7.13, from which values for the rates of scission were calculated by the method of least squares. The following values were obtained,

$$\begin{array}{l} \text{Rate of chain} \\ \text{scission (SX)} \end{array} = (3.09 \pm 0.3) \times 10^{-7} \text{ scissions/monomer unit/sec}$$

$$\begin{array}{l} \text{Rate of chain} \\ \text{scission (BLDX01)} \end{array} = (3.80 \pm 0.3) \times 10^{-7} \text{ scissions/monomer unit/sec}$$

These two sets of results above show that there is no significant difference between the rates of depolymerisation of SX and of BLDX01 at 170°C.

The changes which occur in the molecular weight of SX during isothermal heating at a temperature of 170°C under vacuum were investigated by the method described in Chapter 2.9(i). The results obtained were treated, as for the cases under nitrogen

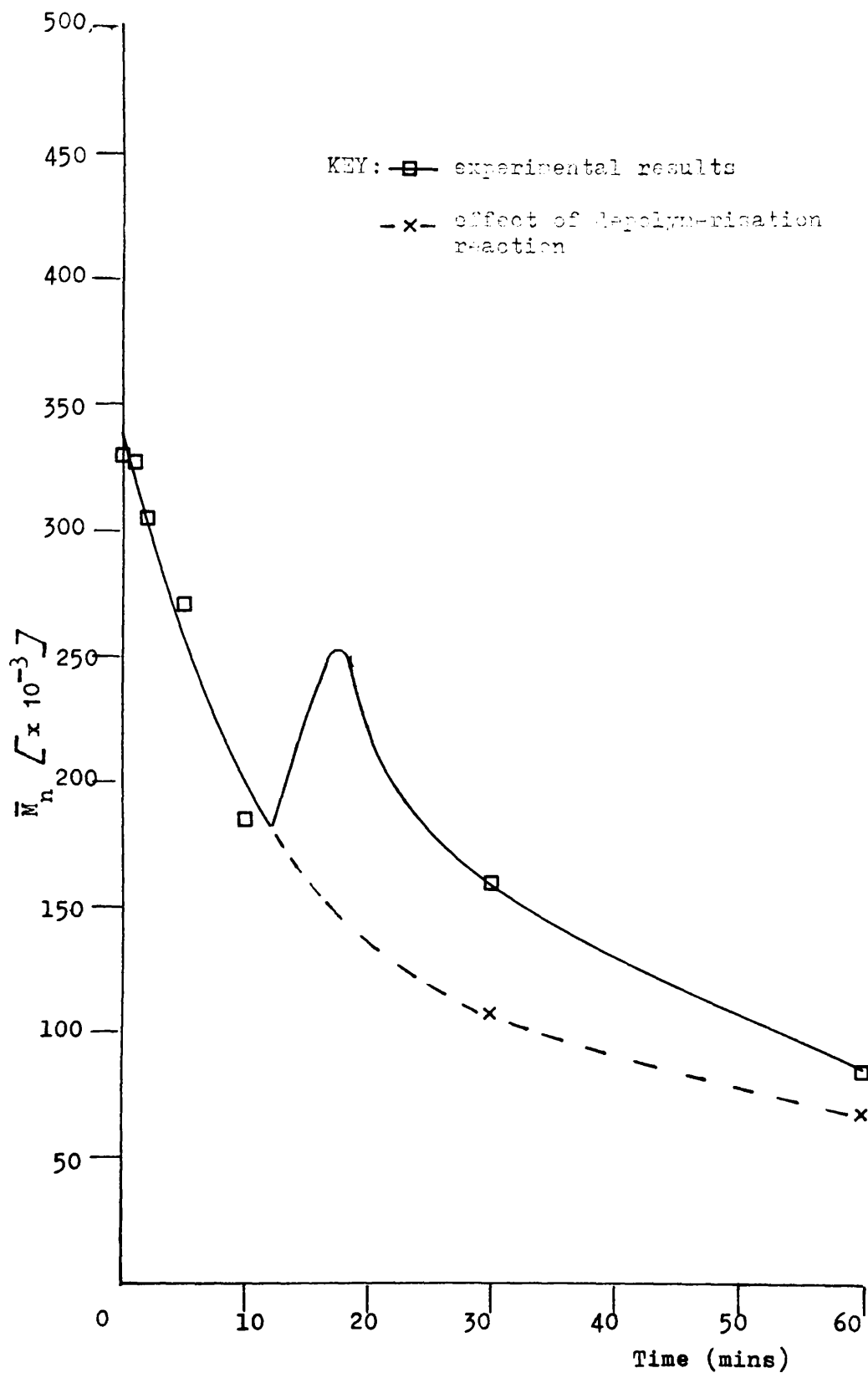


FIGURE 7.11

**CHANGES IN MOLECULAR WEIGHT (\bar{M}_n) WITH TIME OF
HEATING OF SX AT 170°C UNDER STATIC AIR**

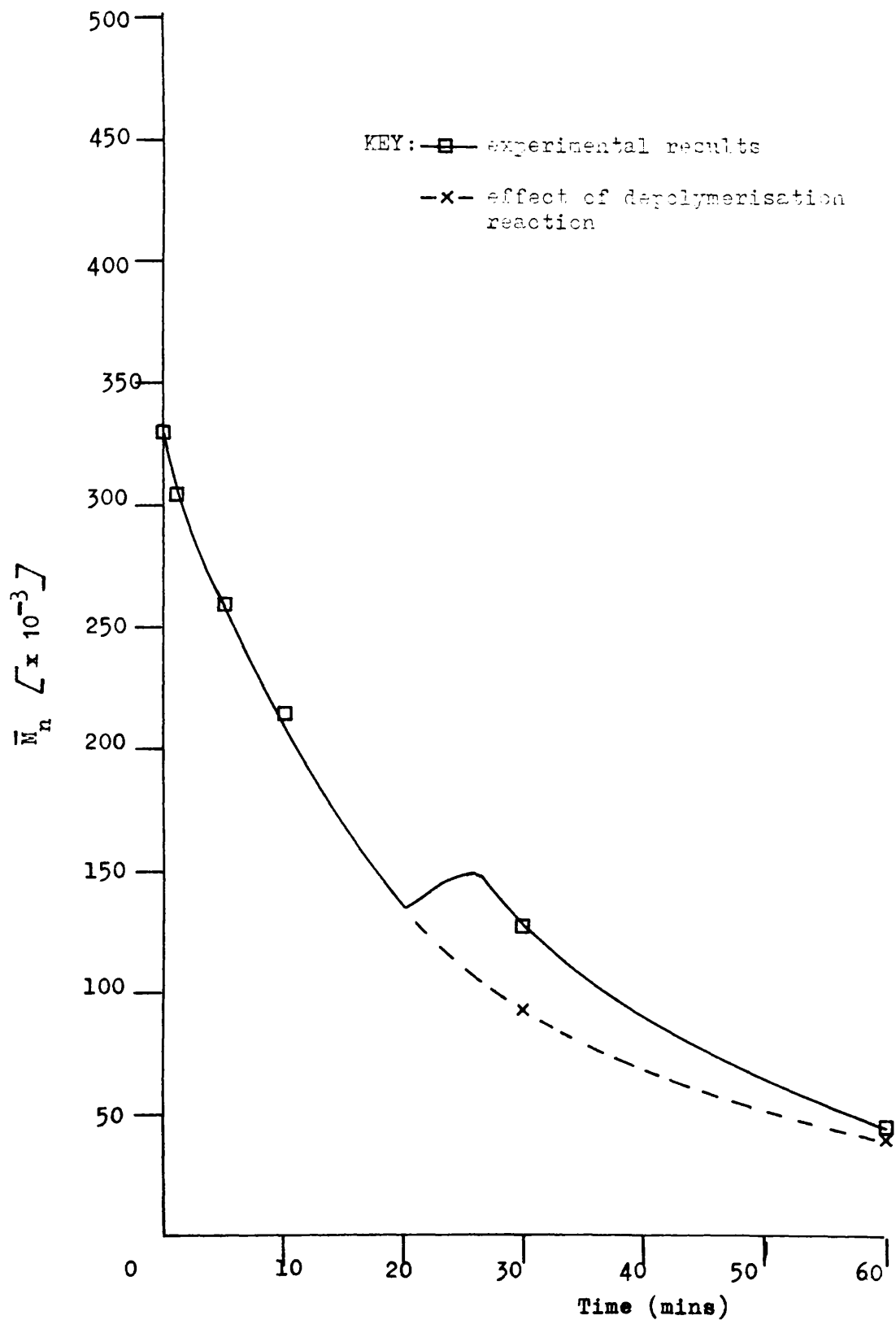


FIGURE 7.12

CHANGES IN MOLECULAR WEIGHT (\bar{M}_n) WITH TIME OF HEATING OF BLDX01 AT 170°C UNDER STATIC AIR

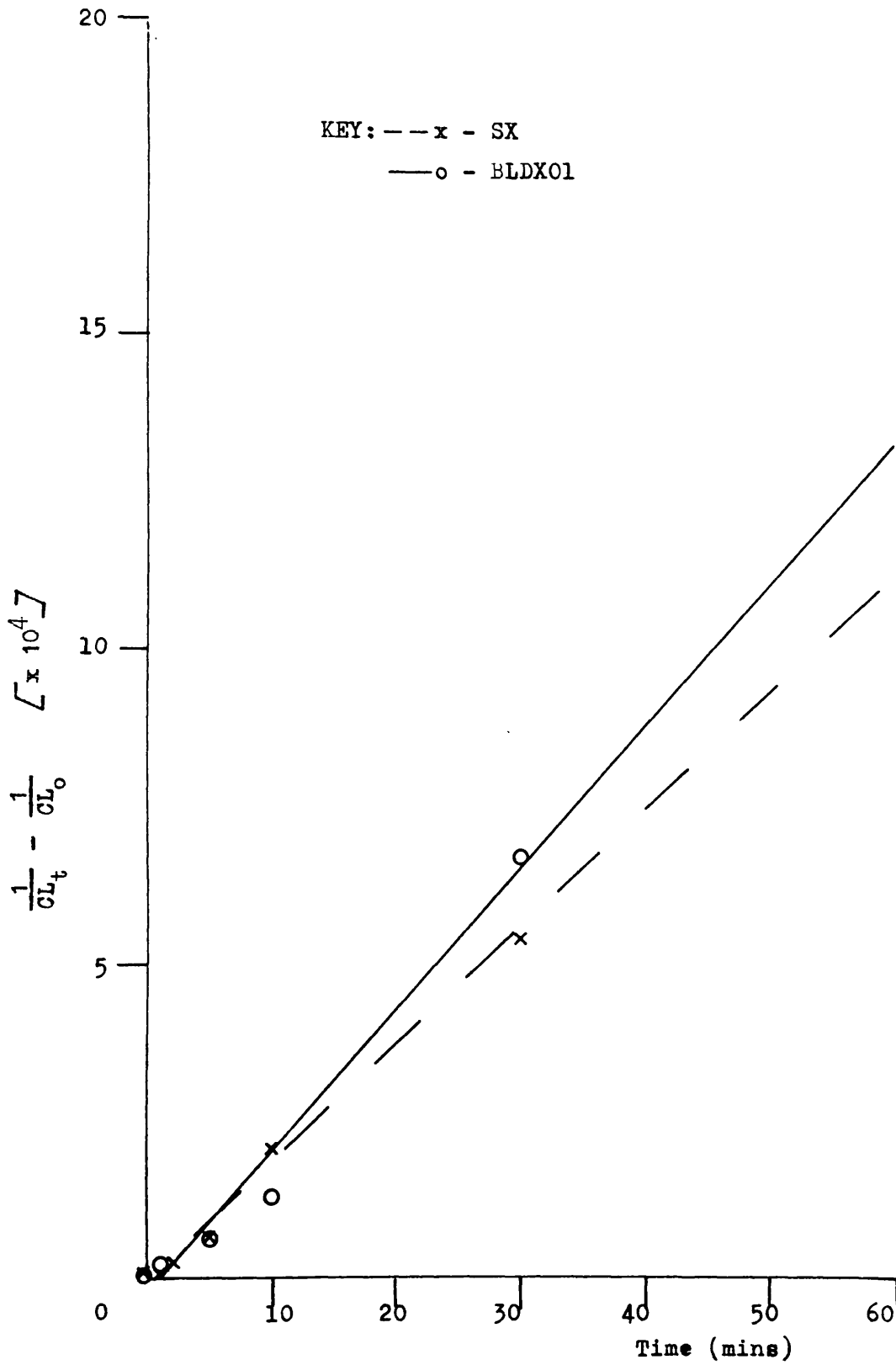


FIGURE 7.13

$\frac{1}{CL_t} - \frac{1}{CL_0}$ VERSUS TIME OF HEATING FOR SX AND BLDX01
AT 170°C UNDER STATIC AIR

and static air above, and gave rise to the curves, Figures 7.14 and 7.15. By a least squares fit on the data of Figure 7.15 the following value for the rate of the depolymerisation reaction was obtained,

$$\text{Rate of chain scission (SX)} = (3.01 \pm 0.5) \times 10^{-7} \text{ scissions/monomer unit/sec}$$

A plot of \bar{M}_w versus time of heating for each of the experiments above is shown in Figure 7.16.

7.9 DISCUSSION AND CONCLUSIONS

It has been shown that there was no significant difference in the rates of the depolymerisation reaction of SX and BLDX01 at 170°C under atmospheres of nitrogen and static air. Therefore increasing the crystallinity of a sample of PHB above that which occurs during rapid precipitation of polymer from solution has no effect on the thermal stability of PHB, as far as the rate of depolymerisation is concerned. The only benefit is the apparent increased tendency for esterification under a nitrogen atmosphere which was reported in Chapter 7.7. This effect suggests a possible pretreatment for PHB to raise the molecular weight prior to processing. Should the endotherm observed at 140°C in the DSC of SX be due to the transformation of one crystal form to another, then the former will have no effect on stability, since it changes to the latter at a temperature where no appreciable degradation occurs on prolonged heating. (PHB has been shown to be thermally stable at 150°C (Ref. 135)).

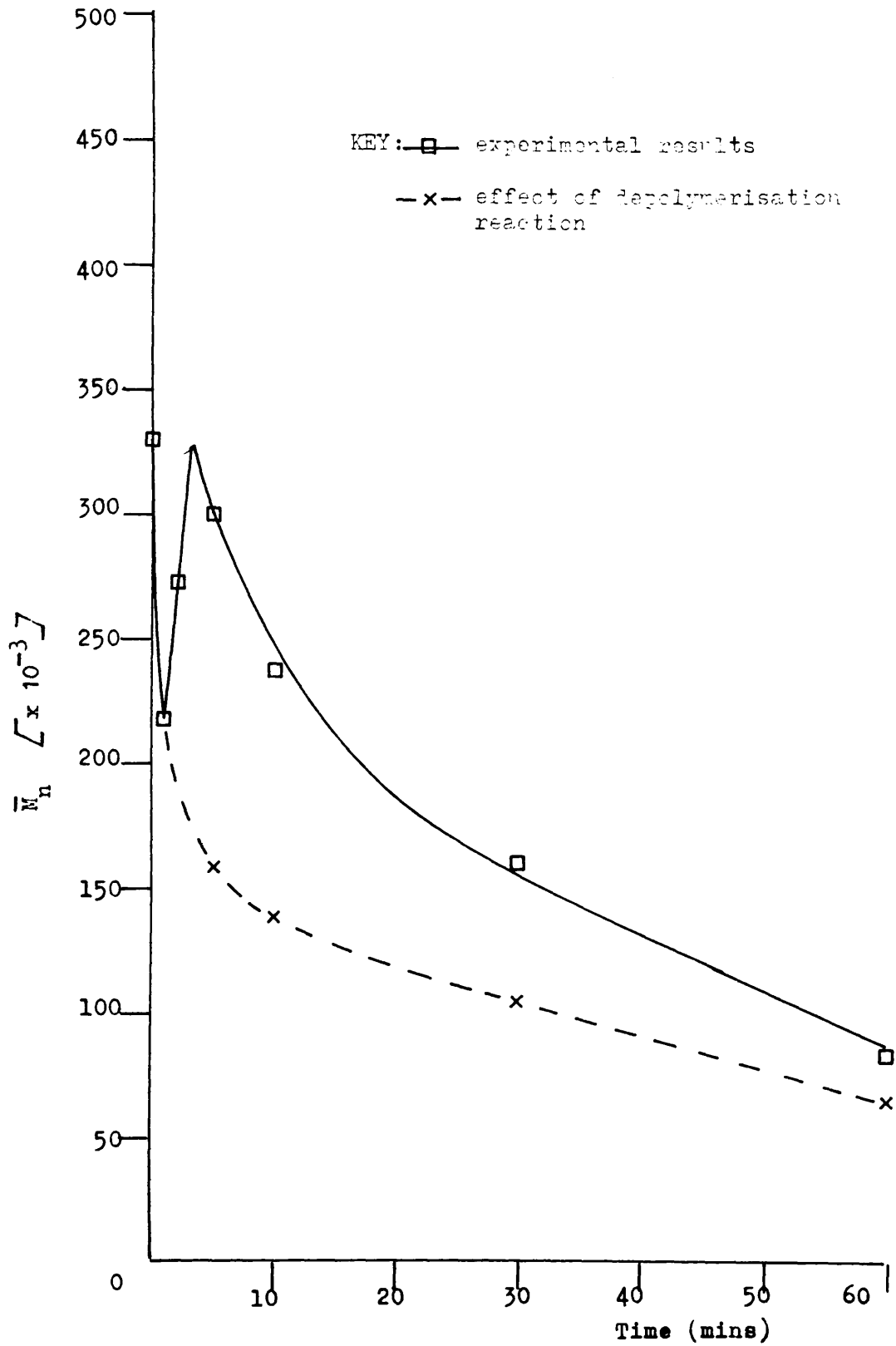


FIGURE 7.14

CHANGES IN MOLECULAR WEIGHT (\bar{M}_n) WITH TIME OF HEATING OF SX at 170°C UNDER VACUUM

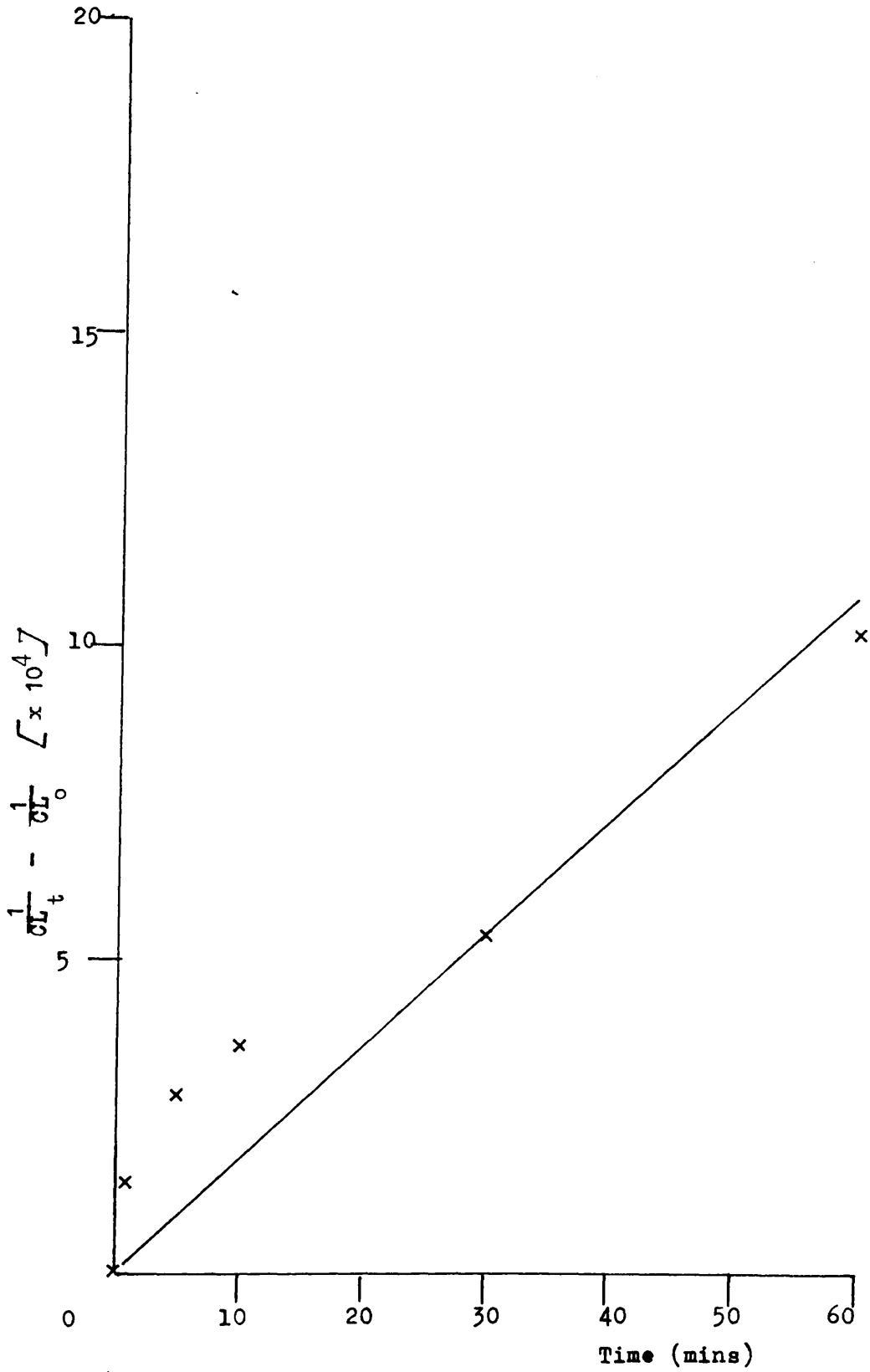


FIGURE 7.15

$\frac{1}{CL_t} - \frac{1}{CL_0}$ VERSUS TIME OF HEATING FOR SX AT 170°C
UNDER VACUUM

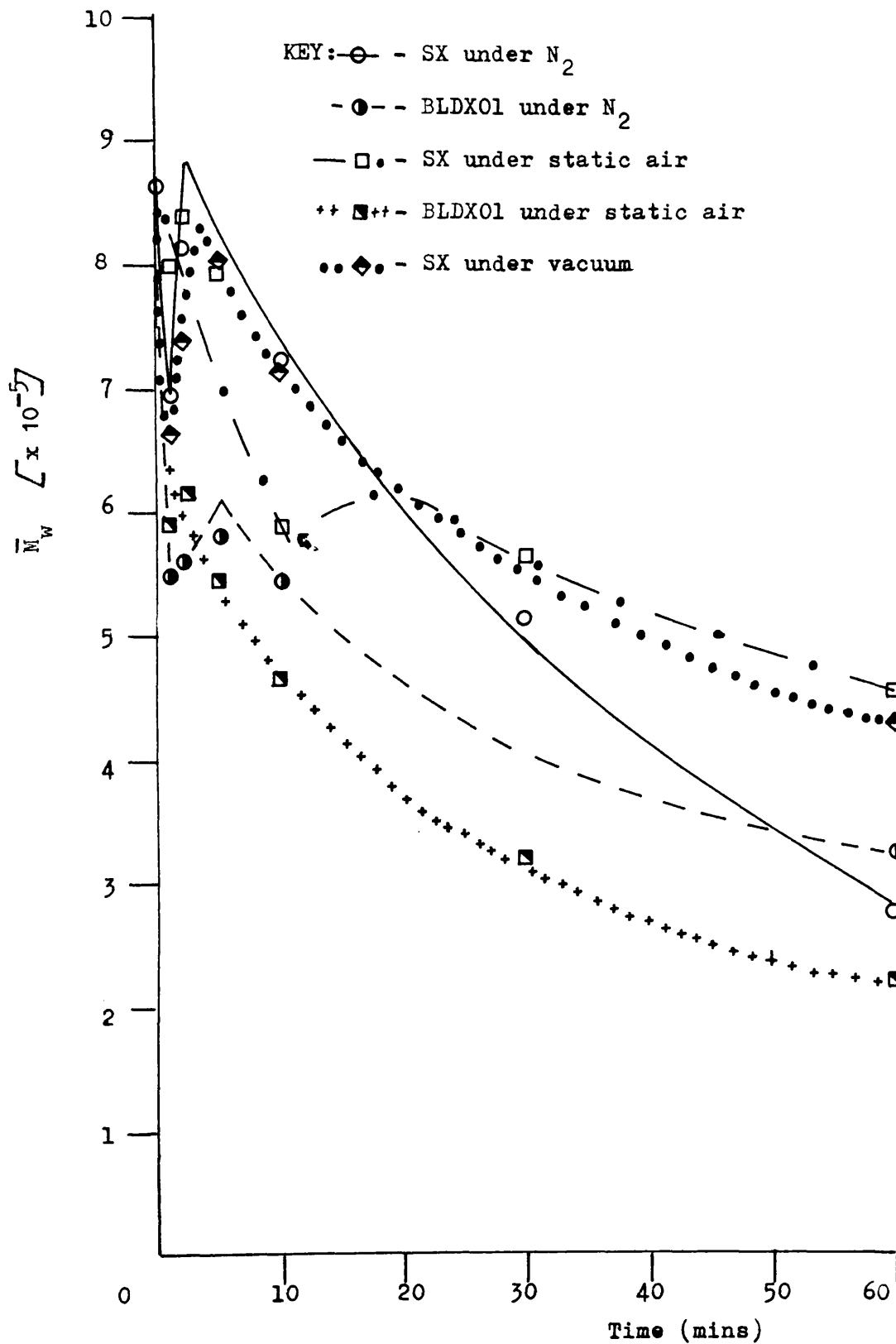


FIGURE 7.16
CHANGES IN \bar{M}_w WITH TIME OF HEATING OF PHB
AT 170°C

The results obtained for the rates of the depolymerisation reaction of SX at 170°C under the three atmospheres have the same value within experimental error. This confirms the results of Chapter 6, where no relationship between atmosphere and rate of degradation was observed.

CHAPTER 8

EFFECT OF INITIAL MOLECULAR WEIGHT ON STABILITY

8.1 INTRODUCTION

In order to investigate the dependence of thermal stability on this initial degree of polymerisation, polymer S1 (See Chapter 2.11) was fractionated, by the method described in Chapter 2.3, giving four fractions with a range of molecular weights, denoted by F1, F2, F3, and F4, in order of decreasing \bar{M}_n . These four fractions, and their precursor S1 were characterised by GPC and trace impurity analysis, the results being recorded in Chapter 2.11. The sources and effects on stability of impurities present in the polymer sample were discussed in Chapter 1.3.

8.2 DIFFERENTIAL SCANNING CALORIMETRY

The DSC traces of the five polymer samples, obtained as described in Chapter 2.4(iii), are illustrated in Figure 8.1. No significant difference was noted in the positions of the degradation endotherms in the five traces but, as expected, the melting endotherms of sample F4 occurred at a lower temperature than that of F1. In each trace small shoulders can be observed in the region of 250°C to 290°C which are thought to be the effects of the esterification reaction (Chapter 6) and the subsequent evaporation of eliminated water. The exact position of these shoulders will depend upon such things as density of the polymer sample, effecting the rate of heat transfer to the polymer and the level of impurities within the sample. These shoulders will be more pronounced the shorter the time interval during which all the hydroxyl chain ends react in

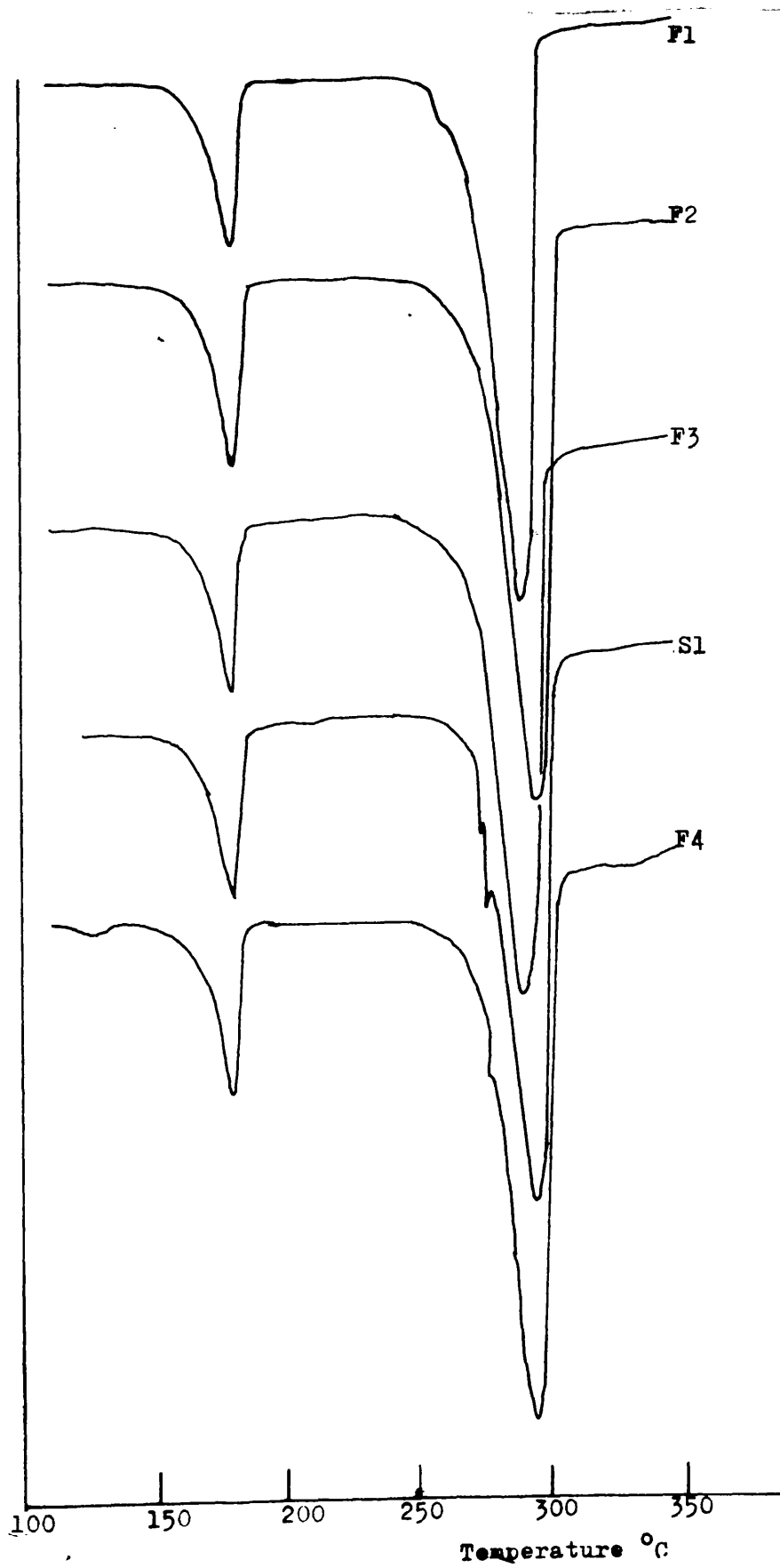


FIGURE 8.1
DSC TRACES OF VARIOUS SAMPLES OF PHB
($10^{\circ}\text{C min}^{-1}$, N_2 $50\text{cm}^3 \text{min}^{-1}$)

the esterification reaction.

The DSC trace of F4 shows a small endotherm at 125°C, 42°C lower than its melting endotherm, similar to that reported in the DSC trace of SX. Possible explanations for this phenomenon have been discussed in Chapter 7.5. Other similarities between F4 and SX were observed: (a) both had a "glassy" appearance and, (b) both SX and F4 were notably denser than any of the other samples listed in Table 2.B, Chapter 2.11. This suggested that F4 was highly crystalline like SX. To test whether this was so, the crystallinities of samples F1 to F4 and S1 were measured by the method outlined in Chapter 7.3, the results being recorded in Table 8.A. From these results it was observed that F4 was notably more crystalline than F1 to F3 and S1.

8.3 THERMAL GRAVIMETRIC ANALYSIS

The traces from programmed TG analyses of samples F1-F4, SX and S1, obtained by the method described in Chapter 2.4(i), are illustrated in Figure 8.2 and the results summarised in Table 8.B. No clear relationship between initial molecular weight and stability was observed. The differences in the traces are probably due to a combination of experimental error and complicated impurity effects.

Isothermal TG analysis, at a temperature of 200°C under nitrogen, was carried out as described in Chapter 2.4(i), on the six polymer samples listed above. The resultant traces are illustrated in Figure 8.3. Again no apparent order was observed in the traces.

A random chain scission mechanism with short zip length was proposed in Chapter 6 for the degradation of PHB. With such a mechanism, the rate of weight loss should be independent of the

TABLE 8.ACRYSTALLINITY OF VARIOUS SAMPLES OF PHB

Polymer Sample	Hfus ^(a) J/g	% Crystallinity ^(b)
SX	107.4	100
F1	87.4	81.4
F2	85.7	79.8
F3	90.5	84.3
F4	102.3	94.8
S1	88.4	82.3

(a) measured by DSC

(b) relative to that in SX

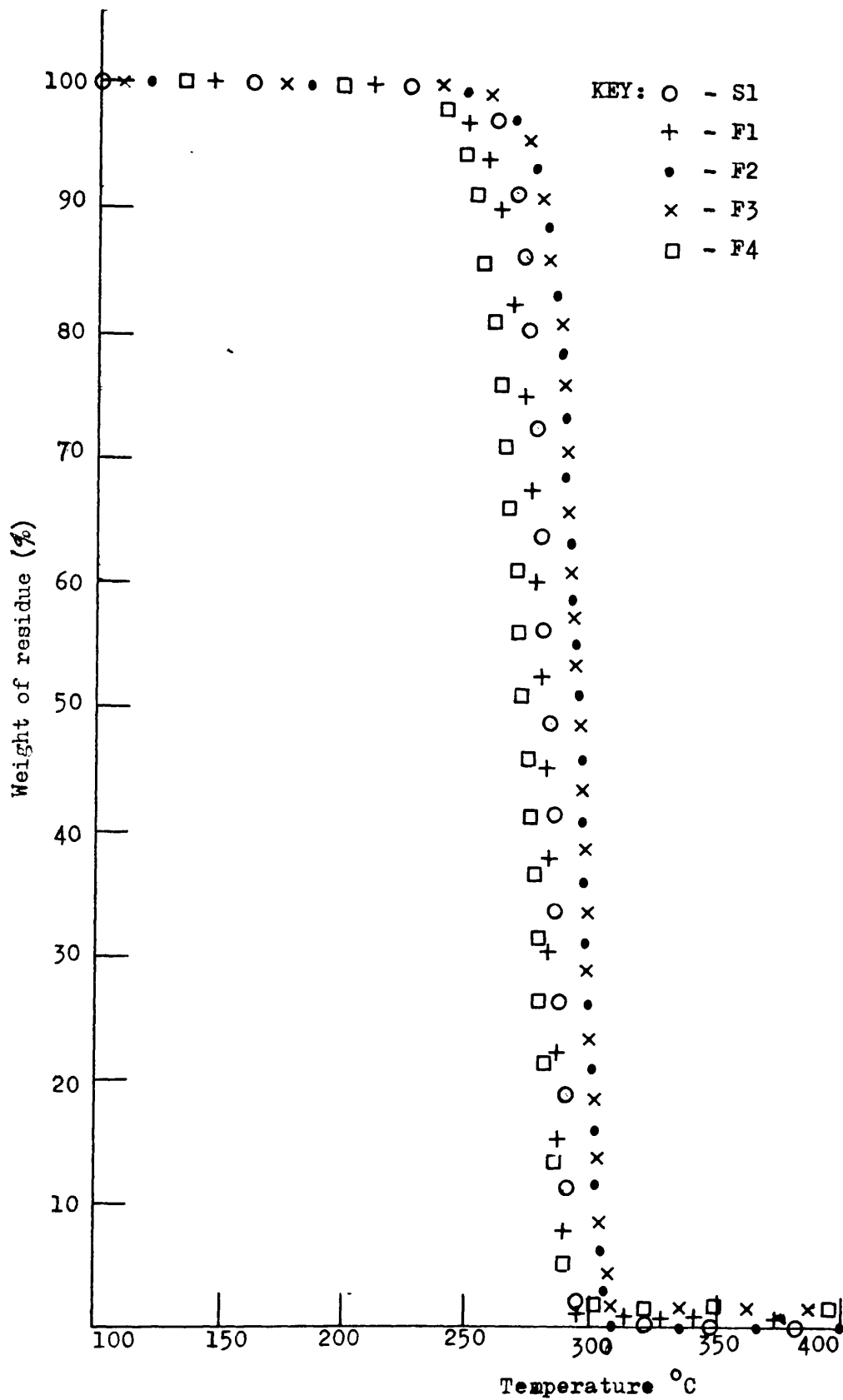


FIGURE 8.2

TG TRACES OF VARIOUS PHB SAMPLES

(heating rate $10^{\circ}\text{C}/\text{min}$, under a flow of $50\text{cm}^3/\text{min}$ of N_2)

TABLE 8.B

RESULTS OF A PROGRAMMED TG ANALYSIS OF VARIOUS SAMPLES OF PHB(10°C min⁻¹, 50cm³ min⁻¹ H₂ flow)

Polymer Sample (Listed in order of decreasing \bar{M}_n)	Temperature of onset of weight loss °C	Temperature at which 50% weight loss recorded °C	Temperature at which weight loss terminated °C	Weight of Residue (% of original weight)
F1	228	281	299	0.5
F2	242	293	310	0.5
F3	240	295	309	1.6
S1	248	285	298	0
SX	235	281	309	1.5
F4	230	275	297	1.0

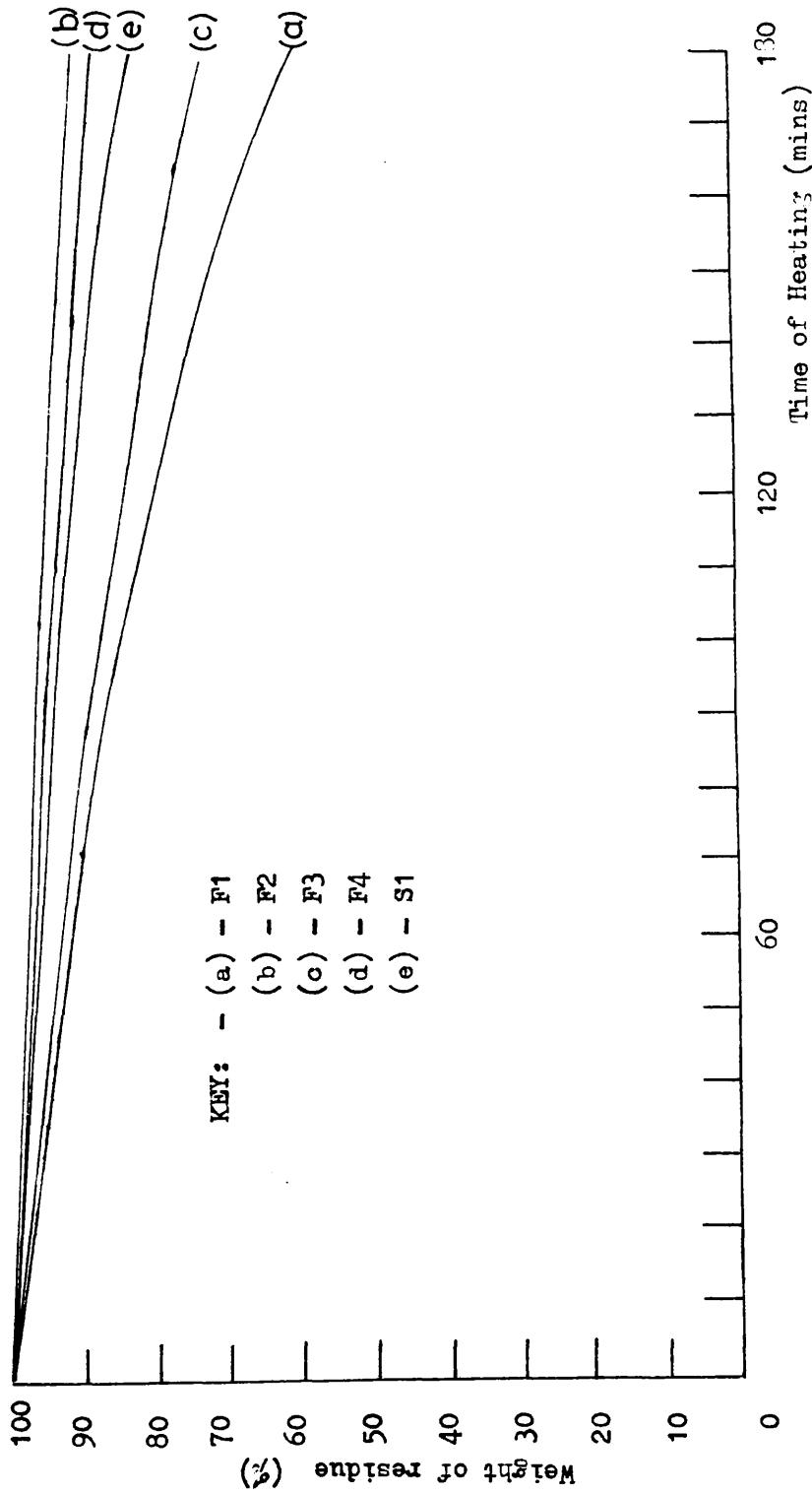


FIGURE 8.3
ISOTHERMAL TG TRACES, AT 200°C OF VARIOUS FIB SAMPLES UNDER NITROGEN

initial degree of polymerisation and this is demonstrated by the data in Figure 8.3.

The variation in stability between the samples must be due to a combination of experimental error and the effects of impurities on the stability of the polymer (see Chapter 1.3).

8.4 THERMAL VOLATILISATION ANALYSIS

Thermal volatilisation analyses of polymer samples F1 to F4 were carried out, as described in Chapter 2.4(iv) in order to investigate the relationship between initial degree of polymerisation and the temperature at which the maximum evolution of volatiles is recorded. The TVA traces obtained were similar to the one illustrated in Figure 3.4 and the results are tabulated in Table 8.C. It can be seen that the polymer samples gave identical traces within experimental accuracy.

8.5 QUANTITATIVE ANALYSIS OF PRODUCTS

In Chapter 5 the products of thermal degradation of polymer S1, under vacuum and nitrogen, were investigated quantitatively. In this section, the results from a similar study carried out on polymers F1, BLDX01 and F4 are reported, and a comparison made between the results obtained and those of polymer S1. A detailed characterisation of these four polymers is recorded in Chapter 2.11. The experimental methods by which the quantitative analysis of the degradation products were obtained are described fully in Chapter 5.2.

The results of a quantitative analysis of the products formed on heating polymers F1, BLDX01 and F4 under TVA conditions to 500°C, along with those of S1, are recorded in Tables 8.D, 8.E and 8.F. The results quoted are averages over four experiments.

TABLE 8.C
RESULTS OF TVA ON POLYMERS P1 to P4

Polymer Sample	Peak (240°C - 310°C)			Peak (> 310°C)
	Temperature at which volatiles first recorded °C	Temperature of maximum evolution of volatiles °C	Temperature of termination of °C	
F1	242	298	305	467
F2	247	296	306	467
F3	246	301	310	473
S1	246	298	305	464
F4	245	300	310	462

TABLE 8.D

QUANTITATIVE ANALYSIS OF THE CONDENSABLE PRODUCTS OF THERMAL DEGRADATION OF

VARIOUS SAMPLES OF PFB

(0°-500°C, 10°C min⁻¹ UNDER VACUUM)

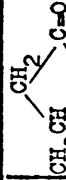
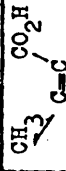
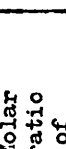
Sample	\bar{M}_n	Units	P R O D U C T S								Molar ratio of CO ₂ :propene
			CO ₂	CH ₂ =CHCH ₃	CH ₂ =C=O	CH ₃ CHO					
F1	658000	Moles/g of initial polymer	3.3×10^{-4}	1.8×10^{-4}	8.6×10^{-5}	1.0×10^{-4}	8.9×10^{-4}	1.7×10^{-4}	2.05×10^{-3}	1.8	
		Moles of product / Moles of monomer unit	2.8×10^{-2}	1.6×10^{-2}	7.4×10^{-3}	8.6×10^{-3}	7.7×10^{-2}	1.5×10^{-2}	0.176		
S1	468400	Moles/g of initial polymer	3.7×10^{-4}	1.7×10^{-4}	8.5×10^{-5}	1.2×10^{-4}	4.7×10^{-4}	1.3×10^{-4}	2.2×10^{-3}	2.2	
		Moles of product / Moles of monomer unit	3.2×10^{-2}	1.5×10^{-2}	7.3×10^{-3}	1.0×10^{-2}	4.0×10^{-2}	1.1×10^{-2}	0.189		
BLDX01	329500	Moles/g of initial polymer	1.8×10^{-4}	1.1×10^{-4}	5.5×10^{-5}	0.94×10^{-4}	4.4×10^{-4}	1.9×10^{-4}	1.7×10^{-3}	1.6	
		Moles of product / Moles of monomer unit	1.5×10^{-2}	9.5×10^{-3}	4.7×10^{-3}	8.1×10^{-3}	3.8×10^{-2}	1.7×10^{-2}	0.15		
F4	62600	Moles/g of initial polymer	3.7×10^{-4}	1.3×10^{-4}	7.9×10^{-5}	0.95×10^{-4}	7.6×10^{-4}	1.5×10^{-4}	2.0×10^{-3}	2.8	
		Moles of product / Moles of monomer unit	3.2×10^{-2}	1.2×10^{-2}	6.8×10^{-3}	8.2×10^{-3}	6.5×10^{-2}	1.6×10^{-2}	0.205		

TABLE 8.E

QUANTITATIVE ANALYSIS OF THE CRF FROM VARIOUS SAMPLES OF PHB
(0-500°C, 10°C min⁻¹ under vacuum)

Polymer Sample	Molecular Weight \bar{M}_n	Weight of CRF % of initial polymer weight \bar{M}_n	Units	monomer of PHB	dimer of PHB	trimer of PHB	tetramer of PHB
F1	658000	76.3	mole % of CRF →	36.7	46.0	16.6	0.7
			moles of product moles of monomer units	0.154	0.194	7.00 x 10 ⁻²	2.75 x 10 ⁻³
S1	468400	77	moles of CRF →	36.9	47.8	14.4	0.9
			moles of product moles of monomer units	0.153	0.205	6.16 x 10 ⁻²	3.35 x 10 ⁻³
BLDX01	329500	81.1	mole % of CRF →	39.8	46.7	13.0	0.6
			moles of product moles of monomer units	0.185	0.217	6.03 x 10 ⁻²	2.75 x 10 ⁻³
F4	62600	68.2	mole % of CRF →	38.8	45.4	15.3	0.4
			moles of product moles of monomer units	0.149	0.175	5.90 x 10 ⁻²	1.75 x 10 ⁻³

TABLE 8.F

MASS BALANCE TABLE FOR DEGRADATION OF VARIOUS SAMPLES OF PHB
TO 500°C UNDER IVA CONDITIONS

Products	% weight of initial polymer				Average Value for the 4 Polymers
	F1	S1	BLDX01	F4	
Carbon Dioxide	1.5	1.6	0.8	1.6	1.4
Propene	0.8	0.7	0.5	0.6	0.7
Ketene	0.2	0.4	0.2	0.3	0.3
Acetaldehyde	0.4	0.5	0.4	0.4	0.4
Water	-	-	-	-	-
β -Butyrolactone	7.7	4.0	3.8	6.5	5.5
iso-crotonic acid	1.5	1.1	1.7	1.6	1.5
crotonic acid (condensable) (CRF)	17.6) 33.0 15.4)	18.9) 34.7 15.8)	15.0) 33.5 18.5)	20.5) 35.4 14.9)	34.2
Dimer of PHB	38.7	41.1	43.4	35.0	39.6
Trimer of PHB	21.0	18.5	18.1	17.7	18.8
Tetramer of PHB	1.1	1.5	1.1	0.7	1.1
Residue	trace	trace	trace	trace	trace
Total	105.9	104.1	103.5	99.8	103.5

NOTE: No measurement was made of water content.

From the data it is obvious that there is little variance in the composition of the condensable products and the CRF, and no noticeable effects that could be attributed to the purity of the polymer sample. The percentage weight of CRF of sample F4 (Table 8.E) was lower than that recorded for F1, F3 and S1, primarily because of a different distribution of crotonic acid between the CRF and the cold trap used to collect the condensable products. No value for water content was obtained but the similar heights of the peak due to water observed in the SATVA traces of the four polymer samples showed that it was constant.

The results of a similar analysis obtained on heating polymers F1, BLDX01 and F4 to 500°C under nitrogen, are recorded along with that of S1, in Tables 8.G, 8.H and 8.I. As under vacuum, no significant differences were found in the product distribution of the four different polymer samples.

The molar ratio of CO₂ : propene was measured for each set of results and recorded in the last column of Tables 8.C and 8.F. This ratio was found to lie in the range 1.6 to 2.9 and the divergence from unity has been fully discussed in Chapter 5.5. Average results for the percentage weight of each degradation product compiled from all experiments undertaken has been recorded in the last column of Tables 8.F and 8.I for degradation under vacuum and nitrogen atmospheres respectively.

8.6 RATE OF DEPOLYMERISATION

The dependance of the rate of degradation on the initial degree of polymerisation was investigated by heating polymers F1, F3 and F4 at a temperature of 190°C for varying lengths of time in the pan of a Du Pont DSC1 instrument under a stream of flowing nitrogen.

TABLE 8.C

QUANTITATIVE ANALYSIS OF THE CONDENSABLE PRODUCTS OF THERMAL DEGRADATION OF VARIOUS SAMPLES OF PHE
(0-500°C, 10°C min⁻¹ UNDER NITROGEN)

Polymer Sample	\bar{M}_n	Units	P R O D U C T S								Molar ratio of $\text{CO}_2:\text{CH}_2=\text{CHCH}_3$
			CO_2	$\text{CH}_2 = \text{CHCH}_3$	$\text{CH}_2 = \text{C} = \text{O}$	CH_3CHO	$\begin{array}{c} \text{CH}_3 \\ \diagdown \\ \text{C}=\text{C} \\ \diagup \\ \text{H} \end{array}$	$\begin{array}{c} \text{H} \\ \diagdown \\ \text{C}=\text{C} \\ \diagup \\ \text{H} \end{array}$	$\begin{array}{c} \text{H} \\ \diagdown \\ \text{C}=\text{C} \\ \diagup \\ \text{CO}_2\text{H} \end{array}$		
F1	658000	Moles/g of initial polymer	1.2×10^{-4}	0.59×10^{-4}	trace	4.1×10^{-5}	2.4×10^{-4}	0.98×10^{-3}	2.0		
		Moles of product moles of monomer unit	1.0×10^{-2}	5.1×10^{-3}	trace	3.4×10^{-3}	2.1×10^{-2}	8.4×10^{-2}			
S1	468400	Moles/g of initial polymer	2.2×10^{-4}	1.1×10^{-4}	trace	5.0×10^{-5}	1.6×10^{-4}	1.0×10^{-3}	2.2		
		Moles of product moles of monomer unit	1.9×10^{-2}	8.6×10^{-3}	trace	4.3×10^{-3}	1.4×10^{-2}	8.6×10^{-2}			
BLDX01	329500	Moles/g of initial polymer	2.2×10^{-4}	0.89×10^{-4}	trace	3.4×10^{-5}	2.66×10^{-4}	0.72×10^{-3}	2.5		
		Moles of product moles of monomer unit	1.9×10^{-2}	7.7×10^{-3}	trace	2.9×10^{-3}	2.3×10^{-2}	6.2×10^{-2}			
F4	62600	Moles/g of initial polymer	2.9×10^{-4}	1.2×10^{-4}	trace	3.9×10^{-5}	1.9×10^{-4}	1.3×10^{-3}	2.4		
		Moles of product moles of monomer unit	2.5×10^{-2}	1.0×10^{-2}	trace	3.4×10^{-3}	1.7×10^{-2}	0.11			

TABLE 3.H

QUANTITATIVE ANALYSIS OF THE CRF FROM VARIOUS SAMPLES OF PHB
 (0-500°C, 10°C min⁻¹ under nitrogen)

Polymer Sample	Molecular weight \bar{M}_n	Monomer molecular % of PHB	Dimer molecular % of PHB	Trimer molecular % of PHB	Tetramer molecular % of PHB
F1	658000	45.0	49.0	5.3	0.7
S1	468400	53.4	41.1	4.9	0.5
BLDX01	329500	48.6	43.9	6.7	0.7
F4	62600	42.4	47.1	9.7	0.8

TABLE 8.I

MASS BALANCE TABLE FOR DEGRADATION OF VARIOUS SAMPLES OF PHB
TO 500°C UNDER NITROGEN

Products	% weight of initial polymer				Average Value for the 4 polymers
	F1	S1	BLDX01	F4	
Carbon Dioxide	0.5	1.0	1.0	1.3	1.0
Propene	0.3	0.4	0.4	0.5	0.4
Ketene	trace	trace	trace	trace	trace
Acetaldehyde	0.2	0.2	0.2	0.2	0.2
Water	-	-	-	-	-
β -Butyrolatone	Nil	Nil	Nil	Nil	Nil
iso-crotonic acid	2.1	1.4	2.3	1.7	1.9
crotonic acid (condensable) (CRF)	8.4) 24.6) 33.0	8.6) 30.9) 39.5	6.2) 27.4) 33.6	11.2) 21.4) 32.6	34.7
Dimer of PHB	53.6	47.6	49.5	47.5	49.6
Trimer of PHB	8.8	8.6	11.3	14.6	10.8
Tetramer of PHB	1.5	1.2	1.6	1.6	1.5
Residue	trace	trace	trace	trace	trace
Total	100	99.9	99.9	100	100.1

- NOTE: (1) No measurement was made of water content.
- (2) The residue accounted for 0 to 1% of initial weight of polymer for each sample (measured by TG).

Each polymer sample was dried for one hour on a fluidised bed of polymer created by a flow of dried nitrogen (120°C) flowing through the polymer prior to degradation. The sample to be degraded was heated in a DSC pan to 190°C , at a rate of $64^{\circ}\text{C}/\text{min}$, the temperature being maintained for a specific length of time after which the polymer residue remaining in the pan was quenched cooled in 8cm^3 of chloroform and its molecular weight determined by GPC, on instrument B, as described in Chapter 2.6(i).

A plot of \bar{M}_n versus time of heating for each of the polymers is illustrated in Figure 8.4. The effect of the esterification reaction on \bar{M}_n is once again observed (see Chapter 6) and the data has been replotted, on the same diagram, to show the changes in \bar{M}_n with time of heating due to the depolymerisation reaction alone, by application of Equation 6.1 to the experimentally measured \bar{M}_n values. Using this amended data the rate of chain scission for each sample was calculated, by a least squares fit, on the respective $\frac{1}{\text{CL}_t} - \frac{1}{\text{CL}_0}$ versus time of heating plot (Figure 8.5), the results being recorded on Table 8.J. A large error is associated with the value quoted for Sample F4, since the lower the molecular weight, the greater, the relative error in \bar{M}_n , the absolute error in $\frac{1}{\text{CL}}$, and hence the rate. The values for the rate of chain scission recorded in Table 8.J agree within experimental error and are comparable with that obtained for polymer S1 $[(1.15 \pm 0.8) \times 10^{-6}$ bond scissions/monomer unit/sec] recorded under similar conditions (Chapter 6.4). Of the two experimental methods used to determine the changes in \bar{M}_n with time of heating, that reported in Chapter 6 is thought to be superior. The main reason for this is that by heating the polymer sample in a degradation tube (see Figure 2.18) as in the method discussed in Chapter 6, rather than in a DSC pan

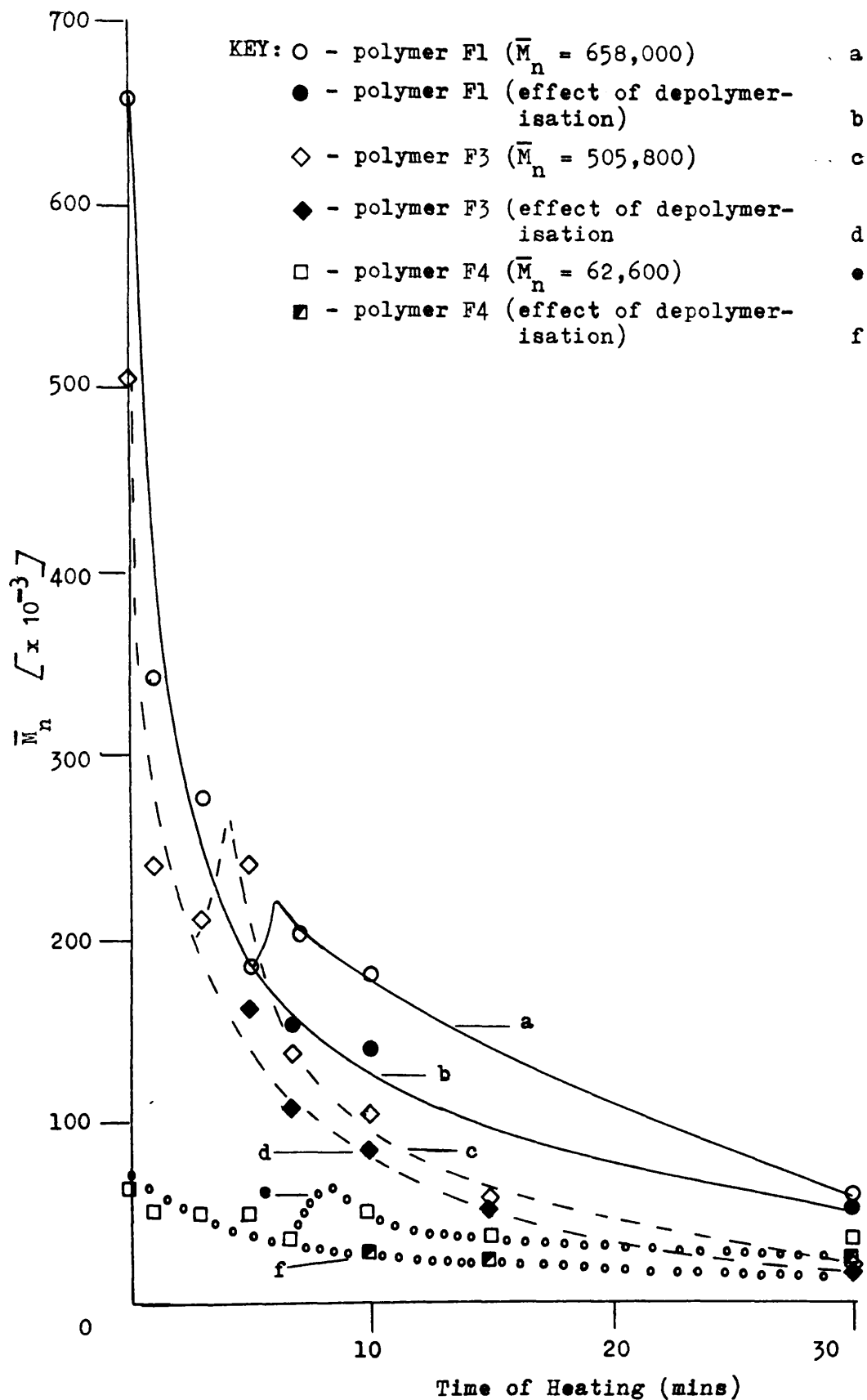


FIGURE 8.4
CHANGES IN \bar{M}_n WITH TIME OF HEATING OF VARIOUS
PHB SAMPLES (190°C, NITROGEN)

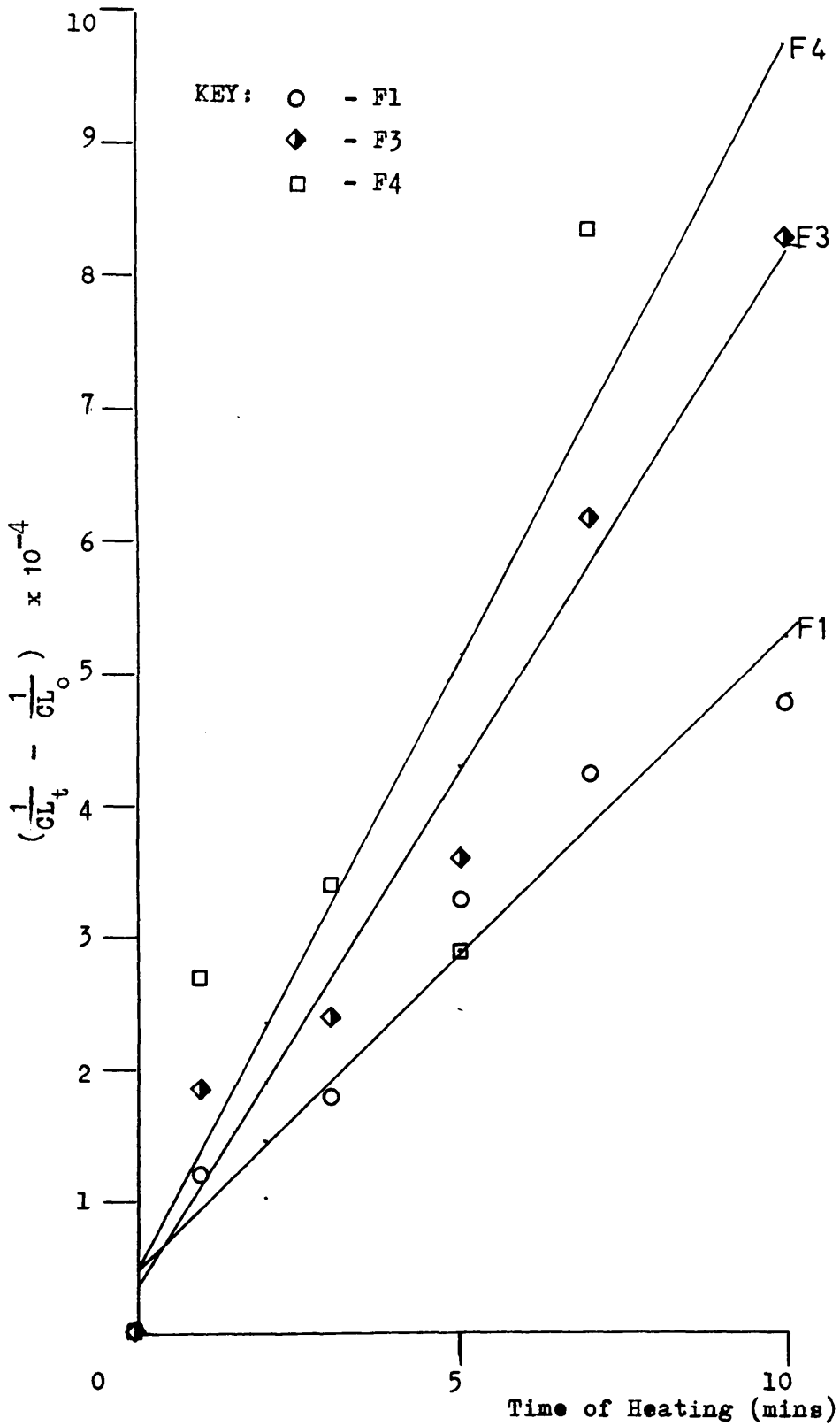


FIGURE 8.5

$(\frac{1}{CL_t} - \frac{1}{CL_o})$ VERSUS TIME OF HEATING FOR VARIOUS
 PHB SAMPLES (190°C, NITROGEN)

TABLE 8.J

RATE OF DEPOLYMERISATION OF SAMPLES OF PHB
WITH DIFFERENT INITIAL MOLECULAR WEIGHTS

Polymer Sample	Rate of Chain Scission (scissions/monomer unit/sec.)
F1	$(8.03 \pm 1) \times 10^{-7}$
F3	$(1.34 \pm 0.1) \times 10^{-6}$
F4	$(1.55 \pm 0.5) \times 10^{-6}$

NOTE: Errors calculated as described in Chapter 2.9
and are expressed as \pm standard deviation.

it is possible to "degrade" a weight of polymer factors of ten larger and to have a thinner layer of polymer, due to the differences in surface area between the base of a degradation tube and that of a DSC pan. Plots of \bar{M}_w versus time of heating (Figure 8.6) show a rise in \bar{M}_w after a similar time of heating to that observed for \bar{M}_n (Figure 8.4).

8.7 CONCLUSIONS

The work described in this chapter has shown that the composition of the degradation products of PHB does not differ significantly from one polymer sample to another. Further evidence for a random chain scission mechanism for the degradation of PHB was obtained from the TG results and rates of depolymerisation of various PHB samples. The complicated nature of the effect of impurities within the polymer sample on stability has been illustrated by the TG traces and highlights the discussion on impurities contained in Chapter 1.3.

Polymer F4 has been shown to exhibit an endotherm in its DSC trace similar to that of SX and was shown to be highly crystalline.

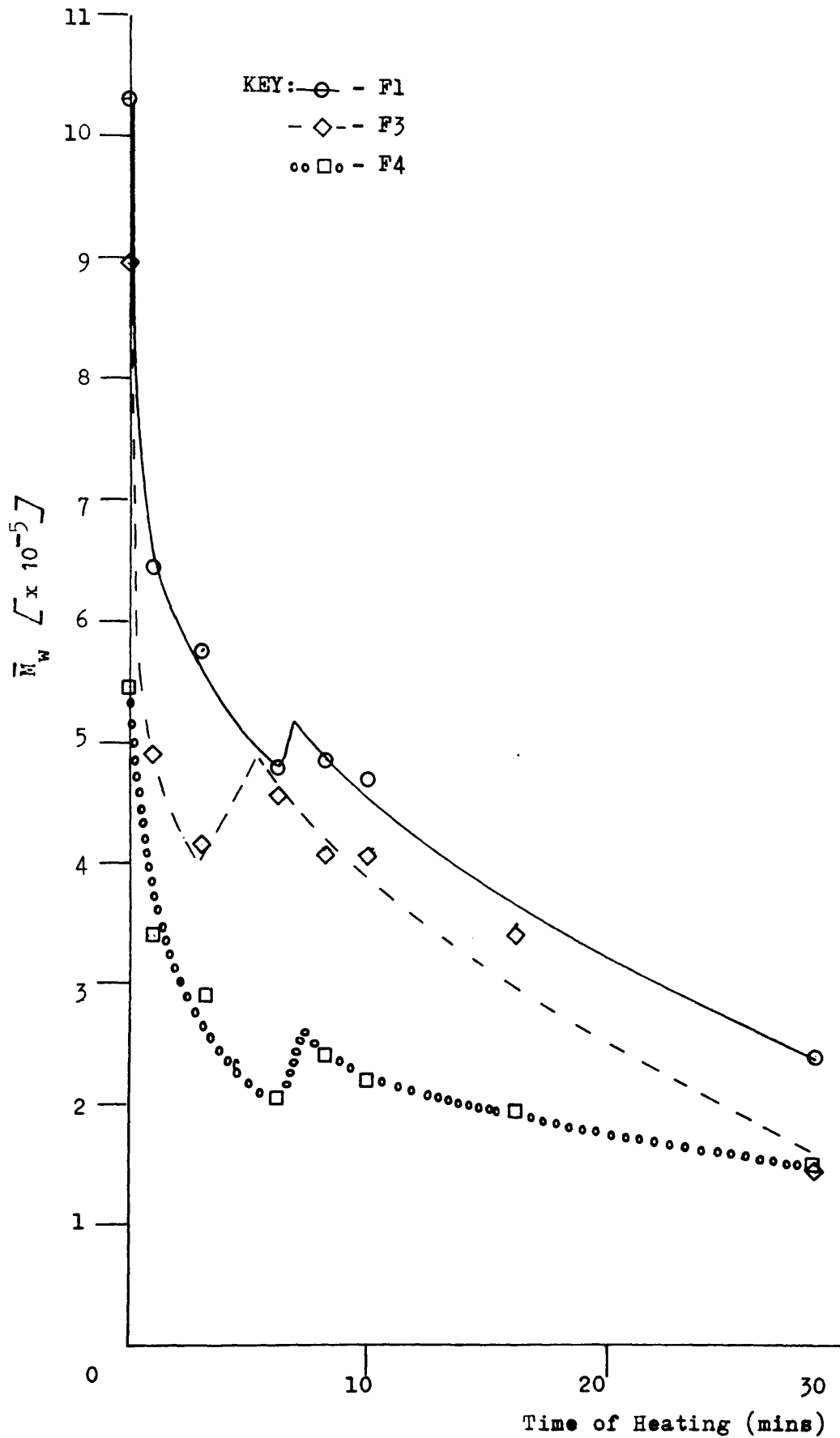


FIGURE 8.6
CHANGES IN \bar{M}_w WITH TIME OF HEATING FOR VARIOUS
PHB SAMPLES (190°C, NITROGEN)

CHAPTER 9GENERAL CONCLUSIONS AND DISCUSSION9.1 GENERAL CONCLUSIONS

The main results of the present study may be summarised in the following way:

- (1) Poly(-(D)- β -hydroxybutyric acid), isolated from a culture of the bacterium *Azotobacter beijerinckii*, undergoes rapid degradation at temperatures in the range 170°C to 200°C via a random chain scission mechanism with short zip length.
- (2) The random chain scission can be explained by an esterpyrolysis mechanism in which a six-membered cyclic transition state is involved.
- (3) During the early stages of such a degradation a competing esterification reaction, of limited duration, occurs which is associated with the condensation of terminal hydroxyl and carboxyl groups.
- (4) No significant difference in the rate of depolymerisation was observed under vacuum or in atmospheres of nitrogen and air. The average rate of chain scission at 170°C, 180°C, 190°C and 200°C is 9.9×10^{-8} scissions/monomer unit/sec., 3.2×10^{-7} scissions/monomer unit/sec., 1.8×10^{-6} scissions/monomer unit/sec. and 6.6×10^{-6} scissions/monomer unit/sec. respectively.

(5) The energy of activation of the depolymerisation reaction was shown to be 250 kJ mol^{-1} .

(6) The following products have been identified during thermal degradation of PHB to 500°C under TVA conditions:

- | | | | |
|------|-------------------------|---|---------------------------------|
| I | Tetramer of PHB | } | (acidic and vinylic end groups) |
| II | Trimer of PHB | | |
| III | Dimer of PHB | | |
| IV | Crotonic Acid | | |
| V | Iso-crotonic acid | | |
| VI | β -Butyrolactone | | |
| VII | Water | | |
| VIII | Acetaldehyde | | |
| IX | Ketene | | |
| X | Propene | | |
| XI | Carbon dioxide | | |
| XII | Carbon monoxide (trace) | | |

(7) Compounds VI to XII are primarily formed at temperatures above 340°C .

(8) There is a tendency to form lower oligomers as the temperature rises.

(9) Identical products to those noted in (6) above, are formed during the thermal degradation of PHB (ambient to 500°C at $10^\circ\text{C}/\text{min}$) under nitrogen.

- (10) A diagrammatical summary of the main routes of thermal breakdown of PHB is illustrated in Figure 9.1.
- (11) Initial degree of polymerisation has no effect on the thermal stability of PHB.
- (12) The main products of the thermal degradation of PHB are, in order of importance, dimer of PHB, crotonic acid, trimer of PHB, accounting for greater than 90% of the weight of the initial polymer.
- (13) No marked increase in stability of PHB was noted on increasing the crystallinity of the polymer above that formed on rapid precipitation from solution.
- (14) The effect of impurities on the stability of PHB is very complicated.
- (15) Some evidence for the existence of two crystalline forms of PHB has been observed.
- (16) A relationship between MFI and \bar{M}_w at 190°C of the form $\log \text{MFI} = 19.8 - 3.49 \log \bar{M}_w$ was shown to exist.

9.2 GENERAL DISCUSSION

As a result of the present study a greater understanding of the kinetics, mechanisms and products involved in the thermal degradation of PHB has been obtained. This information will prove valuable when consideration is given to the possibility of commercial exploitation of PHB as a thermoplastic. To this end, the esterification reaction occurring in PHB when heated, (see Chapter 6), could prove a vital factor. This may enable PHB

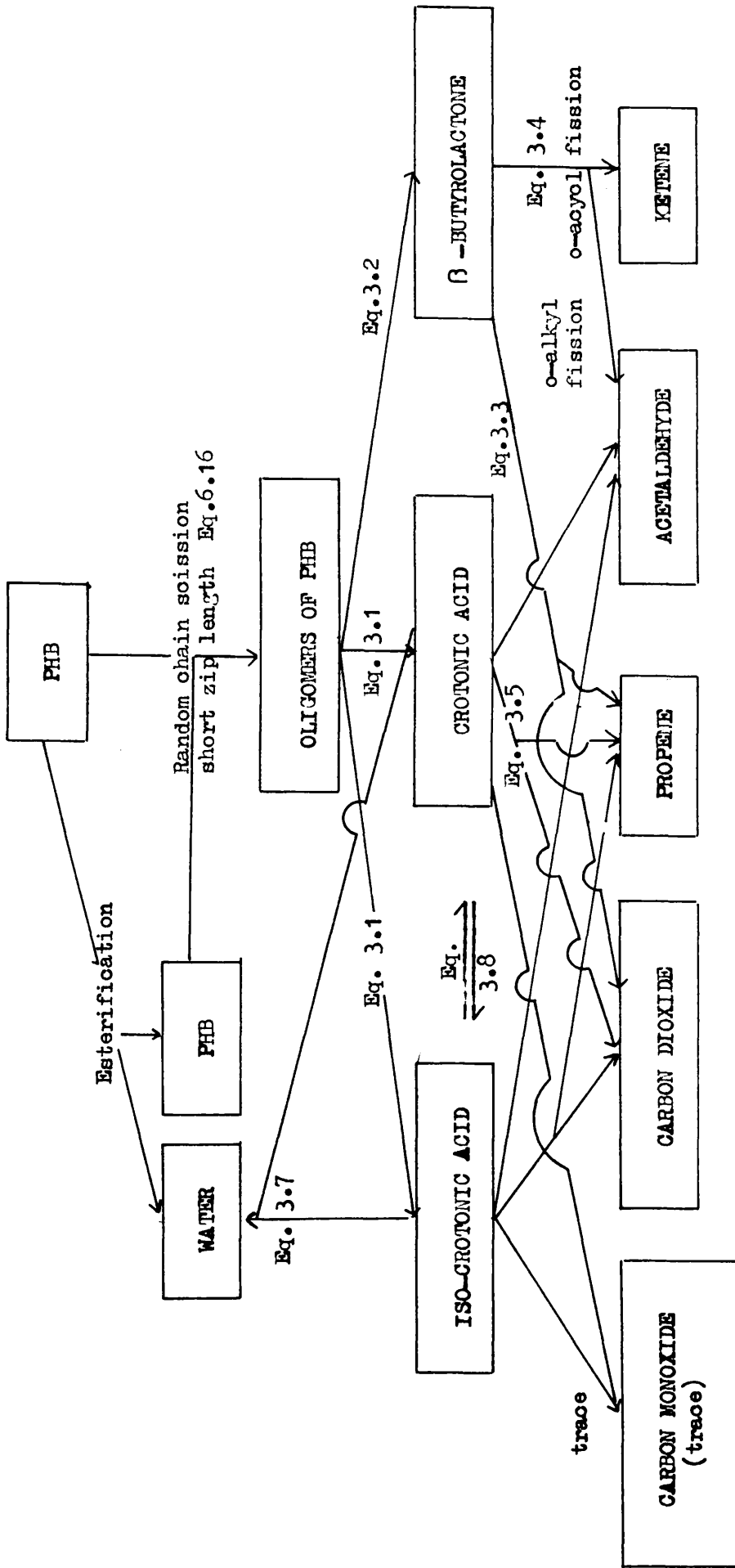


FIGURE 9.1

SUMMARY OF THE THERMAL DEGRADATION PATH OF PHB

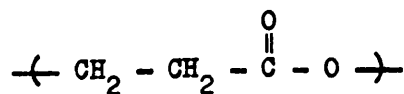
to be processed, with little degradative effect on the molecular weight of the polymer sample, if the effects of the esterification and depolymerisation reactions can be roughly balanced during processing.

9.3 SUGGESTIONS FOR FUTURE WORK

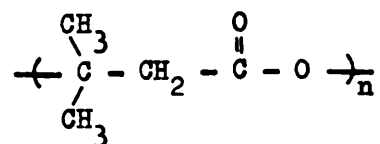
A study of the changes in molecular weight of "synthetic" PHB in the temperature range 170°C to 200°C would yield valuable information on rates of chain scission which on comparison with those of "biological" PHB, reported in this work, would give an indication as to the optimum stability that could be achieved. Use of "synthetic" PHB to study systematically the effects of impurities on stability would help solve the complex puzzle of the effects of the numerous impurities reported in "biological" PHB. Once this information has been obtained a discussion can take place as to the optimum purity of PHB beyond which the cost of purification outweighs the benefits of improved stability.

A useful line of research would be into additives which improve the rheology of PHB for processing in addition to controlling the molecular weight.

The thermal stability of PHB would be expected to be between that of poly(oxy-carbonylethylene) XIII and poly(oxy-carbonyl-2-2-dimethylethylene) XIV.



XIII



XIV

as a direct consequence of the ester-pyrolysis six-centred β -elimination mechanism proposed for the random chain scission reaction observed in PHB in the temperature range 170°C to 200°C. This is due to the steric hinderance, associated with the six-centred transition state, on replacement of β -hydrogen atoms (to the carboxyl group) with increasing numbers of methyl groups. In fact, XIV has been shown to be thermally stable at 200°C (Ref.136), whereas XIII undergoes weight loss at 180°C (Ref.137). A detailed study of the thermal properties, especially kinetics, of XIII and XIV would provide a useful comparison with the results of this work.

The ultimate usefulness of PHB may depend on its stability under normal atmospheric conditions. To this end a parallel study of the photochemical stability of PHB would be vital.

REFERENCES

- 1 J. Gibson, *Chemistry in Britain*, 16(1), 26, (1980)
- 2 Y. Tokiwa, T. Suzuki, *Nature*, 270, 76, (1977)
- 3 R.D. Fields, F. Rodriguez, R.K. Finn,
J. Appl. Polym. Sci., 13, 3571, (1974)
- 4 J.E. Potts, R.A. Clendinning, W.B. Ackart, W.D. Niegisch
Am. Chem. Soc. Polym. Prepr., 13, 629, (1972)
- 5 Y. Tokiwa, T. Ando, T. Suzuki,
Hakko Kagaku Zasshi, 52(8), 603, (1976)
- 6 M. Lemoigne,
Ann. Inst. Pasteur, 41, 148, (1927)
- 7 M. Doudoroff, R.Y. Stanier,
Nature, 183, 1440, (1959)
- 8 N.E. Gibbons, G. Sierra,
Can. J. Microbiol., 8, 225, (1962), 9, 491, (1963)
- 9 H.G. Schlegel, G. Gottschalk, R. Von Bartha,
Nature, 191, 463, (1961)
- 10 D.H. Williamson, J.F. Wilkinson,
J. Gen. Microbiol., 19, 198, (1958)
- 11 H.G. Schlegel, G. Gottschalk,
Angew. Chem., 74, 342, (1962)
- 12 R.M. Macrae, J.F. Wilkinson,
J. Gen. Microbiol., 19, 210, (1958)
- 13 G.A.F. Ritchie, E.A. Dawes,
Biochem. J., 112, 803, (1969)
- 14 G.A.F. Ritchie, P.J. Senior, E.A. Dawes,
Biochem. J., 121, 308, (1971)
- 15 P.J. Senior, E.A. Dawes,
Biochem. J., 125, 55, (1971)
- 16 P.J. Senior, G.A. Beech, G.A.F. Ritchie, E.A. Dawes,
Biochem. J., 128, 1193, (1972)
- 17 P.J. Senior, E.A. Dawes,
Biochem. J., 134, 225, (1973)
- 18 M. Yokouchi, Y. Chatani, H. Tadokora, K. Teranishi, H. Tani,
Polymer, 14, 267, (1973)
- 19 J. Cornibert, R.H. Marchessault,
Macromolecules, 8, 296, (1975)

- 20 R. Alper, D.G. Lundgren, R.H. Marchessault, W.A. Cote,
Biopolymers, 1, 545, (1963)
- 21 D.G. Lundgren, R. Alper, C. Schneitman, R.H. Marchessault,
J. Bacteriol, 89, 245, (1965)
- 22 A.H. de Mola, N. Marx-Figini, R.V. Figini,
Makromol. Chem., 176, 2655, (1975)
- 23 J.N. Baptist, F.X. Werber,
SPE Trans., 4, 245, (1964)
- 24 Chemical and Engineering News, March 18, (1963) pp.40-41
- 25 S. Inoue, Y. Tomoi, T. Tsuruta, J. Furukawa,
Makromol. Chem., 48, 229, (1961)
- 26 Y. Yamashita, Y. Ishikawa, T. Tsuda, S. Miura,
Koggo Kagaka Zasshi, 66, 104, 110, (1963)
- 27 D.E. Agostini, J.B. Lando, J. Reid Shelton,
J. Polym. Sci., Part A1, 9, 2775, (1971)
- 28 J. Reid Shelton, J.B. Lando, D.E. Agostini,
J. Polym. Sci., Part B, 9, 173, (1971)
- 29 J. Vergara, R.V. Figini,
Makromol. Chem., 178, 267, (1977)
- 30 M. Iida, T. Araki, K. Teranishi, H. Tani,
Macromolecules, 10, 275, (1977)
- 31 F.L. Wright, Private communication
- 32 P.A. Holmes, Private communication
- 33 N. Grassie, H.W. Melville;
Proc. R. Soc., A1, 199, 1, 14, 24, (1949)
- 34 N. Grassie, H.W. Melville,
Discuss. Faraday Soc., 2, 378, (1947)
- 35 G.G. Cameron, G.P. Kerr,
Makromol. Chem., 115, 268, (1968)
- 36 P. Bradt, V.H. Dibeler, F.L. Mohler,
J. Res. Natl. Bur. Std., 50, 201, (1953)
- 37 S.L. Madorsky, S. Straus, D. Thompson, L. Williamson,
J. Polym. Sci., 4, 639, (1949)
- 38 Y. Tsuchiya, K. Sumi,
J. Polym. Sci., A1, 6, 415, (1968)
- 39 G.G. Cameron, I.T. McWalter,
Europ. Polym. J., 6 1601, (1970)

- 40 Y. Tsuchiya, K. Sumi,
J. Polym. Sci., A1, 6, 415, (1968)
- 41 R. Simha, L.A. Wall, P.J. Blatz,
J. Polym. Sci., 5, 615, (1950)
- 42 R. Simha, L.A. Wall,
J. Polym. Sci., 6, 39, (1951)
- 43 R. Simha, L.A. Wall,
J. Phys. Chem., 56, 707, (1952)
- 44 N. Grassie, R.S. Roche,
Makromol. Chem., 112, 16, (1963)
- 45 F. Wiloth, Makromol. Chem., 144, 283, (1971)
- 46 E.P. Goodings, Soc. Chem. Ind. Monograph, 13, 211, (1961)
- 47 P.D. Ritchie, Soc. Chem. Ind. Monograph, 13, 106, (1961)
- 48 G.G. Cameron, D.R. Kane,
J. Polym. Sci., Part B, 2, 693, (1964)
- 49 G.G. Cameron, D.R. Kane,
Makromol. Chem., 135, 137, (1970)
- 50 G.G. Cameron, F. Davie,
Makromol. Chem., 149, 169, (1971)
- 51 G.G. Cameron, D.R. Kane,
Makromol. Chem., 109, 194, (1967)
- 52 V.V. Rodé, M.A. Verkhotin, S.R. Rafikov,
Europ. Polym. J. (Supplement), 401, (1969)
- 53 W.C. Geddes, Europ. Polym. J., 3, 267, 733, 747, (1967)
- 54 V.P. Gupta, L.E. St. Pierre,
J. Polym. Sci., Part A1, 8, 37, (1970)
- 55 R.R. Stromberg, S. Straus, B.G. Achhammer,
J. Polym. Sci., 35, 355, (1959)
- 56 N. Grassie, Trans. Faraday Soc., 48, 379, (1952)
- 57 N. Grassie, Trans. Faraday Soc., 49, 835, (1953)
- 58 D.L. Gardner, I.C. McNeill,
J. Therm. Anal., 1, 389, (1969)
- 59 A.B. Blyumenfeld, B.M. Kovarskaya,
Vysokomol. Soyed., A12, 633, (1970)
(Translated in Polym. Sci. U.S.S.R., 12, 710, (1970))

- 60 N. Grassie, J. Hay,
Soc. Chem. Ind. Monograph, 13, 183, (1961)
- 61 N. Grassie, I.C. McNeill,
J. Polym. Sci., 27, 207, (1958)
- 62 H.N. Friedlander, L.H. Peebles, H. Brandrup, J.R. Kirby,
Macromolecules, 1, 79, (1968)
- 63 N. Grassie, D.H. Grant, Polymer, 1, 125, (1960)
- 64 N. Grassie, J.N. Hay, Makromol. Chem., 64, 82, (1963)
- 65 H.H.G. Jellinek, 'Degradation of Vinyl Polymers',
(Academic Press Incorp., New York) (1955)
- 66 N. Grassie, 'Developments in Polymer Degradation - 1',
(Applied Sci. Publ.) (1977)
- 67 S.L. Madorsky, 'Thermal Degradation of Organic Polymers'
(Interscience New York (Publ.)) (1964)
- 68 N. Grassie, in I.U.P.A.C. International Symposium on Macro-
molecular Chemistry, Plenary and Main Lectures,
Akademiai Kiado, Budapest., (1969), p.725
- 69 N. Grassie, E. Parish,
Europ. Polym. J., 3, 619, (1967)
- 70 I.C. McNeill, 'Developments in Polymer Degradation
ed. N. Grassie, Vol.1 171,
(Applied Science Publishers Ltd. London, (1977))
- 71 R.R. Hindersinn, G.W. Wagner,
'Encyclopaedia of Polymer Science and Technology',
Vol.7 Interscience Publ. (1967) p 231
- 72 I.C. McNeill, J. Polymer Sci., A4, 2479, (1966)
- 73 I.C. McNeill, Europ. Polym. J., 3, 409, (1967)
- 74 I.C. McNeill, Europ. Polym. J. 6, 373, (1970)
- 75 I.C. McNeill, D. Neil,
'Thermal Analysis', Vol.1 p.353
R.F. Schwenher, P.D. Cram (Eds)
Academic Press, New York (1969)
- 76 I.C. McNeill, D. Neil, Europ. Polym. J., 7, 115, (1971)
- 77 I.C. McNeill, L. Ackerman, S.N. Gupta, M. Zulifiqar,
S. Zulifiqar,
J. Polym. Sci. 15, 2381, (1977)
- 78 L. Ackerman, W.J. McGill, J.S. Afr. Chem. Inst., 26, 82,
(1973)
- 79 Brymeer, Penny,- "Mass Spectrometry", Butterworth Pub. p.10

- 80 O. Hromatka, W.A. Ave,
Monatsh.Chem. 93, 503, (1962)
- 81 D.W. Grant, 'Gas Liquid Chromatography'
Van Nostrand Reinhold Company (Publ)
- 82 B.W. Hatt, C.E.H. Knapman (Ed) -
"Developments in Chromatography - 1"
Applied Science Publishers Ltd., London pp 157-199
- 83 H.E. Pickett, M.J.R. Canton, J.F. Johnson,
J. Appl. Polym. Sci., 10, 917, (1966)
- 84 A.N. Burgess, Private Communication
- 85 A. Nevin, T.G. Ryan, Private Communication
- 86 R.H. Marchessault, K. Okamura, C.J. Su,
Macromolecules, 3, 735, (1970)
- 87 "Polymer Handbook" Second Edition
J. Brandrup, E.H. Immergut (Eds)
J. Wiley & Sons New York (Publ) (1975) pIV-2
- 88 J. Cornibert, R.H. Marchessault, H. Benoit, G. Weill,
Macromolecules, 3, 741, (1970)
- 89 K. Eckschlager "Errors, Measurements and Results in
Chemical Analysis"
Van Nostrand Reinhold Company (Publ), p 142
- 90 R.H. Pierson, A.N. Fletcher, E. St. Clair Grantz,
Anal. Chem., 28, 1218, (1965)
- 91 American Petroleum Institute Research Project 44, 2, 699
- 92 F. Halverson, V.Z. Williams,
J. Chem. Phys., 15, 552, (1947)
- 93 D. Welti "Infrared Vapour Spectra" -
Heyden & Sons Ltd. (Publ) (1970)
- 94 "The Aldrich Library of Infrared Spectra"
C.J. Pouchert - Aldrich Chemical Co. Inc. Ref. Spectra 310B
- 95 "The Sadtler Standard Spectra" Ref. 14936 K
- 96 C.R.C. "Handbook of Chemistry and Physics" 60th Edition
R.C. Weast, M.J. Astle (Eds) (1979) p C231
- 97 F.W. McLafferty - Anal. Chem. 29, 1782, (1957)
- 98 F.W. McLafferty - "Interpretations of Mass Spectra"
(Second Edition)
W.A. Benjamin Inc. (Publ) (1973), p142
- 99 F.H. Fields, Accounts Chem. Res., 1, 42, (1968)

- 100 "Heterocyclic Compounds Vol. 19²" - A. Weissberger (Ed)
Interscience (Publ) (1964) pp 806 and 787
- 101 R.L. Forman, H.M. MacKinnon, P.D. Ritchie,
J. Chem. Soc., (C)2, 2013, (1968)
- 102 A.L. Brown, P.D. Ritchie, J. Chem. Soc., (C)2, 2007, (1968)
- 103 G.G. Smith, S.E. Blau, J. Phys. Chem., 68, 1231, (1964)
- 104 E.U. Emovan, A. MacColl, J. Chem. Soc., 1, 227, (1964)
- 105 S. De Burgh Norfolk, R. Taylor,
J. Chem. Soc., Perkin II, 280, (1976)
- 106 R. Taylor, Private Communication
- 107 B.L. Van Duvren et al,
J. Nat. Cancer Inst., 37, 325, (1966)
- 108 B.L. Van Duvren et al,
J. Nat. Cancer Inst., 39, 1231, (1967)
- 109 D. Davidson and P. Newman,
J. American Chem. Soc., 74, 1515, (1952)
- 110 N. Grassie - "Encyclopaedia of Polymer Science and Technology"
Vol.4, pp 651-654, Wiley, New York (1966)
- 111 H.H.G. Jellinek, Pure Appl. Chem., 4, 419, (1962)
- 112 H.H.G. Jellinek,
"Degradation of Vinyl Polymers",
Academic Press Inc. (Publ) (1955) Ch 1
- 113 N. Grassie, E.M. Grant,
Europ. Polym. J., 2, 255, (1966)
- 114 W.F. Busse, R. Longworth,
J. Polym. Sci., 58, 49, (1962)
- 115 H.P. Schreiber, E.B. Bagley,
J. Polym. Sci., 58, 29, (1962)
- 116 W.T. Peticolas, J.M. Watkins,
J. Amer. Chem. Soc., 79, 5083, (1957)
- 117 T. Fox, G.S. Gratch, S. Loshaek,
"Rheology, Theory and Applications" F.R. Eirich (Ed).
Academic Press, New York, (1956) Ch.12 pp 442-446
- 118 "Encyclopaedia of Polymer Science and Technology"
Vol. 8, pp 596, 599-600, Wiley, New York (1966)
- 119 F. Bueche, J. Polym. Sci., 43, 527, (1960)
- 120 F. Bueche, J. Chem. Phys., 20, 1959, (1952)

- 121 R.S. Porter, J.F. Johnson,
J. Appl. Polymer Sci., 3, 194, (1960)
- 122 N. Grassie, I.G. MacFarlane,
Europ. Poly. J., 14, 875, (1978)
- 123 T.H. Thomas, T.G. Kendrick,
J. Polym. Sci., Part A-2, 7, 537, (1969)
- 124 L.H. Peebles, M.W. Huffman,
J. Polym. Sci., Part A-1, 9, 1807, (1971)
- 125 T.J. Heman, Private Communication
- 126 P.A. Holmes, Private Communication
- 127 D.G.M. Wood, Private Communication
- 128 R. Taylor, J. Chem. Soc., Perkin II, 1025, (1975)
- 129 S. de Burgh Norfolk, R. Taylor,
J. Chem. Soc., Perkin II, 280, (1976)
- 130 M. Yokouchi, Y. Chatani, H. Tadokora, K. Teranishi,
H. Tani,
Polymer, 14 267, (1973)
- 131 "Encyclopaedia of Polymer Science and Technology,"
B. Ke., (Interscience Publ), Vol. 5, p 41
- 132 "Encyclopaedia of Polymer Science and Technology,"
B. Ke., (Interscience Publ), Vol. 5, pp 53-57
- 133 B.H. Clampitt, R.H. Hughes,
J. Polym. Sci., Part C, 6, 43, (1964)
- 134 C. Teacintor, R.S. Schotland, R.B. Miles,
J. Polym. Sci., Part C, 6, 197, (1964)
- 135 T. Ryan, Private Communication
- 136 Yu. N. Sazanov, N.A. Glukhav, M.M. Koton,
Vysokomol. Soedin., Ser B, 10, 501, (1968)
(read in abstract form only)
- 137 S. Iwabuchi, V. Jaacks, F. Gabil, W. Kern,
Makromol. Chem., 165, 59, (1973)